West Pomeranian University of Technology

Szczecin

Department of Structure Theory

Hanna Weber

Numerical Analysis of Static and Dynamic Sensitivity of Complex Structural Systems with Random Parameters

Supervisor
Dr hab. Tran Duong Hien, prof. ZUT

Praca doktorska finansowana ze środków budżetowych
na naukę w latach 2010-2014 jako projekt badawczy

Szczecin 2014

Summary

Numerical Analysis of Static and Dynamic Sensitivity of Complex Structural Systems with Random Parameters

In the paper the static and dynamic sensitivity problems of structural multi-degree-of-freedom systems are considered in terms of uncertainties in design parameters. Starting from the stochastic version of Lagrange equations, based on the mean-point second-order perturbation method, the hierarchical sets of equations of motion and equilibrium are formulated. The first two probabilistic moments of time-dependent and time-independent structural response as well as the first two probabilistic moments of static and dynamic sensitivity are derived with the mean values and cross-covariances of design parameters on input. It allows one to get not only the deterministic results of static and dynamic structural response and their sensitivities, but also the solution accuracy in the form of the mean values and their cross-covariances.

The formulations are illustrated by a number of numerical examples, cable-stayed bridges and bar domes, for instance. For the suspended bridge, a model with 3563 degrees of freedom, consisting of 154 truss elements, 510 beam elements and 635 shell elements, is adopted. For the 80-bar dome four various models are discussed to verify the influence of finite element setting on numerical results. A few model examples are analyzed and obtained results are compared with exact (analytical) solutions presented in the literature.

The beat effects in the structures with repeated geometry is observed and eliminated by using added masses and dampers. The way of processing and entering the cross-covariances matrix for design random variables is presented in a Fortran procedure.

The problem of systems with repeatable eigenvalues and the influence of parameter selection on the result accuracy are included. In the appendices some computer codes to generating input data of the complex structural model and to forming the cross-covariances matrix of random parameters are shown.

The paper is finished with concluding remarks on the effectiveness of the above-mentioned formulations and with some new aspects related to the future work.

Streszczenie

Numeryczna analiza wrażliwości statycznej i dynamicznej złożonych układów konstrukcyjnych z parametrami losowymi

W pracy rozważono problem statycznej i dynamicznej wrażliwości układów o wielu stopniach swobody, z uwzględnieniem niepewności w parametrach projektowych. Wychodząc ze stochastycznej wersji równań Lagrange'a i stosując metodę perturbacji w otoczeniu wartości średnich, sformułowano hierarchiczne układy równań ruchu i równowagi. Wyprowadzono wyrażenia na pierwsze i drugie momenty probabilistyczne czasowo-zależnej i czasowo-niezależnej reakcji układu oraz na pierwsze i drugie moment probabilistyczne statycznej i dynamicznej wrażliwości, wykorzystując wartości średnie i kowariancje wzajemne parametrów projektowych na wejściu. Pozwala to na uzyskanie nie tylko deterministycznej statycznej i dynamicznej reakcji układu i ich wrażliwości, jak również dokładności otrzymanych wyników w postaci wartości średnich i ich wzajemnych kowariancji.

Sformułowania zilustrowano za pomocą przykładów numerycznych, np. mostu podwieszonego i kopuły prętowej. Dla konstrukcji mostu przyjęto model o 3563 stopniach swobody, składający się z 154 kratowych, 510 belkowych i 635 powłokowych elementów skończonych. Dla kopuły tworzonej przez 80 prętów rozpatrzono cztery różne modele metody elementów skończonych, w celu zbadania wpływu doboru siatki na otrzymane wyniki. Przeanalizowano niektóre przykłady modelowe, których wyniki porównano z dokładnymi (analitycznymi) rezultatami z literatury.

Zaobserwowano effekty dudnienia układów geometrycznie się powtarzających i opisano ich eliminację przy wykorzystaniu dodatkowych mas i tłumików. Przedstawiono także sposób tworzenia i wprowadzenia macierzy kowariancji wzajemnych losowych zmiennych projektowych poprzez procedurę fortranowską.

Ujęto również zagadnienia analizy układu o powtarzających się wartościach własnych i wpływ doboru parametrów analizy dynamicznej na dokładność uzyskanych wyników. W załącznikach do rozprawy zawarto programy do generacji danych dla złożonych układów konstrukcyjnych oraz do tworzenia macierzy kowariancji zmiennych projektowych.

Niektóre uwagi wniosukjące o skuteczności przedstawionych sformułowań kończą rozprawę, wraz z pewnymi nowymi aspektami dotyczącymi dalszej pracy.

Contents

Glossary of Symbols

$(\cdot)^{\mathrm{T}}$	transposed matrix
$\dot{(\cdot)}$	first derivative with respect to time
$\ddot{(\cdot)}$	second derivative with respect to time
$\frac{\mathrm{d}\cdot}{\mathrm{d}b_a}$	absolute partial derivative with respect to design variable vector
$(\cdot)^{-1}$	inverse matrix
α, β	coefficients in damping approximation
γ_m	weight density
γ_f	loads coefficient
$\delta(\cdot)$	Dirac delta distribution
$\delta_{\alpha\beta}$	Kronecker delta
Δt	time step
ϵ	small parameter
$\boldsymbol{\varepsilon}$	strain vector
θ	terminal time condition
λ	modal damping coefficient
λ_α	adjoint vector
ν	Poisson's ratio
$\xi,\ \xi_\beta$	eigenvalue, β-th eigenvalue
ω	natural frequency
$\Omega,\ \Omega_{\alpha\beta}$	diagonal matrix of system eigenvalues
$\boldsymbol{\sigma}$	stress vector
τ	time variable
ϕ	structural response functional
ρ	mass density
φ	dynamic coefficient
A	cross-sectional area
$\mathbf{b},\ b_a$	vector of design variables
$\mathbf{C}$	constitutive matrix
$\mathrm{Cov}(h_r, h_s)$	cross-covariance matrix of nodal random variables
$\mathbf{D},\ \ D_{\alpha\beta}$	damping matrix

E	Young's modulus
E[·]	expectation operator
E_{p}	potential energy
E_{k}	kinetic energy
$\mathbf{F}$	external force vector
g	constant load
G	structural response function
$\mathbf{h}$, h_r	vector of nodal random variables
$\mathbf{H}(\mathbf{x})$	shape function matrix
$\mathbf{I}$	unit matrix
J_i	moment of inertia
$\mathbf{K}_{\mathrm{L}}$	local stiffness matrix
$\mathbf{K}_{\mathrm{e}}$	element's global stiffness matrix
$\mathbf{K}_{\mathrm{G}}$, $K_{\alpha\beta}$	system global stiffness matrix
$\mathbf{L}$	lower triangular matrix
$\mathcal{L}$	total energy of the system
$\mathbf{M}_{\mathrm{L}}$	local mass matrix
$\mathbf{M}_{\mathrm{e}}$	element's global mass matrix
$\mathbf{M}_{\mathrm{G}}$, $M_{\alpha\beta}$	system global mass matrix
N	total number of degrees of freedom of the system
$\mathbf{q}$	nodal displacements vector in the global coordinate system
$\mathbf{q}_{\mathrm{G}}$, q_α	the whole structure's global displacements vector
$\mathbf{Q}_{\mathrm{L}}$	nodal loading vector in the local coordinate system
$\mathbf{Q}_{\mathrm{e}}$	element's nodal loading vector in the global coordinate system
$\mathbf{Q}_{\mathrm{G}}$, Q_α	the whole structure's nodal loading vector in the global coordinate system
t	time
$\mathbf{T}$	coordinate transformation matrix
$\mathbf{T}(b_a)$	terminal time function
$\mathbf{u}(\mathbf{x}, t)$	displacement vector at point inside a finite element
$\mathbf{u}^*(t)$	vector of nodal displacements in continuum
$\mathbf{U}$	upper triangular matrix
V	capacity
Var(·)	variance function
w_i	wind load
W	external force work
x_i	random variable vector
$\mathbf{y}$, $y_{\alpha\beta}$	eigenvector matrix
$\mathbf{z}$	normal coordinate vector

Chapter 1

Introduction

Contemporary technology and computer studies are developing in an amazing pace. Computers and machines have become the basis of functioning in the world today. Therefore, every new discovery in this area affects other fields of knowledge such as science, industry, medicine, communication, astronautics, etc. Otherwise, for the technology development we would not be at the level of life that we are now. The last 60 years show the real revolution in those fields — the total transition from the huge computing machines taking entire rooms with processing power comparable to modern calculators to super microcomputers, with astonishing floating-point operations per second, memory capacities and small enough to fit in an average person's hand. Owing to that, we can send people to the Moon, quickly diagnose various diseases and find cures for them. It is also possible to conduct complex operations, transport ourselves from one point in the world to another in a matter of hours, or at any time to speak face to face to a person being at any place on the Earth.

This high speed is also noticeable in civil engineering. Designers compete in creating structures, crossing the current barriers of height, span, slenderness, etc. This is reflected in developments of modern programs designed both for creating and calculating selected models. Contemporary building objects are usually complex systems with irregular shapes, various structural material properties and support conditions. All those elements make that the solution for such a complex scheme, becomes impossible from analytical point of view. Therefore, with the development of computational technology, with years of scientific and experimental research, the Finite Element Method (FEM) was formulated. Shortly, it has become the basis of modern numerical tools for structural design, and many others. Dating back to the 1940s, a number of works dealing with this method were written. Some of the first papers that contributed to the development of FEM are [14] and [31]. A rapid advancement of this method took place since the 1970s. Thereafter tens of books concerning this problem were published, [3,4,11,32,37,54,68], for instance.

Since FEM is an approximate method, it requires great knowledge and experience to interpret obtained results. In one of the approaches, it allows to designate the values of internal forces in the system at hand, from computed displacements at characteristic points from external loads. This method challenges for creating a model of selected structures and dividing it into the finite elements. This means that a continuous system is modelled through a set of discretized elements connected to each other by the so-called nodal points, or nodes. That is described in details in [3,54,68], for instance. Depending on the element type, a set of nodal displacements is

appropriately specified. Because civil engineering structures are complex objects, even the simplest ones consist of at least a few finite elements, which makes them, after applying boundary conditions, multi-degree-of-freedom (MDOF) systems. Due to fast improvement in computer technology, analysis of this kind of structures becomes available. In order to compute the system as a whole in the base of generalized coordinates, we need to form the mass and stiffness matrices for the model from corresponding local matrices, which are defined for specific elements. All procedures necessary to carry out this process can be found in [3,68].

Today's constructors dream is to develop a way for optimal designing, that is find the best design point between the considered basic aspects, related to adopted object functions — maximum permissible load, allowable displacements, execution time, etc. Contemporary tender procedures additionally require to achieve the lowest cost of the whole design. Among these factors, the most important aspect — the safety of future users of the object, must not be ignored. There are many papers about this issue, [5,6,12,50,51], for instance.

One of conditions of optimal designing is to create a model which most appropriately describes the reality. It is equivalent to that, all factors that influence the system's work, for example the finite element setting, the external loads, etc., must be chosen and entered to the analysis in a correct way. It is of great significance for both, making new structures and renovating the old ones. Technological developments have a great impact on improvement in communication. When drawing blueprints of bridges and viaducts, which were built in the past centuries, only "simplified" calculations of loads were considered. Therefore, many of them as historic building, often require adjusting to contemporary conditions. This involves designing special strengthening elements, which impose the need for precise computations.

Not only validity of the adopted static scheme and finite element setting is the condition of creating a model which best reflects the reality. The most appropriate inclusion of any factors that affect the system has the great importance in this issue. It is commonly known that the dead load of the specified structural elements may easily be computed by taking into account their cross-sectional areas and the characteristics of used materials. Support in including the proper type and values of external loads, and entering them during data processing, are the rules in civil engineering [69,70,71] etc.

Due to the change of time, most modern structures, are exposed to dynamic factors, which results that each point in the system experiences the time-dependent displacements under their influence. When we create a model of a structure located in real world, there are many factors that affect the system, which should be taken into account. Except the dynamic load there are some elements that have an influence on the object, for example — contact between various materials, connections between components, resistance to motion, hydrodynamics, aerodynamics, thermal effects, etc., that causes the gradual disappearance of the vibration in time. The above-mentioned factors contribute to the damping effect. When this effect is omitted in the dynamic analysis, the amplitude of vibration under the constant impulse in time, should be unchangeable, however in practise this kind of situation can not occur. For the systems with one degree of freedom, the damping is widely discussed in world literature, for instance [13,55,57]. There are some models of this effect, for example viscous, hysteretic and coulomb damping, that can be successfully applied in this type of system. But it is impossible to use them for describing the damping in complex structures, with many degrees of freedom, due to the fact that this problem is very difficult to be solved. For that reason, in our numerical examples we choose the Rayleigh's damping, because it turns out that this model presents this phenomenon

more appropriately in complex systems computed by FEM. The Rayleigh's damping matrix is treated as linear combination of stiffness and mass terms, multiplied by coefficients obtained in experimental way, (cf. [3,57]).

Recently, there is a tendency to create slim and slender forms, which give the impression as if they were built opposing the nature's laws. They are the results of striving to overcome the existing constraints. That leads to the formation of a structure group, which is highly vulnerable to any changes in loads as well as in design parameters. It is known that larger value of cross-sectional areas or structural members is advantageous for the load capacity of the considered object in terms of statics. However it may in several cases contribute to increasing the amplitude of vibration, which consequently can cause the damage of the system. One of the most important questions in the designing is that how the variation of design parameters affect the change of the system response. Sensitivity analysis gives the answer to that, cf. [9,28,12,15,16,23,48,49].

The sensitivity problem for deterministic systems have been discussed extensively in the literature [23,]. There exist various approaches and methodologies. In this type of analysis, we are going to find the sensitivity gradient, which is defined by the changes of the structural response with respect to the design parameters. As the structural response, the displacements, stresses, buckling loads or natural frequencies may be considered, while the elements cross-sectional areas, the plate thickness, the Young modulus or mass destiny can be treated as design variables.

Stochastic analysis [1,20,26,30,60,35,40] includes randomness of structural parameters (geometrical dimensions of the elements, material properties) or external factors (loads, support conditions). In the context of research of existing objects it turned out that even small uncertainties in the above mentioned factors have a significant influence to load capacity of the system. For this reason, in case of a complex structure, changes in the entire model are involved. Due to the spatially distribution of the uncertainties over the structural system, which is required to be modelled as random fields and complexity of the scheme, this problems must be considered by numerical methods, because analytical analysis is impossible.

We can distinguish three basic trends in determining the values of structural response that were discussed in international papers and publications. The first involves perturbation approach and includes description of linear dependence between the reaction and the random variables using the Taylor series with retaining terms up to second order [22,40,42]. The second way is called Monte Carlo simulation and was created by Gauss. It is a statistical method consisting in random selection of the variables according to pre-assumed probability distribution. The numbers are then used for appointing set of random numbers on the basis of the reactions' equation, in order to verify the type of uncertainty. Accuracy of the results is directly dependent on the number of attempts [36,18]. The third trend is Neumanns' expansion [30,43], rarely used in structures' analysis unless it is combined with Monte-Carlo Simulation.

Considering current trends in design, requirements for modern objects and loads which this complex structures are exposed to, an insightful analysis of combined issues of sensitivity and stochastics seems to be necessary [34,35,53,58], which is currently rare occurred. Therefore the main goal of the paper is numerical nonstatistical analysis of statics, dynamics and sensitivity for the complex systems with deterministic and random parameters. In stochastic computations we are basing on the second-order version of methodology using the perturbation approach, that is described above. This is a version of FEM, that includes the randomness in geometry and material properties, the same as in adopted load.

The Second chapter is devoted to the deterministic models. In first sections, we obtained the set of equations of motion for the complex structures with many degrees of freedom, using the set of Lagrange's equations of the second type and the formula for the total energy of the system. In section 2.3, the specific finite elements are presented, with description of possible displacements and corresponding internal forces and additionally with stiffness matrix formulation. Then, there is shown a detailed description of receiving the modal damping coefficient, from Rayleigh damping matrix by the mode superposition method, and its entering to the program during data processing. In section 2.5 the static and dynamic sensitivity of the system with respect to the change of the design parameters is presented. In this analysis the displacements, buckling loads, stresses or natural frequencies in particular nodes may be considered as measures of the structural response, while the cross-section areas of main elements, Young Modulus and mass density may be treated as design variables.

In the third chapter the models in terms of uncertainties in design parameters are prescribed. The scope of the previous sections is to formulate the hierarchical set of equations of motion and equilibrium using the stochastic version of Lagrange's equation of the second type and mean-point second-order perturbation method. Based on the first two probabilistic moments of design random variables, the first to probabilistic moments of static and dynamic response and their sensitivity will be received. It allows to obtain the deterministic results of time-dependent and time-independent structural response and their sensitivities, with the solution accuracy in the form of the mean values and their cross-covariances.

A valuable part of this doctoral dissertation is the illustration of the theoretical considerations in practical examples. During the research, in graphical and computational programme, the models of selected structures inspired by real objects are created. First we enter the FEM setting, support conditions, characteristics of particular elements and designated external loads, then the static, dynamic and sensitivity analysis for the deterministic and stochastic systems with many degrees of freedom is made. Obtained results are summarized in tables and presented in graphs.

Thorough deterministic analysis is made on the basis of a model of suspended bridge, created according to a real object, named Seri Wawasan Bridge, located in Putrajaya, Malaysia [72]. For this example the static, dynamic and sensitivity analysis is made. The geometry characteristics of structural member are adopted in simplified form. During the load cases determining, the dynamic effects on the bridge are intentionally omitted. Dynamic analysis is made from a constant impulse put at the top of the pylon. The courses of vibration of selected nodes show periodical changes of the amplitudes, which is called beat effect. From the point of view of material fatigue, it may be treated as a disadvantageous phenomenon. Therefore, an attempt to eliminate this phenomenon by using the damping and added mass, is made. The design sensitivity response of displacements in selected nodes with respect to the cross-sectional areas of particular elements, allows to find the most vulnerable point in the structure.

The last section of third chapter presents the numerical computations of statics, dynamics and sensitivity of bar dome with deterministic and random parameters. After the studies, the results obtained for truss and beam models are compared. The influence of the model division into the beam elements to the precision of the received displacements and internal forces, is examined. In Section 3.6, the programs to generating the nodes' coordinates and procedures for determining the covariances matrices, are shown. Due to the symmetry of the system, the beat effect is observed and an attempt to its elimination is made. In dynamic analysis the influence of time

step choosing to the accuracy of yielding results, is written. The problem of time-dependent computations for the models with repeatable values of natural frequencies is prescribed. In this part, we present the impact of the static and dynamic sensitivity analysis results on the view of structures work.

The guiding goal of this paper is to create a new computer tool, which combines the possibility of making the sensitivity analysis for complex structures with many degrees of freedom with using the deterministic and random parameters. It can have an important meaning in practical designing of the building objects and significantly improve this process. Main scope is to optimize the so-called design point for the real system consisting of many elements, which have not been carried out, yet.

Chapter 2

Deterministic Systems

2.1 Set of Lagrange's Equation of the Second Type

The scope of this section is to formulate the equation of motion by using the expression for total energy of the system, as the terms for kinetic and potential energy and external force work. During analysis, the system is first discretized into a finite element mesh, then the nodal displacements are computed and, consequently, the internal forces are obtained.

Let us consider $\mathbf{u}(\mathbf{x}) = \{u_1, u_2, u_3\}$ as the displacement vector at a arbitrary point inside the finite element, described in the local coordinate system. If $\mathbf{x} = \{x_1, x_2, x_3\}$ and $\mathbf{H}(\mathbf{x})$ are assumed as the coordinate vector and the shape function matrix, respectively, the equation for $\mathbf{u}(\mathbf{x})$ can be approximated in the form

$$\mathbf{u}(\mathbf{x}) = \mathbf{H}(\mathbf{x})\,\mathbf{u}^* \tag{2.1}$$

with $\mathbf{u}^* = \{u_1^*, u_2^*, u_3^*, ..., u_k^*\}$ being the element vector of nodal displacements, described in local coordinate system.

It is known that the strain vector can be expressed as the first derivatives of $\mathbf{u}(\mathbf{x})$ with respect to $\mathbf{x}$. The strain vector, $\boldsymbol{\varepsilon} = \{\varepsilon_x, \varepsilon_y, \varepsilon_z, \sqrt{2}\varepsilon_{xy}, \sqrt{2}\varepsilon_{yz}, \sqrt{2}\varepsilon_{zx}\}$ reads

$$\boldsymbol{\varepsilon}(\mathbf{x}) = \frac{\mathrm{d}\mathbf{u}(\mathbf{x})}{\mathrm{d}\mathbf{x}} = \mathbf{B}(\mathbf{x})\,\mathbf{u}^* \tag{2.2}$$

where the derivative of shape function matrix with respect to the local coordinates' vector is written symbolically as

$$\mathbf{B}(\mathbf{x}) = \frac{\mathrm{d}\mathbf{H}(\mathbf{x})}{\mathrm{d}\mathbf{x}} \tag{2.3}$$

The stress vector $\boldsymbol{\sigma} = \{\sigma_x, \sigma_y, \sigma_z, \sqrt{2}\sigma_{xy}, \sqrt{2}\sigma_{yz}, \sqrt{2}\sigma_{zx}\}$, in accordance with the generalized Hooke's law, can be expressed as the product of the strain vector and an elastic constitutive matrix $\mathbf{C}$, i.e.

$$\boldsymbol{\sigma} = \mathbf{C}\varepsilon = \mathbf{C}\mathbf{B}(\mathbf{x})\mathbf{u}^* \tag{2.4}$$

Specific entries of the constitutive matrix are described through via on the basis of the characteristics of the structural material, such as the Young's Modulus E and the Poisson's ratio ν.

This matrix is determined for each finite element of the system. The general forms of **C** are given in [3,68], for instance.

If we assume $\mathbf{u}(\mathbf{x}, t)$ is the time-dependent displacement vector of any point inside the element, the Eq.(2.1) is rewritten in the form

$$\mathbf{u}(\mathbf{x}, t) = \mathbf{H}(\mathbf{x})\, \mathbf{u}^*(t) \tag{2.5}$$

Implying the first and second derivatives of $\mathbf{u}(\mathbf{x}, t)$ with respect to time, respectively as

$$\begin{aligned} \dot{\mathbf{u}}(\mathbf{x}, t) &= \mathbf{H}(\mathbf{x})\, \dot{\mathbf{u}}^*(t), \\ \ddot{\mathbf{u}}(\mathbf{x}, t) &= \mathbf{H}(\mathbf{x})\, \ddot{\mathbf{u}}^*(t), \end{aligned} \tag{2.6}$$

Each of the finite elements in the mesh, which is described in its local system, has to be now transformed into a global coordinate system. That is, Fig. 2.1.

$$\mathbf{u}^* = \mathbf{T}\, \mathbf{q}_\mathrm{e} \tag{2.7}$$

with $\mathbf{T}$ and $\mathbf{q}_\mathrm{e}$ being the transformation matrix, containing directional cosine entries, and the nodal displacement vector of the element in the global coordinate system. For example, in the two-dimensional (2D) case we have, Fig.2.1.

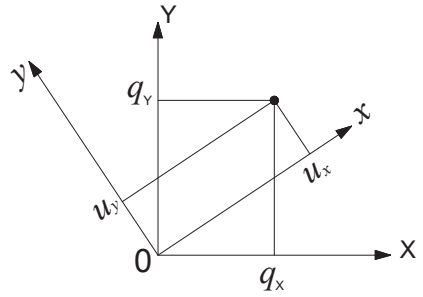

Figure 2.1 Local and global coordinate systems

That is written in matrix notation as, cf. Eq. (2.7)

$$\begin{bmatrix} u_x \\ u_y \end{bmatrix} = \begin{bmatrix} \cos(x, X) & \cos(x, Y) \\ \cos(y, X) & \cos(y, Y) \end{bmatrix} \begin{bmatrix} q_X \\ q_Y \end{bmatrix} \tag{2.8}$$

Generally, for a 3D coordinate system the transformation matrix is given as

$$\mathbf{T} = \begin{bmatrix} \cos(x, X) & \cos(x, Y) & \cos(x, Z) \\ \cos(y, X) & \cos(y, Y) & \cos(y, Z) \\ \cos(z, X) & \cos(z, Y) & \cos(z, Z) \end{bmatrix} \tag{2.9}$$

Substituting Eq. (2.7) into Eq. (2.1) yields

$$\mathbf{u}(\mathbf{x}) = \mathbf{H}(\mathbf{x})\, \mathbf{T}\, \mathbf{q}_\mathrm{e} \tag{2.10}$$

Using the transformation matrix, the equations for stress and strain have the form

$$\boldsymbol{\varepsilon} = \mathbf{B}(\mathbf{x})\mathbf{T}\mathbf{q}_\mathrm{e} \tag{2.11}$$

and

$$\boldsymbol{\sigma} = \mathbf{C}\mathbf{B}(\mathbf{x})\mathbf{T}\mathbf{q}_\mathrm{e} \tag{2.12}$$

The vector of time-dependent displacements and its first two derivatives with respect to time, including the Eq. (2.7), read

$$\begin{aligned}\mathbf{u}(\mathbf{x},t) &= \mathbf{H}(\mathbf{x})\,\mathbf{T}\,\mathbf{q}_{\mathrm{e}}(t)\\ \dot{\mathbf{u}}(\mathbf{x},t) &= \mathbf{H}(\mathbf{x})\mathbf{T}\dot{\mathbf{q}}_{\mathrm{e}}(t)\\ \ddot{\mathbf{u}}(\mathbf{x},t) &= \mathbf{H}(\mathbf{x})\mathbf{T}\ddot{\mathbf{q}}_{\mathrm{e}}(t)\end{aligned} \tag{2.13}$$

The goal of the section is to formulate the equation of motion in the deterministic terms on. Hence, the total energy of the system is adopted in the form

$$\mathcal{L} = E_{\mathrm{k}} - E_{\mathrm{p}} + W \tag{2.14}$$

where E_{k} and E_{p} are kinetic and potential energy of the system, respectively, while W the external force work. If $\mathbf{q}$ denotes the generalized coordinates' vector, the set of Lagrange's equation of the second type can be written out as

$$\frac{\partial \mathcal{L}}{\partial \mathbf{q}} - \frac{\mathrm{d}}{\mathrm{d}t}\left(\frac{\partial \mathcal{L}}{\partial \dot{\mathbf{q}}}\right) = 0 \tag{2.15}$$

To obtain the equation of motion using Eq. (2.15), the specific terms of Eq. (2.14) are needed explicitly, and presented in the next section. The derivations of the mentioned equations in details can be found in [63].

2.2 Equations of Motion and Equilibrium

2.2.1 Potential Energy

Potential energy for a linear elastic system can be expressed via its elastic deformation energy. Therefore E_{p} is determined as an integral for capacity from stress and strain product, i.e.

$$E_{\mathrm{p}} = \int_V \frac{1}{2}\boldsymbol{\sigma}^{\mathrm{T}}\boldsymbol{\varepsilon}\,\mathrm{d}V \tag{2.16}$$

Substituting Eqs. (2.2) and (2.4) into Eq. (2.16) and using the advantage of matrices transposing laws (compare [63]) , potential energy of the considered element is obtained in the form

$$E_{\mathrm{pe}} = \frac{1}{2}\mathbf{u}^{*\mathrm{T}}\mathbf{K}_{\mathrm{L}}\mathbf{u}^{*} \tag{2.17}$$

with $\mathbf{K}_{\mathrm{L}}$, being the element stiffness matrix, described in the local coordinate system and expressed by the equation

$$\mathbf{K}_{\mathrm{L}} = \int_V \mathbf{B}^{\mathrm{T}}\mathbf{C}\mathbf{B}\,\mathrm{d}V \tag{2.18}$$

leading to the element stiffness matrix

$$\mathbf{K}_{\mathrm{e}} = \mathbf{T}^{\mathrm{T}}\mathbf{K}_{\mathrm{L}}\,\mathbf{T} \tag{2.19}$$

and the element potential energy for the global system as

$$E^{*}_{\mathrm{pe}} = \frac{1}{2}\mathbf{q}_{\mathrm{e}}^{\mathrm{T}}\mathbf{K}_{\mathrm{e}}\mathbf{q}_{\mathrm{e}} \tag{2.20}$$

Aggregating the global stiffness matrix for the whole system from the local element stiffness matrices, according to the equation

$$\mathbf{K}_{\mathrm{G}} = \sum_{\mathrm{e}} \mathbf{K}_{\mathrm{e}} \tag{2.21}$$

and including boundary conditions, we receive symmetric and positive definite system matrix $\mathbf{K}_{\mathrm{G}}$. Denoting by N the total number of the system degrees of freedom (DOF), the dimension of $\mathbf{K}_{\mathrm{G}}$ is NxN. The potential energy of the system is consequently given by

$$E_{\mathrm{p}} = \frac{1}{2}\mathbf{q}^{\mathrm{T}}\mathbf{K}_{\mathrm{G}}\mathbf{q} \tag{2.22}$$

2.2.2 Kinetic Energy

If ρ is denoted as the mass density, kinetic energy E_{k}, which is dependent on the velocity of a point, can be expressed by the equation

$$E_{\mathrm{k}} = \int_V \frac{1}{2}\rho\, \dot{\mathbf{u}}^{\mathrm{T}}\dot{\mathbf{u}}\, \mathrm{d}V \tag{2.23}$$

Let us consider the element's mass matrix in a local coordinate system as

$$\mathbf{M}_{\mathrm{L}} = \int_V \rho\, \mathbf{H}^{\mathrm{T}}\mathbf{H}\, \mathrm{d}V \tag{2.24}$$

Using Eqs. $(2.6)_1$, and including matrices transposing laws, Eq. (2.23) is rewritten to

$$E_{\mathrm{ke}} = \frac{1}{2}\, \dot{\mathbf{u}}^{*\mathrm{T}}\mathbf{M}_{\mathrm{L}}\, \dot{\mathbf{u}}^{*} \tag{2.25}$$

with E_{ke} being the element kinetic energy. Transposing it to the global coordinate system leads to

$$E^{*}_{\mathrm{ke}} = \frac{1}{2}\dot{\mathbf{q}}_{\mathrm{e}}^{\mathrm{T}}\mathbf{M}_{\mathrm{e}}\, \dot{\mathbf{q}}_{\mathrm{e}} \tag{2.26}$$

where $\mathbf{M}_{\mathrm{e}}$ is the element global mass matrix, expressed by the equation

$$\mathbf{M}_{\mathrm{e}} = \mathbf{T}^{\mathrm{T}}\mathbf{M}_{\mathrm{L}}\mathbf{T} \tag{2.27}$$

The global mass matrix of the whole structure $\mathbf{M}_{\mathrm{G}}$ is the sum of mass matrices of the specific elements, therefore the kinetic energy of the system is equal

$$E_{\mathrm{k}} = \frac{1}{2}\dot{\mathbf{q}}^{\mathrm{T}}\mathbf{M}_{\mathrm{G}}\, \dot{\mathbf{q}} \tag{2.28}$$

2.2.3 External Force Work

Let us consider work done by the external force vector $\mathbf{F}$ on the displacement vector $\mathbf{u}$ in the form

$$W = \int_V \mathbf{u}^{\mathrm{T}}\mathbf{F}\, \mathrm{d}V \tag{2.29}$$

Assuming the vector of nodal loads written in the local coordinate system, i.e.

$$\mathbf{Q}_{\mathrm{L}} = \int_V \mathbf{H}^{\mathrm{T}}\mathbf{F}\,\mathrm{d}V \tag{2.30}$$

and using Eq. (2.1), the work for an element is determined by

$$W_{\mathrm{e}} = \mathbf{u}^{*\mathrm{T}}\mathbf{Q}_{\mathrm{L}} \tag{2.31}$$

Transforming Eq. (2.31) into the global coordinate system results in

$$W_{\mathrm{e}}^{*} = \mathbf{q}_{\mathrm{e}}^{\mathrm{T}}\mathbf{Q}_{\mathrm{e}} \tag{2.32}$$

where

$$\mathbf{Q}_{\mathrm{e}} = \mathbf{T}^{\mathrm{T}}\mathbf{Q}_{\mathrm{L}} \tag{2.33}$$

denotes the element vector of the global nodal loads. The whole structure work is expressed by the equation

$$W = \mathbf{q}^{\mathrm{T}}\mathbf{Q}_{\mathrm{G}} \tag{2.34}$$

with $\mathbf{q}$ and $\mathbf{Q}_{\mathrm{G}}$ being the vectors of generalized coordinates and nodal loads, respectively.

2.2.4 FEM Equations of Motion

So far, the terms of potential and kinetic energy and external force work in matrix form were determined, using the vectors of generalized coordinates — $\mathbf{q}$, nodal loads — $\mathbf{Q}_{\mathrm{G}}$, and the matrices of stiffness — $\mathbf{K}_{\mathrm{G}}$ and mass — $\mathbf{M}_{\mathrm{G}}$. Substituting Eqs. (2.22), (2.28) and (2.34) into Eq. (2.14) leads to the total energy of the system

$$\mathcal{L} = \frac{1}{2}\dot{\mathbf{q}}^{\mathrm{T}}\mathbf{M}_{\mathrm{G}}\dot{\mathbf{q}} - \frac{1}{2}\mathbf{q}^{\mathrm{T}}\mathbf{K}_{\mathrm{G}}\mathbf{q} + \mathbf{q}^{\mathrm{T}}\mathbf{Q}_{\mathrm{G}} \tag{2.35}$$

Partial derivatives of $\mathcal{L}$ with respect to $\mathbf{q}$ and $\dot{\mathbf{q}}$ and taking the advantage of matrices $\mathbf{K}_{\mathrm{G}}$ and $\mathbf{M}_{\mathrm{G}}$ symmetry, can be expressed respectively

$$\frac{\partial \mathcal{L}}{\partial \mathbf{q}} = -\mathbf{K}_{\mathrm{G}}\mathbf{q} + \mathbf{Q}_{\mathrm{G}} \tag{2.36}$$

and

$$\frac{\partial \mathcal{L}}{\partial \dot{\mathbf{q}}} = \mathbf{M}_{\mathrm{G}}\dot{\mathbf{q}} \tag{2.37}$$

Differentiation Eq. (2.37) with respect to time t, yields

$$\frac{\mathrm{d}}{\mathrm{d}t}\left(\frac{\partial \mathcal{L}}{\partial \dot{\mathbf{q}}}\right) = \mathbf{M}_{\mathrm{G}}\ddot{\mathbf{q}} \tag{2.38}$$

Including Eqs. (2.36) and (2.38) into Eq. (2.15) and after summing up, the set of the equations of motion for the whole system is received

$$\mathbf{M}_{\mathrm{G}}\ddot{\mathbf{q}} + \mathbf{K}_{\mathrm{G}}\mathbf{q} = \mathbf{Q}_{\mathrm{G}} \tag{2.39}$$

Entering the damping effects into the analysis with **D** being the damping matrix, Eq. (2.39) takes form

$$\mathbf{M}_{\mathrm{G}}\ddot{\mathbf{q}} + \mathbf{D}\dot{\mathbf{q}} + \mathbf{K}_{\mathrm{G}}\mathbf{q} = \mathbf{Q}_{\mathrm{G}}(t) \tag{2.40}$$

For the complex structures with many degrees of freedom (MDOF), it can not be used the same model of damping as for the systems with one DOF. Therefore, during the analysis of complex systems, the Rayleigh's damping matrix is taken into account, which is assumed as a linear combination of mass and stiffness terms

$$\mathbf{D} = \alpha\mathbf{M} + \beta\mathbf{K} \tag{2.41}$$

with α and β being the coefficients obtained in an experimental way. More information about complying the damping effects in data processing is presented in section 2.4.

2.2.5 Equilibrium Equations

Statics may be treated as the special case of the dynamics, where the inertial and damping effects are neglected because of time-independent vector of generalized coordinated. According to that the set of equations of motion, describing the equilibrium of the whole system, is rewritten in matrix recording as

$$\mathbf{K}_{\mathrm{G}}\mathbf{q} - \mathbf{Q}_{\mathrm{G}} = 0 \tag{2.42}$$

Multiplying Eq. (2.40) by the inverse of stiffness matrix leads to obtaining an unknown vector of generalized coordinates

$$\mathbf{q} = \mathbf{K}_{\mathrm{G}}^{-1}\mathbf{Q}_{\mathrm{G}} \tag{2.43}$$

with N being the total number degrees of freedom. The specific terms in Eq. (2.40) have the following dimensions: $N \times N$ for the stiffness matrix $\mathbf{K}_{\mathrm{G}}$ and $N \times 1$ for the both vectors of the generalized (nodal) coordinates $\mathbf{q}$ and external loading $\mathbf{Q}_{\mathrm{G}}$.

2.3 Finite Elements

2.3.1 Truss Element

Let us consider a 2D truss element presented in Fig.(2.2.), where only axial forces are taken into account.

The displacement $\mathbf{u}(x)$ at any point inside the element is adopted as

$$u_x(x) = \alpha_1 + \alpha_2 x \tag{2.44}$$

or, in matrix notation, as

$$u_x(x) = \begin{bmatrix} 1 & x \end{bmatrix} \begin{bmatrix} \alpha_1 \\ \alpha_2 \end{bmatrix} \tag{2.45}$$

Using Eq. (2.44) we can write the values of the nodal displacements as

$$\begin{aligned} u_x^i &= u(0) = \alpha_1 \\ u_x^j &= u(L) = \alpha_1 + L\alpha_2 \end{aligned}$$

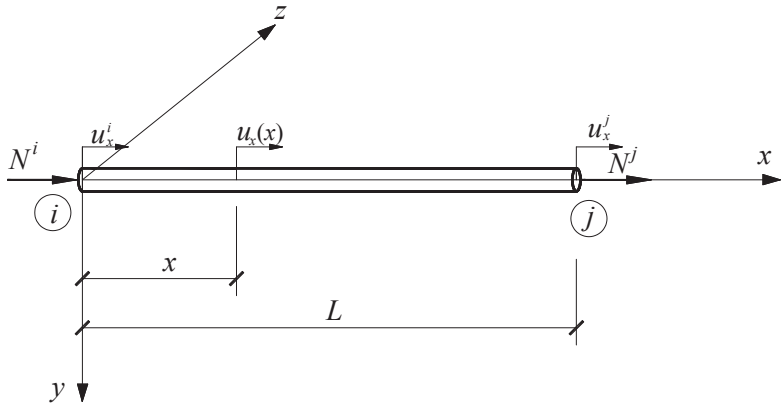

Figure 2.2 2D truss element

That is

$$\begin{bmatrix} u_x^i \\ u_x^j \end{bmatrix} = \begin{bmatrix} 1 & 0 \\ 0 & L \end{bmatrix} \begin{bmatrix} \alpha_1 \\ \alpha_2 \end{bmatrix} \tag{2.46}$$

or, in the concise form

$$\mathbf{u}^* = \mathbf{A}\boldsymbol{\alpha} \tag{2.47}$$

and solved for $\boldsymbol{\alpha}$, yields

$$\boldsymbol{\alpha} = \mathbf{A}^{-1}\mathbf{u}^* \tag{2.48}$$

Using Eq. (2.46), the above equation takes the form

$$\begin{bmatrix} \alpha_1 \\ \alpha_2 \end{bmatrix} = \frac{1}{L} \begin{bmatrix} L & 0 \\ -1 & 1 \end{bmatrix} \begin{bmatrix} u_x^i \\ u_x^j \end{bmatrix} \tag{2.49}$$

Substituting Eq. (2.49) into Eq. (2.45) we get

$$u_x(x) = \mathbf{H}(\mathbf{x})\ \mathbf{u}^* \tag{2.50}$$

where

$$\mathbf{H}(\mathbf{x}) = \begin{bmatrix} 1 & x \end{bmatrix} \frac{1}{L} \begin{bmatrix} L & 0 \\ -1 & 1 \end{bmatrix} \tag{2.51}$$

is the shape function matrix for the element, while the matrix $\mathbf{B}(\mathbf{x})$ being the first derivative $\mathbf{H}(\mathbf{x})$ with respect to $\mathbf{x}$, is equal to, cf. Eq. (2.3)

$$\mathbf{B}(\mathbf{x}) = \begin{bmatrix} 0 & 1 \end{bmatrix} \frac{1}{L} \begin{bmatrix} L & 0 \\ -1 & 1 \end{bmatrix} = \frac{1}{L} \begin{bmatrix} -1 & 1 \end{bmatrix} \tag{2.52}$$

Using Eq. (2.4), the expression for the stress vector can now be written as

$$\boldsymbol{\sigma} = E \frac{1}{L} \begin{bmatrix} -1 & 1 \end{bmatrix} \begin{bmatrix} u_x^i \\ u_x^j \end{bmatrix} \tag{2.53}$$

For the truss element with constant cross-sectional area A, Eq. (2.18) can be rewritten as

$$\mathbf{K}_{\mathrm{L}} = \mathbf{B}^{\mathrm{T}}\mathbf{C}\mathbf{B}AL \tag{2.54}$$

Using Eqs. (2.52) and $\mathbf{C} = E$, Eq. (2.54) for the local stiffness matrix for the 2D truss element is expressed as

$$\mathbf{K}_{\mathrm{L}} = \frac{1}{L}\begin{bmatrix} -1 \\ 1 \end{bmatrix} E \frac{1}{L}\begin{bmatrix} -1 & 1 \end{bmatrix} AL = \frac{AE}{L}\begin{bmatrix} 1 & -1 \\ -1 & 1 \end{bmatrix} \tag{2.55}$$

In the three-dimensional (3D) truss element we are consider three translational displacements, and corresponding them internal forces that are presented in Fig. 2.3.

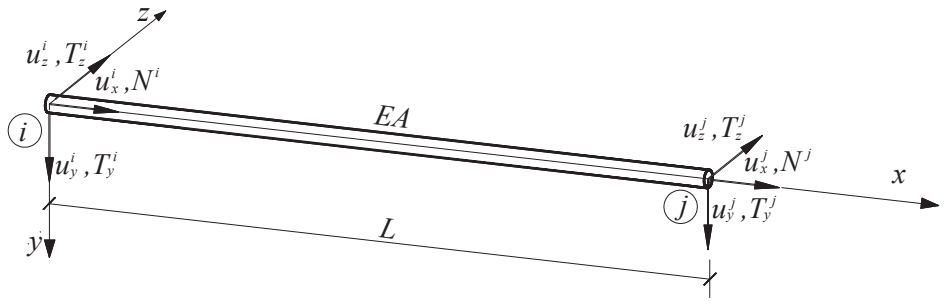

Figure 2.3 3D truss element in the local coordinate system

Consequently, to the 2D truss element, the stiffness matrix for a 3D one, according to Fig. 2.3. is developed as

$$\frac{AE}{L}\begin{bmatrix} 1 & 0 & 0 & -1 & 0 & 0 \\ & 0 & 0 & 0 & 0 & 0 \\ & & 0 & 0 & 0 & 0 \\ & & & 1 & 0 & 0 \\ & & \text{symm.} & & 0 & 0 \\ & & & & & 0 \end{bmatrix} \begin{bmatrix} u_x^i \\ u_y^i \\ u_z^i \\ u_x^j \\ u_y^j \\ u_z^j \end{bmatrix} = \begin{bmatrix} N^i \\ 0 \\ 0 \\ N^j \\ 0 \\ 0 \end{bmatrix} \tag{2.56}$$

or, in matrix notation, as

$$\mathbf{K}_{\mathrm{L}}\mathbf{u}^* = \mathbf{Q}_{\mathrm{L}} \tag{2.57}$$

where $\mathbf{K}_{\mathrm{L}}$ and $\mathbf{Q}_{\mathrm{L}}$ are the stiffness matrix and nodal load vector described in the local coordinate system.

2.3.2 Beam Element

The 2D beam element can be formulated by the superposition of the truss and bending-only-beam elements. First, we designate the local stiffness matrix for the z-bending element, Fig. 2.4, then we add the previously appointed matrix for the 2D truss element, cf. Eq. (2.56).
The vertical displacement at any point inside the element is assumed as

$$u_y(x) = \alpha_1 + \alpha_2 x + \alpha_3 x^2 + \alpha_4 x^3 \tag{2.58}$$

or, in matrix notation, as

$$u_y(x) = \begin{bmatrix} 1 & x & x^2 & x^3 \end{bmatrix} \begin{bmatrix} \alpha_1 \\ \alpha_2 \\ \alpha_3 \\ \alpha_4 \end{bmatrix} \tag{2.59}$$

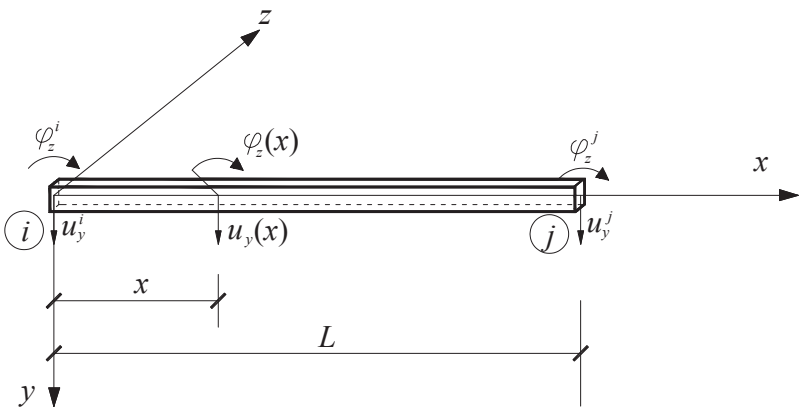

Figure 2.4 Local displacements in z-bending element

The slope at the point is defined as the first derivative of the displacement $u_y(x)$ with respect to x as

$$\varphi_z = \frac{\mathrm{d}u_y(x)}{\mathrm{d}x} = \alpha_2 + 2\alpha_3 x + 3\alpha_4 x^2 \tag{2.60}$$

Approving the boundary conditions with accordance to the Fig. 2.4, we have

$$\begin{aligned}
u_y^i &= u_y(0) = \alpha_1, \\
\varphi_z^i &= \left.\frac{\mathrm{d}u_y}{\mathrm{d}x}\right|_{x=0} = \alpha_2, \\
u_y^j &= u_y(L) = \alpha_1 + L\alpha_2 + L^2\alpha_3 + L^3\alpha_4, \\
\varphi_z^j &= \left.\frac{\mathrm{d}u_y}{\mathrm{d}x}\right|_{x=L} = \alpha_2 + 2L\alpha_3 + 3L^2\alpha_4
\end{aligned}$$

or, in matrix notation

$$\mathbf{u}^* = \mathbf{A}\boldsymbol{\alpha} = \begin{bmatrix} 1 & 0 & 0 & 0 \\ 0 & 1 & 0 & 0 \\ 1 & L & L^2 & L^3 \\ 0 & 1 & 2L & 3L^2 \end{bmatrix} \begin{bmatrix} \alpha_1 \\ \alpha_2 \\ \alpha_3 \\ \alpha_4 \end{bmatrix} \tag{2.61}$$

These equations are solved for $\boldsymbol{\alpha}$ to get

$$\boldsymbol{\alpha} = \mathbf{A}^{-1}\mathrm{u}^* = \begin{bmatrix} 1 & 0 & 0 & 0 \\ 0 & 1 & 0 & 0 \\ -\frac{3}{L^2} & -\frac{2}{L} & \frac{3}{L^2} & -\frac{1}{L} \\ \frac{2}{L^3} & \frac{1}{L^2} & -\frac{2}{L^3} & \frac{1}{L^2} \end{bmatrix} \begin{bmatrix} u_y^i \\ \varphi_z^i \\ u_y^j \\ \varphi_z^j \end{bmatrix} \tag{2.62}$$

that, substituted into Eq. (2.61), leads to the shape function matrix for the bending element of the form

$$u_y(x) = \begin{bmatrix} 1 & x & x^2 & x^3 \end{bmatrix} \begin{bmatrix} 1 & 0 & 0 & 0 \\ 0 & 1 & 0 & 0 \\ -\frac{3}{L^2} & -\frac{2}{L} & \frac{3}{L^2} & -\frac{1}{L} \\ \frac{2}{L^3} & \frac{1}{L^2} & -\frac{2}{L^3} & \frac{1}{L^2} \end{bmatrix} \begin{bmatrix} u_y^i \\ \varphi_z^i \\ u_y^j \\ \varphi_z^j \end{bmatrix} = \mathbf{H}(x)\mathbf{u}^* \tag{2.63}$$

We treat the vector of nodal forces by means of the local stiffness matrix and the nodal displacement vector as

$$\mathbf{Q}_{\mathrm{L}} = \left\{ \begin{array}{cccc} T_y^i & M_z^i & T_y^j & M_z^j \end{array} \right\} \tag{2.64}$$

Notations of the nodal forces presented in Eq.(2.65) are assumed on the basis on Fig. 2.5.

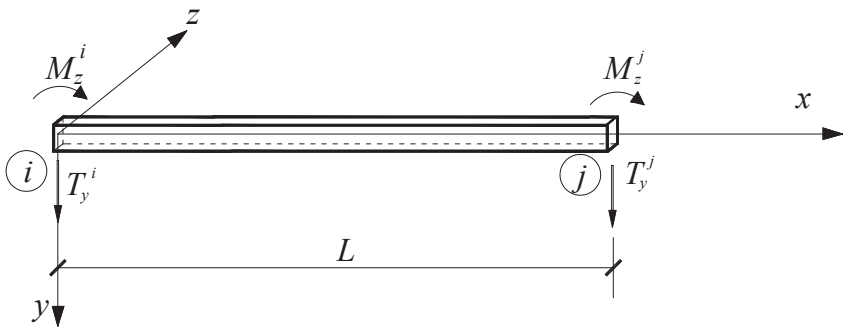

Figure 2.5 Nodal forces in z-bending element

Applying the Euler's equation and differential relationship between external forces and displacements, the equations for bending moments and shear forces of the z-bending element are received as

$$M_z(x) = -EJ_z \frac{\mathrm{d}^2 u_y(x)}{\mathrm{d}x^2} \tag{2.65}$$

and

$$T_y(\mathrm{x}) = \frac{\mathrm{d}M_z(x)}{\mathrm{d}x} = -EJ_z \frac{\mathrm{d}^3 u_y(x)}{\mathrm{d}x^3} \tag{2.66}$$

where J_z is the moment of inertia of the element's cross-section. The first, second and third derivatives of the displacement $u_y(x)$ with respect to x, are expressed respectively, by

$$\begin{aligned} \frac{\mathrm{d}u_y(x)}{\mathrm{d}x} &= \left[\begin{array}{cccc} 0 & 1 & 2x & 3x^2 \end{array} \right] \mathbf{A}^{-1}\mathbf{u}^* \\ \frac{\mathrm{d}^2 u_y(x)}{\mathrm{d}x^2} &= \left[\begin{array}{cccc} 0 & 0 & 2 & 6x \end{array} \right] \mathbf{A}^{-1}\mathbf{u}^* \\ \frac{\mathrm{d}^3 u_y(x)}{\mathrm{d}x^3} &= \left[\begin{array}{cccc} 0 & 0 & 0 & 6 \end{array} \right] \mathbf{A}^{-1}\mathbf{u}^* \end{aligned} \tag{2.67}$$

Using boundary conditions, the values of nodal forces for the bending element are obtained in the form

$$\begin{aligned}
M_z^i = -EJ_z \left.\frac{\mathrm{d}^2 u_y(x)}{\mathrm{d}x^2}\right|_{x=0} &= -EJ_z \begin{bmatrix} 0 & 0 & 2 & 0 \end{bmatrix} \mathbf{A}^{-1}\mathbf{u}^* \\
&= EJ_z \begin{bmatrix} \frac{6}{L^2} & \frac{4}{L} & -\frac{6}{L^2} & \frac{2}{L} \end{bmatrix} \mathbf{u}^* \\
M_z^j = EJ_z \left.\frac{\mathrm{d}^2 u_y(x)}{\mathrm{d}x^2}\right|_{x=L} &= EJ_z \begin{bmatrix} 0 & 0 & 2 & 6L \end{bmatrix} \mathbf{A}^{-1}\mathbf{u}^* \\
&= EJ_z \begin{bmatrix} \frac{6}{L^2} & \frac{2}{L} & -\frac{6}{L^2} & \frac{4}{L} \end{bmatrix} \mathbf{u}^* \\
T_y^i = EJ_z \left.\frac{\mathrm{d}^3 u_y(x)}{\mathrm{d}x^3}\right|_{x=0} &= EJ_z \begin{bmatrix} 0 & 0 & 0 & 6 \end{bmatrix} \mathbf{A}^{-1}\mathbf{u}^* \\
&= EJ_z \begin{bmatrix} \frac{12}{L^3} & \frac{6}{L^2} & -\frac{12}{L^3} & \frac{6}{L^2} \end{bmatrix} \mathbf{u}^* \\
T_y^j = -EJ_z \left.\frac{\mathrm{d}^3 u_y(x)}{\mathrm{d}x^3}\right|_{x=L} &= -EJ_z \begin{bmatrix} 0 & 0 & 0 & 6 \end{bmatrix} \mathbf{A}^{-1}\mathbf{u}^* \\
&= EJ_z \begin{bmatrix} -\frac{12}{L^3} & -\frac{6}{L^2} & \frac{12}{L^3} & -\frac{6}{L^2} \end{bmatrix} \mathbf{u}^*
\end{aligned} \tag{2.68}$$

Substituting the vectors obtained in Eqs.(2.69) into Eq.(2.65), the local stiffness matrix for the z-bending element is determined

$$\begin{bmatrix} T_y^i \\ M_z^i \\ T_y^j \\ M_z^j \end{bmatrix} = EJ_z \begin{bmatrix} \frac{12}{L^3} & \frac{6}{L^2} & -\frac{12}{L^3} & \frac{6}{L^2} \\ & \frac{4}{L} & -\frac{6}{L^2} & \frac{2}{L} \\ & \text{symm.} & \frac{12}{L^3} & -\frac{6}{L^2} \\ & & & \frac{4}{L} \end{bmatrix} \begin{bmatrix} u_y^i \\ \varphi_z^i \\ u_y^j \\ \varphi_z^j \end{bmatrix} \tag{2.69}$$

that is,

$$\mathbf{Q}_\mathrm{L} = \mathbf{K}_\mathrm{L} * \mathbf{u}^* \tag{2.70}$$

If we add the longitudinal displacements and the normal forces to the presented z-bending element, a 2D beam element is obtained (see Figs. 2.6 and 2.7).

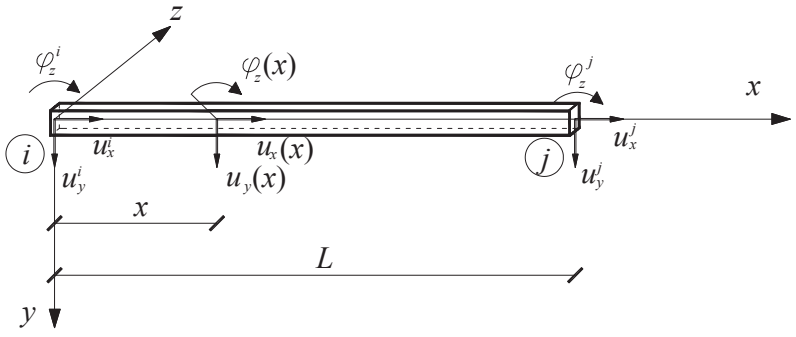

Figure 2.6 2D beam element -displacements

Its local stiffness matrix is formed by the superposition of the matrices designated for the 2D truss and z-bending elements.

$$\begin{bmatrix} N^i \\ T_y^i \\ M_z^i \\ N^j \\ T_y^j \\ M_z^j \end{bmatrix} = \begin{bmatrix} \frac{AE}{L} & 0 & 0 & -\frac{AE}{L} & 0 & 0 \\ & \frac{12EJ_z}{L^3} & \frac{6EJ_z}{L^2} & 0 & -\frac{12EJ_z}{L^3} & \frac{6EJ_z}{L^2} \\ & & \frac{4EJ_z}{L} & 0 & -\frac{6EJ_z}{L^2} & \frac{2EJ_z}{L} \\ & & & \frac{AE}{L} & 0 & 0 \\ & \text{symm.} & & & \frac{12EJ_z}{L^3} & -\frac{6EJ_z}{L^2} \\ & & & & & \frac{4EJ_z}{L} \end{bmatrix} \begin{bmatrix} u_x^i \\ u_y^i \\ \varphi_z^i \\ u_x^j \\ u_y^j \\ \varphi_z^j \end{bmatrix} \tag{2.71}$$

All forces that are considered in 2D beam element are presented on Fig. 2.7.

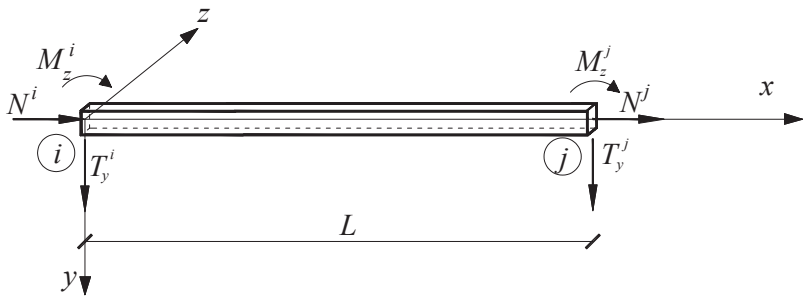

Figure 2.7 2D beam element - forces

Analogically to the z-bending element, presented in Figs.2.4 and 2.5, the y-bending one is formed. Fig. 2.8 shows the displacements in the y-bending element, while Fig. 2.9, corresponding them nodal forces.

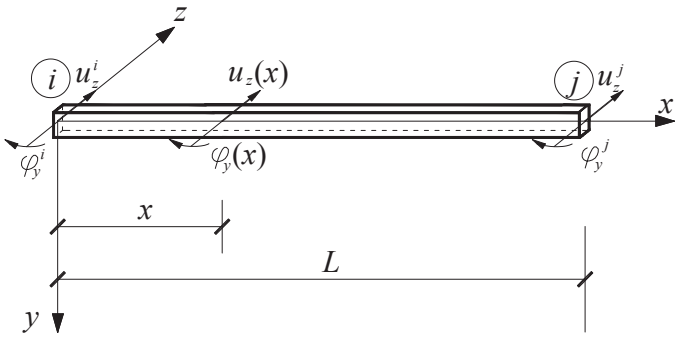

Figure 2.8 Local displacements in y-bending element

The local stiffness matrix for the y-bending element is made on the basis of the z-bending one

and after including the boundary conditions is expressed in the form

$$\begin{bmatrix} T_z^i \\ M_y^i \\ T_z^j \\ M_y^j \end{bmatrix} = EJ_y \begin{bmatrix} \frac{12}{L^3} & -\frac{6}{L^2} & -\frac{12}{L^3} & -\frac{6}{L^2} \\ & \frac{4}{L} & \frac{6}{L^2} & \frac{2}{L} \\ & \text{symm.} & \frac{12}{L^3} & \frac{6}{L^2} \\ & & & \frac{4}{L} \end{bmatrix} \begin{bmatrix} u_z^i \\ \varphi_y^i \\ u_z^j \\ \varphi_y^j \end{bmatrix} \tag{2.72}$$

The notations of the nodal forces in Eq. (2.72) are adopted according to the Fig. 2.9

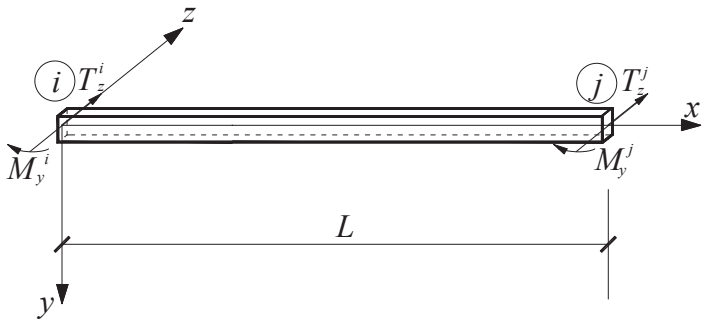

Figure 2.9 Nodal forces in y-bending element

In 3D beam element, each of two nodal points has the 6 DOFs - three translational components and three rotational ones, and, correspondingly, 12 nodal load components, Fig. 2.11. Before, we will determine its local stiffness matrix, one more element must be defined - that includes the torsion moments, Fig. 2.10.

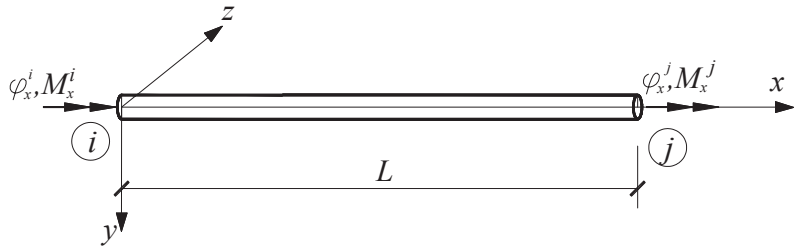

Figure 2.10 Torsion element

The local stiffness matrix for the torsion element is obtained analogically to the 2D truss element ones, and reads

$$\begin{bmatrix} M_x^i \\ M_x^j \end{bmatrix} = \frac{GJ_x}{L} \begin{bmatrix} 1 & -1 \\ -1 & 1 \end{bmatrix} \begin{bmatrix} \varphi_x^i \\ \varphi_x^j \end{bmatrix} \tag{2.73}$$

with G being the bulk modulus equals

$$G = \frac{E}{2(1+\nu)} \tag{2.74}$$

where E and ν are the Young's Modulus and Poisson's ratio of the structural material, respectively.

The stiffness matrix for the 3D beam element is formulated by the superposition of the mentioned four types of elements: truss, torsion, y- and z-bending.

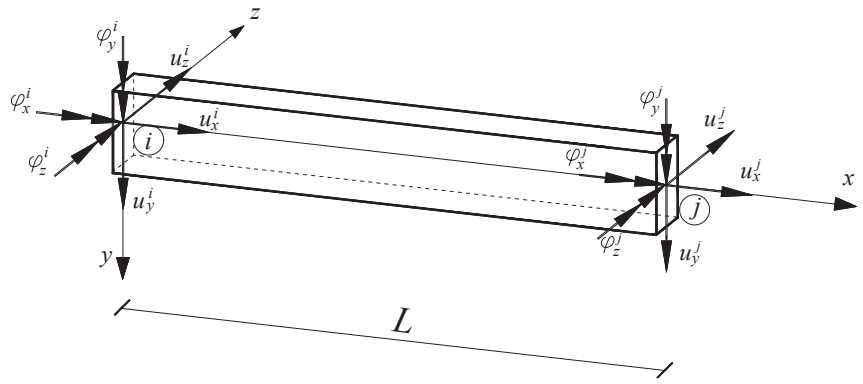

Figure 2.11 3D beam element

For the nodal displacement vector $\mathbf{u}^* = \{u_x^i, u_y^i, u_z^i, \varphi_x^j, \varphi_y^j, \varphi_z^j\}$ written for the element from fig. 2.11 and corresponding to it nodal force vector $\mathbf{Q_L} = \{N^i, T_y^i, T_z^i, M_x^j, M_y^j, M_z^j\}$, the local stiffness matrix can be expressed as

$$\begin{bmatrix}
\frac{EA_x}{L} & 0 & 0 & 0 & 0 & 0 & -\frac{EA_x}{L} & 0 & 0 & 0 & 0 & 0 \\
 & \frac{12EJ_z}{L^3} & 0 & 0 & 0 & \frac{6EJ_z}{L^2} & 0 & -\frac{12EJ_z}{L^3} & 0 & 0 & 0 & \frac{6EJ_z}{L^2} \\
 & & \frac{12EJ_y}{L^3} & 0 & -\frac{6EJ_y}{L^2} & 0 & 0 & 0 & -\frac{12EJ_y}{L^3} & 0 & -\frac{6EJ_y}{L^2} & 0 \\
 & & & \frac{GJ_x}{L} & 0 & 0 & 0 & 0 & 0 & -\frac{GJ_x}{L} & 0 & 0 \\
 & & & & \frac{4EJ_y}{L} & 0 & 0 & 0 & \frac{6EJ_y}{L^2} & 0 & \frac{2EJ_y}{L} & 0 \\
 & & & & & \frac{4EJ_z}{L} & 0 & -\frac{6EJ_z}{L^2} & 0 & 0 & 0 & \frac{2EJ_z}{L} \\
 & & & & & & \frac{EA_x}{L} & 0 & 0 & 0 & 0 & 0 \\
 & & & & & & & \frac{12EJ_z}{L^3} & 0 & 0 & 0 & -\frac{6EJ_z}{L^2} \\
 & & & \text{symm.} & & & & & \frac{12EJ_y}{L^3} & 0 & \frac{6EJ_y}{L^2} & 0 \\
 & & & & & & & & & \frac{GJ_x}{L} & 0 & 0 \\
 & & & & & & & & & & \frac{4EJ_y}{L} & 0 \\
 & & & & & & & & & & & \frac{4EJ_z}{L}
\end{bmatrix}$$

2.3.3 Shell Element

A shell element is created by superposing the plate and membrane elements, symbolically as

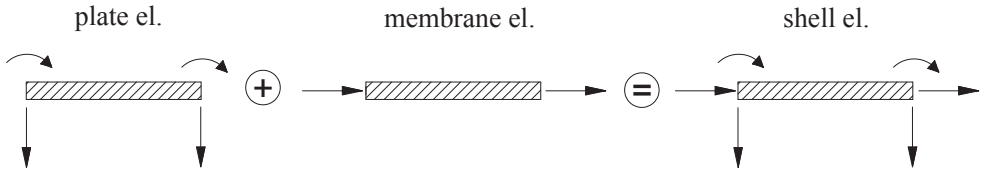

Figure 2.12 Shell element

Each node in the shell element has 6 DOFs - 3 translational components and 3 rotational ones. Accordingly, when a quadrilateral shell element is considered, the total number of degrees of freedom are equal 24 — specific forms of shell elements can be found in [3,68], for instance.

2.4 Damping Effects

Every object is exposed to many external factors, which have influence on the nodal displacements and consequently, the internal forces in a finite element. Contemporary research and modern numerical codes aim to simulate real work of the structure most exactly. Therefore, the considered system may be designed optimally, say, maximum of bearing capacity at minimum cost of production and realization. One of problems that are encountered by creating models of real objects is how to include damping effects in the analysis.

If the system with one degree of freedom is considered, it is not a problem to take this effect into account. There are a few types of damping models for such a kind of structures, described in the world literature. For example, the viscous, hysteretic and coulomb damping can be found in [57]. The situation becomes more complicated when we consider a complex structure with many degrees of freedom. The damping effect in a real object is caused by several different factors, known as the dry friction, such as hydrodynamics, aerodynamics, thermal effects etc. It is unavailable to use all the above mentioned models for including damping effects. The simplest damping model in computational implementation is described by the Rayleigh's matrix **D** which is treated as linear combination of mass and stiffness terms.

The goal of this section, is incorporating the damping to the numerical program. During the data processing a modal damping coefficient λ is used. It can be easily obtained by rewriting the equation of motion in terms of modal analysis. With N denoting the number of normalized mode shapes, the vector of generalized coordinates can be adopted in the form

$$\mathbf{q} = \mathbf{yz} \tag{2.75}$$

where $\mathbf{z} = z_1, z_2, ..., z_N$ and $\mathbf{y} = [y_1, y_2, ..., y_N]$ are the normal (modal) coordinate vector and the eigenvector matrix, respectively. The latter is received as the solution of generalized eigenproblem expressed by the equation

$$(\mathbf{K_G} - \Omega\mathbf{M_G})\mathbf{y} = 0 \tag{2.76}$$

where K_G and M_G are the previously obtained stiffness and mass matrices, while Ω is a diagonal matrix with entries being the squares of natural frequencies, amount in the finite element implementation

$$\Omega = \lceil \omega_{(1)}^2, \omega_{(2)}^2, ..., \omega_{(N)}^2 \rfloor \tag{2.77}$$

Substituting Eqs. (2.75) and their first and second derivatives with respect to time into Eq. (2.40) and premultiplying by $\mathbf{y}^{\mathrm{T}}$ we arrive at

$$\mathbf{y}^{\mathrm{T}}\mathbf{M_G}\mathbf{y}\ddot{\mathbf{z}} + \mathbf{y}^{\mathrm{T}}\mathbf{D}\mathbf{y}\dot{\mathbf{z}} + \mathbf{y}^{\mathrm{T}}\mathbf{K_G}\mathbf{yz} = \mathbf{y}^{\mathrm{T}}\mathbf{Q_G} \tag{2.78}$$

According to [3], when the mass orthonormality and stiffness orthogonality conditions are assumed as

$$\mathbf{y}^{\mathrm{T}}\mathbf{My} = \mathbf{I}, \quad \mathbf{y}^{\mathrm{T}}\mathbf{Ky} = \Omega \tag{2.79}$$

with **I** being the identity matrix, an uncoupled system of equations is obtained in the form

$$\ddot{z}_{(n)} + 2\lambda_{(n)}\omega_{(n)}\dot{z}_{(n)} + \omega_{(n)}^2 z_{(n)} = y_{(n)}^{\mathrm{T}} Q_{(n)} \tag{2.80}$$

where the following expression is adopted

$$D_{(n)} = \mathbf{y}_{(n)}^{\mathrm{T}} \mathbf{D} \mathbf{y}_{(n)} = 2\lambda_{(n)} \omega_{(n)} \tag{2.81}$$

In Eqs. (2.80) and (2.81) the symbols $z_{(n)}$, $\lambda_{(n)}$ and $\omega_{(n)}$ denote the normal displacement, modal damping coefficient and natural frequency of the system corresponding to the n-th mode shape. In order to get the $\lambda_{(n)}$, the Rayleigh's damping matrix is considered. Side-wise postmultiplying Eq. (2.41) by $\mathbf{y}$ and premultiplying by $\mathbf{y}^{\mathrm{T}}$ lead to

$$\mathbf{y}^{\mathrm{T}} \mathbf{D} \mathbf{y} = \alpha \mathbf{y}^{\mathrm{T}} \mathbf{M_G} \mathbf{y} + \beta \mathbf{y}^{\mathrm{T}} \mathbf{K_G} \mathbf{y} \tag{2.82}$$

Using conditions (2.79), the damping related to the n-th mode shape is received as

$$D_{(n)} = \mathbf{y}_{(n)}^{\mathrm{T}} \mathbf{D} \mathbf{y}_{(n)} = \alpha + \beta \omega_{(n)}^2 \tag{2.83}$$

From Eqs. (2.81) and (2.83) we obtain the expression for the n-th modal damping coefficient

$$\lambda_{(n)} = \frac{1}{2} \left(\frac{\alpha}{\omega_{(n)}} + \beta \omega_{(n)} \right) \tag{2.84}$$

Let $\bar{\omega}$ be the value of the natural frequency which leads to the minimum value of the modal damping coefficient denoted as $\bar{\lambda}$. The equation for α and β can be rewritten in the form

$$\alpha = \bar{\lambda} \bar{\omega}, \quad \text{and} \quad \beta = \frac{\bar{\lambda}}{\bar{\omega}} \tag{2.85}$$

Substituting Eqs. (2.85) into (2.84)

$$\lambda_{(n)} = \frac{\bar{\lambda}}{2} \left(\frac{T_{(n)}}{\bar{T}} + \frac{\bar{T}}{T_{(n)}} \right) \tag{2.86}$$

where $T_{(n)}$ and $\bar{T}$ are the periods of the system's vibrations corresponding to the natural frequencies $\omega_{(n)}$ and $\bar{\omega}$. In this section $\bar{\lambda}$ is the same damping factor as the input data in the numerical processing. On its basis, during the data analysis, the particular coefficients $\lambda_{(n)}$ related to the n-th mode shape are computed.

2.5 Static and Dynamic Sensitivity

2.5.1 Design Sensitivity Analysis

Structural design sensitivity analysis is a field which studies the influence of the design variables' changes to the structural response limited by boundary conditions. Displacements, buckling loads, stresses or natural frequencies in specific nodes of the system may be treated as the measures of the structural response, while cross-sectional areas of main elements, thickness of the plate or shell, Young's Modulus, mass density etc. can be considered as design variables. In literature there are many papers about static design sensitivity for 1D and 2D systems, therefore this issue can be considered to be thoroughly discussed. But opposing it, the dynamic design sensitivity for bodies which can be deformed needs to be developed. In this chapter, this problem is examined by using numerical analysis with direct differentiation and adjoint variable methods.

Let us assume that $\tau,\ \tau \in [0, \mathbf{T}(\mathbf{b}_a)]$ indicates the time variable and $\mathbf{b} = \{b_a\},\ a = 1, 2, ..., A$, the design variable vector. According to [25,35], for multi-degree-of freedom (MDOF) systems the structural response can be defined by the functional

$$\phi = \int_0^{\boldsymbol{T}(b_a)} G\left[\mathbf{q}(\tau, \mathbf{b}), \mathbf{b}\right] \mathrm{d}\tau \tag{2.87}$$

where $T(b_a)$ is the terminal time function assumed via

$$\theta[\mathbf{q}(T, \mathbf{b}), \dot{\mathbf{q}}(T, \mathbf{b}), \mathbf{b}] = 0 \tag{2.88}$$

Additionally, $\mathbf{q}(\tau, \mathbf{b})$ presents the generalized coordinate vector, $\mathbf{q}(\tau, \mathbf{b}) = \{q_\alpha(\tau, b_a)\},\ \alpha = 1, 2, ..., N$. For the sake of presentation transparency, the summation notation is included from now on. On this basis, the mass, damping and stiffness matrices are rewritten to the $\mathbf{M}(\mathbf{b}) = [M_{\alpha\beta}(b_a)],\ \mathbf{D}(\mathbf{b}) = [D_{\alpha\beta}(b_a)],\ \mathbf{K}(\mathbf{b}) = [K_{\alpha\beta}(b_a)]$, respectively, and load vector of the system is $\mathbf{Q}(\tau, \mathbf{b}) = \{Q_\alpha(\tau, b_a)\}$, where $\alpha, \beta = 1, 2, ..., N$. The equations of motion (2.40) takes then the general form

$$M_{\alpha\beta}(b_a)\ddot{q}_\beta(\tau, b_a) + D_{\alpha\beta}(b_a)\dot{q}_\beta(\tau, b_a) + K_{\alpha\beta}(b_a)q_\beta(\tau, b_a) = Q_\alpha(\tau, b_a) \tag{2.89}$$

with the initial conditions being prescribed as

$$\mathbf{q}(0, \mathbf{b}) = \mathbf{q}^0(\mathbf{b}), \qquad \dot{\mathbf{q}}(0, \mathbf{b}) = \dot{\mathbf{q}}^0(\mathbf{b}) \tag{2.90}$$

The problems of time-independent and time-dependent sensitivity will be analyzed below, in the next sections constantly.

2.5.2 Static Sensitivity

In the statics case, the vectors of generalized coordinates and external loads are time-independent. Therefore, the structural response of the system is reduced to

$$\phi = G[q_\alpha(b_a), b_a] \tag{2.91}$$

with the equilibrium equations being expressed in the form

$$K_{\alpha\beta}(b_a)q_\beta(b_a) = Q_\alpha(b_a) \tag{2.92}$$

The static sensitivity analysis aims to get $\mathrm{d}\phi/\mathrm{d}b_a$, which describes the change in the structural response functional with respect to the design variables. Let us assume that $K_{\alpha\beta}(b_a)$ and $Q_\alpha(b_a)$ are twice times continuously differentiable with respect to b_a, so do $q_\alpha(b_a)$. The chain rule of differentiation leads to

$$\frac{\mathrm{d}\phi}{\mathrm{d}b_a} = \frac{\partial G}{\partial b_a} + \frac{\partial G}{\partial q_\alpha}\frac{\mathrm{d}q_\alpha}{\mathrm{d}b_a}, \quad \alpha = 1, 2, ..., N;\ \ a = 1, 2, ..., A \tag{2.93}$$

The partial derivatives $\partial G/\partial b_a$ and $\partial G/\partial q_\alpha$ are known, because of G being an explicit function of b_a and q_α. The goal of the following considerations is to obtain $\mathrm{d}q_\alpha/\mathrm{d}b_a$, so all the terms in Eq. (2.92) are differentiated with respect to b_a to obtain

$$\frac{\partial K_{\alpha\beta}}{\partial b_a}q_\beta + K_{\alpha\beta}\frac{\mathrm{d}q_\beta}{\mathrm{d}b_a} = \frac{\partial Q_\alpha}{\partial b_a} \tag{2.94}$$

For further derivation the direct differentiation method (DDM) [35] is used. Due to symmetry of the stiffness matrix, $K_{\alpha\beta}$ inverted can also be written as ${K_{\alpha\beta}}^{-1}$. All members of the Eq. (2.94) are then multiplied by ${K_{\alpha\beta}}^{-1}$ to received

$$K_{\alpha\beta}^{-1}\frac{\partial K_{\alpha\gamma}}{\partial b_a}q_\gamma + \frac{\mathrm{d}q_\beta}{\mathrm{d}b_a} = K_{\alpha\beta}^{-1}\frac{\partial Q_\alpha}{\partial b_a}, \qquad \alpha, \beta, \gamma = 1, 2, ..., N \tag{2.95}$$

or, in terms of the displacement sensitivities, as

$$\frac{\mathrm{d}q_\beta}{\mathrm{d}b_a} = K_{\alpha\beta}^{-1}\left(\frac{\partial Q_\alpha}{\partial b_a} - \frac{\partial K_{\alpha\gamma}}{\partial b_a}q_\gamma\right) \tag{2.96}$$

Substituting Eq. (2.96) into Eq. (2.93) yields

$$\frac{\mathrm{d}\phi}{\mathrm{d}b_a} = \frac{\partial G}{\partial b_a} + \frac{\partial G}{\partial q_\beta}K_{\alpha\beta}^{-1}\left(\frac{\partial Q_\alpha}{\partial b_a} - \frac{\partial K_{\alpha\gamma}}{\partial b_a}q_\gamma\right) \tag{2.97}$$

Instead of the DDM presented above, we can formulate the static sensitivity problem by using the so-called adjoint system method (ASM) as an alternative. To this end we define an adjoint vector of the form

$$\lambda_\alpha = K_{\alpha\beta}^{-1}\frac{\partial G}{\partial q_\beta} \tag{2.98}$$

so that Eq. (2.97) becomes

$$\frac{\mathrm{d}\phi}{\mathrm{d}b_a} = \frac{\partial G}{\partial b_a} + \lambda_\alpha\left(\frac{\partial Q_\alpha}{\partial b_a} - \frac{\partial K_{\alpha\gamma}}{\partial b_a}q_\gamma\right) \tag{2.99}$$

where the adjoint vector is solved for from the adjoint equations system

$$K_{\alpha\beta}\lambda_\alpha = \frac{\partial G}{\partial q_\beta} \tag{2.100}$$

2.5.3 Unit Impulse and Dirac-δ Distribution

For better understanding the mathematical derivations presented in Sections from 2.5.4 to 2.5.6., this section will deal with Dirac-δ distribution. In the sense of computational engineering, it is considered as a unit impulse being a significant element in system dynamics. From the viewpoint of mathematical analysis, the Dirac-δ Distribution is not differentiated as an ordinary function, because its derivative is equal 0 in the variable range $x \neq 0$, while for point $x = 0$ it is undetermined [26,27,35].

To illustrate Dirac-δ distribution, let us consider the piecewise function $f(x)$, mathematically written as

$$f(x) = \begin{cases} \dfrac{1}{x_1} & \text{for} \quad x \in \left[\dfrac{-x_1}{2}, \dfrac{x_1}{2}\right] \\ 0 & \text{for} \quad x \neq \in \left[\dfrac{-x_1}{2}, \dfrac{x_1}{2}\right] \end{cases} \tag{2.101}$$

that is presented in Fig. 2.13.

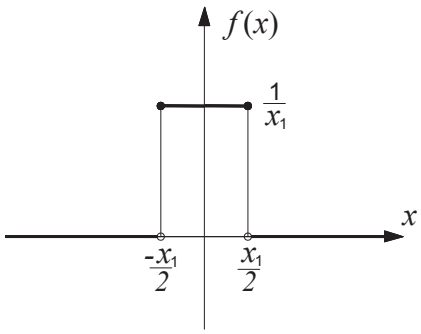

Figure 2.13 The piecewise function

Geometrically, $f(x)$ may describe the rectangle of the base x_1 and hight $1/x_1$. The area of the rectangle from Fig. 2.13, specified by $f(x)$, is the product of the height and base length. Regardless the value of x_1, it will be always equal 1. The base length of the rectangle is pulse duration. When x_1 approaches 0, the figure's height tends to infinity, and then, function $f(x)$ tends to $\delta(x)$, which can be shown by Eq. (2.102).

$$\delta(x) = \lim_{x_1 \to 0} f(x) \begin{cases} \infty & \text{for} \quad x = 0 \\ 0 & \text{for} \quad x \neq 0 \end{cases} \tag{2.102}$$

Due to the constancy of the integral of the function $\delta(x)$ [26,27,35], the area of the figure for a small positive parameter ε is expressed by the equation

$$\int_{-\varepsilon}^{\varepsilon} \delta(x)\mathrm{d}x = \lim_{x_1 \to 0} \int_{-x_1/2}^{x_1/2} f(x)\mathrm{d}x = \lim_{x_1 \to 0} \int_{-x_1/2}^{x_1/2} \frac{1}{x_1}\mathrm{d}x = \lim_{x_1 \to 0} \frac{1}{x_1} \int_{-x_1/2}^{x_1/2} \mathrm{d}x = 1 \tag{2.103}$$

When function $f(x)$ is not symmetric with respect to the line given by the equation $x = 0$, but to $x = x_0$ one, we change the variable x into $(x_0 - x)$ [26,27,35], and then Eq. (2.102) takes the form

$$\delta(x_0 - x) = \begin{cases} \infty & \text{for} \quad x = x_0 \\ 0 & \text{for} \quad x \neq x_0 \end{cases} \tag{2.104}$$

and the integral given by the Eq. (2.103) is rewritten to the expression

$$\int_{x_0-\varepsilon}^{x_0+\varepsilon} \delta(x_0 - x)\mathrm{d}x = 1 \tag{2.105}$$

Due to a nature of the Dirac-δ distribution, this type of generalized function is regarded to be specified and derived. Therefore, on the basis of [26,27,35], Dirac-δ is defined by the equation

$$\int_{-\infty}^{+\infty} g(x)\delta(x_0 - x)\mathrm{d}x = g(x_0) \tag{2.106}$$

where the test function $g(x)$ is continuous and differential at point $x = x_0$ and it takes zero value outside a prescribed interval. Integral in Eq. (2.106) takes the value of the test function at point $x = x_0$. Because of the $\delta(x)$-parity, cf. Eqs. (2.105) and (2.106), the below equalities hold true

$$\begin{aligned} \delta(x - x_0) &= \delta(x_0 - x) \\ \delta(x) &= \delta(-x) \end{aligned} \tag{2.107}$$

The convolution given by the Eq. (2.106) is symmetric with respect to the generalized function $g(x)$ and $\delta(x - x_0)$ [26,27,35]. Adopting dummy variables x and ς and putting expression $x = x_0 - \varsigma$ into Eq. (2.106) we obtain

$$g(x_0) = -\int_{-\infty}^{+\infty} g(x_0 - \varsigma)\delta(\varsigma)\mathrm{d}\varsigma = \int_{-\infty}^{+\infty} g(x_0 - x)\delta(x)\mathrm{d}x \tag{2.108}$$

Therefore, we can write

$$\int_{-\infty}^{+\infty} g(x_0 - x)\delta(x)\mathrm{d}x = \int_{-\infty}^{+\infty} g(x)\delta(x_0 - x)\mathrm{d}x \tag{2.109}$$

When $x_0 = 0$, we get

$$\int_{-\infty}^{+\infty} g(x)\delta(-x)\mathrm{d}x = \int_{-\infty}^{+\infty} g(-x)\delta(x)\mathrm{d}x = \int_{-\infty}^{+\infty} g(x)\delta(x)\mathrm{d}x = g(0) \tag{2.110}$$

In the conventional sense of mathematical analysis, the derivative of $\delta(x)$ is equal 0 with $x \neq 0$, for $x = 0$ it does not uniquely exist. However, we can define the derivative of $\delta(x)$ in an integral form as

$$\int_{-\infty}^{+\infty} g(x)\delta'(x)\mathrm{d}x = -\int_{-\infty}^{+\infty} g'(x)\delta(x)\mathrm{d}x \tag{2.111}$$

that will be used in the following form for

$$\int_{-\infty}^{+\infty} g(x)\delta'(x)\mathrm{d}x = -g'(0) \tag{2.112}$$

The Dirac-δ is a significant element in the discrete data processing in numerical methods. When entering data into a program, the continuous signals are previously discretized to the signals being determined at the so-called sampling points $\gamma_{(n)}$, $n = 0, 1, ...$ of discrete variable γ [26,27,35]. The continuous signals are divided into equal sampling intervals $\Delta\gamma_n = \Delta\gamma$ between given $\gamma_{(n)}$. Therefore we have

$$\gamma_n = n\Delta\gamma;\ \ n = 0, 1, ... \tag{2.113}$$

Using the concept of zero-order hold,[26,27,35], we can express

$$f_n = f(\gamma_n) = f(n\Delta\gamma); \quad \gamma_n \in [n\Delta\gamma, (n+1)\Delta\gamma],\ n = 0, 1, ... \tag{2.114}$$

where $f(\gamma_n)$ is the n-th value of the sample function being generated from the output signal $f(\gamma)$. Due to the continuity of $f(\gamma)$ function at points γ_n, the value of sample function at point n can be written by Dirac-δ distribution.

Applying an engineering, staircase implementation, $\delta(x)$ can be interpreted simply by the well-known Kronecker delta δ_{jn} (see [26,27,35])

$$\delta_{jn} = \delta(j - n) \begin{cases} 1 \text{ for } j = n \\ \\ 0 \text{ for } j \neq n \end{cases} \quad j, n = 0, 1, ... \tag{2.115}$$

Therefore, the convolution given by the Eq. (2.106) takes the form

$$f_n = \sum_j f(j)\delta(n - j) = \sum_j f_j\delta_{nj}; \quad n, j = 0, 1, ... \tag{2.116}$$

2.5.4 Eigenvalue Sensitivity

Let us consider a special example of equations of motion. Omitting the damping coefficients and external loads, Eq. (2.87) takes the form of an undamped free vibration system as

$$M_{\alpha\beta}(b_a)\ddot{q}_\beta(b_a) + K_{\alpha\beta}(b_a)q_\beta(b_a) = 0 \tag{2.117}$$

We are going to find β-th eigenvalue $\xi_{(\beta)}(\mathbf{b}) = \xi_{(\beta)}(b_a) = \omega^2_{(\beta)}$. It should be noted that the indexes in round bracket as (β) are not subject to the summation convention. Let us adopted that $\mathbf{y}(\mathbf{b}) = \{y_{\alpha\beta}(b_a)\}$ is the eigenvector matrix (compare Section 2.4). Assuming that

$$\phi_{(\beta)} = \xi_{(\beta)}(b_a); \quad \beta = 1, 2, ..., N \tag{2.118}$$

The $K_{\alpha\beta}$-orthogonality and $M_{\alpha\beta}$-orthonormality conditions (cf. Eq. (2.79)) are now rewritten to the form

$$\begin{aligned} y^{\mathrm{T}}_{\alpha\gamma} K_{\alpha\beta}\, y_{\beta\eta} &= \Omega_{(\bar{\alpha}\bar{\beta})}\delta_{\gamma\eta} \\ y^{\mathrm{T}}_{\alpha\gamma} M_{\alpha\beta}\, y_{\beta\eta} &= \delta_{\gamma\eta} \end{aligned} \tag{2.119}$$

with $\alpha, \beta, \gamma, \eta = 1, 2, ..., N$ and $\Omega_{(\bar{\alpha}\bar{\beta})}$ being the diagonal matrix of N eigenvalues. The symbol $\delta_{\gamma\eta}$ used in Eqs. (2.119) is the Kroneker delta, described in details in Section 2.5.3. Pre-multiplying Eq. $(2.119)_1$ by $y_{\alpha\beta}$ gives

$$K_{\alpha\beta}\, y_{\beta\gamma} = \Omega_{(\bar{\alpha}\bar{\beta})} y_{\alpha\eta}\delta_{\gamma\eta} \tag{2.120}$$

Substituting Eq. $(2.119)_2$ to Eq. (2.120), leads to

$$K_{\alpha\beta}\, y_{\beta\gamma} = \Omega_{(\bar{\alpha}\bar{\beta})} M_{\alpha\beta} y_{\beta\gamma} \tag{2.121}$$

Because we are aiming to the design sensitivity of the β-th eigenvalue and we consider undamped free vibration system, Eq. (2.121) is rewritten as

$$K_{\alpha\beta}(b_a)\, y_{\beta\gamma}(b_a) = \xi_{(\beta)}(b_a) M_{\alpha\beta}(b_a) y_{\beta\gamma}(b_a) \tag{2.122}$$

Now, the structural design sensitivity for the eigenvalue response of the generalized eigenproblem will be derived. Differentiating both sides of Eq. (2.122) with respect to design variable, leads to

$$\frac{\partial K_{\alpha\beta}}{\partial b_a} y_{\beta\gamma} + K_{\alpha\beta}\frac{\mathrm{d}y_{\beta\gamma}}{\mathrm{d}b_a} = \frac{\mathrm{d}\xi_{(\beta)}}{\mathrm{d}b_a} M_{\alpha\beta} y_{\beta\gamma} + \xi_{(\beta)}\frac{\partial M_{\alpha\beta}}{\partial b_a} y_{\beta\gamma} + \xi_{(\beta)} M_{\alpha\beta}\frac{\mathrm{d}y_{\beta\gamma}}{\mathrm{d}b_a} \tag{2.123}$$

where $\alpha, \beta, \gamma = 1, 2, .., N$, $a = 1, 2, ..., A$. Eq. (2.123) is then rewritten to get

$$\frac{\mathrm{d}\xi_{(\beta)}}{\mathrm{d}b_a} M_{\alpha\beta} y_{\beta\gamma} = \left(\frac{\partial K_{\alpha\beta}}{\partial b_a} - \xi_{(\beta)}\frac{\partial M_{\alpha\beta}}{\partial b_a}\right) y_{\beta\gamma} + \left(K_{\alpha\beta} - \xi_{(\beta)} M_{\alpha\beta}\right)\frac{\mathrm{d}y_{\beta\gamma}}{\mathrm{d}b_a} \tag{2.124}$$

that, side-wise multiplied by the transposed eigenvector matrix, leads to

$$\frac{\mathrm{d}\xi_{(\beta)}}{\mathrm{d}b_a} y^{\mathrm{T}}_{\alpha\eta} M_{\alpha\beta} y_{\beta\gamma} = y^{\mathrm{T}}_{\alpha\eta}\left[\left(\frac{\partial K_{\alpha\beta}}{\partial b_a} - \xi_{(\beta)}\frac{\partial M_{\alpha\beta}}{\partial b_a}\right) y_{\beta\gamma} + \left(K_{\alpha\beta} - \xi_{(\beta)} M_{\alpha\beta}\right)\frac{\mathrm{d}y_{\beta\gamma}}{\mathrm{d}b_a}\right] \tag{2.125}$$

Using the orthonormality condition of the mass matrix, Eq. $(2.119)_2$ gives

$$\frac{\mathrm{d}\xi_{(\beta)}}{\mathrm{d}b_a}\delta_{\eta\gamma} = y^{\mathrm{T}}_{\alpha\eta}\left(\frac{\partial K_{\alpha\beta}}{\partial b_a} - \xi_{(\beta)}\frac{\partial M_{\alpha\beta}}{\partial b_a}\right) y_{\beta\gamma} + y^{\mathrm{T}}_{\alpha\eta}\left(K_{\alpha\beta} - \xi_{(\beta)} M_{\alpha\beta}\right)\frac{\mathrm{d}y_{\beta\gamma}}{\mathrm{d}b_a} \tag{2.126}$$

Eq. (2.122) is firstly post-multiplying and then pre-multiplying by the transposed eigenvectors matrix, to obtain

$$y^{\mathrm{T}}_{\beta\gamma} K_{\alpha\beta} = \xi_{(\beta)} y^{\mathrm{T}}_{\beta\gamma} M_{\alpha\beta} \tag{2.127}$$

According to that, Eq. (2.126) is converted to the formula

$$\frac{\mathrm{d}\xi_{(\beta)}}{\mathrm{d}b_a}\delta_{\eta\gamma} = y^{\mathrm{T}}_{\alpha\eta}\left(\frac{\partial K_{\alpha\beta}}{\partial b_a} - \xi_{(\beta)}\frac{\partial M_{\alpha\beta}}{\partial b_a}\right) y_{\beta\gamma} \tag{2.128}$$

2.5.5 Time Interval Sensitivity

In this section, we aiming to obtain the dynamic sensitivity, when time is considered on a given interval. Let us assumed that the matrices $K_{\alpha\beta}$, $M_{\alpha\beta}$ and $D_{\alpha\beta}$ and the vector of nodal loads Q_α are twice continuously differentiable with respect to the b_a and additionally the mass matrix is nonsingular. Consequently to that $q_\alpha(\tau, b_a)$ is twice times continuously differentiable with respect to design variable. In this case we consider the structural response given by the Eq. (2.87). Differentiating functional with respect to design variable with applying the Leibniz rule yields to

$$\frac{\mathrm{d}\phi}{\mathrm{d}b_a} = \int_0^{\boldsymbol{T}(b_a)} \frac{\mathrm{d}G\left[\mathbf{q}(\tau, \mathbf{b}), \mathbf{b}\right]}{\mathrm{d}b_a}\, \mathrm{d}\tau \; + G\Big|_{\tau=T} \frac{\mathrm{d}T}{\mathrm{d}b_a} \tag{2.129}$$

The second term of right-side of Eq. (2.129) results from differentiation under the integral. The chain rule of differentiation gives

$$\frac{\mathrm{d}\phi}{\mathrm{d}b_a} = G\Big|_{\tau=T} \frac{\mathrm{d}T}{\mathrm{d}b_a} + \int_0^{\boldsymbol{T}(b_a)} \left(\frac{\partial G}{\partial b_a} + \frac{\partial G}{\partial q_\alpha}\frac{\mathrm{d}q_\alpha}{\mathrm{d}b_a}\right) \mathrm{d}\tau \tag{2.130}$$

Differentiating the terminal-time condition, defined by Eq. (2.88) with respect to the design variable b_a leads to

$$\frac{\partial\theta[q_\beta(T, b_a), \dot{q}_\beta(T, b_a), b_a]}{\partial b_a} = \frac{\partial\theta}{\partial b_a} + \frac{\partial\theta}{\partial q_\beta}\frac{\mathrm{d}q_\beta}{\mathrm{d}b_a} + \frac{\partial\theta}{\partial\dot{q}_\beta}\frac{\mathrm{d}\dot{q}_\beta}{\mathrm{d}b_a} = 0 \tag{2.131}$$

It should be observed that the symbol $\mathrm{d}\cdot/\mathrm{d}b_a$ mean the absolutely partial derivative with respect to b_a. Because $T(b_a)$ is also an explicit function of the design variable, the first and second derivatives of generalized coordinate vector with respect to b_a are expressed as

$$\frac{\mathrm{d}q_\beta(T)}{\mathrm{d}b_a} = \left(\frac{\partial q_\beta(T)}{\partial b_a} + \frac{\partial q_\beta(T)}{\partial T}\frac{\mathrm{d}T}{\mathrm{d}b_a}\right) \tag{2.132}$$

and

$$\frac{\mathrm{d}\dot{q}_\beta(T)}{\mathrm{d}b_a} = \left(\frac{\partial \dot{q}_\beta(T)}{\partial b_a} + \frac{\partial \dot{q}_\beta(T)}{\partial T}\frac{\mathrm{d}T}{\mathrm{d}b_a}\right) \tag{2.133}$$

Substituting Egs. (2.132) and (2.133) into Eq. (2.131) we get

$$\begin{aligned}
&\frac{\partial\theta}{\partial b_a} + \frac{\partial\theta}{\partial q_\alpha}\left[\frac{\partial q_\alpha}{\partial b_a} + \frac{\partial q_\alpha}{\partial T}\frac{\mathrm{d}T}{\mathrm{d}b_a}\right]_{\tau=T} + \frac{\partial\theta}{\partial\dot{q}_\alpha}\left[\frac{\partial\dot{q}_\alpha}{\partial b_a} + \frac{\partial\dot{q}_\alpha}{\partial T}\frac{\mathrm{d}T}{\mathrm{d}b_a}\right]_{\tau=T} \\
&= \frac{\partial\theta}{\partial b_a} + \left[\frac{\partial\theta}{\partial q_\alpha}\frac{\partial q_\alpha}{\partial b_a} + \frac{\partial\theta}{\partial\dot{q}_\alpha}\frac{\partial\dot{q}_\alpha}{\partial b_a}\right]_{\tau=T} + \left(\frac{\partial\theta}{\partial q_\alpha}\frac{\partial q_\alpha}{\partial T} + \frac{\partial\theta}{\partial\dot{q}_\alpha}\frac{\partial\dot{q}_\alpha}{\partial T}\right)\frac{\mathrm{d}T}{\mathrm{d}b_a} \\
&= \frac{\partial\theta}{\partial b_a} + \left[\frac{\partial\theta}{\partial q_\alpha}\frac{\partial q_\alpha}{\partial b_a} + \frac{\partial\theta}{\partial\dot{q}_\alpha}\frac{\partial\dot{q}_\alpha}{\partial b_a}\right]_{\tau=T} + \dot{\theta}\frac{\mathrm{d}T}{\mathrm{d}b_a} = 0
\end{aligned} \tag{2.134}$$

where

$$\dot{\theta} = \frac{\partial\theta}{\partial q_\alpha}\frac{\partial q_\alpha}{\partial T} + \frac{\partial\theta}{\partial\dot{q}_\alpha}\frac{\partial\dot{q}_\alpha}{\partial T} \tag{2.135}$$

Eq. (2.134) is solved for $\frac{\mathrm{d}T}{\mathrm{d}b_a}$, to get

$$\frac{\mathrm{d}T}{\mathrm{d}b_a} = -\frac{1}{\dot{\theta}}\left[\frac{\partial\theta}{\partial b_a} + \frac{\partial\theta}{\partial q_\alpha}\frac{\partial q_\alpha}{\partial b_a} + \frac{\partial\theta}{\partial\dot{q}_\alpha}\frac{\partial\dot{q}_\alpha}{\partial b_a}\right]_{\tau=T} \tag{2.136}$$

Substituting Eq. (2.136) into Eq. (2.130) yields to

$$\frac{\mathrm{d}\phi}{\mathrm{d}b_a} = -\frac{G}{\dot{\theta}}\left[\frac{\partial\theta}{\partial b_a} + \frac{\partial\theta}{\partial q_\alpha}\frac{\partial q_\alpha}{\partial b_a} + \frac{\partial\theta}{\partial\dot{q}_\alpha}\frac{\partial\dot{q}_\alpha}{\partial b_a}\right]_{\tau=T} + \int_0^{T(b_a)}\left(\frac{\partial G}{\partial b_a} + \frac{\partial G}{\partial q_\alpha}\frac{\mathrm{d}q_\alpha}{\mathrm{d}b_a}\right)\mathrm{d}\tau \quad (2.137)$$

The derivatives $\mathrm{d}q_\alpha/\mathrm{d}b_a$ and $\mathrm{d}\dot{q}_\alpha/\mathrm{d}b_a$ are still unknown, therefore removing them by adjoint variable method is the next step of the following consideration. To do this, both sides of Eq. (2.89) are first differentiated with respect to b_a to get

$$\frac{\partial M_{\alpha\beta}}{\partial b_a}\ddot{q}_\beta + M_{\alpha\beta}\frac{\mathrm{d}\ddot{q}_\beta}{\mathrm{d}b_a} + \frac{\partial D_{\alpha\beta}}{\partial b_a}\dot{q}_\beta + D_{\alpha\beta}\frac{\mathrm{d}\dot{q}_\beta}{\mathrm{d}b_a} + \frac{\partial K_{\alpha\beta}}{\partial b_a}q_\beta + K_{\alpha\beta}\frac{\mathrm{d}q_\beta}{\mathrm{d}b_a} = \frac{\partial Q_\alpha}{\partial b_a} \quad (2.138)$$

and then they are postmultiplied by the adjoint vector $\lambda_\alpha(\tau)$

$$\begin{aligned}\left(\frac{\partial M_{\alpha\beta}}{\partial b_a}\ddot{q}_\beta + M_{\alpha\beta}\frac{\mathrm{d}\ddot{q}_\beta}{\mathrm{d}b_a} + \frac{\partial D_{\alpha\beta}}{\partial b_a}\dot{q}_\beta + D_{\alpha\beta}\frac{\mathrm{d}\dot{q}_\beta}{\mathrm{d}b_a} + \frac{\partial K_{\alpha\beta}}{\partial b_a}q_\beta + K_{\alpha\beta}\frac{\mathrm{d}q_\beta}{\mathrm{d}b_a}\right)\lambda_\alpha(\tau)\\ = \frac{\partial Q_\alpha}{\partial b_a}\lambda_\alpha(\tau)\end{aligned} \quad (2.139)$$

and integrated over the time domain $[\,0,\,T\,]$ to obtain

$$\begin{aligned}\int_0^T\Bigg(\frac{\partial M_{\alpha\beta}}{\partial b_a}\ddot{q}_\beta\lambda_\alpha + M_{\alpha\beta}\lambda_\alpha\frac{\mathrm{d}\ddot{q}_\beta}{\mathrm{d}b_a} + \frac{\partial D_{\alpha\beta}}{\partial b_a}\dot{q}_\beta\lambda_\alpha + D_{\alpha\beta}\lambda_\alpha\frac{\mathrm{d}\dot{q}_\beta}{\mathrm{d}b_a} + \frac{\partial K_{\alpha\beta}}{\partial b_a}q_\beta\lambda_\alpha\\ + K_{\alpha\beta}\lambda_\alpha\frac{\mathrm{d}q_\beta}{\mathrm{d}b_a}\Bigg)\mathrm{d}\tau = \int_0^T\frac{\partial Q_\alpha}{\partial b_a}\lambda_\alpha\mathrm{d}\tau\end{aligned} \quad (2.140)$$

It is known that the integral from the sum of expressions is equal to the sum of the integrals. Therefore the separate terms of the above equation are first considered and then they are composed as a whole formula. We start form the term involving $\mathrm{d}\dot{q}_\alpha/\mathrm{d}b_a$ and integrate it by parts with respect to τ, which gives

$$\int_0^T D_{\alpha\beta}\lambda_\alpha\frac{\mathrm{d}\dot{q}_\beta}{\mathrm{d}b_a}\mathrm{d}\tau = D_{\alpha\beta}\lambda_\alpha\frac{\mathrm{d}q_\beta}{\mathrm{d}b_a}\bigg|_{\tau=T} - \int_0^T D_{\alpha\beta}\dot{\lambda}_\alpha\frac{\mathrm{d}q_\beta}{\mathrm{d}b_a}\mathrm{d}\tau \quad (2.141)$$

Next, the term having $\mathrm{d}\ddot{q}_\alpha/\mathrm{d}b_a$ is twice integrated by parts with respect to τ. The first integral is equal

$$\int_0^T M_{\alpha\beta}\lambda_\alpha\frac{\mathrm{d}\ddot{q}_\beta}{\mathrm{d}b_a}\mathrm{d}\tau = M_{\alpha\beta}\lambda_\alpha\frac{\mathrm{d}\dot{q}_\beta}{\mathrm{d}b_a}\bigg|_{\tau=T} - \int_0^T M_{\alpha\beta}\dot{\lambda}_\alpha\frac{\mathrm{d}\dot{q}_\beta}{\mathrm{d}b_a}\mathrm{d}\tau \quad (2.142)$$

and the second is written as

$$\int_0^T M_{\alpha\beta}\dot{\lambda}_\alpha\frac{\mathrm{d}\dot{q}_\beta}{\mathrm{d}b_a}\mathrm{d}\tau = M_{\alpha\beta}\dot{\lambda}_\alpha\frac{\mathrm{d}q_\beta}{\mathrm{d}b_a}\bigg|_{\tau=T} - \int_0^T M_{\alpha\beta}\ddot{\lambda}_\alpha\frac{\mathrm{d}q_\beta}{\mathrm{d}b_a}\mathrm{d}\tau \quad (2.143)$$

so that, Eq. (2.142) takes the form

$$\int_0^T M_{\alpha\beta}\lambda_\alpha\frac{\mathrm{d}\ddot{q}_\beta}{\mathrm{d}b_a}\mathrm{d}\tau = M_{\alpha\beta}\lambda_\alpha\frac{\mathrm{d}\dot{q}_\beta}{\mathrm{d}b_a}\bigg|_{\tau=T} - M_{\alpha\beta}\dot{\lambda}_\alpha\frac{\mathrm{d}q_\beta}{\mathrm{d}b_a}\bigg|_{\tau=T} + \int_0^T M_{\alpha\beta}\ddot{\lambda}_\alpha\frac{\mathrm{d}q_\beta}{\mathrm{d}b_a}\mathrm{d}\tau \quad (2.144)$$

Substituting Eqs. (2.141) and (2.144) into Eq. (2.140) and rearranging all the terms, we obtain

$$\begin{aligned}- \quad & (M_{\alpha\beta}\dot{\lambda}_\alpha - D_{\alpha\beta}\lambda_\alpha)\frac{\mathrm{d}q_\beta}{\mathrm{d}b_a}\bigg|_{\tau=T} + \int_0^T(M_{\alpha\beta}\ddot{\lambda}_\alpha - D_{\alpha\beta}\dot{\lambda}_\alpha + K_{\alpha\beta}\lambda_\alpha)\frac{\mathrm{d}q_\beta}{\mathrm{d}b_a}\mathrm{d}\tau\\ + \quad & M_{\alpha\beta}\lambda_\alpha\frac{\mathrm{d}\dot{q}_\beta}{\mathrm{d}b_a}\bigg|_{\tau=T} = \int_0^T\lambda_\alpha\left(\frac{\partial Q_\alpha}{\partial b_a} - \frac{\partial M_{\alpha\beta}}{\partial b_a}\ddot{q}_\beta - \frac{\partial D_{\alpha\beta}}{\partial b_a}\dot{q}_\beta - \frac{\partial K_{\alpha\beta}}{\partial b_a}q_\beta\right)\mathrm{d}\tau\end{aligned} \quad (2.145)$$

Comparing the terms including $\mathrm{d}q_\alpha/\mathrm{d}b_a$ at $\tau \in [0, T]$ of the second term under integration of Eq. (2.145) and of the last term under integration of Eq.(2.137), we arrive at the adjoint equations system of the form

$$\frac{\partial G}{\partial q_\beta} = M_{\beta\alpha}(b_a)\ddot{\lambda}_\alpha(\tau) - D_{\beta\alpha}(b_a)\dot{\lambda}_\alpha(\tau) + K_{\beta\alpha}(b_a)\lambda_\alpha(\tau) \tag{2.146}$$

Further comparing the term involving $\mathrm{d}q_\alpha/\mathrm{d}b_a$ and $\mathrm{d}\dot{q}_\alpha/\mathrm{d}b_a$ at $\tau = T$ from Eq. (2.145) and Eq.(2.137), the terminal conditions for the adjoint generalized coordinates and velocities are received in the form

$$\begin{aligned} M_{\beta\alpha}\lambda_\alpha(T) &= -\frac{G}{\dot{\theta}}\frac{\partial\theta}{\partial\dot{q}_\beta} \\ M_{\beta\alpha}\dot{\lambda}_\alpha(T) &= D_{\beta\alpha}\lambda_\alpha(T) + \frac{G}{\dot{\theta}}\frac{\partial\theta}{\partial q_\beta} \end{aligned} \tag{2.147}$$

Introducing Eqs. (2.146) and (2.147) into Eq. (2.145) leads to

$$\begin{aligned} &- \frac{G}{\dot{\theta}}\frac{\partial\theta}{\partial\dot{q}_\beta}\frac{\mathrm{d}\dot{q}_\beta}{\mathrm{d}b_a}\bigg|_{\tau=T} - \frac{G}{\dot{\theta}}\frac{\partial\theta}{\partial q_\beta}\frac{\mathrm{d}q_\beta}{\mathrm{d}b_a}\bigg|_{\tau=T} + \int_0^T \frac{\partial G}{\partial q_\beta}\frac{\mathrm{d}q_\beta}{\mathrm{d}b_a}\mathrm{d}\tau \\ &= \int_0^T \lambda_\alpha\left(\frac{\partial Q_\alpha}{\partial b_a} - \frac{\partial M_{\alpha\beta}}{\partial b_a}\ddot{q}_\beta - \frac{\partial D_{\alpha\beta}}{\partial b_a}\dot{q}_\beta - \frac{\partial K_{\alpha\beta}}{\partial b_a}q_\beta\right)\mathrm{d}\tau \end{aligned} \tag{2.148}$$

or, after rearranging the terms

$$\begin{aligned} &- \frac{G}{\dot{\theta}}\left[\frac{\partial\theta}{\partial\dot{q}_\beta}\frac{\mathrm{d}\dot{q}_\beta}{\mathrm{d}b_a} + \frac{\partial\theta}{\partial q_\beta}\frac{\mathrm{d}q_\beta}{\mathrm{d}b_a}\right]_{\tau=T} = -\int_0^T \frac{\partial G}{\partial q_\beta}\frac{\mathrm{d}q_\beta}{\mathrm{d}b_a}\mathrm{d}\tau \\ &+ \int_0^T \lambda_\alpha\left(\frac{\partial Q_\alpha}{\partial b_a} - \frac{\partial M_{\alpha\beta}}{\partial b_a}\ddot{q}_\beta - \frac{\partial D_{\alpha\beta}}{\partial b_a}\dot{q}_\beta - \frac{\partial K_{\alpha\beta}}{\partial b_a}q_\beta\right)\mathrm{d}\tau \end{aligned} \tag{2.149}$$

Substituting Eq. (2.149) into Eq. (2.137) we receive the sensitivity gradient coefficients for the general dynamic problem as

$$\begin{aligned} \frac{\mathrm{d}\phi}{\mathrm{d}b_a} &= -\frac{G}{\dot{\theta}}\frac{\partial\theta}{\partial b_a}\bigg|_{\tau=T} - \int_0^{\boldsymbol{T}(b_a)} \frac{\partial G}{\partial q_\beta}\frac{\mathrm{d}q_\beta}{\mathrm{d}b_a}\mathrm{d}\tau + \int_0^{\boldsymbol{T}(b_a)}\left(\frac{\partial G}{\partial b_a} + \frac{\partial G}{\partial q_\beta}\frac{\mathrm{d}q_\beta}{\mathrm{d}b_a}\right)\mathrm{d}\tau \\ &\quad + \int_0^{\boldsymbol{T}(b_a)} \lambda_\alpha\left(\frac{\partial Q_\alpha}{\partial b_a} - \frac{\partial M_{\alpha\beta}}{\partial b_a}\ddot{q}_\beta - \frac{\partial D_{\alpha\beta}}{\partial b_a}\dot{q}_\beta - \frac{\partial K_{\alpha\beta}}{\partial b_a}q_\beta\right)\mathrm{d}\tau \end{aligned} \tag{2.150}$$

Converting the above formula we obtain

$$\begin{aligned} \frac{\mathrm{d}\phi}{\mathrm{d}b_a} &= -\frac{G}{\dot{\theta}}\frac{\partial\theta}{\partial b_a}\bigg|_{\tau=T} + \int_0^{\boldsymbol{T}(b_a)} \frac{\partial G}{\partial b_a}\,\mathrm{d}\tau \\ &\quad + \int_0^{\boldsymbol{T}(b_a)} \lambda_\alpha\left(\frac{\partial Q_\alpha}{\partial b_a} - \frac{\partial M_{\alpha\beta}}{\partial b_a}\ddot{q}_\beta - \frac{\partial D_{\alpha\beta}}{\partial b_a}\dot{q}_\beta - \frac{\partial K_{\alpha\beta}}{\partial b_a}q_\beta\right)\mathrm{d}\tau \end{aligned} \tag{2.151}$$

2.5.6 Time Instant Sensitivity

In case of the time instant sensitivity, the sensitivity gradient is computed for a specific time within the time interval $[\,0, T\,]$. In other word the sensitivity of an instantaneous value of

function G is searched. For simplification the terminal time condition θ is implied as an explicit function with respect to the terminal time T, according to that Eq.(2.88) is prescribed to

$$\theta[\mathbf{q}(b_a); \dot{\mathbf{q}}(b_a); T; b_a] = 0 \tag{2.152}$$

At this point we can use the signal theory presented in the previous section. The functional of the structural response is considered as a series of successive impulses in infinitely small time. Treating t as the running terminal time and $\delta(t-\tau)$ as the Dirac-delta measure, we describe the structural response functional in the form [26]

$$\phi = \int_0^t G[q_\beta(b_a, \tau); b_a]\delta(t-\tau)\mathrm{d}\tau, \tag{2.153}$$

where $t \in [\,0, T\,]$; $\beta = 1, 2, ..., N$; $a = 1, 2, ..., A$. The function $G[\,q_\beta(b_a, \tau); b_a\,]$ is supposed to be continuous in the whole time interval $\tau \in [\,0, T\,]$.

Differentiating Eq. (2.153) with respect to design variables b_a, at a fixed $\tau = t$, gives

$$\frac{\mathrm{d}\phi}{\mathrm{d}b_a} = \frac{\partial G}{\partial b_a} + \int_0^t \frac{\partial G}{\partial q_\beta}\frac{\mathrm{d}q_\beta}{\mathrm{d}b_a}\delta(t-\tau)\mathrm{d}\tau \tag{2.154}$$

Using Eq. $(2.107)_1$ we have

$$\frac{\partial G(\tau)}{\partial q_\beta}\delta(t-\tau) = \frac{\partial G(t)}{\partial q_\beta}\delta(t-\tau) \tag{2.155}$$

Following the same lines as in Section 2.5.5. Eq. (2.145) is now rewritten for the new time condition $\tau \in [\,0, t\,]$ and $t \in [\,0, T\,]$, in the form

$$\begin{aligned} - \quad & (M_{\alpha\beta}\dot{\lambda}_\alpha - D_{\alpha\beta}\lambda_\alpha)\frac{\mathrm{d}q_\beta}{\mathrm{d}b_a}\bigg|_{\tau=t} + \int_0^t (M_{\alpha\beta}\ddot{\lambda}_\alpha - D_{\alpha\beta}\dot{\lambda}_\alpha + K_{\alpha\beta}\lambda_\alpha)\frac{\mathrm{d}q_\beta}{\mathrm{d}b_a}\mathrm{d}\tau \\ + \quad & M_{\alpha\beta}\lambda_\alpha\frac{\mathrm{d}\dot{q}_\beta}{\mathrm{d}b_a}\bigg|_{\tau=t} = \int_0^t \lambda_\alpha\left(\frac{\partial Q_\alpha}{\partial b_a} - \frac{\partial M_{\alpha\beta}}{\partial b_a}\ddot{q}_\beta - \frac{\partial D_{\alpha\beta}}{\partial b_a}\dot{q}_\beta - \frac{\partial K_{\alpha\beta}}{\partial b_a}q_\beta\right)\mathrm{d}\tau \end{aligned} \tag{2.156}$$

Improving the terminal time conditions

$$\lambda_\alpha(t) = 0 \ \text{ and } \ \dot{\lambda}_\alpha(t) = 0 \tag{2.157}$$

and comparing the terms involving $\mathrm{d}q_\alpha/\mathrm{d}b_a$ at $\tau \in [0, t]$ under integration from Eqs. (2.154) and (2.156), we get the adjoint equations of motion

$$M_{\alpha\beta}(b_a)\ddot{\lambda}_\alpha(\tau) - D_{\alpha\beta}(b_a)\dot{\lambda}_\alpha(\tau) + K_{\alpha\beta}\lambda_\alpha(\tau) = \frac{\partial G}{\partial q_\beta}\delta(t-\tau) \tag{2.158}$$

Substituting Eq. (2.158) into Eq. (2.156) and taking the terminal conditions (2.157) into account we get

$$\int_0^t \frac{\partial G}{\partial q_\beta}\delta(t-\tau)\frac{\mathrm{d}q_\beta}{\mathrm{d}b_a}\mathrm{d}\tau = \int_0^t \lambda_\alpha\left(\frac{\partial Q_\alpha}{\partial b_a} - \frac{\partial M_{\alpha\beta}}{\partial b_a}\ddot{q}_\beta - \frac{\partial D_{\alpha\beta}}{\partial b_a}\dot{q}_\beta - \frac{\partial K_{\alpha\beta}}{\partial b_a}q_\beta\right)\mathrm{d}\tau \tag{2.159}$$

that, substituted into Eq. (2.154), leads to the sensitivity gradient for the time instant sensitivity of the form

$$\frac{\mathrm{d}\phi}{\mathrm{d}b_a} = \frac{\partial G}{\partial b_a} + \int_0^t \lambda_\alpha(\tau)\left[\frac{\partial Q_\alpha(\tau)}{\partial b_a} - \frac{\partial M_{\alpha\beta}}{\partial b_a}\ddot{q}_\beta(\tau) - \frac{\partial D_{\alpha\beta}}{\partial b_a}\dot{q}_\beta(\tau) - \frac{\partial K_{\alpha\beta}}{\partial b_a}q_\beta(\tau)\right]\mathrm{d}\tau \tag{2.160}$$

for any fixed time $t \in [\,0, T\,]$.

2.6 A Model Numerical Examples

2.6.1 Three-Bar Truss System

Let us consider a three-bar truss structure presented in details in Fig. 2.14, that was described in [12]. The goal of this section is to obtain the values of nodal displacements and static design sensitivity for this system by POLSAP, and comparing them with the results given in [12].

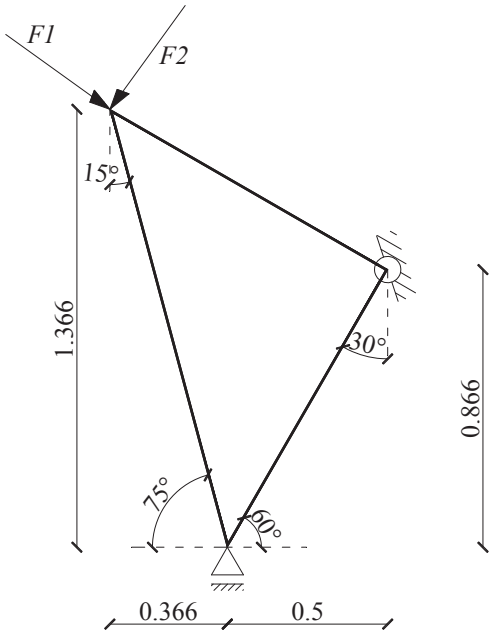

Figure 2.14 Three-bar truss structure dimensions

To simplify the process of entering the data into the program, three-bar truss from [12] is rotated, as it is shown in Fig. 2.14. Adopted FEM setting and global coordinate system is presented in Fig. 2.15. If we consider $F1 = F2 = 1$, the nodal forces are equal $Fx = 0.366$ and $Fy = 1.366$. To the numerical computations the following values are assumed, the cross-sectional areas of specific elements $A_1 = A_2 = A_3 = 1$, the Young modulus $E = 1$ and mass density $\varrho = 1$. To compare the results received from POLSAP with those given in [12], the latter must be multiplied by appropriate trigonometric functions of $\alpha = 30°$. Displacements obtained by POLSAP and from [12], are summarized in Table 2.1 for the coordinate system from Fig. 2.15.

Table 2.1 Nodal static displacements for three-bar truss system

node	coordinate	[12]	POSAP
1	x	1.4641	1.4639
	y	0.0000	0.0000
2	x	0.0000	0.0000
	y	0.0000	0.0000
3	x	−1.6822	−1.6821
	y	2.9136	2.9134

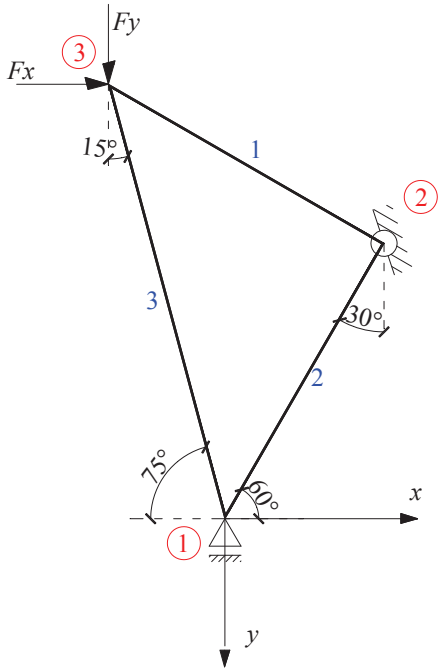

Figure 2.15 FEM setting and nodal forces

Table 2.2 includes the values of the static sensitivity of node displacements with cross-sectional areas of particular elements considered as design variables. During the numerical computation we received very similar results as in [12]. That proves the effectiveness of the presented analysis.

Table 2.2 Design sensitivity of node displacements with respect to cross-sectional area of specific elements

node	displacement direction	design sensitivity results [12]	POSAP
cross − sectional area of el.no. 1 as design variable			
1	x	0.000	0.000
3	x	0.000	0.000
3	y	0.000	0.000
cross − sectional area of el.no. 2 as design variable			
1	x	−1.4641	−1.4639
3	x	−0.2679	−0.2679
3	y	−0.4641	−0.4640
cross − sectional area of el.no. 3 as design variable			
1	x	0.000	0.000
3	x	−1.4142	−1.4142
3	y	−2.4495	−2.4494

Now, we are going to present the design sensitivity of the eigenvalue problem for this model. For this type of analysis according to [12], we adopted $E = 1$, $\varrho = 1$, $A_1 = A_2 = 1$ and $A3 = 2\sqrt{2}$. The first eigenvalues obtained by POLSAP including above characteristics is equal $\xi = 0.08036$ which is very similar to the result given by [12] $\xi_{[12]} = 0.08038$.

Table 2.3 presents the eigenvalue design sensitivity with respect to cross-sectional areas of specific elements, received by POLSAP. It should be noticed, that all results in this section are given for the global coordinate system presented in Fig. 2.15.

Table 2.3 Eigenvalue design sensitivity with respect to element cross-sectional areas

Design variable	POSAP
A_1	-0.0106
A_2	0.0294
A_3	-0.0785

2.6.2 Cantilever Beam - Eigenvalue Sensitivity

We present the numerical computations obtained for the cantilever beam shown in Fig. 2.16, the analytical results of this type of structure can be found in [12,23]. The following values are assumed during data processing: Youngh's modulus $E = 2.0E + 5$, Poisson's ration $\nu = 0.3$, mass density $\varrho = 7.87E - 4$, length of the beam $L = 1.0$, axial area $A = 0.005$, the moments of inertia $J_y = J_z = 4.17E - 5$ and the torsion moment $J_x = 8.35E - 5$.

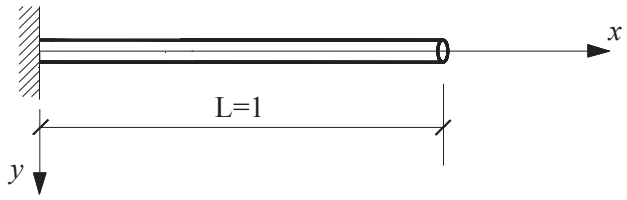

Figure 2.16 Cantilever Beam

The FEM model consisting of 100 beam elements is adopted during the numerical computations. The aim of the analysis is to find design sensitivity of eigenvalue with respect to the cross-sectional area of specific elements. Obtained results are shown in Fig. 2.17.

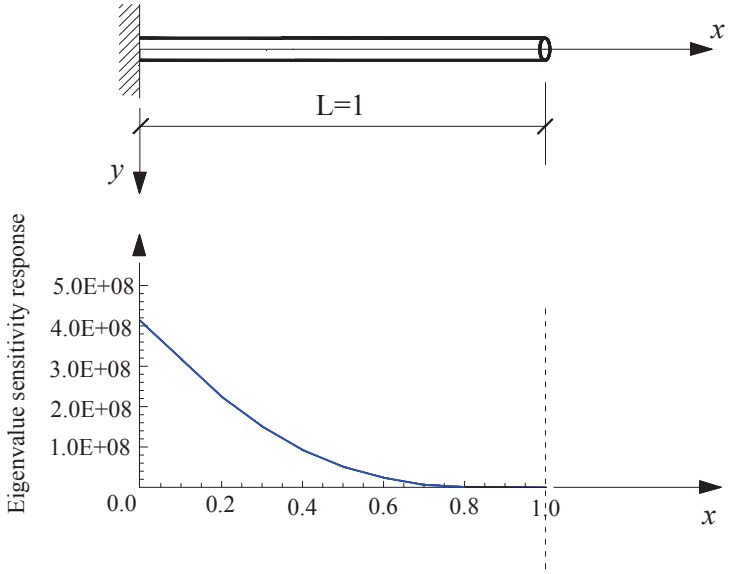

Figure 2.17 Design sensitivity of eigenvalue

The values presented in Fig. 2.17, are received with taking into account one eigenvalue in the numerical analysis. Maximum number of iterations required during data processing is 16, convergence of tolerance 1.0E-5. Considering Fig. 2.17, we may draw a conclusion that the first eigenvalue is more sensitive with respect to the change of cross-sectional areas of clamped end than the free one, which seems to be natural from the point of view of this structure work.

2.7 An Example of Deterministic Analysis of Cable-Stayed Bridges

2.7.1 Structure Description

Inspiration to creating the following model of cable-stayed bridge becomes the real structure named Seri Wawasan Bridge, located in Putrajaya, Malaysia. It was designed by PJS International Sdn. Bhd. and built by Muhibbah Engineering (M) Bhd. It has been in use since 2003 [72]. This asymmetric bridge resembles a sail ship, Fig. 2.18.

Figure 2.18 Seri Wawasan Bridge [72]

Its total length is equal 240m. Main span with dimensions 168.5x37.2m is suspended on 62 symmetrical steel cables to the inverted-Y pylon with 85m height. Additionally, the pylon is stabilized in its position by 58 steel ties with smaller cross-sectional areas, joined by hinges to the steel arches.

On the basis of gained information, the model with similar dimensions is created (cf. Fig. 2.19) — pylon, the main span and bridge's total length are equal 104m, 160m and 220m, respectively, while deck's total width is 40m. During static analysis all loads, characteristics of materials and requirements are selected according to the polish rules of civil engineering, as if the object was located in Poland.

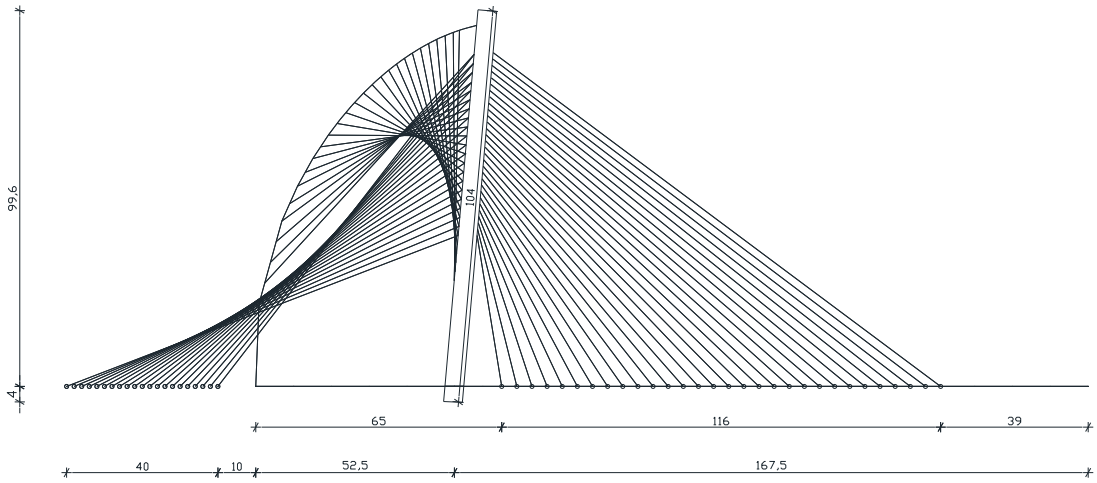

Figure 2.19 Main dimensions inputting to the programm [63]

For simplification instead of inverted-Y shape we accepted a non-forked pylon with a box cross-section. It is assumed to be fixed in the ground and supported by steel bars and arches, connected by hinges. Steel arches are also rigidly fixed. The main span besides the suspension on cables is supported in several points by pins.

Accepted static scheme is presented in Fig. 2.20

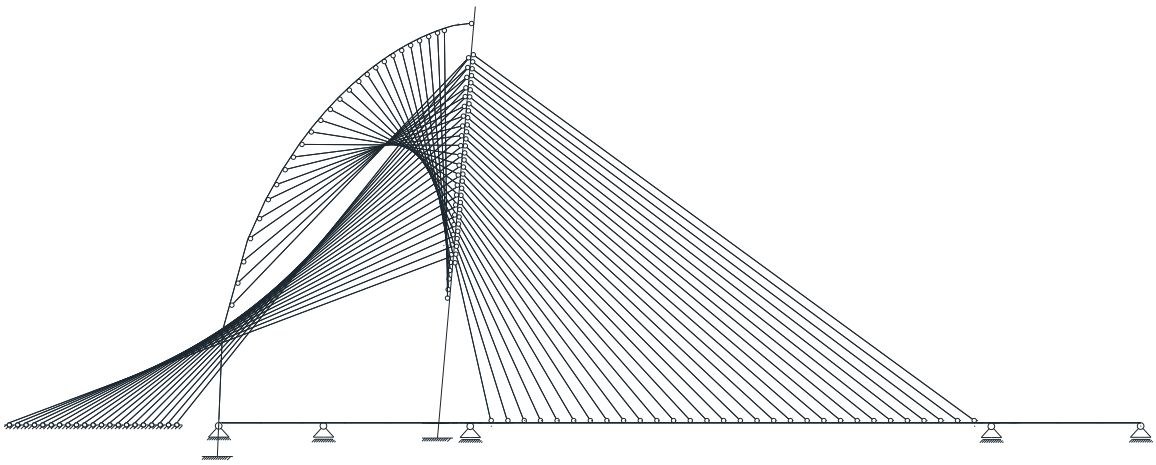

Figure 2.20 Accepted static scheme [63]

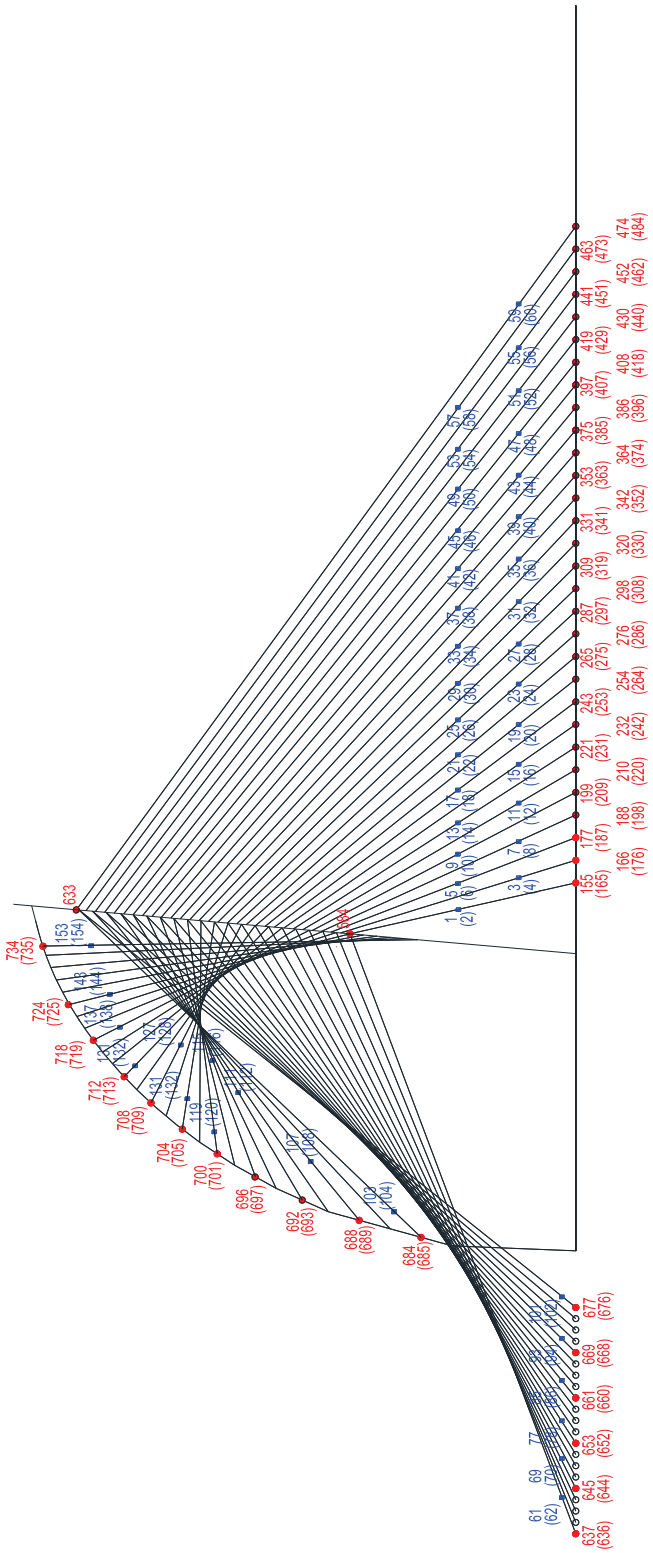

Figure 2.21 Truss elements

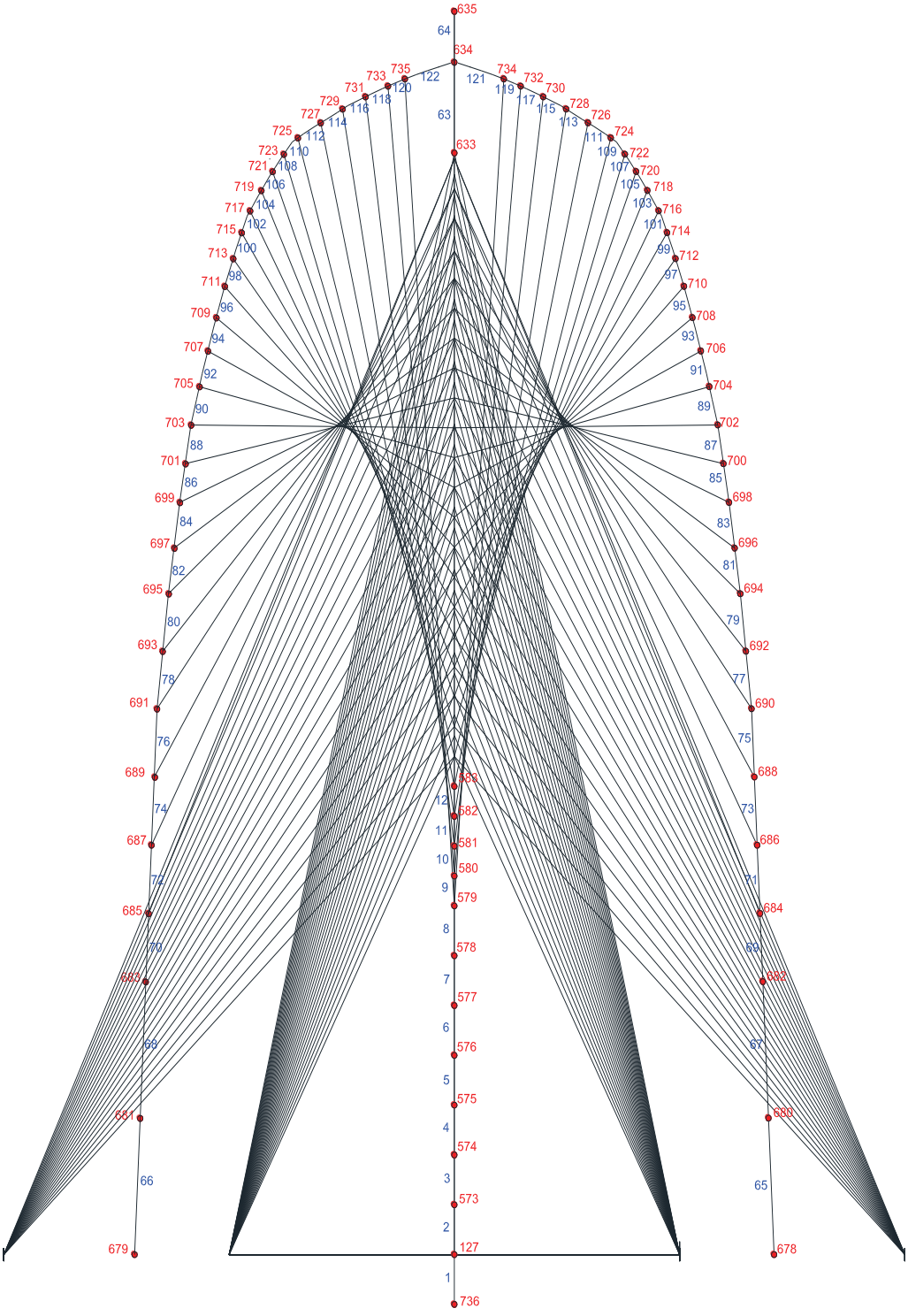

Figure 2.22 Beam elements

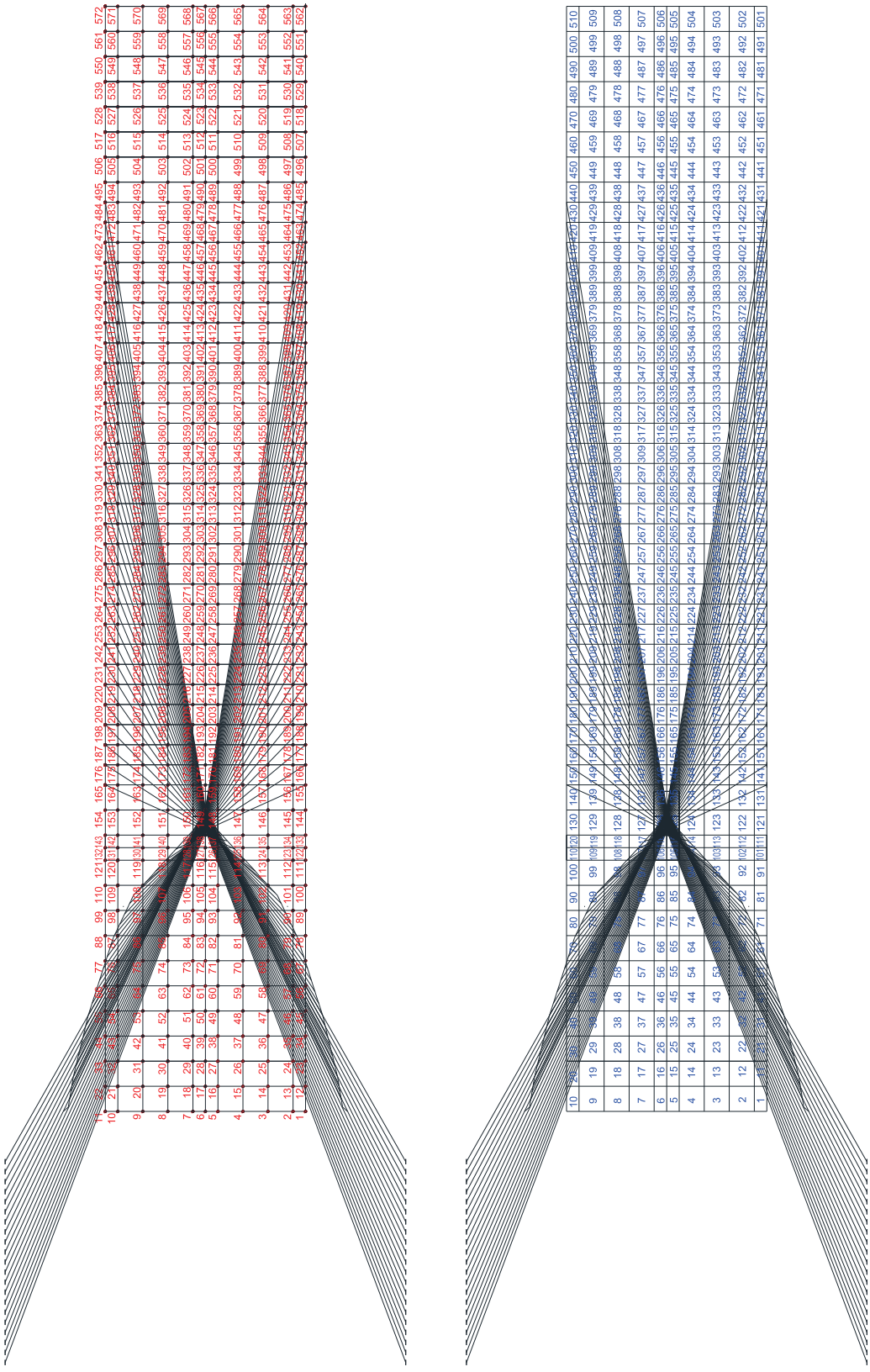

Figure 2.23 Shell elements[63]

2.7.2 Finite Element Mesh

The finite element setting is assumed on the basis of work manner of the main structural members, support conditions and type of connections [7,39,44,45]. The model of suspended-bridge is created by using three specific finite elements — truss, beam and shell.

Cables suspending the bridge and bars connecting the pylon with the arches are anchored by a hinge. Because, there are only axial forces, these members are implemented to the numerical programm as truss elements with total number 154. All details of their distribution are presented in Fig.2.21.

Suspended span is adopted as a reinforced concrete plate with the thickness equal 30cm, strengthened by steel ribs. The plate is divided into 510 rectangular shell elements cf. Fig. 2.23.

For simplification the pylon, arches and steel ribs are split into smaller beam elements in the number 675 (Fig. 2.22). According to the above mentioned assumptions, after complying boundary conditions, a system with 3536 degrees of freedom is obtained.

2.7.3 Geometry and Material Properties of Structural Members

In this section a short descriptions of cross-sectional areas chosen for main elements of the structures are presented. Additionally the geometrical and material characteristics for particular members of the object [7,10,19,21,41,47] that are put to the program at the stage of creating the model. All details of the equation that were used by determining the obtained values can be found in [63].

2.7.3.1 Pylon

Seri Wawasan Bridge becomes an inspiration of making this examples, however in the process of creating the model, the concept of the pylon with the shape of an inverted-Y, is rejected. For simplification of the scheme the caisson cross-section, that is presented n Fig.2.24, is assumed.

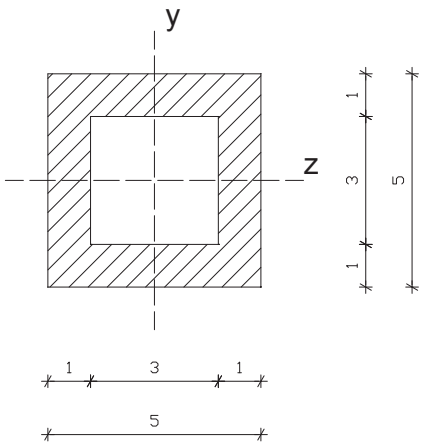

Figure 2.24 Adopted caisson cross-section of the pylon [m]

For the proper giving the characteristics of the adopted cross-section, that are input data to the numerical programm, the local axis ordination of the element needs to be defined. Therefore they can be found in Fig. 2.25.

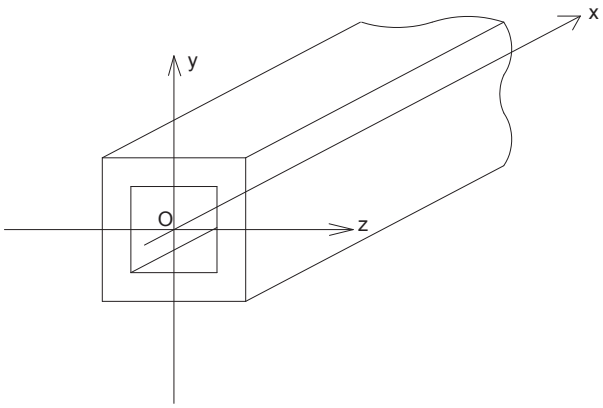

Figure 2.25 Pylon's local coordinate system

Moments of inertia with respect to local axis [52], presented in Fig. 2.25, read

$$J_{py} = J_{pz} = \frac{5 \times 5^3}{12} - \frac{3 \times 3^3}{12} = 45,33(3)\,\mathrm{m}^4$$
$$J_{px} = 45,33 + 45,33 = 90,66\,\mathrm{m}^4$$

The cross-section area of the considered element is expressed by the equation

$$A_p = 5 \times 5 - 3 \times 3 = 16\,\mathrm{m}^2$$

Assuming that $\gamma_{pm} = 25\ \mathrm{kN/m}^3$ is the self weight of reinforced concrete, and γ_f is the safety coefficient, the characteristic G_{pk} and computational G_{pd} values of pylon's dead load are equal respectively

$$G_{pk} = A_p \gamma_{pm} = 16 \times 25 = 400\,\mathrm{kN/m}$$
$$G_{pd} = A_p \gamma_{pm} \gamma_f = 16 \times 25 \times 1,2 = 480\,\mathrm{kN/m}$$

2.7.3.2 Arches

It is possible to model lengthwise variable cross-section of the arches by using shell elements, but this approach will make the computation much more complicated. Therefore, the constant values of the arches' cross-section area are adopted to the input data — see Fig. 2.26.

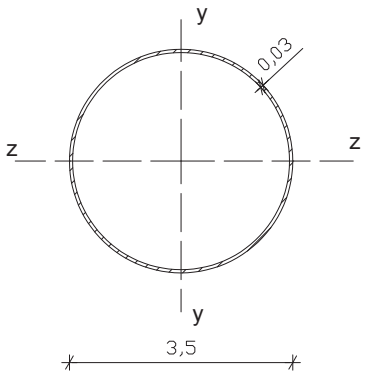

Figure 2.26 Accepted pipe cross-section of the arches [m]

The characteristics for the described beam element are obtained on the basis of following local coordinate system — Fig. 2.27.

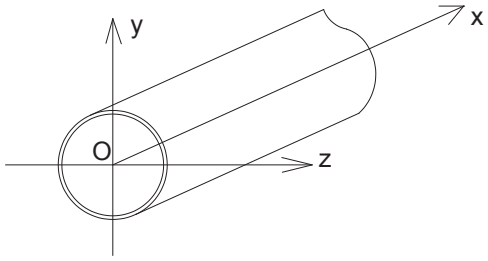

Figure 2.27 Local axis ordination in the arches' beam elements

Moments of inertia received for local axes from Fig. 2.27 are equal

$$J_{ay2} = J_{z2} = \frac{\pi}{4}(1,75^4 - 1,72^4) = 0,4922684758\,\mathrm{m}^4$$
$$J_{ax2} = 0,4922684758 + 0,4922684758 = 0,9845369516\,\mathrm{m}^4$$

The cross-section area of the single arch is given by the below formula

$$A_a = \pi(1,75^2 - 1,72^2) = 0,32704\,\mathrm{m}^2$$

It should be noticed that the most suitable material for the structure with this kind of shape is steel. Therefore for gaining the characteristic and computational values of arch's dead load — G_{ak} and G_{ad}, the unit-volume weight $\gamma_{am} = 78,5\ \mathrm{kN/m^3}$ is assumed

$$G_{ak} = A_a\gamma_{am} = 0,32704 \times 78,5 = 25,67\,\mathrm{kN/m}$$
$$G_{ad} = A_a\gamma_a m\gamma_f = 0,32704 \times 78,5 \times 1,2 = 30,81\,\mathrm{kN/m}$$

2.7.3.3 Span

In the created model of suspended bridge, the following dimensions of main span are adopted: width — 40 m, total length — 220 m. At first, it was designed as a reinforced concrete plate with the thickness equal 30 cm. Due to the large values of obtained vertical displacements from the static loads, the plate is strengthened with longitudinal and crosswise steel ribs. When entering the model to the program some simplifications are applied. We assumed that the thickness center of the plate coincide with the middle points of the ribs' hight — mentioned problem is illustrated in Fig. 2.28. Accurate reflection of the span's work and connection between the elements may encounter many problems and makes the computations much more time-consuming.

The necessary input data for the plate are the components of constitutive matrix (see section 2.1), that can be expressed by the equation

$$\begin{bmatrix} \sigma_{xx} \\ \sigma_{yy} \\ \sigma_{xs} \end{bmatrix} = \begin{bmatrix} C_{xx} & C_{xy} & C_{xs} \\ & C_{yy} & C_{ys} \\ \text{sym.} & & G_{xy} \end{bmatrix} \begin{bmatrix} \epsilon_{xx} \\ \epsilon_{yy} \\ \gamma_{xs} \end{bmatrix}$$

During following data processing, the maximum vertical displacement of the plate turns out to be to large. Therefore by the council from the experts, we took characteristics of special composite material:E =10000 $\frac{\text{kN}}{\text{cm}^2}$ and $\nu = 0,25$ for research. Using this values the particular terms of constitutive matrix are obtained

$$C_{xx} = C_{yy} = \frac{E}{1-\nu^2} = 10666,67\frac{\text{kN}}{\text{cm}^2}$$
$$C_{xy} = \frac{E\nu}{1-\nu^2} = 2666,67\frac{\text{kN}}{\text{cm}^2}$$
$$C_{xs} = C_{ys} = 0$$
$$G_{xy} = \frac{E}{2(1+\nu)} = 4000\frac{\text{kN}}{\text{cm}^2}$$

Assuming $\gamma_{plm} = 25\ \text{kN/m}^3$, and plate's thickness $d = 30cm$, we obtain the characteristic and computational values of plate's dead load

$$G_{plk} = d\gamma_{plm} = 0,30 \times 25 = 7,5\,\text{kN/m}^2$$
$$G_{pld} = d\gamma_{plm}\gamma_f = 0,30 \times 25 \times 1,2 = 9,00\,\text{kN/m}^2$$

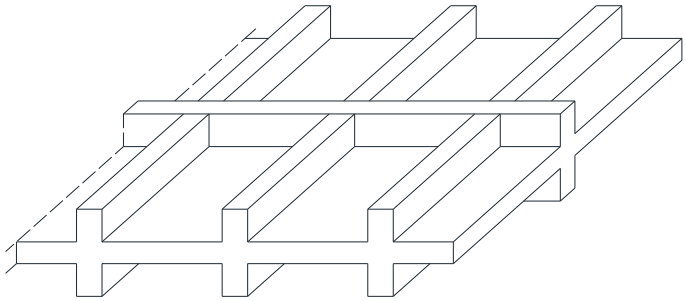

Figure 2.28 Simplified view of plate model design for the experiment

2.7.3.4 Ribs

The plate is strengthened by steel instead of reinforced concrete ribs, according to Fig. 2.29.

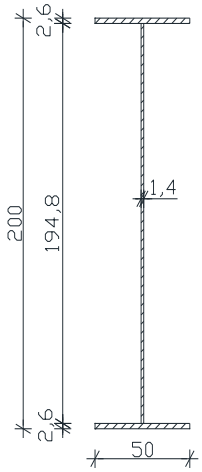

Figure 2.29 Dimensions of rib's cross-sections [cm]

Geometry properties are adopted on the basis of [8]. Moments of inertia are equal respectively

$$\begin{aligned} J_{ry} &= 3395400\,\mathrm{cm}^4 \\ J_{rz} &= 54210\,\mathrm{cm}^4 \\ J_{rx} &= J_{ry} + J_{rz} = 3449610\,\mathrm{cm}^4 \end{aligned} \tag{2.161}$$

Cross-section area for element from Fig. 2.23 is

$$A_r = 532\,\mathrm{cm}^2$$

Values of rib's dead load are given in the form

$$\begin{aligned} G_{rk} &= = 4,256\,\mathrm{kN/m} \\ G_{rd} &= G_{rk}\gamma_f = 4,256 \times 25 \times 1,2 = 5,1072\,\mathrm{kN/m} \end{aligned}$$

2.7.3.5 Cables

In data processing the ropes in the form of seven galvanized wires ϕ5mm in the HDPE coat, are adopted — see Fig. 2.30. This type of cables are the most widespread. The main material characteristics are assumed on the basis of [7,38]: yield stress — $\sigma_c = 1670\,\mathrm{MPa}$, breaking strength — $R_{pk} = 1870\,\mathrm{MPa}$, and elasticity modulus — $E_c = 200\,\mathrm{GPa}$.

Appointing the necessary values of cross-section areas the main cables is a quite complex issue and for this example it is shown in details in [63]. This values for particular cables are between $25,57\mathrm{cm}^2$ and $38,29\mathrm{cm}^2$. For simplification, the constant values of cross-section areas of these suspension structures are adopted. In receiving the necessary areas of cables, the load of the reinforced ribs is not included, the larger cross-section is accepted in the computations $A_c = 63,02\,\mathrm{cm}^2$.

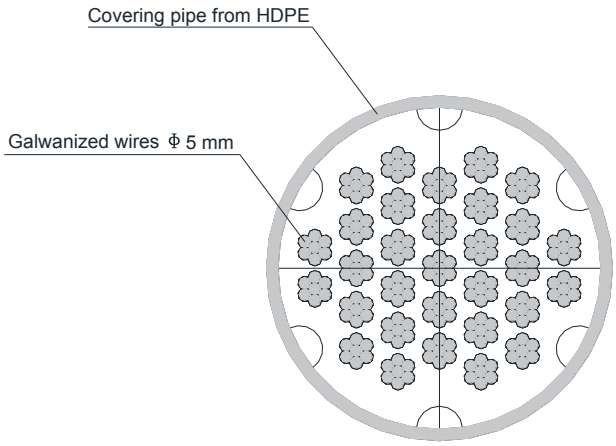

Figure 2.30 Exemplary cable's cross-section

The second ties' group that connect the pylon and arches is less strenuous than the main cables, therefore the solid bar with 36mm diameter is adopted to the computation , $A_{c2} = 10,18\,\mathrm{cm}^2$. According to [7], the Young'h modulus $E = 210\mathrm{GPa}$ for these elements is implied.

2.7.4 Loading Combinations

In order to perform the static analysis for the previously described bridge, the following loads need to be taken into account: constant load from the weight of bridges' elements, surface load from systems of roadway and pavement's layers, but also moving, crowd and wind load.

2.7.4.1 Constant surface load

Figs. 2.31 present the system of roadway and pavement's layers with the values of thickness. On this basis and using simultaneously the provisions contained in the polish rules of civil engineering [69,70], the characteristic and computational values of particular loads are received. They are summarized in tables 2.4 and 2.5.

a)

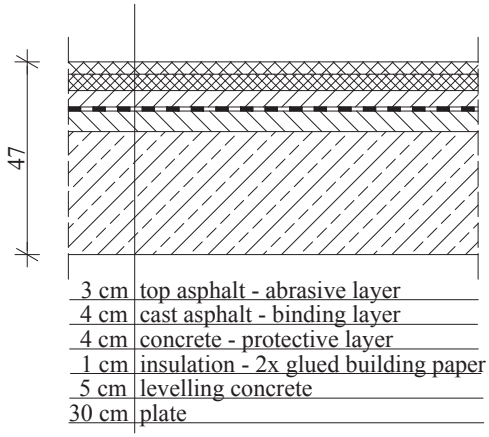

b)

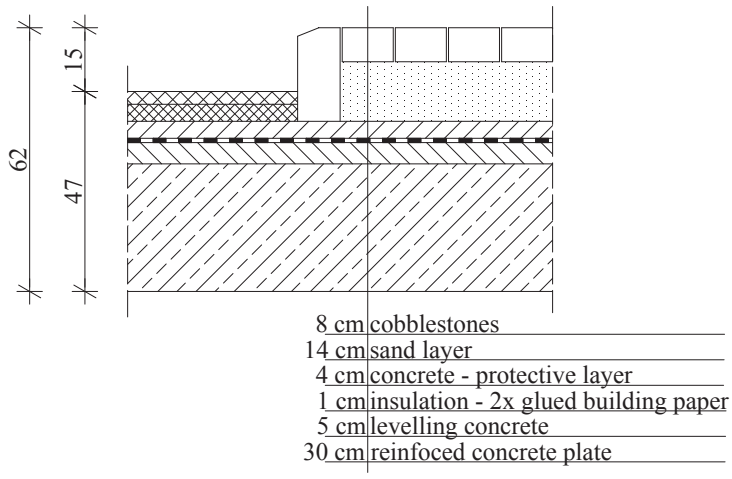

Figure 2.31 The system of a) roadway's layers; b) pavement's layers

Table 2.4 Loads from the roadway layers

Layer	Thickness [m]	γ_m [kN/m^3]	Characteristic load [kN/m^2]	γ_f	Computational load [kN/m^2]
1. Plate	0.30	25	7.50	1.2	9.000
2. Leveling concrete	0.05	24	1.20	1.5	1.800
3. Insulation	0.01	14	0.14	1.50	0.210
4. Concrete	0.04	24	0.96	1.50	1.440
5. Cast asphalt	0.04	23	0.92	1.5	1.380
6. Top asphalt	0.03	23	0.69	1.5	1.035
			$\sum g_{1k} = 11.41$		$\sum g_{1d} = 14.865$

The above computation are subsequently repeated to obtain the loads from pavement's system.

Table 2.5 Pavement layers' design data

Layer	Thickness [m]	γ_m [kN/m^3]	Characteristic load [kN/m^2]	γ_f	Computational load [kN/m^2]
1. Reinforced concrete plate	0.30	25	7.50	1.2	9.00
2. Leveling concrete	0.05	24	1.20	1.5	1.80
3. Insulation	0.01	14	0.14	1.5	0.21
4. Concrete	0.04	24	0.96	1.5	1.44
5. Sand layer	0.14	17	2.38	1.5	3.57
6. Cobblestones	0.08	27	2.16	1.5	3.24
			$\sum g_{2k} = 14.34$		$\sum g_{2d} = 19.26$

2.7.4.2 Constant Linear Load

When the surface loads are obtained it is necessary to add the linear load from a kerbstone and a cornice. Received values are summarized in Table 2.6.

Table 2.6 Constant linear load

Element	Size of cross-section [mxm]	γ_m [kN/m^3]	Characteristic load [kN/m]	γ_f	Computational load [kN/m]
Kerbstone	0.1x0.22	27	0.594	1.5	0.891
Cornice	0.15x0.77	25	2.88	1.5	4.331

2.7.4.3 Moving Load of Road Bridge Objects and Crowd Load

Due to the fact that the considered object is a road bridge, the crowd and moving load need to be taken into account [7,69]. The specific moving load is presented in simple form in Fig. 2.32.

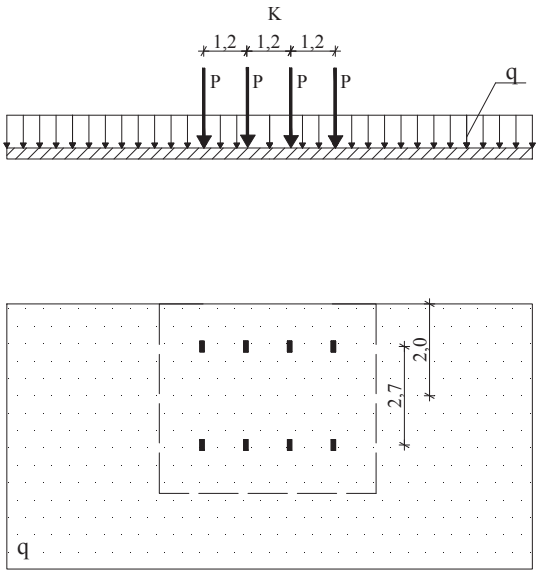

Figure 2.32 Moving load on the fragment of the span

For this structure A class of object is adopted. Therefore the following values of constant loads are applied [69]:
— $\mathrm{q} = 4,0\mathrm{kN/m}^2$ - for main elements
— $\mathrm{K} = 800\mathrm{kN}$ - car's train
— $P = 200kN$ - pressure on axle

All details for the above calculations can be found in [63]. Assuming dynamic coefficient $\varphi = 1.0$ [69], and safety factor $\gamma_f = 1,5$ the computational values of the obtained loads are equal

$$q_d = 6\,\mathrm{kN/m}^2$$
$$P_{obl} = 200 \times 1.5 \times 1.0 = 300\,\mathrm{kN}$$

The crowd pressure on the pavement is included as a constant surface load. Using safety factor $\gamma_f = 1.3$ and [69] we receive

$$q_{tk} = 2,5\frac{\mathrm{kN}}{\mathrm{m}^2}$$
$$q_{td} = 3,25\frac{\mathrm{kN}}{\mathrm{m}^2}$$

2.7.4.4 Static Wind Load

Because of scientific research character of this paper, the static wind effect is adopted including some simplifications [7]. Examples of loads acting on different parts of the bridge are illustrated in Fig. 2.33.

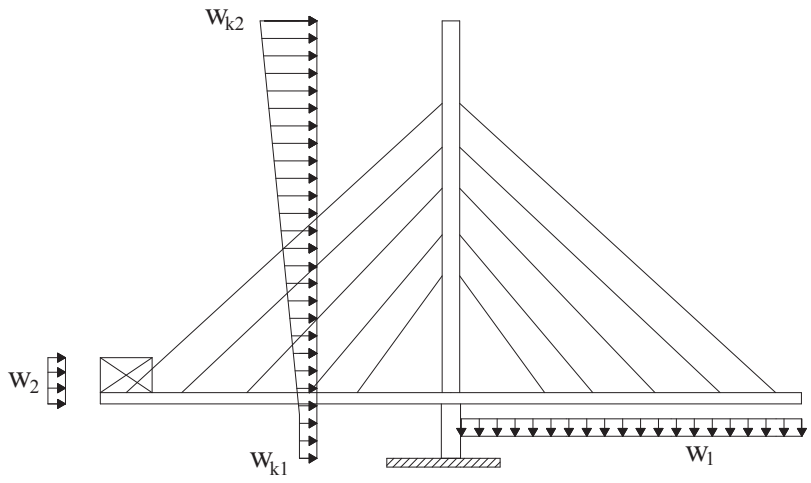

Figure 2.33 Cases of wind load

To obtain the above presented values of wind, the location of the object is necessary to be chosen. During data processing, we decided that this suspended bridge will be designed for the Szczecin conditions. The safety factor for the wind influence is equal 1.3. Characteristic and computational values of particular wind loads on the plate are:$w_{1k} = 0$, 5kPa, $w_{1d} = 0$, 65kPa, $w_{2k} = 1$, 25kPa, $w_{2d} = 1$, 625kPa. The static values of the wind load on the pylon are accepted according to Fig. 2.34.

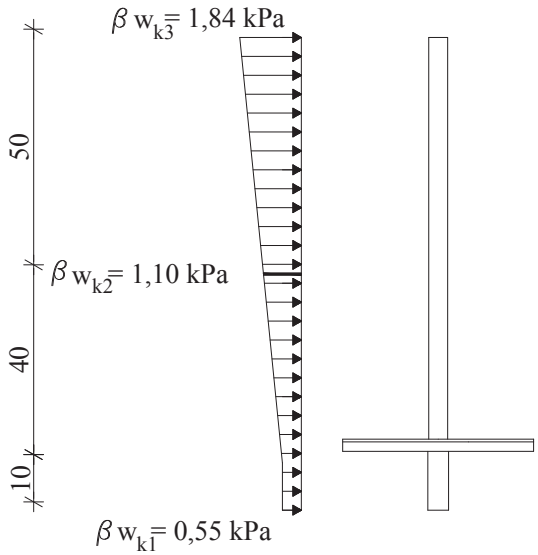

Figure 2.34 Static wind load on the pylon

During data processing, this pressure is reduced to the concentrated forces put in the nodal points.

2.7.5 Static analysis

Because of the theoretical character of this dissertation, the static analysis is made with some simplification. Displacements and internal forces are obtained for the maximum combination

of the previously described loads: dead weight of the main parts of the system, moving loads of road bridge object, crowd and static wind pressures. In the case of real structure designing it would be necessary to include additionally: weight of the equipment elements, thermal impacts, installation load at different stages of construction, internal forces created as a result of changing the static scheme caused by damage of the cable, difference in supports subsidence, dynamic wind and rain influences (specific loads for the suspended bridge).

It should be noticed, that various combinations of the above cases need to be considered in real designing of this type of bridge. However the goal of this example is to show in details the dynamic and sensitivity results for suspended bridge. Therefore, the statics is used to confirm the validity of the adopted scheme and cross-section areas of main elements. Because of symmetry of the bridge with respect to x axis, the results of displacements and internal forces obtained for the corresponding nodes should be equal.

Statics is the analysis which encounter many model problems associated with too large values of received displacements in the span. Using in the bridge only reinforced concrete plate suspended on the cables, makes the maximum vertical movement reach about 9 meters. To stiffen the main span, seven longitudinal rows of steel ribs were designed and spacing of transverse ribs ranges from 4 to 5 meters. Unfortunately, the treatment improved the situation but did not give fully expected results. By the council of experts instead of the reinforced concrete for the plate the modern composite material is used, with the properties assumed as follows: Young modulus — $E = 100$GPa, Poisson's ratio — $\nu = 0,25$. The composite is generally the specific material strengthened by glass, graphite or carbon fibers. It is relatively expensive and therefore rarely used in civil engineering, but has much better mechanical and strength features and at the same time has a low specific gravity. However, in spite of the structural material change, deflection of the span was still to large.

Only assistance from the members of the Building Mechanic Unit in Szczecin West Pomeranian University of Technology allowed to find a solution of this issue. The large dimensions of the bridge cause the length of main cables reach even up to 150m. It turns out that the cables do not fulfill their function and work like springs. It proved necessary to apply initial tension of those structures to minimize the span's displacements. To accomplish this, vertical forces imitating the initial tension were placed at the pylon and plate, by using the experimental method. Some methods about the modeling of bridges initial tension can be found in [46]. This treatment not only reduced the deflection of suspended part of the span, but also resulted in getting the greater part of the load by a plate's fragment rested on supports. The summation of the final displacements in selected nodes obtained after assuming the composite plate strengthened by longitudinal and transverse ribs, is presented in table 2.7. The results include the implied initial tension to the suspended part of the bridge.

If we look at many model problems that were encountered in static analysis, we come to the conclusion that the initial up-deflection of the span, should be considered in this type of structure. Properly matched bent arrow may reduce the values of vertical displacements. The results received for the nodes from plate that are given in table 2.7, confirm correctness of the adopted system — symmetrical points have the same values of movements. It can be also noticed that the closer to the fixed end of the pylon and the arches the lover values of x- and z-displacements are. On this basis we may conclude that the accepted model works properly. In tables 2.8 and 2.9 the internal forces obtained for the selected points in beam and plate elements are presented.

Table 2.7 Displacements of the representative nodal points in different part of the structure

Nodal point	X Translation [cm]	Y Translation [cm]	Z Translation [cm]	XX Rotation [rad]	YY Rotation [rad]	ZZ Rotation [rad]
a) pylon						
635	9.411E-01	-9.150E-13	-4.451E-01	1.846E-16	3.228E-05	4.780E-16
610	7.061E-01	-4.390E-13	-3.888E-01	1.555E-16	1.005E-04	3.292E-16
580	2.969E-01	-9.370E-14	-2.321E-01	7.470E-17	1.229E-04	1.504E-16
b) plate — max. static displacements						
309	1.745E-02	4.472E-04	-8.985E-01	-3.453E-02	-8.047E-04	0.0
310	1.744E-02	3.585E-04	-9.561E+00	-3.407E-02	-8.493E-04	0.0
311	1.733E-02	2.388E-04	-2.503E+01	-2.776E-02	-6.448E-04	0.0
312	1.722E-02	1.419E-04	-3.693E+01	-1.871E-02	-3.805E-04	0.0
313	1.716E-02	4.747E-05	-4.289E+01	-5.256E-03	-3.120E-04	0.0
314	1.715E-02	-1.188E-15	-4.350E+01	-1.090E-16	-3.207E-04	0.0
315	1.716E-02	-4.747E-05	-4.289E+01	5.256E-03	-3.120E-04	0.0
316	1.722E-02	-1.419E-04	-3.693E+01	1.871E-02	-3.805E-04	0.0
317	1.733E-02	-2.388E-04	-2.503E+01	2.776E-02	-6.448E-04	0.0
318	1.744E-02	-3.585E-04	-9.561E+00	3.407E-02	-8.493E-04	0.0
319	1.745E-02	-4.472E-04	-8.985E-01	3.453E-02	-8.047E-04	0.0
c) arches						
682	-2.376E-01	-2.573E-01	-6.056E-02	2.221E-04	3.834E-05	6.001E-05
683	-2.376E-01	2.573E-01	-6.056E-02	-2.221E-04	3.834E-05	-6.001E-05
702	1.726E+00	-1.200E+00	-9.793E-01	2.551E-04	4.810E-04	3.456E-04
703	1.726E+00	1.200E+00	-9.793E-01	-2.551E-04	4.810E-04	-3.456E-04
724	1.582E+00	-4.747E-01	-1.064E+00	2.106E-04	-2.043E-04	5.677E-04
725	1.582E+00	4.747E-01	-1.064E+00	-2.106E-04	-2.043E-04	-5.677E-04

Summing up this part of computations, despite many problems that were encountered in creating the model, the issue of inputting the initial tension of the cables in suspended bridges and increasing stiffness of the plate, is very interesting and gives many prospects in future works. It is undoubtedly worth to be developed in further research.

Table 2.8 Internal forces in the representative beam elements

Element number	XX Axial Force [kN]	YY Shear Force [kN]	YY Shear Force [kN]	XX Bending Moment [kNcm]	YY Bending Moment [kNcm]	XY Torsion Moment [kNcm]
10	2.677E+04	8.474E+01	1.446E-12	-7.966E-07	-3.648E-07	2.299E+05
	-2.677E+04	-8.474E+01	-1.446E-12	7.966E-07	3.648E-07	-2.095E+05
64	0.000E+00	-1.310E-10	7.782E-12	-3.078E-10	-2.134E-09	8.475E-08
	0.000E+00	1.310E-10	-7.782E-12	3.078E-10	-1.223E-09	1.546E-07
121	6.956E+01	5.870E+02	3.146E+01	5.285E+04	-2.266E+05	-2.544E+05
	-6.956E+01	-5.870E+02	-3.146E+01	-5.285E+04	2.002E+05	7.473E+05

Table 2.9 Internal forces in the representative plate elements

Element number	XX Membrane Stress [kN/cm^2]	YY Membrane Stress [kN/cm^2]	YY Membrane Stress [kN/cm^2]	XX Bending Moment [kNcm]	YY Bending Moment [kNcm]	XY Torsion Moment [kNcm]
85	1.784E-03	5.365E-03	-1.845E-03	-1.548E+02	4.970E+01	-2.259E+01
195	1.890E-02	1.989E-03	-2.307E-04	-1.926E+02	-3.908E+02	1.713E+01
315	1.214E-02	1.307E-03	-1.187E-04	-1.500E+02	-4.923E+02	-5.341E+00
475	7.661E-04	-7.193E-04	-1.208E-04	-3.522E+02	-9.312E+01	5.104E+00

2.7.6 Dynamic Analysis

The road suspended bridge is a special example of structure, therefore in practice it may be exposed to various dynamic loads, for example:
— influence of wind and rain,
— forces from a sudden movement of vehicle,
— vehicles colliding into bridge's structure,
— vibrations induced by a crowd of pedestrians,
— earthquakes, etc.
These problems are very complex and their analysis requires comprehensive knowledge, experiences and especially an engineering instinct. However not only the above-mentioned types of loads should be included. In the age of uncertain times, terroristic threat is equally likely as the earthquake, therefore dynamic analysis in this kind of objects seems to be necessary. In research we decided to consider a case of a sudden hit of a constant force during 40seconds. The impulse with the value of 10000kN is applied at the top of the pylon, parallel to the longitudinal axis of the bridge (cf. Fig. 2.35). We justify this choice by the fact, that the loads given this way may cause the largest damage of the structure, in our opinion.

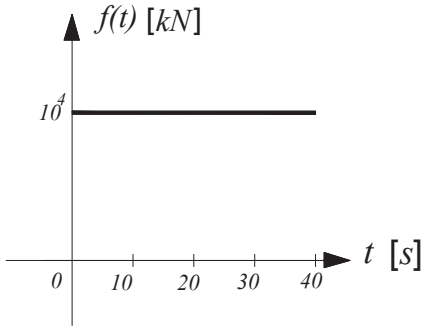

Figure 2.35 Dynamic force

The eigenproblem is solved for the first 12 eigenpairs and convergence is reached at the iteration step no. 11. The number of most dominated eigenvalues is 12. Maximum number of iteration required during the data processing is adopted as 20. The tolerance convergence is equal 1e-05. The results of the first seven circular frequencies and their corresponding periods are presented in Table 2.10, compare [64].

Dynamic analysis is made by the mode superposition method with 10000 time steps Δt with $0,004$s, each. The obtained results are presented for two approaches, with and without including the modal damping coefficient $\lambda = 0.01$. Dynamic longitudinal displacements are the largest for the top of the pylon (node 635), where the impulse of excitation is put. This seems to be natural for two reasons, the time-dependent force acts on this node and it is the highest point in the pylon, that is fixed in the ground. What was predictable, under the dynamic force the most significant vertical vibrations occur in the middle of the suspended part of the plate, while in other points are slight. The static analysis shows that the largest z-axis displacement takes place in the middle point of the plate — node 315, however the most significant dynamic movement turns out to be in node 358, therefore this point is chosen to present further computation results.

Table 2.10 Circular frequencies and periods of the undamped system

Mode number	Circular frequency [rad/s]	Period [s]
1	4.68	1.34
2	4.97	1.26
3	7.14	0.88
4	7.77	0.81
5	8.06	0.78
6	10.60	0.59
7	11.52	0.55

Fig. 2.35 shows the time-dependent vertical displacement for the chosen node of the plate and longitudinal displacement for the selected point of the pylon. Looking at these graphs, the specific course of vibrations can be noticed. Namely, the amplitude is changing periodically in time. This may indicate the presence of the beat effect in our model. This phenomenon is often observed in structures with regular, repetitive segments of geometry and for this type of objects it is a consequence of overlapping vibrations with almost equal frequencies. Considering the results from Table 2.10, it can be seen that the two adjacent frequencies have very similar values.

From the point of view of the material fatigue the beat phenomenon may be treated as an undesirable effect, and therefore in some cases it must be eliminated. It is commonly known, that if we consider the work of a real structure it is impossible to observe the time-dependent displacements without damping influence, because of many factors that are involved in. During the numerical computations, the elements that inhibit the vibrations are taken into account by the modal damping coefficient $\lambda = 0.01$.

Looking at the Fig. 2.35, one can mistakenly draw a conclusion about damping being sufficient to eliminate the beat effect. However if we see at the graphs that present time-dependent internal forces (compare figs. 2.31-2.32), it is noticeable that the use of coefficient λ results in gradual decay of vibration but the periodical changes of the amplitude are still present. Further attempts to avoid the beat phenomenon are taken by analysis of the symmetrical bar dome and are described in details in section 3.6.

Fig. 2.37 shows the internal forces for the selected beam elements in the pylon. The component no. 10 is in one third of the height measured from the fixed end in the ground, while the 64'th is on the top.

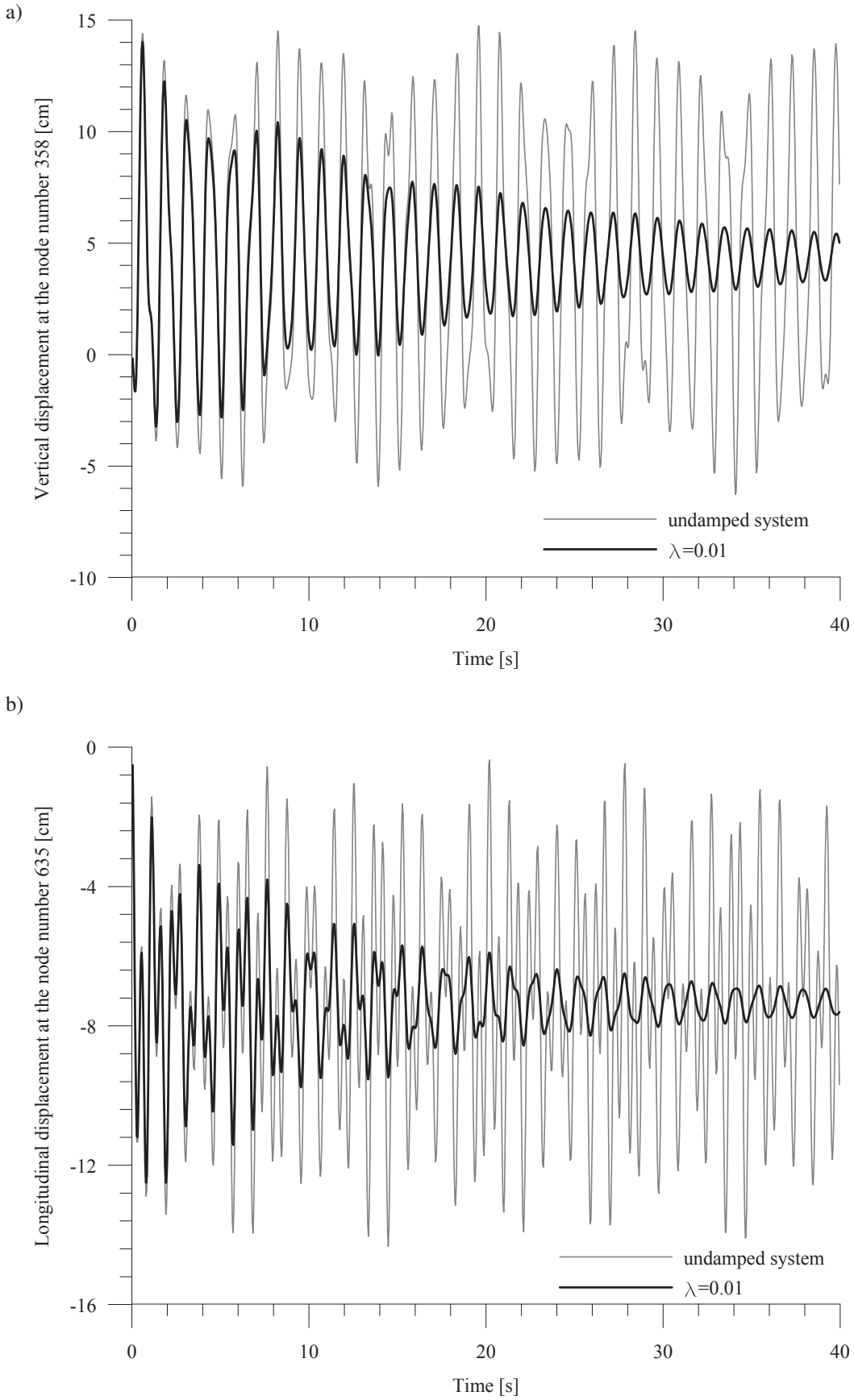

Figure 2.36 a) Vertical displacements at the mid point of the plate; b) Longitudinal displacements at the top of the pylon

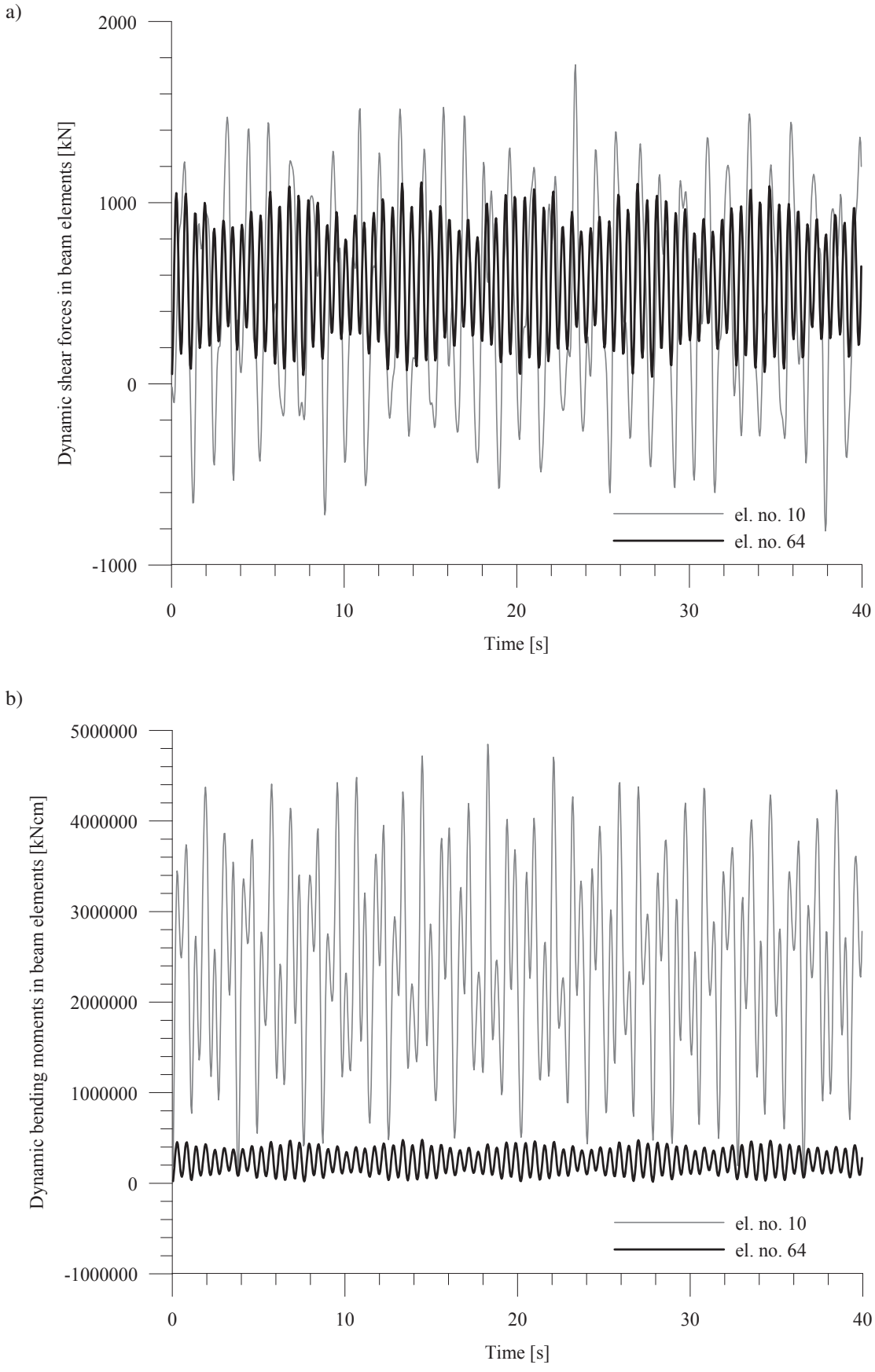

Figure 2.37 Dynamic internal forces in selected pylon's beam elements a) shear forces; b) YY-bending moments

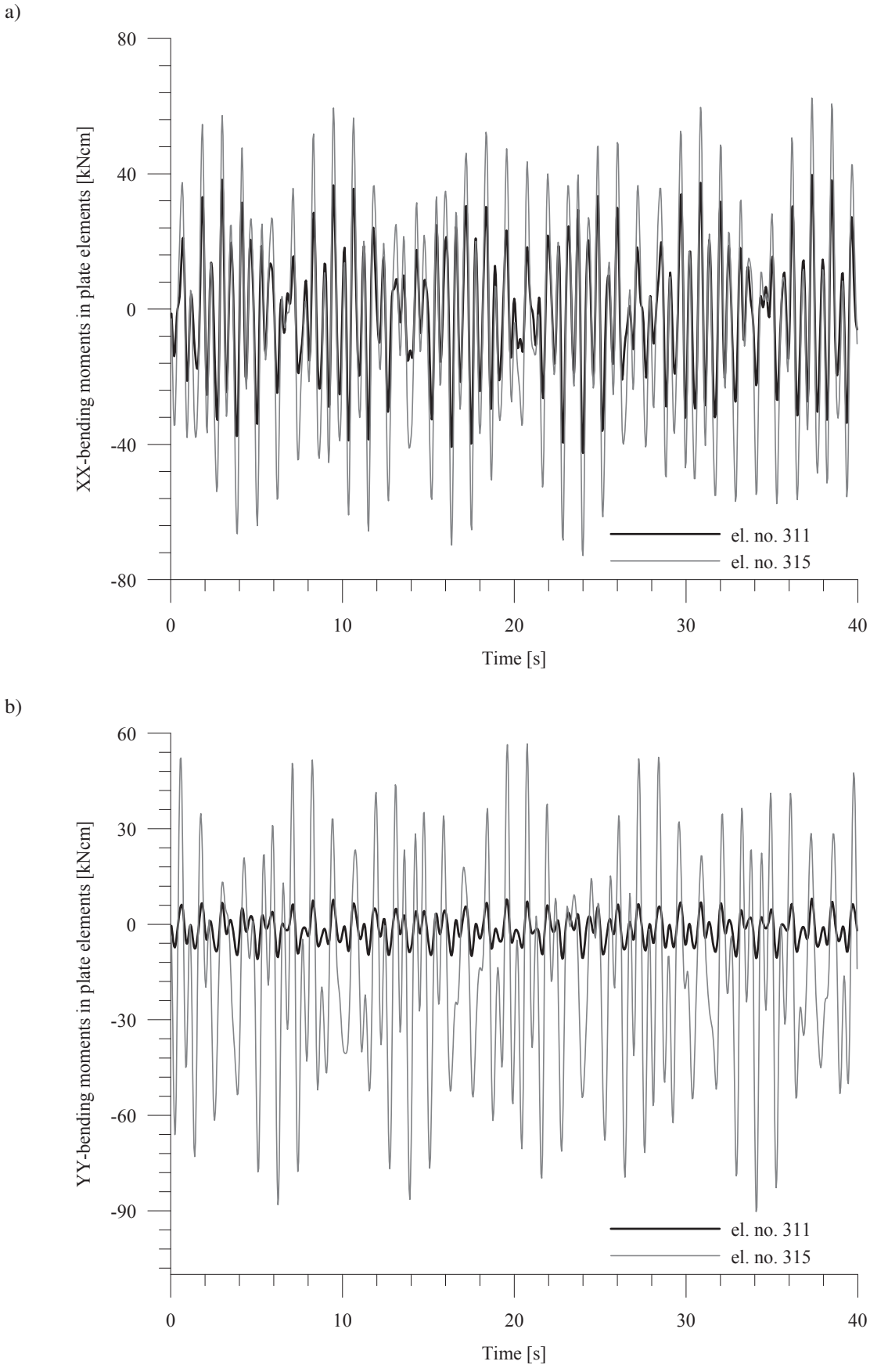

Figure 2.38 Dynamic bending moments in selected plate's elements a) XX; b) YY

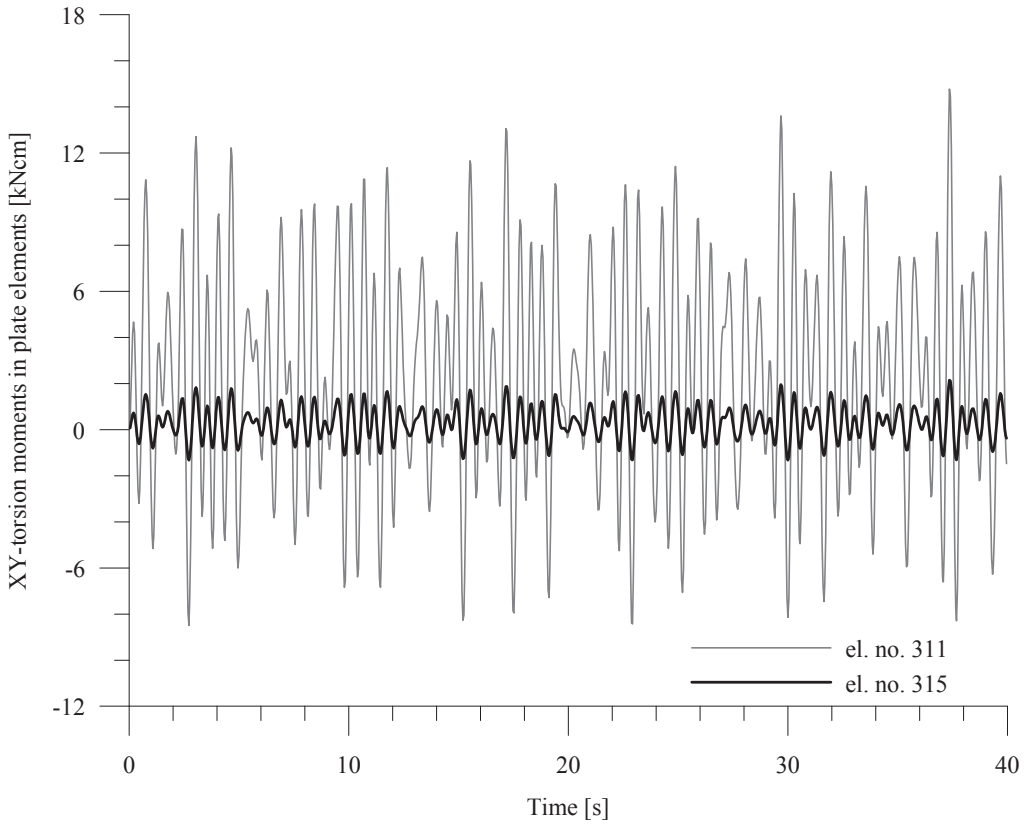

Figure 2.39 XY-torsion moments in selected plate's elements

As it is seen in the graph, the shear forces are larger for the members which are located near the basis, however the difference between the values is not so significant. The same regularity can be observed in the case of the second type of internal forces, except that the bending moment for the beam component lying at a lower height is several times greater than at the top. Obtained result seems to be obvious due to higher distance between the 10'th element and the point of application of the dynamic load.

In Figs. 2.38 and 2.39 are presented the comparisons of the internal moments received for two plate member, from the middle of the suspended part of the span. 315'th element is adjacent to the longitudinal axis of the bridge while the 311'th is on the edge of the plate. Looking at fig. 2.38 we can conclude that the XX- and YY-bending moments in cross-section of the plate are larger for the components that are lying closer to the center of the span. In contrast to the previously described internal forces, XY-torsional moment, exposed in fig. 2.39, achieves the maximum values for elements placed on the edge of the plate, while the minimum for the middle part of the span.

As it is shown in the mentioned graphs, the XY-torsional moment's values are twice smaller than bending one's. The described internal forces for the span behave the same as for normal plate in a complex stress state, namely, the larger displacements in nodes the higher values of bending moments, the smaller distance of the considered element from the symmetry axis of the span the lower torsional moments.

2.7.7 Eigenvalue sensitivity

In this section we consider the sensitivity of eigenvalues with respect to the cross-sectional areas of specific truss and beam elements and with respect to the thickness of the plate components. Table 2.11 presents selected results obtained for first three eigenvalues. It can be noticed that the eigenvalues are the most sensitive with respect to the change of the cross-sectional areas of back cables, that connected the pylon with the arches, and that stabilizing the pylon.

During the statics and dynamics this cables was treated as secondary truss elements, only sensitivity analysis change the view on theirs meaning in the whole structure's work. According to that, we may presume that those components are highly probable to become crucial members at this structure.

Table 2.11 Eigenvalues design sensitivity

Element number	design sensitivity of the eigenvalue first	second	third
a) with respect to the cross-sectional area of the truss element			
102	0.00761	0.00257	0.00143
127	0.01005	0.00274	0.00537
b) with respect to the cross-sectional area of the beam element			
65	0.00040	0.00012	0.00347
121	0.00017	0.00000	0.00132
c) with respect to the thickness of the plate element			
132	0.00020	0.00010	0.00009
439	0.00010	0.00046	0.00003

2.7.8 Dynamic Sensitivity

Dynamic sensitivity analysis is focused on checking how a change of cross-section area of particular elements influences displacements in selected nodes. First of all we consider dynamic sensitivity of the deflection of the span's middle point with respect to the cross-sectional areas of chosen plates', beams', and trusses' elements. The functional of structural response in numerical computations is assumed in the form

$$\phi = \frac{|q_\alpha|}{q_{\text{all}}} - 1 < 0 \tag{2.162}$$

where q_α, q_{all} mean displacement of selected node and allowable displacement at this point, respectively. According to that, the limit value of vertical movement in 358'th plate's node is determined to 15cm. The most significant results of structural response received for this point are presented in fig. 2.40 for two cases — with and without damping. If we look at the course of the mentioned graph, the periodical changes of the amplitude are noticed, which confirms the presence of beat phenomenon.

a)

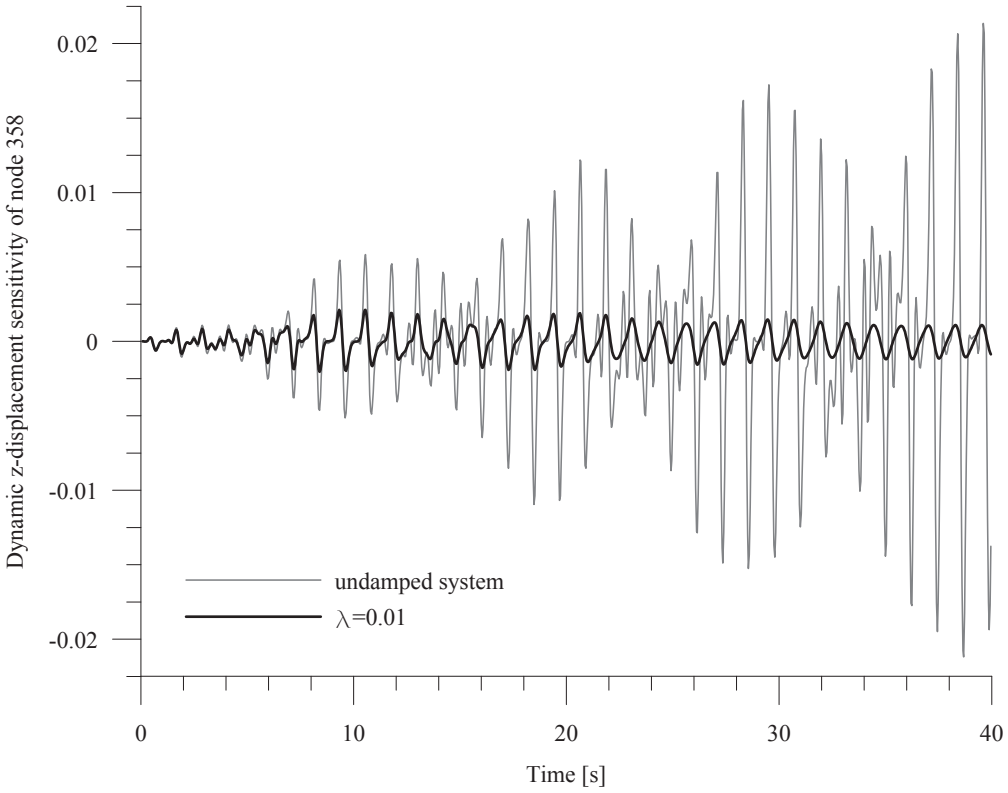

b)

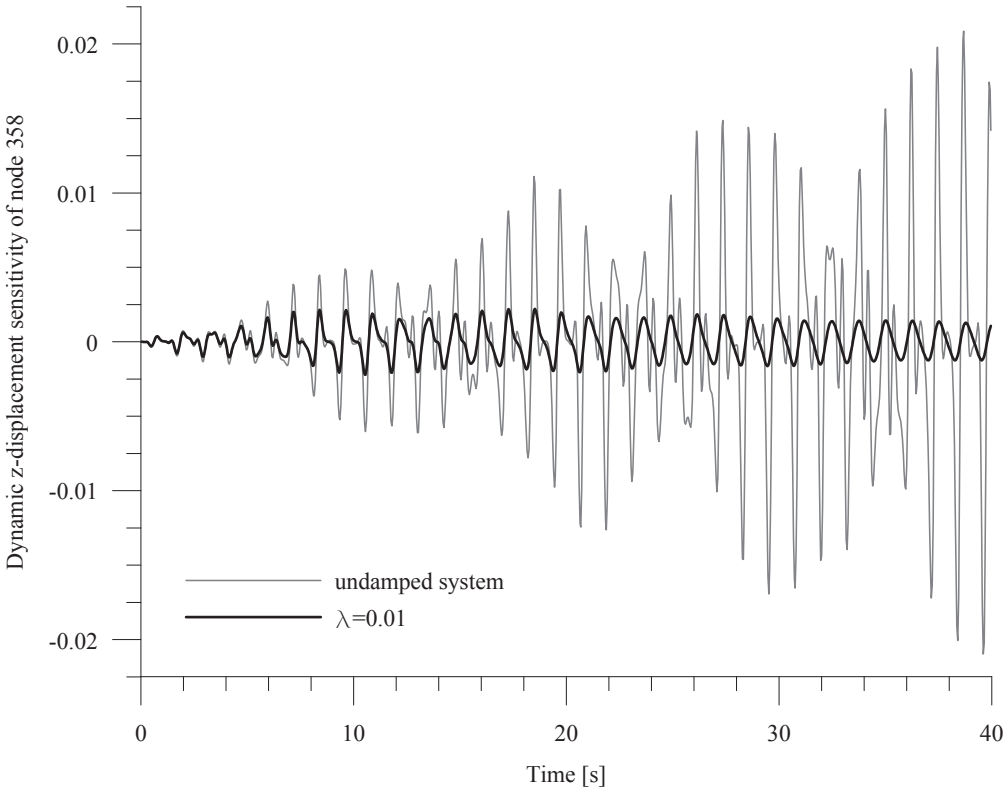

Figure 2.40 Dynamic sensitivity of the mid point in the plate by the change the cross-section area of a) truss element no. 37; b) plate element no. 324

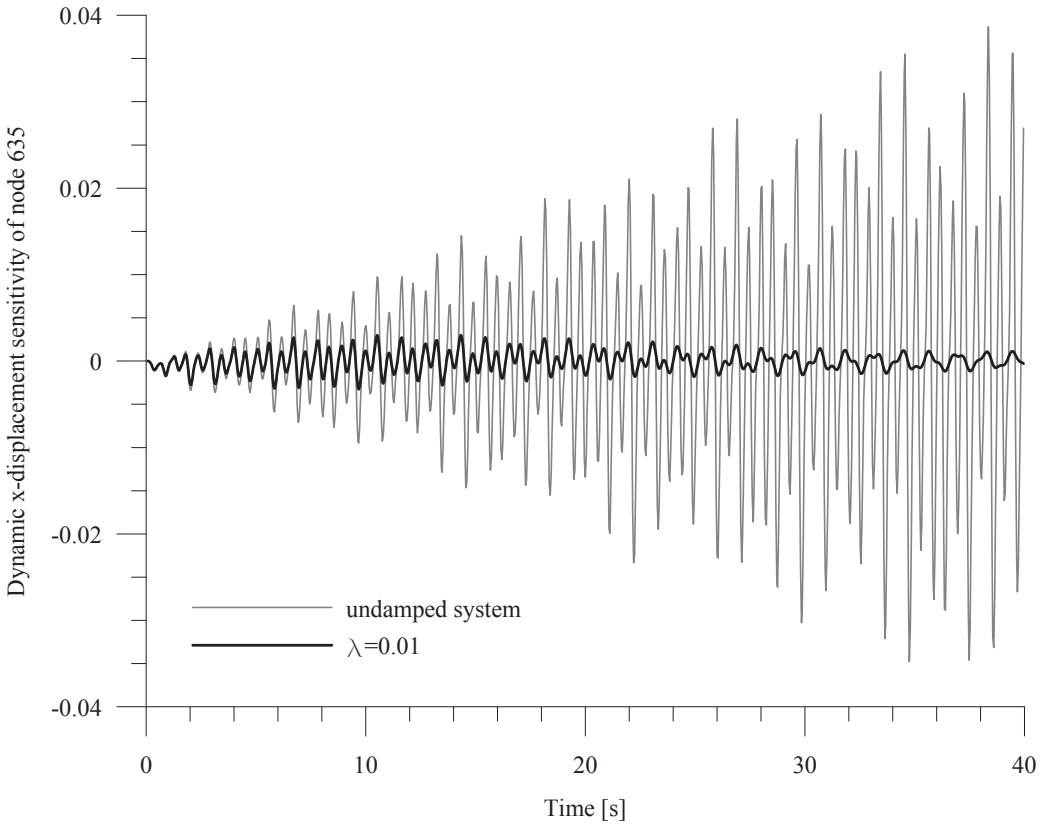

Figure 2.41 Dynamic sensitivity at the top point of the pylon by the change the cross-section area of the truss element no. 60

Generally, the displacement sensitivity of selected node gains the largest values with respect to the change of geometric or material characteristics of the elements in its domain compare [66]. However this stage of the analysis gives surprising conclusions. During the numerical computations, it turns out that the z-direction displacement of node 358 is the most sensitive to the change of the cross-sectional area one from main cable's — truss el. no. 37, suspended the span to the pylon in point with the same x-coordinate as examined node.

That give us a different view on the importance of the main elements in considered bridge. Previous static and dynamic studies didn't show that the role of that cable is the most significant for the deflection of the plate. Only sensitivity analysis reveals the validity of this component.

Second part of the computations applies to the longitudinal displacement of the top of the pylon. The limit value of x-direction movement of 635'th node is determined to 10cm. Analogically as in the case of the plate it turns out that this point is the most sensitive to change of main cable's cross-section area — truss element no. 60, that connects the top of the pylon and the span. The mentioned results are presented in fig. 2.41.

On all the above graphs we can observe the increase of the dynamic sensitivity in time, additionally they show the presence of the beat phenomenon in this analysis as well. If we take coefficient of modal damping into account, the amplitude of the response decreases but it still changing periodical in time. In further research we try to eliminate the mentioned effect by using an added lumped mass in selected nodes. This method is described in details in the section no. 3.6.

In theoretical point of view it is possible to correct the beat phenomenon for such kind of suspended bridge by adding lumped mass but taking into account the practical possibility this type of treatment becomes impossible. Dynamic sensitivity analysis proves that for eliminating this effect the material of lumped mass would have to has the large value of inertia, which cannot be achieved in our reality.

2.8 Summarizing Remarks

Most of objects in the civil engineering are complex structural systems with MDOF, which makes them impossible to be considered by analytical method. In computational examples we prove that the numerical methods may be successfully used in designing process of this type of schemes. After creating a model and inputting it into the program, we can obtain the results comparable to the analytical ones.

Consideration of such kind of suspended bridge is a very complex issue. The problem is not only the FEM setting but also proper selection of materials. The results presented in Section 2.7 show a great importance of dynamic and sensitivity analysis in structure designing nowadays. These numerical computations provide new insight into structures work and show unnoticed so far meaning of the individual elements.

The course of time-dependent displacements in selected nodes of the bridge discloses the presence of beat effect. This phenomenon is largely caused by the symmetry of the geometry. If we are trying to design that kind of slender structure we should first analyze all possible loads which our object can be exposed to. Dynamic and sensitivity analysis seem to be necessary if we want to create a safe and stable bridge.

Chapter 3

Stochastic Dynamic Systems

3.1 Stochastic Version of Lagrange's Equations

The previous chapter is about the deterministic systems where we have a defined value of the function for every argument. In this analysis is obtained only one result of the variable, for example force or displacement at a given point. However, for determining the error measure of the received results, it is necessary to include the stochastic analysis which is related to the systems described by random variables $x_r(\tau)$. We cannot predict the value of the random variables $x_r(\tau)$ for every τ, because it is not a known function of any argument. The history of $x_r(\tau)$ for specific r is called a sample function. The random process contains the whole set of possible histories, $\{x_r(\tau)\},\ r = 1, 2, ..., \hat{r}$, in the object considered in this section [26,27,35].

3.1.1 Mean-Point Second Moment Perturbation Method

We define the vector of time-independent random variables in the form $\mathbf{h} = \{h_r\},\ r = 1, 2, ..., \hat{r}$, given by their first two central moments — means $\bar{\mathbf{h}} = \{\bar{h}_r\}$ and cross-covariances $[\mathrm{Cov}(h_r, h_s)]$; $r, s = 1, 2, ..., \hat{r}$, i.e.

$$[\mathrm{Cov}(h_r, h_s)] = \begin{bmatrix} \mathrm{Var}(h_1) & \mathrm{Cov}(h_1, h_2) & \dots & \mathrm{Cov}(h_1, h_{\hat{r}}) \\ & \mathrm{Var}(h_2) & \dots & \mathrm{Cov}(h_2, h_{\hat{r}}) \\ \mathrm{sym} & & \ddots & \vdots \\ & & & \mathrm{Var}(h_{\hat{r}}) \end{bmatrix} \tag{3.1}$$

Let us consider the vector $\mathbf{x} = \{x_i(\mathbf{h})\},\ i = 1, 2, ..., \hat{i}$, which is a function of $\mathbf{h}$. We tend to obtain the equations for the first two probabilistic moments, $\mathrm{E}[x_i]$ and $\mathrm{Cov}[x_i, x_j]$; $i, j = 1, 2, ..., \hat{i}$, by using the second moment perturbation method (SMPM) [26,35] . For the clarity of presentation, the whole procedure will initially be shown with the first order precision, subsequently the process will be repeated with the terms up to the second order.

Starting considerations, the random variables $x_i(\mathbf{h})$ are expanded in Taylor series up to first order around the means $\bar{h}_r$ as

$$x_i(\mathbf{h}) \;=\; x_i(\bar{\mathbf{h}}) + \left.\frac{\partial x_i}{\partial h_r}\right|_{\mathbf{h}=\bar{\mathbf{h}}} (h_r - \bar{h}_r) \tag{3.2}$$

Aiming to receive the mean values of $\{\bar{x}_i(\mathbf{h})\}$ using the linear transform [26], we get the mean values of particular terms from Eq. (3.2). The derivatives $\partial x_i/\partial h_r$ at $\mathbf{h} = \bar{\mathbf{h}}$ are constant, therefore the mean values of the second terms of Eq. (3.2) concern in the brackets containing the random variables h_r and their means

$$\bar{x}_i(\mathbf{h}) = \mathrm{E}[x_i] = \mathrm{E}[x_i(\bar{\mathbf{h}})] + \left.\frac{\partial x_i}{\partial h_r}\right|_{\mathbf{h}=\bar{\mathbf{h}}} \underbrace{\mathrm{E}[(h_r - \bar{h}_r)]}_{=0} = x_i(\bar{\mathbf{h}}) \tag{3.3}$$

The dispersions of the random variables $\{x_i\}$ about their means $\{\bar{x}_i\}$ are given by

$$x_i - \bar{x}_i \;=\; x_i(\bar{\mathbf{h}}) + \left.\frac{\partial x_i}{\partial h_r}\right|_{\mathbf{h}=\bar{\mathbf{h}}} (h_r - \bar{h}_r) - x_i(\bar{\mathbf{h}}) = \left.\frac{\partial x_i}{\partial h_r}\right|_{\mathbf{h}=\bar{\mathbf{h}}} (h_r - \bar{h}_r) \tag{3.4}$$

Analogically, we have

$$x_j - \bar{x}_j = \left.\frac{\partial x_j}{\partial h_s}\right|_{\mathbf{h}=\bar{\mathbf{h}}} (h_s - \bar{h}_s) \tag{3.5}$$

The cross-covariances $\mathrm{Cov}(x_i,\ x_j)$ may be obtained by definition

$$\mathrm{Cov}(x_i, x_j) = \mathrm{E}[(x_i - \bar{x}_i)(x_j - \bar{x}_j)] \tag{3.6}$$

Substituting Eq. (3.4) and (3.5) into (3.6), we receive

$$\begin{aligned} \mathrm{Cov}(x_i, x_j) \;&=\; \mathrm{E}\left[\left.\frac{\partial x_i}{\partial h_r}\frac{\partial x_j}{\partial h_s}\right|_{\mathbf{h}=\bar{\mathbf{h}}} (h_r - \bar{h}_r)(h_s - \bar{h}_s)\right] \\ &=\; \left.\frac{\partial x_i}{\partial h_r}\frac{\partial x_j}{\partial h_s}\right|_{\mathbf{h}=\bar{\mathbf{h}}} \mathrm{E}[(h_r - \bar{h}_r)(h_s - \bar{h}_s)] = \left.\frac{\partial x_i}{\partial h_r}\frac{\partial x_j}{\partial h_s}\right|_{\mathbf{h}=\bar{\mathbf{h}}} \mathrm{Cov}(h_r, h_s) \end{aligned} \tag{3.7}$$

Now the process of determining the first two probabilistic moments is rewritten with expanding the random variables in power series up to second order around the means $\bar{h}_r$

$$x_i(\mathbf{h}) \;=\; x_i(\bar{\mathbf{h}}) + \left.\frac{\partial x_i}{\partial h_r}\right|_{\mathbf{h}=\bar{\mathbf{h}}} (h_r - \bar{h}_r) + \frac{1}{2}\left.\frac{\partial^2 x_i}{\partial h_r\, \partial h_s}\right|_{\mathbf{h}=\bar{\mathbf{h}}} (h_r - \bar{h}_r)(h_s - \bar{h}_s) \tag{3.8}$$

The values of $x_i(\bar{\mathbf{h}})$ and derivatives $\partial x_i/\partial h_r$ and $\partial^2 x_i/\partial h_r\, \partial h_s$ at $\mathbf{h} = \bar{\mathbf{h}}$ are constant. Using Eq. (3.3), the means of the random variables form Eq. (3.8) are presented by the formula

$$\begin{aligned} \bar{x}_i \;&=\; x_i(\bar{\mathbf{h}}) + \left.\frac{\partial x_i}{\partial h_r}\right|_{\mathbf{h}=\bar{\mathbf{h}}} \underbrace{\mathrm{E}[(h_r - \bar{h}_r)]}_{=0} + \frac{1}{2}\left.\frac{\partial^2 x_i}{\partial h_r\, \partial h_s}\right|_{\mathbf{h}=\bar{\mathbf{h}}} \underbrace{\mathrm{E}[(h_r - \bar{h}_r)(h_s - \bar{h}_s)]}_{\mathrm{Cov}(h_r, h_s)} \\ &=\; x_i(\bar{\mathbf{h}}) + \frac{1}{2} x_i^{(2)} \end{aligned} \tag{3.9}$$

where

$$x_i^{(2)} = \left.\frac{\partial^2 x_i}{\partial h_r\, \partial h_s}\right|_{\mathbf{h}=\bar{\mathbf{h}}} \mathrm{Cov}(h_r, h_s) \tag{3.10}$$

and this symbol will be used from now on in the text, i.e.

$$(\cdot)^{(2)} = \left.\frac{\partial^2 (\cdot)}{\partial h_r\, \partial h_s}\right|_{\mathbf{h}=\bar{\mathbf{h}}} \mathrm{Cov}(h_r, h_s) \tag{3.11}$$

The spreads of the variables x_i around their means $\bar{x}_i$ are

$$\begin{aligned} x_i - \bar{x}_i &= x_i(\bar{\mathbf{h}}) + \frac{\partial x_i}{\partial h_r}\bigg|_{\mathbf{h}=\bar{\mathbf{h}}} (h_r - \bar{h}_r) + \frac{1}{2}\frac{\partial^2 x_i}{\partial h_r\, \partial h_s}\bigg|_{\mathbf{h}=\bar{\mathbf{h}}} (h_r - \bar{h}_r)(h_s - \bar{h}_s) \\ &\quad - x_i(\bar{\mathbf{h}}) - \frac{1}{2}x_i^{(2)} \\ &= \frac{\partial x_i}{\partial h_r}\bigg|_{\mathbf{h}=\bar{\mathbf{h}}} (h_r - \bar{h}_r) + \frac{1}{2}\frac{\partial^2 x_i}{\partial h_r\, \partial h_s}\bigg|_{\mathbf{h}=\bar{\mathbf{h}}} (h_r - \bar{h}_r)(h_s - \bar{h}_s) - \frac{1}{2}x_i^{(2)} \end{aligned} \tag{3.12}$$

Analogically, the subtraction of the second variables x_j and their means $\bar{x}_j$ is expressed as

$$x_j - \bar{x}_j = \frac{\partial x_j}{\partial h_s}\bigg|_{\mathbf{h}=\bar{\mathbf{h}}} (h_s - \bar{h}_s) + \frac{1}{2}\frac{\partial^2 x_j}{\partial h_r\, \partial h_s}\bigg|_{\mathbf{h}=\bar{\mathbf{h}}} (h_r - \bar{h}_r)(h_s - \bar{h}_s) - \frac{1}{2}x_j^{(2)} \tag{3.13}$$

The result of Eqs. (3.12) and (3.13) multiplication, excluding the terms higher than second order is

$$\begin{aligned} (x_i - \bar{x}_i)(x_j - \bar{x}_j) &= -\frac{1}{2}\frac{\partial x_i}{\partial h_r}\bigg|_{\mathbf{h}=\bar{\mathbf{h}}} (h_r - \bar{h}_r)x_j^{(2)} - \frac{1}{2}\frac{\partial x_j}{\partial h_s}\bigg|_{\mathbf{h}=\bar{\mathbf{h}}} (h_s - \bar{h}_s)x_i^{(2)} \\ &\quad + \frac{\partial x_i}{\partial h_r}\frac{\partial x_j}{\partial h_s}\bigg|_{\mathbf{h}=\bar{\mathbf{h}}} (h_r - \bar{h}_r)(h_s - \bar{h}_s) + \frac{1}{4}x_i^{(2)}x_j^{(2)} \\ &\quad - \frac{1}{4}\frac{\partial^2 x_i}{\partial h_r\, \partial h_s}\bigg|_{\mathbf{h}=\bar{\mathbf{h}}} (h_r - \bar{h}_r)(h_s - \bar{h}_s)x_j^{(2)} \\ &\quad - \frac{1}{4}\frac{\partial^2 x_j}{\partial h_r\, \partial h_s}\bigg|_{\mathbf{h}=\bar{\mathbf{h}}} (h_r - \bar{h}_r)(h_s - \bar{h}_s)x_i^{(2)} \end{aligned} \tag{3.14}$$

Using Eq. (3.6), the mean values of Eq. (3.14) lead to the formula for the cross-covariances of two random variables with the second order precision

$$\begin{aligned} &E[(x_i - \bar{x}_i)(x_j - \bar{x}_j)] = \\ &= -\frac{1}{2}\frac{\partial x_i}{\partial h_r}\bigg|_{\mathbf{h}=\bar{\mathbf{h}}} \underbrace{\mathrm{E}[(h_r - \bar{h}_r)]}_{0} x_j^{(2)} - \frac{1}{2}\frac{\partial x_j}{\partial h_s}\bigg|_{\mathbf{h}=\bar{\mathbf{h}}} \underbrace{\mathrm{E}[(h_s - \bar{h}_s)]}_{0} x_i^{(2)} \\ &\quad + \left[\frac{\partial x_i}{\partial h_r}\frac{\partial x_j}{\partial h_s} - \frac{1}{4}\frac{\partial^2 x_i}{\partial h_r\, \partial h_s}x_j^{(2)} - \frac{1}{4}\frac{\partial^2 x_j}{\partial h_r\, \partial h_s}x_i^{(2)}\right]_{\mathbf{h}=\bar{\mathbf{h}}} \underbrace{\mathrm{E}[(h_r - \bar{h}_r)(h_s - \bar{h}_s)]}_{\mathrm{Cov}(h_r,\, h_s)} \\ &\quad + \frac{1}{4}x_i^{(2)}x_j^{(2)} \end{aligned} \tag{3.15}$$

After reducing similar terms we have

$$\mathrm{Cov}(x_i,\, x_j) = \frac{\partial x_i}{\partial h_r}\frac{\partial x_j}{\partial h_s}\bigg|_{\mathbf{h}=\bar{\mathbf{h}}} \mathrm{Cov}(h_r,\, h_s) - \frac{1}{4}x_i^{(2)}x_j^{(2)} \tag{3.16}$$

To sum up this section, there are some disadvantages of the SMPM in comparison to the Monte Carlo simulation [26]. Namely, we obtain only the first two probabilistic moments and the random variables x_i are supposed to have the small fluctuation and be continuous at $\bar{h}_r$. However, the SMPM has also the considerably positive sides. There are no requirements of defining the normal distribution of $\{x_i\}$. Only mean values and the cross-covariances of $\mathbf{h}$ are necessary to be entered on input. To obtain the results with the same precision only $\hat{r}$ order of equations system is considered no $\hat{r}^3$, like in Monte Carlo simulation. The last advantage comes from replacing the $\hat{r}^2$ vectors $\partial^2 x_i/\partial h_r \partial h_s$ $(r, s = 1, 2, ..., \hat{r})$ with single vector of the form $\{x_i^{(2)}(\bar{h}_r)\}$, presented in Eq. (3.10).

3.2 Solving Systems of Hierarchical Equations

The second moment perturbation method concerns solving the system of linear differential equation with $\hat{i}$ degrees of freedom and receiving the unknown vector of output signals $\{x_i\}$, $i = 1, 2, ..., \hat{i}$. The input signal vector $\mathbf{f} = \{f_i(h_r, \tau)\}$ is defined to be an explicit function with respect to time and the previously presented random parameters vector $\mathbf{h} = h_r$, $r = 1, 2, ..., \hat{r}$ that is specified by first two central moments $\bar{\mathbf{h}} = \{\bar{h}_r\}$ and $[\mathrm{Cov}(h_r, h_s)]$. The components of vector $\mathbf{f}$ are assumed to be twice differentiable with respect to $\mathbf{h}$ and τ.

The relationship between the vectors of input and output signals, can be presented by the system of linear differential equation in the form [26]

$$\mathbf{L}\mathbf{x} = \mathbf{f}(\mathbf{h}, \tau) \tag{3.17}$$

where $\mathbf{L}$ is a differential operator whose matrices are explicit functions of $\mathbf{h}$ being supposed to be twice differentiable with respect to $\mathbf{h}$. Solving Eq. (3.17) to obtain the unknown vector, shows that $\mathbf{x} = \{x_i(h_r, \tau)\}$ is an implicit function of random parameters vector and time. In accordance with the requirements of the task, the components of vector $\{x_i\}$ are also assumed to be twice differentiable with respect to $\mathbf{h}$ and τ.

The goal of the considered perturbation method is to obtain first two probabilistic moments for $\{x_i\}$: the mean values vector $\{\mathrm{E}[x_i(\tau = t)]\}$ and the cross-covariances matrix $[\mathrm{Cov}(x_i(\tau = t_1); x_j(\tau = t_2)]$, $i = 1, 2, ..., \hat{i}$. For the sake of concise derivations, all terms of Eq. (3.17) are moved to the right-hand side of the equation, and they are written in the residual form [26] as

$$\mathbb{R} = \mathbf{f}(\mathbf{h}, \tau) - \mathbf{L}\mathbf{x} = 0 \tag{3.18}$$

Next, all the functions of $\{h_r\}$ from Eq. (3.18) are expanded in Taylor series up to the second order around the means $\bar{h}_r$, to the formula

$$\begin{aligned} \mathbb{R}(\mathbf{h}) &= \mathbb{R}(\bar{\mathbf{h}}) + \delta\mathbb{R}(\bar{\mathbf{h}}) + \frac{1}{2}\delta^2\mathbb{R}(\bar{\mathbf{h}}) \\ &= \mathbb{R}(\bar{\mathbf{h}}) + \frac{\mathrm{d}\mathbb{R}}{\mathrm{d}h_r}\bigg|_{\mathbf{h}=\bar{\mathbf{h}}}\delta h_r + \frac{1}{2}\frac{\mathrm{d}^2\mathbb{R}}{\mathrm{d}h_r\mathrm{d}h_s}\bigg|_{\mathbf{h}=\bar{\mathbf{h}}}\delta h_r\delta h_s = 0 \end{aligned} \tag{3.19}$$

with δh_r being the first variations h_r about $\bar{h}_r$. For any small parameter ϵ, we have

$$\delta h_r = \epsilon\,(h_r - \bar{h_r}) \tag{3.20}$$

Analogically, the second mixed variation of h_r and h_s about their means $\bar{h}_r$ and $\bar{h}_s$, can be expressed by

$$\delta h_r\delta h_s = \epsilon^2\,(h_r - \bar{h}_r)(h_s - \bar{h}_s) \tag{3.21}$$

Using the above notations, Eq. (3.19) is rewritten to the form

$$\mathbb{R}(\mathbf{h}) = \mathbb{R}(\bar{\mathbf{h}}) + \frac{\mathrm{d}\mathbb{R}}{\mathrm{d}h_r}\bigg|_{\mathbf{h}=\bar{\mathbf{h}}}\epsilon\,(h_r - \bar{h}_r) + \frac{1}{2}\frac{\mathrm{d}^2\mathbb{R}}{\mathrm{d}h_r\mathrm{d}h_s}\bigg|_{\mathbf{h}=\bar{\mathbf{h}}}\epsilon^2\,(h_r - \bar{h}_r)(h_s - \bar{h}_s) = 0 \tag{3.22}$$

The terms of Eq. (3.19) are explicit, implicit or explicit-implicit functions of the variables $\mathbf{h}$ and τ. Therefore, the first absolute partial derivative $\mathbb{R}(\mathbf{h})$ with respect to h_r for a fixed r is presented by

$$\frac{\mathrm{d}\mathbb{R}}{\mathrm{d}h_r} = \frac{\partial\mathbf{f}}{\partial h_r} - \frac{\mathrm{d}}{\mathrm{d}h_r}\big(\mathbf{L}\mathbf{x}\big) = \frac{\partial\mathbf{f}}{\partial h_r} - \frac{\partial\mathbf{L}}{\partial h_r}\mathbf{x} - \mathbf{L}\frac{\mathrm{d}\mathbf{x}}{\mathrm{d}h_r} = 0 \tag{3.23}$$

Differentiating Eq. (3.23) with respect to h_s leads to the mixed second absolutely partial derivatives, expressed by the equation

$$\frac{\mathrm{d}^2\mathbb{R}}{\mathrm{d}h_r\mathrm{d}h_s} = \frac{\partial^2\mathbf{f}}{\partial h_r\partial h_s} - \frac{\partial^2\mathbf{L}}{\partial h_r\partial h_s}\mathbf{x} - \frac{\partial\mathbf{L}}{\partial h_r}\frac{\mathrm{d}\mathbf{x}}{\mathrm{d}h_s} - \frac{\partial\mathbf{L}}{\partial h_s}\frac{\mathrm{d}\mathbf{x}}{\mathrm{d}h_r} - \mathbf{L}\frac{\mathrm{d}^2\mathbf{x}}{\mathrm{d}h_r\mathrm{d}h_s} = 0 \tag{3.24}$$

Since variations $\{\delta h_r\}$ are mutually independent and arbitrary, the hierarchical set of equations is obtained in the form

$$\begin{aligned} \mathbb{R}(\bar{\mathbf{h}}) &= 0 \\ \left.\frac{\mathrm{d}\mathbb{R}}{\mathrm{d}h_r}\right|_{\mathbf{h}=\bar{\mathbf{h}}} &= 0;\ r = 1, 2, ..., \hat{r} \\ \left.\frac{\mathrm{d}^2\mathbb{R}}{\mathrm{d}h_r\mathrm{d}h_s}\right|_{\mathbf{h}=\bar{\mathbf{h}}} &= 0;\ r, s = 1, 2, ..., \hat{r} \end{aligned} \tag{3.25}$$

because of disappearing the zero, first and second derivatives from Eq. (3.19) at $\{h_r\} = \{\bar{h}_r\}$. The hierarchical system presented in Eq. (3.25) is made by the following equations: one of the zeroth-order, $\hat{r}$ of the first-order and $\hat{r}(\hat{r}+1)/2$ of the second-order. Receiving the mean values of the second order terms from Eq. (3.22), we have

$$\begin{aligned} \mathrm{E}\left[\left.\frac{\mathrm{d}^2\mathbb{R}}{\mathrm{d}h_r\mathrm{d}h_s}\right|_{\mathbf{h}=\bar{\mathbf{h}}} \epsilon^2\,(h_r - \bar{h}_r)(h_s - \bar{h}_s)\right] &= \epsilon^2\left.\frac{\mathrm{d}^2\mathbb{R}}{\mathrm{d}h_r\mathrm{d}h_s}\right|_{\mathbf{h}=\bar{\mathbf{h}}} \mathbf{E}[(h_r - \bar{h}_r)(h_s - \bar{h}_s)] \\ &= \epsilon^2\left.\frac{\mathrm{d}^2\mathbb{R}}{\mathrm{d}h_r\mathrm{d}h_s}\right|_{\mathbf{h}=\bar{\mathbf{h}}} \mathrm{Cov}(h_r,\ h_s) \\ &= \epsilon^2\mathbb{R}^{(2)} = 0 \end{aligned} \tag{3.26}$$

Substituting Eq. (3.24) into Eq. (3.26), we get

$$\epsilon^2\left(\frac{\partial^2\mathbf{f}}{\partial h_r\partial h_s} - \frac{\partial^2\mathbf{L}}{\partial h_r\partial h_s}\mathbf{x} - \frac{\partial\mathbf{L}}{\partial h_r}\frac{\mathrm{d}\mathbf{x}}{\mathrm{d}h_s} - \frac{\partial\mathbf{L}}{\partial h_s}\frac{\mathrm{d}\mathbf{x}}{\mathrm{d}h_r} - \mathbf{L}\frac{\mathrm{d}^2\mathbf{x}}{\mathrm{d}h_r\mathrm{d}h_s}\right)\mathrm{Cov}(h_r,\ h_s) = 0 \tag{3.27}$$

Because the cross-covariances matrix is symmetrical, the terms $\frac{\partial\mathbf{L}}{\partial h_r}\frac{\mathrm{d}\mathbf{x}}{\mathrm{d}h_s}$ and $\frac{\partial\mathbf{L}}{\partial h_s}\frac{\mathrm{d}\mathbf{x}}{\mathrm{d}h_r}$ are equal after multiplying by $[\mathrm{Cov}(h_r,\ h_s)]$. Therefore, the following equation holds

$$\left(\frac{\partial\mathbf{L}}{\partial h_r}\frac{\mathrm{d}\mathbf{x}}{\mathrm{d}h_s} + \frac{\partial\mathbf{L}}{\partial h_s}\frac{\mathrm{d}\mathbf{x}}{\mathrm{d}h_r}\right)\mathrm{Cov}(h_r,\ h_s) = 2\frac{\partial\mathbf{L}}{\partial h_r}\frac{\mathrm{d}\mathbf{x}}{\mathrm{d}h_s}\mathrm{Cov}(h_r,\ h_s) \tag{3.28}$$

Using Eqs. (3.27), Eq. (3.26) is rewritten in the form

$$\mathbf{L}x^{(2)} = \mathbf{f}^{(2)} - \left[2\frac{\partial\mathbf{L}}{\partial h_r}\frac{\mathrm{d}\mathbf{x}}{\mathrm{d}h_s} + \frac{\partial^2\mathbf{L}}{\partial h_r\partial h_s}\mathbf{x}\right]_{\mathbf{h}=\bar{\mathbf{h}}}\mathrm{Cov}(h_r,\ h_s) \tag{3.29}$$

Solving the Eqs. (3.22) with respect to $\mathbf{L}\frac{\mathrm{d}\mathbf{x}}{\mathrm{d}h_r}$ leads to

$$\left.\mathbf{L}\frac{\mathrm{d}\mathbf{x}}{\mathrm{d}h_r}\right|_{\mathbf{h}=\bar{\mathbf{h}}} = \left[\frac{\partial\mathbf{f}}{\partial h_r} - \frac{\partial\mathbf{L}}{\partial h_r}\mathbf{x}\right]_{\mathbf{h}=\bar{\mathbf{h}}} \tag{3.30}$$

Based on the Eqs. (3.17), (3.29) and (3.30), the hierarchical system of linear perturbation about the mean values, can be presented as follows

$$\begin{aligned} \mathbf{L}\mathbf{x}|_{\mathbf{h}=\bar{\mathbf{h}}} &= \mathbf{f}(\bar{\mathbf{h}},\ \tau) \\ \left.\mathbf{L}\frac{\mathrm{d}\mathbf{x}}{\mathrm{d}h_r}\right|_{\mathbf{h}=\bar{\mathbf{h}}} &= \left[\frac{\partial\mathbf{f}}{\partial h_r} - \frac{\partial\mathbf{L}}{\partial h_r}\mathbf{x}\right]_{\mathbf{h}=\bar{\mathbf{h}}} \\ \left.\mathbf{L}x^{(2)}\right|_{\mathbf{h}=\bar{\mathbf{h}}} &= \mathbf{f}^{(2)} - \left[2\frac{\partial\mathbf{L}}{\partial h_r}\frac{\mathrm{d}\mathbf{x}}{\mathrm{d}h_s} + \frac{\partial^2\mathbf{L}}{\partial h_r\partial h_s}\mathbf{x}\right]_{\mathbf{h}=\bar{\mathbf{h}}}\mathrm{Cov}(h_r,\ h_s) \end{aligned} \tag{3.31}$$

with $r, s = 1, 2, ..., \hat{r}$. The set from Eq. (3.31) consist of the equations: one of the zeroth-order, $\hat{r}$ of the first-order and one of the second-order.

Assuming x_i be the time-dependent vector of the random variables, the first two central moments are respectively equal [26] : the mean values for definite time $\tau = t$ are

$$\bar{x}_i(t) = x_i(\bar{\mathbf{h}}; t) + \frac{1}{2}x_i^{(2)}(t) \tag{3.32}$$

and the cross-covariances for the specific variables x_i (for $\tau = t_1$), x_j (for $\tau = t_2$) are, cf. Eq. (3.16)

$$\mathrm{Cov}\big(x_i(t_1);\ x_j(t_2)\big) \ = \ \frac{\partial x_i(t_1)}{\partial h_r}\frac{\partial x_j(t_2)}{\partial h_s}\bigg|_{\mathbf{h}=\bar{\mathbf{h}}} \mathrm{Cov}(h_r,\ h_s) - \frac{1}{4}x_i^{(2)}(t_1)x_j^{(2)}(t_2) \tag{3.33}$$

3.3 System Total Energy and Lagrange's Equations of the Second Type

For the general case of the dynamic stochastic analysis the matrices — stiffness $K_{\alpha\beta}(h_r)$, masses $M_{\alpha\beta}(h_r)$ and damping $D_{\alpha\beta}(h_r)$ and the vector of nodal loads $Q_\alpha(h_r; \tau)$ are considered as explicit functions of the random variable vector h_r, while the generalized coordinate vector of the $q_\alpha(h_r; \tau)$ as an implicit one. Using the above notation, the equation for the total energy of the system — Eq. (2.35), is rewritten to

$$\begin{aligned}\mathcal{L}(h_r) \ &= \ \frac{1}{2}\dot{q}_\alpha^{\mathrm{T}}(h_r; \tau)M_{\alpha\beta}(h_r)\dot{q}_\beta(h_r; \tau) - \frac{1}{2}{q_\alpha}^{\mathrm{T}}(h_r; \tau)K_{\alpha\beta}(h_r)q_\beta(h_r; \tau) \\ &+ \ q_\alpha^{\mathrm{T}}(h_r; \tau)Q_\alpha(h_r; \tau)\end{aligned} \tag{3.34}$$

where $\alpha, \beta = 1, 2, .., N,\ r = 1, 2, ..., \hat{r}$. Therefore, the Lagrange's equations of the second type can be expressed in the form (compare Eq. (2.15))

$$\frac{\partial \mathcal{L}}{\partial q_\alpha(h_r; \tau)} - \frac{\mathrm{d}}{\mathrm{d}t}\left(\frac{\partial \mathcal{L}}{\partial \dot{q}_\alpha(h_r; \tau)}\right) = 0; \quad \alpha = 1, 2, .., N \tag{3.35}$$

Since the generalized coordinate vector is an implicit function of the random parameters and time, Eqs. (2.36) and (2.38) read

$$\frac{\partial \mathcal{L}}{\partial q_\alpha} = -K_{\alpha\beta}(h_r)q_\beta(h_r; \tau) + Q_\alpha(h_r; \tau) \tag{3.36}$$

and

$$\frac{\mathrm{d}}{\mathrm{d}t}\left(\frac{\partial \mathcal{L}}{\partial \dot{q}_\alpha}\right) = M_{\alpha\beta}(h_r)\ddot{q}_\beta(h_r; \tau) \tag{3.37}$$

Substituting Eqs. (3.37) and (3.38) into (3.35), including the damping effect, and after rearranging the similar terms we receive

$$M_{\alpha\beta}(h_r)\ddot{q}_\beta(h_r; \tau) + D_{\alpha\beta}(h_r)\dot{q}_\beta(h_r; \tau) + K_{\alpha\beta}(h_r)q_\beta(h_r; \tau) = Q_\alpha(h_r; \tau) \tag{3.38}$$

with $D_{\alpha\beta}(h_r)$ being the damping matrix of the system.

3.4 Hierarchical Equations of Motion and Equilibrium

For simplification, we begin with the static case, for which the equilibrium equation stands

$$K_{\alpha\beta}(h_r)q_\beta(h_r) = Q_\alpha(h_r) \tag{3.39}$$

Using Eq. (3.9), we expand the stiffness matrix and the vectors of nodal displacements and external loads in Taylor series up to the second order around the mean values $\bar{h}_r$

$$\begin{aligned} K_{\alpha\beta}(h_r) &= K_{\alpha\beta}(\bar{\mathbf{h}}) + \left[\frac{\partial K_{\alpha\beta}}{\partial h_r}\delta h_r + \frac{1}{2}\frac{\partial^2 K_{\alpha\beta}}{\partial h_r \partial h_s}\delta h_r \delta h_s\right]_{\mathbf{h}=\bar{\mathbf{h}}} \\ q_\beta(h_r) &= q_\beta(\bar{\mathbf{h}}) + \left[\frac{\mathrm{d}q_\beta}{\mathrm{d}h_r}\delta h_r + \frac{1}{2}\frac{\mathrm{d}^2 q_\beta}{\mathrm{d}h_r \mathrm{d}h_s}\delta h_r \delta h_s\right]_{\mathbf{h}=\bar{\mathbf{h}}} \\ Q_\alpha(h_r) &= Q_\alpha(\bar{\mathbf{h}}) + \left[\frac{\partial Q_\alpha}{\partial h_r}\delta h_r + \frac{1}{2}\frac{\partial^2 Q_\alpha}{\partial h_r \partial h_s}\delta h_r \delta h_s\right]_{\mathbf{h}=\bar{\mathbf{h}}} \end{aligned} \tag{3.40}$$

Substituting Eqs. (3.40) into (3.39) and excluding the terms higher than second order, we obtain

$$\begin{aligned} Q_\alpha(\bar{\mathbf{h}}) &+ \left[\frac{\partial Q_\alpha}{\partial h_r}\delta h_r + \frac{1}{2}\frac{\partial^2 Q_\alpha}{\partial h_r \partial h_s}\delta h_r \delta h_s\right]_{\mathbf{h}=\bar{\mathbf{h}}} = K_{\alpha\beta}(\bar{\mathbf{h}})q_\beta(\bar{\mathbf{h}}) \\ &+ \left[K_{\alpha\beta}\frac{\mathrm{d}q_\beta}{\mathrm{d}h_r} + \frac{\partial K_{\alpha\beta}}{\partial h_r}q_\beta\right]_{\mathbf{h}=\bar{\mathbf{h}}}\delta h_r \\ &+ \frac{1}{2}\left[K_{\alpha\beta}\frac{\mathrm{d}^2 q_\beta}{\mathrm{d}h_r \mathrm{d}h_s} + q_\beta\frac{\partial^2 K_{\alpha\beta}}{\partial h_r \partial h_s} + 2\frac{\partial K_{\alpha\beta}}{\partial h_r}\frac{\mathrm{d}q_\beta}{\mathrm{d}h_s}\right]_{\mathbf{h}=\bar{\mathbf{h}}}\delta h_r \delta h_s \end{aligned} \tag{3.41}$$

Comparing the terms in the same order from Eq. (3.41) we receive the hierarchical system of the equilibrium equations consisting of:

— one system of N linear equation of the zeroth-order

$$K_{\alpha\beta}(\bar{\mathbf{h}})q_\beta(\bar{\mathbf{h}}) = Q_\alpha(\bar{\mathbf{h}}) \tag{3.42}$$

— $\hat{r}$ systems of N linear equation of the first-order

$$K_{\alpha\beta}\frac{\mathrm{d}q_\beta}{\mathrm{d}h_r}\bigg|_{\mathbf{h}=\bar{\mathbf{h}}} = \left[\frac{\partial Q_\alpha}{\partial h_r} - \frac{\partial K_{\alpha\beta}}{\partial h_r}q_\beta\right]_{\mathbf{h}=\bar{\mathbf{h}}} \tag{3.43}$$

— one system of N linear equation of the second-order

$$K_{\alpha\beta}(\bar{\mathbf{h}})\, q_\beta^{(2)} = Q_\alpha^{(2)} - K_{\alpha\beta}^{(2)}\, q_\beta(\bar{\mathbf{h}}) - 2\frac{\partial K_{\alpha\beta}}{\partial h_r}\frac{\mathrm{d}q_\beta}{\mathrm{d}h_s}\bigg|_{\mathbf{h}=\bar{\mathbf{h}}}\mathrm{Cov}(h_r,\, h_s) \tag{3.44}$$

Equation (3.44) is obtained by reducing $\hat{r}^2$ systems of equations to the one, because of multiplying the second-order terms by the cross-covariances matrix and summing them up.

Aiming to find the most general form of the time-dependent equations of motion in the stochastic version, the following expressions are needed

$$\begin{aligned}
M_{\alpha\beta}(h_r) &= M_{\alpha\beta}(\bar{\mathbf{h}}) + \left[\frac{\partial M_{\alpha\beta}}{\partial h_r}\delta h_r + \frac{1}{2}\frac{\partial^2 M_{\alpha\beta}}{\partial h_r \partial h_s}\delta h_r \delta h_s\right]_{\mathbf{h}=\bar{\mathbf{h}}} \\
D_{\alpha\beta}(h_r) &= D_{\alpha\beta}(\bar{\mathbf{h}}) + \left[\frac{\partial D_{\alpha\beta}}{\partial h_r}\delta h_r + \frac{1}{2}\frac{\partial^2 D_{\alpha\beta}}{\partial h_r \partial h_s}\delta h_r \delta h_s\right]_{\mathbf{h}=\bar{\mathbf{h}}} \\
\dot{q}_\beta(h_r;\tau) &= \dot{q}_\beta(\bar{\mathbf{h}}) + \left[\frac{\mathrm{d}\dot{q}_\beta}{\mathrm{d}h_r}\delta h_r + \frac{1}{2}\frac{\mathrm{d}^2\dot{q}_\beta}{\mathrm{d}h_r \mathrm{d}h_s}\delta h_r \delta h_s\right]_{\mathbf{h}=\bar{\mathbf{h}}} \\
\ddot{q}_\beta(h_r;\tau) &= \ddot{q}_\beta(\bar{\mathbf{h}}) + \left[\frac{\mathrm{d}\ddot{q}_\beta}{\mathrm{d}h_r}\delta h_r + \frac{1}{2}\frac{\mathrm{d}^2\ddot{q}_\beta}{\mathrm{d}h_r \mathrm{d}h_s}\delta h_r \delta h_s\right]_{\mathbf{h}=\bar{\mathbf{h}}}
\end{aligned} \tag{3.45}$$

Putting Eqs. (3.40) and (3.45) into Eg. (3.38) leads to obtain

$$\begin{aligned}
Q_\alpha(\bar{\mathbf{h}};\tau) &+ \left[\frac{\partial Q_\alpha}{\partial h_r}\delta h_r + \frac{1}{2}\frac{\partial^2 Q_\alpha}{\partial h_r \partial h_s}\delta h_r \delta h_s\right]_{\mathbf{h}=\bar{\mathbf{h}}} = \\
&+ M_{\alpha\beta}(\bar{\mathbf{h}})\ddot{q}_\beta(\bar{\mathbf{h}};\tau) + \left[M_{\alpha\beta}\frac{\mathrm{d}\ddot{q}_\beta}{\mathrm{d}h_r} + \frac{\partial M_{\alpha\beta}}{\partial h_r}\ddot{q}_\beta(\tau)\right]_{\mathbf{h}=\bar{\mathbf{h}}}\delta h_r \\
&+ \frac{1}{2}\left[M_{\alpha\beta}\frac{\mathrm{d}^2\ddot{q}_\beta}{\mathrm{d}h_r \mathrm{d}h_s} + \ddot{q}_\beta(\tau)\frac{\partial^2 M_{\alpha\beta}}{\partial h_r \partial h_s} + 2\frac{\partial M_{\alpha\beta}}{\partial h_r}\frac{\mathrm{d}\ddot{q}_\beta}{\mathrm{d}h_s}\right]_{\mathbf{h}=\bar{\mathbf{h}}}\delta h_r \delta h_s \\
&+ D_{\alpha\beta}(\bar{\mathbf{h}})\dot{q}_\beta(\bar{\mathbf{h}};\tau) + \left[D_{\alpha\beta}\frac{\mathrm{d}\dot{q}_\beta}{\mathrm{d}h_r} + \frac{\partial D_{\alpha\beta}}{\partial h_r}\dot{q}_\beta(\tau)\right]_{\mathbf{h}=\bar{\mathbf{h}}}\delta h_r \\
&+ \frac{1}{2}\left[D_{\alpha\beta}\frac{\mathrm{d}^2\dot{q}_\beta}{\mathrm{d}h_r \mathrm{d}h_s} + \dot{q}_\beta(\tau)\frac{\partial^2 D_{\alpha\beta}}{\partial h_r \partial h_s} + 2\frac{\partial D_{\alpha\beta}}{\partial h_r}\frac{\mathrm{d}\dot{q}_\beta}{\mathrm{d}h_s}\right]_{\mathbf{h}=\bar{\mathbf{h}}}\delta h_r \delta h_s \\
&+ K_{\alpha\beta}(\bar{\mathbf{h}})q_\beta(\bar{\mathbf{h}};\tau) + \left[K_{\alpha\beta}\frac{\mathrm{d}q_\beta}{\mathrm{d}h_r} + \frac{\partial K_{\alpha\beta}}{\partial h_r}q_\beta(\tau)\right]_{\mathbf{h}=\bar{\mathbf{h}}}\delta h_r \\
&+ \frac{1}{2}\left[K_{\alpha\beta}\frac{\mathrm{d}^2 q_\beta}{\mathrm{d}h_r \mathrm{d}h_s} + q_\beta(\tau)\frac{\partial^2 K_{\alpha\beta}}{\partial h_r \partial h_s} + 2\frac{\partial K_{\alpha\beta}}{\partial h_r}\frac{\mathrm{d}q_\beta}{\mathrm{d}h_s}\right]_{\mathbf{h}=\bar{\mathbf{h}}}\delta h_r \delta h_s
\end{aligned} \tag{3.46}$$

The comparison of the same order terms in Eq. (3.47) tends to receiving the hierarchical set of equations of motion, composing from:

— one system of N equations of the zeroth-order

$$Q_\alpha(\bar{\mathbf{h}};\tau) = M_{\alpha\beta}(\bar{\mathbf{h}})\ddot{q}_\beta(\bar{\mathbf{h}};\tau) + D_{\alpha\beta}(\bar{\mathbf{h}})\dot{q}_\beta(\bar{\mathbf{h}};\tau) + K_{\alpha\beta}(\bar{\mathbf{h}})q_\beta(\bar{\mathbf{h}};\tau) \tag{3.47}$$

— $\hat{r}$ systems of N linear equations of the first-order

$$\begin{aligned}
&\left[M_{\alpha\beta}\frac{\mathrm{d}\ddot{q}_\beta}{\mathrm{d}h_r} + D_{\alpha\beta}\frac{\mathrm{d}\dot{q}_\beta}{\mathrm{d}h_r} + K_{\alpha\beta}\frac{\mathrm{d}q_\beta}{\mathrm{d}h_r}\right]_{\mathbf{h}=\bar{\mathbf{h}}} = \\
&\left[\frac{\partial Q_\alpha}{\partial h_r} - \frac{\partial M_{\alpha\beta}}{\partial h_r}\ddot{q}_\beta(\tau) - \frac{\partial D_{\alpha\beta}}{\partial h_r}\dot{q}_\beta(\tau) - \frac{\partial K_{\alpha\beta}}{\partial h_r}q_\beta(\tau)\right]_{\mathbf{h}=\bar{\mathbf{h}}}
\end{aligned} \tag{3.48}$$

— one system of N linear equations of the second-order

$$\begin{aligned}
M_{\alpha\beta}(\bar{\mathbf{h}})\ddot{q}_\beta^{(2)} &+ D_{\alpha\beta}(\bar{\mathbf{h}})\dot{q}_\beta^{(2)} + K_{\alpha\beta}(\bar{\mathbf{h}})q_\beta^{(2)} = \\
&Q_\alpha^{(2)} - \ddot{q}_\beta(\bar{\mathbf{h}};\tau)M_{\alpha\beta}^{(2)} - \dot{q}_\beta(\bar{\mathbf{h}};\tau)D_{\alpha\beta}^{(2)} - q_\beta(\bar{\mathbf{h}};\tau)K_{\alpha\beta}^{(2)} \\
&- 2\left[\frac{\partial M_{\alpha\beta}}{\partial h_r}\frac{\mathrm{d}\ddot{q}_\beta}{\mathrm{d}h_s} + \frac{\partial D_{\alpha\beta}}{\partial h_r}\frac{\mathrm{d}\dot{q}_\beta}{\mathrm{d}h_s} + \frac{\partial K_{\alpha\beta}}{\partial h_r}\frac{\mathrm{d}q_\beta}{\mathrm{d}h_s}\right]_{\mathbf{h}=\bar{\mathbf{h}}}\mathrm{Cov}(h_r,\, h_s)
\end{aligned} \tag{3.49}$$

3.5 Output Probabilistic Moments

In this section we are aiming to obtain the expectations at any time $\tau = t$ for the nodal displacements and the cross-covariances of $q_\alpha(t_1)$ and $q_\beta(t_1)$, both with including the terms up to the second order. This can be received by using the Eqs. (3.32) and (3.33). The mean values of $q_\alpha(t)$ are

$$\mathrm{E}[q_\alpha(t)] = q_\alpha(\bar{\mathbf{h}}; t) + \frac{1}{2} q_\alpha^{(2)}(t) \tag{3.50}$$

and the cross-covariances of variables q_α (for $\tau = t_1$), q_β (for $\tau = t_2$) read

$$\mathrm{Cov}\big(q_\alpha(t_1);\ q_\beta(t_2)\big) = \frac{\mathrm{d}q_\alpha(t_1)}{\mathrm{d}h_r} \frac{\mathrm{d}q_\beta(t_2)}{\mathrm{d}h_s}\bigg|_{\mathbf{h}=\bar{\mathbf{h}}} \mathrm{Cov}(h_r,\ h_s) - \frac{1}{4} q_\alpha^{(2)}(t_1) q_\beta^{(2)}(t_2) \tag{3.51}$$

In accordance with Eqs. (2.2) and (2.3), we can express the strain tensor at any point inside the element $x = x_\alpha$ by

$$\varepsilon_{ij}(x_\alpha; \tau) = B_{ij\beta}(x_\alpha) \left[q_\beta + \frac{\mathrm{d}q_\beta}{\mathrm{d}h_r} \delta h_r + \frac{1}{2} \frac{\mathrm{d}^2 q_\beta}{\mathrm{d}h_r \mathrm{d}h_s} \delta h_r \delta h_s \right]_{\mathbf{h}=\bar{\mathbf{h}}}; \quad i, j = 1, 2, 3 \tag{3.52}$$

The second-order expectation values at any time $\tau = t$ and the cross-covariances of the strain members are obtained in the form

$$\mathrm{E}[\varepsilon_{ij}(x_\alpha; t)] = B_{ij\beta}(x_\alpha) \left[q_\beta(t) + \frac{1}{2} q_\beta(t)^{(2)} \right] \tag{3.53}$$

and

$$\begin{aligned} &\mathrm{Cov}\big(\varepsilon_{ij}(t_1)\ ;\ \varepsilon_{kl}(t_2)\big) \\ &\quad = B_{ij\alpha} B_{kl\beta} \left[\frac{\mathrm{d}q_\alpha(t_1)}{\mathrm{d}h_r} \frac{\mathrm{d}q_\beta(t_2)}{\mathrm{d}h_s}\bigg|_{\mathbf{h}=\bar{\mathbf{h}}} \mathrm{Cov}(h_r,\ h_s) - \frac{1}{4} q_\alpha^{(2)}(t_1) q_\beta^{(2)}(t_2) \right] \end{aligned} \tag{3.54}$$

with $\alpha, \beta = 1, 2, ..., N$ and $i, j, k, l = 1, 2, 3$.

3.6 Stochastic Sensitivity of Statics and Dynamics

3.6.1 Static Sensitivity

Since the linear elastic complex structure with N degrees of freedom is considered, the static response can be expressed by the functional

$$\phi = G[q_\alpha(b_a, h_r), b_a] \tag{3.55}$$

where $a = 1, 2, .., A;\ \alpha = 1, 2, .., N,\ r = 1, 2, ..., \bar{r}$. The symbols $q_\alpha,\ b_a,\ h_r$ are defined as the vectors of the generalized coordinates, the design variables and the random variables, respectively. Aiming to present the design sensitivity of the stochastic systems, the equation of motion for static case — cf. Eqs. (2.95) and (3.40), is rewritten to

$$K_{\alpha\beta}(b_a, h_r) q_\beta(b_a, h_r) = Q_\alpha(b_a, h_r) \tag{3.56}$$

In assumption, the stiffness matrix $K_{\alpha\beta}$ and the nodal load vector Q_α are explicit functions of the design parameter and the random variable vectors. Solving Eq. (3.56) with respect to the q_β (Eq. 3.57) proves that the nodal displacement vector is an implicit function of b_a and h_r.

$$q_\beta(b_a, h_r) = K^{-1}_{\alpha\beta}(b_a, h_r) Q_\alpha(b_a, h_r) \tag{3.57}$$

Our goal is to estimate the probabilistic distribution of the static structural response with respect to the design parameters. Therefore, we are using Eq. (2.96) to obtain the absolute partial derivative of the functional ϕ with respect to b_a.

The adjoint variable vector is assumed to be an implicit function of b_a and h_r and is written in the form $\lambda = \{\lambda_\alpha(b_a, h_r)\},\ \alpha = 1, 2, ..., N$. Owing to that, the adjoint equations (cf. Eq. 2.100) are given as

$$K_{\alpha\beta}(b_a, h_r)\lambda_\beta(b_a, h_r) = \frac{\partial G}{\partial q_\alpha}(b_a, h_r) \tag{3.58}$$

Using Eq. (3.58) we receive the same solution as for the deterministic system sensitivity — Eq. (2.103), except that all terms are simultaneously functions of the design parameter and the random variable vectors now

$$\frac{\mathrm{d}\phi}{\mathrm{d}b_a} = \frac{\partial G}{\partial b_a} + \lambda_\alpha\left(\frac{\partial Q_\alpha}{\partial b_a} - \frac{\partial K_{\alpha\beta}}{\partial b_a} q_\beta\right) \tag{3.59}$$

We are expanding in power series around the means $\bar{h}_r$ the vectors of generalized coordinates q_α and the nodal loads Q_α and the stiffness matrix $K_{\alpha\beta}$, respectively as

$$\begin{aligned}
q_\beta(b_a; h_r) &= q_\beta(\bar{\mathbf{h}}) + \left[\frac{\mathrm{d}q_\beta}{\mathrm{d}h_r}\delta h_r + \frac{1}{2}\frac{\mathrm{d}^2 q_\beta}{\mathrm{d}h_r \mathrm{d}h_s}\delta h_r \delta h_s\right]_{\mathbf{h}=\bar{\mathbf{h}}} \\
Q_\alpha(b_a; h_r) &= Q_\alpha(\bar{\mathbf{h}}) + \left[\frac{\partial Q_\alpha}{\partial h_r}\delta h_r + \frac{1}{2}\frac{\partial^2 Q_\alpha}{\partial h_r \partial h_s}\delta h_r \delta h_s\right]_{\mathbf{h}=\bar{\mathbf{h}}} \\
K_{\alpha\beta}(b_a; h_r) &= K_{\alpha\beta}(\bar{\mathbf{h}}) + \left[\frac{\partial K_{\alpha\beta}}{\partial h_r}\delta h_r + \frac{1}{2}\frac{\partial^2 K_{\alpha\beta}}{\partial h_r \partial h_s}\delta h_r \delta h_s\right]_{\mathbf{h}=\bar{\mathbf{h}}}
\end{aligned} \tag{3.60}$$

To including the influence of the randomness in the design parameters like material, geometry, etc. on the final results of the computation, the adjoint variable vector is expanded in Taylor series up to the second order around the mean values of the random variables $\bar{h}_r$

$$\lambda_\alpha(b_a, h_r) = \lambda_\alpha(\bar{\mathbf{h}}) + \left[\frac{\mathrm{d}\lambda_\alpha}{\mathrm{d}h_r}\delta h_r + \frac{1}{2}\frac{\mathrm{d}^2\lambda_\alpha}{\mathrm{d}h_r \mathrm{d}h_s}\delta h_r \delta h_s\right]_{\mathbf{h}=\bar{\mathbf{h}}} \tag{3.61}$$

Expanding in power series up to the second order, the first partial derivative of the functional with respect to the generalized coordinate vector, yields to

$$\frac{\partial G}{\partial q_\alpha}(b_a, h_r) = \frac{\partial G}{\partial q_\alpha}(\bar{\mathbf{h}}) + \left[\frac{\partial^2 G}{\partial h_r \partial q_\alpha}\delta h_r + \frac{1}{2}\frac{\partial^3 G}{\partial h_r \partial h_s \partial q_\alpha}\delta h_r \delta h_s\right]_{\mathbf{h}=\bar{\mathbf{h}}} \tag{3.62}$$

Substituting Eqs. (3.58) into Eq. (3.54) and Eqs. $(3.58)_3$, (3.59) and (3.60) into Eq.(3.56) and comparing the same order terms, gives the primary and adjoint systems of equations [35]

— one pair of systems of N linear algebraic equations of zeroth-order

$$\begin{aligned} K_{\alpha\beta}(b_a,\bar{\mathbf{h}})q_\beta(b_a,\bar{\mathbf{h}}) &= Q_\alpha(b_a,\bar{\mathbf{h}}) \\ K_{\alpha\beta}(b_a,\bar{\mathbf{h}})\lambda_\beta(b_a,\bar{\mathbf{h}}) &= \frac{\partial G}{\partial q_\alpha}(b_a,\bar{\mathbf{h}}) \end{aligned} \tag{3.63}$$

— $\hat{r}$ pairs of systems of N linear algebraic equations of the first-order

$$\begin{aligned} K_{\alpha\beta}(b_a,\bar{\mathbf{h}})\frac{\mathrm{d}q_\beta}{\mathrm{d}b_a,\mathrm{d}h_r} &= \frac{\partial Q_\alpha}{\partial h_r}(\mathrm{d}b_a,\bar{\mathbf{h}}) - \frac{\partial K_{\alpha\beta}}{\partial h_r}(b_a,\bar{\mathbf{h}})q_\beta(b_a,\bar{\mathbf{h}}) \\ K_{\alpha\beta}(b_a,\bar{\mathbf{h}})\frac{\mathrm{d}\lambda_\beta}{\mathrm{d}b_a,\mathrm{d}h_r} &= \frac{\partial G^2}{\partial h_r\partial q_\alpha}(b_a,\bar{\mathbf{h}}) - \frac{\partial K_{\alpha\beta}}{\partial h_r}(b_a,\bar{\mathbf{h}})\lambda_\beta(b_a,\bar{\mathbf{h}}) \end{aligned} \tag{3.64}$$

— one pair of systems of N linear algebraic equations of the second-order

$$\begin{aligned} K_{\alpha\beta}(b_a,\bar{\mathbf{h}})\, q^{(2)}_\beta(b_a,\bar{\mathbf{h}}) &= Q^{(2)}_\alpha(b_a,\bar{\mathbf{h}}) - K^{(2)}_{\alpha\beta}(b_a,\bar{\mathbf{h}})q_\beta(b_a,\bar{\mathbf{h}}) \\ &\quad -2\frac{\partial K_{\alpha\beta}}{\partial h_r}(b_a,\bar{\mathbf{h}})\frac{\mathrm{d}q_\beta}{\mathrm{d}h_s}(b_a,\bar{\mathbf{h}})\mathrm{Cov}(h_r,\ h_s) \\ K_{\alpha\beta}(b_a,\bar{\mathbf{h}})\,\lambda^{(2)}_\beta(b_a,\bar{\mathbf{h}}) &= \left[\frac{\partial G^3}{\partial h_r\partial h_s\partial q_\alpha}(b_a,\bar{\mathbf{h}}) - 2\frac{\partial K_{\alpha\beta}}{\partial h_r}(b_a,\bar{\mathbf{h}})\frac{\mathrm{d}\lambda_\beta}{\mathrm{d}h_s}(b_a,\bar{\mathbf{h}})\right] \\ &\quad \times\mathrm{Cov}(h_r,\ h_s) - K^{(2)}_{\alpha\beta}(b_a,\bar{\mathbf{h}})\lambda_\beta(b_a,\bar{\mathbf{h}}) \end{aligned} \tag{3.65}$$

From the definition [26,27,35], the first probabilistic moment for the sensitivity gradient can be expressed as

$$E\left[\frac{\mathrm{d}\phi}{\mathrm{d}b_a}\right] = \underbrace{\int_{-\infty}^{+\infty}\int_{-\infty}^{+\infty}\ldots\int_{-\infty}^{+\infty}}_{A-\text{fold}}\frac{\mathrm{d}\phi}{\mathrm{d}b_a}p_A(b_1,b_2,\ldots,b_A)\mathrm{d}b_1\mathrm{d}b_2\ldots\mathrm{d}b_A \tag{3.66}$$

and the second probabilistic moment is respectively equal

$$\mathrm{Cov}\left(\frac{\mathrm{d}\phi}{\mathrm{d}b_a},\frac{\mathrm{d}\phi}{\mathrm{d}b_b}\right) = E\left[\left(\frac{\mathrm{d}\phi}{\mathrm{d}b_a} - E\left[\frac{\mathrm{d}\phi}{\mathrm{d}b_a}\right]\right)\left(\frac{\mathrm{d}\phi}{\mathrm{d}b_b} - E\left[\frac{\mathrm{d}\phi}{\mathrm{d}b_b}\right]\right)\right] \tag{3.67}$$

Substituting Eq. (3.59) into Eqs. (3.66) and (3.67), the mean value of sensitivity gradient may be written as

$$\begin{aligned} E\left[\frac{\mathrm{d}\phi}{\mathrm{d}b_a}\right] &= E\left[\frac{\partial G}{\partial b_a} + \lambda_\alpha\left(\frac{\partial Q_\alpha}{\partial b_a} - \frac{\partial K_{\alpha\beta}}{\partial b_a}q_\beta\right)\right] \\ &= E\left[\frac{\partial G}{\partial b_a}\right] + E\left[\lambda_\alpha\frac{\partial Q_\alpha}{\partial b_a}\right] - E\left[\lambda_\alpha\frac{\partial K_{\alpha\beta}}{\partial b_a}q_\beta\right] \end{aligned} \tag{3.68}$$

while the covariances-matrix is given in the form

$$\begin{aligned} \mathrm{Cov}\left(\frac{\mathrm{d}\phi}{\mathrm{d}b_a},\frac{\mathrm{d}\phi}{\mathrm{d}b_b}\right) &= E\left[\left(\frac{\partial G}{\partial b_a} + \lambda_\alpha\left(\frac{\partial Q_\alpha}{\partial b_a} - \frac{\partial K_{\alpha\beta}}{\partial b_a}q_\beta\right) - E\left[\frac{\mathrm{d}\phi}{\mathrm{d}b_a}\right]\right)\right. \\ &\quad \times \left.\left(\frac{\partial G}{\partial b_b} + \lambda_\gamma\left(\frac{\partial Q_\gamma}{\partial b_b} - \frac{\partial K_{\gamma\delta}}{\partial b_b}q_\delta\right) - E\left[\frac{\mathrm{d}\phi}{\mathrm{d}b_b}\right]\right)\right] \end{aligned} \tag{3.69}$$

In order to determine the Eqs. (3.68) and (3.69), the partial derivatives of the gradient sensitivity, the stiffness matrix and the nodal load vector with respect to the design variable vector, are expanded in Taylor series up to the second order around the means $\bar{h}_r$

$$\begin{aligned}
\frac{\partial G}{\partial b_a}(b_a, h_r) &= \frac{\partial G}{\partial b_a}(\bar{\mathbf{h}}) + \left[\frac{\partial^2 G}{\partial h_r \partial b_a}\delta h_r + \frac{1}{2}\frac{\partial^3 G}{\partial h_r \partial h_s \partial b_a}\delta h_r \delta h_s\right]_{\mathbf{h}=\bar{\mathbf{h}}} \\
\frac{\partial K_{\alpha\beta}}{\partial b_a}(b_a, h_r) &= \frac{\partial K_{\alpha\beta}}{\partial b_a}(\bar{\mathbf{h}}) + \left[\frac{\partial^2 K_{\alpha\beta}}{\partial h_r \partial b_a}\delta h_r + \frac{1}{2}\frac{\partial^3 K_{\alpha\beta}}{\partial h_r \partial h_s \partial b_a}\delta h_r \delta h_s\right]_{\mathbf{h}=\bar{\mathbf{h}}} \\
\frac{\partial Q_\alpha}{\partial b_a}(b_a, h_r) &= \frac{\partial Q_\alpha}{\partial b_a}(\bar{\mathbf{h}}) + \left[\frac{\partial^2 Q_\alpha}{\partial h_r \partial b_a}\delta h_r + \frac{1}{2}\frac{\partial^3 Q_\alpha}{\partial h_r \partial h_s \partial b_a}\delta h_r \delta h_s\right]_{\mathbf{h}=\bar{\mathbf{h}}}
\end{aligned} \tag{3.70}$$

The mean value of $\partial G/\partial b_a$ is equal

$$E\left[\frac{\partial G}{\partial b_a}\right] = \frac{\partial G}{\partial b_a}(\bar{\mathbf{h}}) + \frac{1}{2}\frac{\partial^3 G}{\partial h_r \partial h_s \partial b_a}\bigg|_{h=\bar{h}} \mathrm{Cov}(h_r,\, h_s) \tag{3.71}$$

Using Eqs. (3.61) and $(3.70)_3$, the product $\lambda_\alpha \frac{\partial Q_\alpha}{\partial b_a}$ limited to the second order terms is received as

$$\begin{aligned}
\lambda_\alpha \frac{\partial Q_\alpha}{\partial b_a} &= \lambda_\alpha(\bar{\mathbf{h}})\frac{\partial Q_\alpha}{\partial b_a}(\bar{\mathbf{h}}) + \left[\lambda_\alpha \frac{\partial^2 Q_\alpha}{\partial h_r \partial b_a} + \frac{\mathrm{d}\lambda_\alpha}{\mathrm{d}h_r}\frac{\partial Q_\alpha}{\partial b_a}\right]_{\mathbf{h}=\bar{\mathbf{h}}}\delta h_r \\
&+ \frac{1}{2}\left[\lambda_\alpha \frac{\partial^3 Q_\alpha}{\partial h_r \partial h_s \partial b_a} + 2\frac{\mathrm{d}\lambda_\alpha}{\mathrm{d}h_r}\frac{\partial^2 Q_\alpha}{\partial h_s \partial b_a} + \frac{\mathrm{d}^2\lambda_\alpha}{\mathrm{d}h_r \mathrm{d}h_s}\frac{\partial Q_\alpha}{\partial b_a}\right]_{\mathbf{h}=\bar{\mathbf{h}}}\delta h_r \delta h_s
\end{aligned} \tag{3.72}$$

Analogically, after multiplying Eqs. (3.61), $(3.70)_2$ and $(3.60)_1$ and excluding the terms higher than second order, we obtain

$$\begin{aligned}
\lambda_\alpha \frac{\partial K_{\alpha\beta}}{\partial b_a} q_\beta &= \lambda_\alpha(\bar{\mathbf{h}})\frac{\partial K_{\alpha\beta}}{\partial b_a}(\bar{\mathbf{h}})q_\beta(\bar{\mathbf{h}}) \\
&+\left[\lambda_\alpha\left(\frac{\partial^2 K_{\alpha\beta}}{\partial h_r \partial b_a}q_\beta + \frac{\partial K_{\alpha\beta}}{\partial b_a}\frac{\mathrm{d}q_\beta}{\mathrm{d}h_r}\right) + \frac{\mathrm{d}\lambda_\alpha}{\mathrm{d}h_r}\frac{\partial K_{\alpha\beta}}{\partial b_a}q_\beta\right]_{\mathbf{h}=\bar{\mathbf{h}}}\delta h_r \\
&+\left[\frac{1}{2}\left(\lambda_\alpha \frac{\partial^3 K_{\alpha\beta}}{\partial h_r \partial h_s \partial b_a} + 2\frac{\mathrm{d}\lambda_\alpha}{\mathrm{d}h_r}\frac{\partial^2 K_{\alpha\beta}}{\partial h_s \partial b_a} + \frac{\mathrm{d}^2\lambda_\alpha}{\mathrm{d}h_r \mathrm{d}h_s}\frac{\partial K_{\alpha\beta}}{\partial b_a}\right)q_\beta\right. \\
&\left.+\left(\lambda_\alpha \frac{\partial^2 K_{\alpha\beta}}{\partial h_r \partial b_a} + \frac{\mathrm{d}\lambda_\alpha}{\mathrm{d}h_r}\frac{\partial K_{\alpha\beta}}{\partial b_a}\right)\frac{\mathrm{d}q_\beta}{\mathrm{d}h_s} + \frac{1}{2}\lambda_\alpha \frac{\partial K_{\alpha\beta}}{\partial b_a}\frac{\mathrm{d}^2 q_\beta}{\mathrm{d}h_r \mathrm{d}h_s}\right)\right]_{\mathbf{h}=\bar{\mathbf{h}}}\delta h_r \delta h_s
\end{aligned} \tag{3.73}$$

The mean values of Eq. (3.72) is equal,

$$\begin{aligned}
E\left[\lambda_\alpha \frac{\partial Q_\alpha}{\partial b_a}\right] &= \lambda_\alpha(\bar{\mathbf{h}})\frac{\partial Q_\alpha}{\partial b_a}(\bar{\mathbf{h}}) + \frac{1}{2}\lambda_\alpha^{(2)}\frac{\partial Q_\alpha}{\partial b_a} \\
&+\frac{1}{2}\left[\lambda_\alpha \frac{\partial^3 Q_\alpha}{\partial h_r \partial h_s \partial b_a} + 2\frac{\mathrm{d}\lambda_\alpha}{\mathrm{d}h_r}\frac{\partial^2 Q_\alpha}{\partial h_s \partial b_a}\right]_{\mathbf{h}=\bar{\mathbf{h}}}\mathrm{Cov}(h_r, h_s)
\end{aligned} \tag{3.74}$$

Similarly, for Eq. (3.73) we have

$$
\begin{aligned}
E\left[\lambda_\alpha \frac{\partial K_{\alpha\beta}}{\partial b_a} q_\beta\right] &= \lambda_\alpha(\bar{\mathbf{h}}) \frac{\partial K_{\alpha\beta}}{\partial b_a}(\bar{\mathbf{h}}) q_\beta(\bar{\mathbf{h}}) + \frac{1}{2}\left(\lambda_\alpha^{(2)} \frac{\partial K_{\alpha\beta}}{\partial b_a} q_\beta(\bar{\mathbf{h}}) + \lambda_\alpha(\bar{\mathbf{h}}) \frac{\partial K_{\alpha\beta}}{\partial b_a}(\bar{\mathbf{h}}) q_\beta^{(2)}\right) \\
&+ \frac{1}{2}\left[\lambda_\alpha\left(\frac{\partial^3 K_{\alpha\beta}}{\partial h_r \partial h_s \partial b_a} q_\beta + 2 \frac{\partial^2 K_{\alpha\beta}}{\partial h_r \partial b_a} \frac{\mathrm{d}q_\beta}{\mathrm{d}h_s}\right)\right. \\
&\left. + 2 \frac{\mathrm{d}\lambda_\alpha}{\mathrm{d}h_r}\left(\frac{\partial^2 K_{\alpha\beta}}{\partial h_s \partial b_a} q_\beta + \frac{\partial K_{\alpha\beta}}{\partial b_a} \frac{\mathrm{d}q_\beta}{\mathrm{d}h_s}\right)\right]_{\mathbf{h}=\bar{\mathbf{h}}} \mathrm{Cov}(h_r, h_s)
\end{aligned} \tag{3.75}
$$

Substituting Eqs. (3.71), (3.74) and (3.75) into Eq. (3.68) results in obtaining the mean values of the sensitivity gradient expression

$$
\begin{aligned}
E\left[\frac{\mathrm{d}\phi}{\mathrm{d}b_a}\right] &= \frac{\partial G}{\partial b_a}(\bar{\mathbf{h}}) - \frac{1}{2}\lambda_\alpha(\bar{\mathbf{h}}) \frac{\partial K_{\alpha\beta}}{\partial b_a}(\bar{\mathbf{h}}) q_\beta^{(2)} \\
&+ \left(\lambda_\alpha(\bar{\mathbf{h}}) + \frac{1}{2}\lambda_\alpha^{(2)}\right)\left(\frac{\partial Q_\alpha}{\partial b_a}(\bar{\mathbf{h}}) - \frac{\partial K_{\alpha\beta}}{\partial b_a}(\bar{\mathbf{h}}) q_\beta(\bar{\mathbf{h}})\right) \\
&+ \frac{1}{2}\left[\frac{\partial^3 G}{\partial h_r \partial h_s \partial b_a} + 2 \frac{\mathrm{d}\lambda_\alpha}{\mathrm{d}h_r}\left(\frac{\partial^2 Q_\alpha}{\partial h_s \partial b_a} - \frac{\partial^2 K_{\alpha\beta}}{\partial h_s \partial b_a} q_\beta - \frac{\partial K_{\alpha\beta}}{\partial b_a} \frac{\mathrm{d}q_\beta}{\mathrm{d}h_s}\right)\right. \\
&\left. + \lambda_\alpha\left(\frac{\partial^3 Q_\alpha}{\partial h_r \partial h_s \partial b_a} - \frac{\partial^3 K_{\alpha\beta}}{\partial h_r \partial h_s \partial b_a} q_\beta - 2 \frac{\partial^2 K_{\alpha\beta}}{\partial h_r \partial b_a} \frac{\mathrm{d}q_\beta}{\mathrm{d}h_s}\right)\right]_{\mathbf{h}=\bar{\mathbf{h}}} \mathrm{Cov}(h_r, h_s)
\end{aligned} \tag{3.76}
$$

By entering the following notations

$$
\begin{aligned}
\mathfrak{A}_{\alpha a} &= \frac{\partial Q_\alpha}{\partial b_a}(\bar{\mathbf{h}}) - \frac{\partial K_{\alpha\beta}}{\partial b_a}(\bar{\mathbf{h}}) q_\beta(\bar{\mathbf{h}}) \qquad (3.77) \\
\mathfrak{B}_{\alpha s a} &= \frac{\partial^2 Q_\alpha}{\partial h_s \partial b_a} - \frac{\partial^2 K_{\alpha\beta}}{\partial h_s \partial b_a} q_\beta(\bar{\mathbf{h}}) - \frac{\partial K_{\alpha\beta}}{\partial b_a}(\bar{\mathbf{h}}) \frac{\mathrm{d}q_\beta}{\mathrm{d}h_s} \\
\mathfrak{C}_{\alpha r s a} &= \frac{\partial^3 Q_\alpha}{\partial h_r \partial h_s \partial b_a} - \frac{\partial^3 K_{\alpha\beta}}{\partial h_r \partial h_s \partial b_a} q_\beta(\bar{\mathbf{h}}) - 2 \frac{\partial^2 K_{\alpha\beta}}{\partial h_r \partial b_a} \frac{\mathrm{d}q_\beta}{\mathrm{d}h_s}
\end{aligned}
$$

Eq. (3.76) can be written in a simpler form as

$$
\begin{aligned}
E\left[\frac{\mathrm{d}\phi}{\mathrm{d}b_a}\right] &= \frac{\partial G}{\partial b_a} - \frac{1}{2}\lambda_\alpha(\bar{\mathbf{h}}) \frac{\partial K_{\alpha\beta}}{\partial b_a} q_\beta^{(2)} + \mathfrak{A}_{\alpha a}\left(\lambda_\alpha(\bar{\mathbf{h}}) + \frac{1}{2}\lambda_\alpha^{(2)}\right) \qquad (3.78) \\
&+ \frac{1}{2}\left[\frac{\partial^3 G}{\partial h_r \partial h_s \partial b_a} + 2 \frac{\mathrm{d}\lambda_\alpha}{\mathrm{d}h_r} \mathfrak{B}_{\alpha s a} + \lambda_\alpha \mathfrak{C}_{\alpha r s a}\right]_{\mathbf{h}=\bar{\mathbf{h}}} \mathrm{Cov}(h_r, h_s)
\end{aligned}
$$

Analogically to Eq. (3.78), the equation for $E\left[\frac{\mathrm{d}\phi}{\mathrm{d}b_b}\right]$ reads

$$
\begin{aligned}
E\left[\frac{\mathrm{d}\phi}{\mathrm{d}b_b}\right] &= \frac{\partial G}{\partial b_b} - \frac{1}{2}\lambda_\gamma(\bar{\mathbf{h}}) \frac{\partial K_{\gamma\delta}}{\partial b_b} q_\delta^{(2)} + \mathfrak{A}_{\gamma b}\left(\lambda_\gamma(\bar{\mathbf{h}}) + \frac{1}{2}\lambda_\gamma^{(2)}\right) \qquad (3.79) \\
&+ \frac{1}{2}\left[\frac{\partial^3 G}{\partial h_r \partial h_s \partial b_b} + 2 \frac{\mathrm{d}\lambda_\gamma}{\mathrm{d}h_r} \mathfrak{B}_{\gamma s b} + \lambda_\gamma \mathfrak{C}_{\gamma r s b}\right]_{\mathbf{h}=\bar{\mathbf{h}}} \mathrm{Cov}(h_r, h_s)
\end{aligned}
$$

After multiplying the particular members in Eq. (3.69), the formula for the covariances can be written in the form

$$\begin{aligned}\mathrm{Cov}\left(\frac{\mathrm{d}\phi}{\mathrm{d}b_a},\frac{\mathrm{d}\phi}{\mathrm{d}b_b}\right) = E\Bigg[&\frac{\partial G}{\partial b_a}\frac{\partial G}{\partial b_b}+\frac{\partial G}{\partial b_a}\lambda_\gamma\left(\frac{\partial Q_\gamma}{\partial b_b}-\frac{\partial K_{\gamma\delta}}{\partial b_b}q_\delta\right)+\frac{\partial G}{\partial b_b}\lambda_\alpha\left(\frac{\partial Q_\alpha}{\partial b_a}-\frac{\partial K_{\alpha\beta}}{\partial b_a}q_\beta\right)\\ &-\lambda_\alpha\left(\frac{\partial Q_\alpha}{\partial b_a}-\frac{\partial K_{\alpha\beta}}{\partial b_a}q_\beta\right)E\left[\frac{\mathrm{d}\phi}{\mathrm{d}b_b}\right]-\lambda_\gamma\left(\frac{\partial Q_\gamma}{\partial b_b}-\frac{\partial K_{\gamma\delta}}{\partial b_b}q_\delta\right)E\left[\frac{\mathrm{d}\phi}{\mathrm{d}b_a}\right]\\ &+\lambda_\alpha\lambda_\gamma\left(\frac{\partial Q_\alpha}{\partial b_a}-\frac{\partial K_{\alpha\beta}}{\partial b_a}q_\beta\right)\left(\frac{\partial Q_\gamma}{\partial b_b}-\frac{\partial K_{\gamma\delta}}{\partial b_b}q_\delta\right)\\ &-\frac{\partial G}{\partial b_a}E\left[\frac{\mathrm{d}\phi}{\mathrm{d}b_b}\right]-\frac{\partial G}{\partial b_b}E\left[\frac{\mathrm{d}\phi}{\mathrm{d}b_a}\right]+E\left[\frac{\mathrm{d}\phi}{\mathrm{d}b_a}\right]E\left[\frac{\mathrm{d}\phi}{\mathrm{d}b_b}\right]\Bigg]\end{aligned} \tag{3.80}$$

From now on, the terms $E[\mathrm{d}\phi/\mathrm{d}b_a]$ and $E[\mathrm{d}\phi/\mathrm{d}b_b]$ are treated as the final products, given by Egs. (3.78) and (3.79). Therefore they are not developed during the consideration of following expressions. For simplification, all members of (Eq. 3.80) are initially received by using Eqs. (3.60), (3.61) and (3.70) with including the terms only to the second-order. After ordering individual terms, first formula is

$$\begin{aligned}E\left[\frac{\partial G}{\partial b_a}\frac{\partial G}{\partial b_b}\right] = &\frac{\partial G}{\partial b_a}(\bar{\mathbf{h}})\frac{\partial G}{\partial b_b}(\bar{\mathbf{h}})+\frac{1}{2}\Bigg[\frac{\partial G}{\partial b_a}\frac{\partial^3 G}{\partial h_r\partial h_s\partial b_b}+\frac{\partial G}{\partial b_b}\frac{\partial^3 G}{\partial h_r\partial h_s\partial b_a}\\ &+2\frac{\partial^2 G}{\partial h_r\partial b_a}\frac{\partial^2 G}{\partial h_s\partial b_b}\Bigg]_{\mathbf{h}=\bar{\mathbf{h}}}\mathrm{Cov}(h_r,h_s)\end{aligned} \tag{3.81}$$

The second and the third terms, due to the similarity, are obtained together in the form

$$\begin{aligned}&E\left[\lambda_\gamma\frac{\partial G}{\partial b_a}\left(\frac{\partial Q_\gamma}{\partial b_b}-\frac{\partial K_{\gamma\delta}}{\partial b_b}q_\delta\right)\right]+E\left[\lambda_\alpha\frac{\partial G}{\partial b_b}\left(\frac{\partial Q_\alpha}{\partial b_a}-\frac{\partial K_{\alpha\beta}}{\partial b_a}q_\beta\right)\right]=\\ &\quad\lambda_\gamma(\bar{\mathbf{h}})\frac{\partial G}{\partial b_a}(\bar{\mathbf{h}})\mathfrak{A}_{\gamma b}+\lambda_\alpha(\bar{\mathbf{h}})\frac{\partial G}{\partial b_b}(\bar{\mathbf{h}})\mathfrak{A}_{\alpha a}\\ &+\quad\frac{1}{2}\Bigg\{\mathfrak{A}_{\gamma b}\left[2\frac{\partial^2 G}{\partial h_r\partial b_a}\frac{\mathrm{d}\lambda_\gamma}{\mathrm{d}h_s}+\frac{\partial G}{\partial b_a}\frac{\mathrm{d}^2\lambda_\gamma}{\mathrm{d}h_r\mathrm{d}h_s}+\lambda_\gamma\frac{\partial^3 G}{\partial h_r\partial h_s\partial b_a}\right]_{\mathbf{h}=\bar{\mathbf{h}}}\\ &+\quad\mathfrak{A}_{\alpha a}\left[2\frac{\partial^2 G}{\partial h_r\partial b_b}\frac{\mathrm{d}\lambda_\alpha}{\mathrm{d}h_s}+\frac{\partial G}{\partial b_b}\frac{\mathrm{d}^2\lambda_\alpha}{\mathrm{d}h_r\mathrm{d}h_s}+\lambda_\alpha\frac{\partial^3 G}{\partial h_r\partial h_s\partial b_b}\right]_{\mathbf{h}=\bar{\mathbf{h}}}\\ &+\quad\lambda_\gamma(\bar{\mathbf{h}})\frac{\partial G}{\partial b_a}(\bar{\mathbf{h}})\left[\mathfrak{C}_{\gamma rsb}-\frac{\partial K_{\gamma\delta}}{\partial b_b}\frac{\mathrm{d}^2 q_\delta}{\mathrm{d}h_r\mathrm{d}h_s}\right]_{\mathbf{h}=\bar{\mathbf{h}}}\\ &\quad+\lambda_\alpha(\bar{\mathbf{h}})\frac{\partial G}{\partial b_b}(\bar{\mathbf{h}})\left[\mathfrak{C}_{\alpha rsa}-\frac{\partial K_{\alpha\beta}}{\partial b_a}\frac{\mathrm{d}^2 q_\beta}{\mathrm{d}h_r\mathrm{d}h_s}\right]_{\mathbf{h}=\bar{\mathbf{h}}}\\ &+\quad2\mathfrak{B}_{\gamma sb}\left[\lambda_\gamma\frac{\partial^2 G}{\partial h_r\partial b_a}+\frac{\partial G}{\partial b_a}\frac{\mathrm{d}\lambda_\gamma}{\mathrm{d}h_r}\right]_{\mathbf{h}=\bar{\mathbf{h}}}\\ &\quad+2\mathfrak{B}_{\alpha sa}\left[\lambda_\alpha\frac{\partial^2 G}{\partial h_r\partial b_b}+\frac{\partial G}{\partial b_b}\frac{\mathrm{d}\lambda_\alpha}{\mathrm{d}h_r}\right]_{\mathbf{h}=\bar{\mathbf{h}}}\Bigg\}\mathrm{Cov}(h_r,h_s)\end{aligned} \tag{3.82}$$

The fourth equation is given by

$$
\begin{aligned}
E\left[\lambda_\alpha\lambda_\gamma\left(\frac{\partial Q_\alpha}{\partial b_a}-\frac{\partial K_{\alpha\beta}}{\partial b_a}q_\beta\right)\left(\frac{\partial Q_\gamma}{\partial b_b}-\frac{\partial K_{\gamma\delta}}{\partial b_b}q_\delta\right)\right] &= \\
= \quad \lambda_\alpha(\bar{\mathbf{h}})\lambda_\gamma(\bar{\mathbf{h}})\mathfrak{A}_{\alpha a}\mathfrak{A}_{\gamma b} & \\
+ \quad \frac{1}{2}\Bigg\{\lambda_\alpha(\bar{\mathbf{h}})\lambda_\gamma(\bar{\mathbf{h}})\Bigg(\mathfrak{A}_{\alpha a}\left[\mathfrak{C}_{\gamma rsb}-\frac{\partial K_{\gamma\delta}}{\partial b_b}\frac{\mathrm{d}^2 q_\delta}{\mathrm{d}h_r\mathrm{d}h_s}\right]_{\mathbf{h}=\bar{\mathbf{h}}}+2\mathfrak{B}_{\alpha ra}\mathfrak{B}_{\gamma sb}\Bigg) & \\
+ \quad \lambda_\alpha(\bar{\mathbf{h}})\lambda_\gamma(\bar{\mathbf{h}})\mathfrak{A}_{\gamma b}\left[\mathfrak{C}_{\alpha rsa}-\frac{\partial K_{\alpha\beta}}{\partial b_a}\frac{\mathrm{d}^2 q_\beta}{\mathrm{d}h_r\mathrm{d}h_s}\right]_{\mathbf{h}=\bar{\mathbf{h}}} & \\
+ \quad \mathfrak{A}_{\alpha a}\mathfrak{A}_{\gamma b}\left[\lambda_\alpha\frac{\mathrm{d}^2\lambda_\gamma}{\mathrm{d}h_r\mathrm{d}h_s}+\lambda_\gamma\frac{\mathrm{d}^2\lambda_\alpha}{\mathrm{d}h_r\mathrm{d}h_s}+2\frac{\mathrm{d}\lambda_\alpha}{\mathrm{d}h_r}\frac{\mathrm{d}\lambda_\gamma}{\mathrm{d}h_t}\right]_{\mathbf{h}=\bar{h}} & \\
+ \quad 2\left(\lambda_\alpha(\bar{\mathbf{h}})\frac{\mathrm{d}\lambda_\gamma}{\mathrm{d}h_r}+\lambda_\gamma(\bar{\mathbf{h}})\frac{\mathrm{d}\lambda_\alpha}{\mathrm{d}h_r}\right)\left(\mathfrak{A}_{\alpha a}\mathfrak{B}_{\gamma sb}+\mathfrak{A}_{\gamma b}\mathfrak{B}_{\alpha sa}\right)\Bigg\}\mathrm{Cov}(h_r,h_s) & \qquad (3.83)
\end{aligned}
$$

Five and six members, are gained simultaneously

$$
\begin{aligned}
E\left[\frac{\partial G}{\partial b_a}E\left[\frac{\mathrm{d}\phi}{\mathrm{d}b_b}\right]\right]+E\left[\frac{\partial G}{\partial b_b}E\left[\frac{\mathrm{d}\phi}{\mathrm{d}b_a}\right]\right] = & \\
\left(\frac{\partial G}{\partial b_a}(\bar{\mathbf{h}})+\frac{1}{2}\frac{\partial^3 G}{\partial h_r\partial h_s\partial b_a}\bigg|_{h=\bar{h}}\mathrm{Cov}(h_r,h_s)\right)E\left[\frac{\mathrm{d}\phi}{\mathrm{d}b_b}\right] & \\
+ \quad \left(\frac{\partial G}{\partial b_b}(\bar{\mathbf{h}})+\frac{1}{2}\frac{\partial^3 G}{\partial h_r\partial h_s\partial b_b}\bigg|_{h=\bar{h}}\mathrm{Cov}(h_r,h_s)\right)E\left[\frac{\mathrm{d}\phi}{\mathrm{d}b_a}\right] & \qquad (3.84)
\end{aligned}
$$

The last two equations are achieve as

$$
\begin{aligned}
E \quad \left[\lambda_\alpha\left(\frac{\partial Q_\alpha}{\partial b_a}-\frac{\partial K_{\alpha\beta}}{\partial b_a}q_\beta\right)E\left[\frac{\mathrm{d}\phi}{\mathrm{d}b_b}\right]\right]+E\left[\lambda_\gamma\left(\frac{\partial Q_\gamma}{\partial b_b}-\frac{\partial K_{\gamma\delta}}{\partial b_b}q_\delta\right)E\left[\frac{\mathrm{d}\phi}{\mathrm{d}b_a}\right]\right] = & \\
\lambda_\alpha(\bar{\mathbf{h}})\mathfrak{A}_{\alpha a}E\left[\frac{\mathrm{d}\phi}{\mathrm{d}b_b}\right]+\lambda_\gamma(\bar{\mathbf{h}})\mathfrak{A}_{\alpha b}E\left[\frac{\mathrm{d}\phi}{\mathrm{d}b_a}\right] & \\
+ \frac{1}{2}\Bigg\{\left(\lambda_\alpha(\bar{\mathbf{h}})\left[\mathfrak{C}_{\alpha rsa}-\frac{\partial K_{\alpha\beta}}{\partial b_a}\frac{\mathrm{d}^2 q_\beta}{\mathrm{d}h_r\mathrm{d}h_s}\right]_{\mathbf{h}=\bar{\mathbf{h}}}+\mathfrak{A}_{\alpha a}\frac{\mathrm{d}^2\lambda_\alpha}{\mathrm{d}h_r\mathrm{d}h_s}+2\frac{\mathrm{d}\lambda_\alpha}{\mathrm{d}h_r}\mathfrak{B}_{\alpha sa}\right)E\left[\frac{\mathrm{d}\phi}{\mathrm{d}b_b}\right] & \\
+ \left(\lambda_\gamma(\bar{\mathbf{h}})\left[\mathfrak{C}_{\gamma rsb}-\frac{\partial K_{\gamma\delta}}{\partial b_b}\frac{\mathrm{d}^2 q_\delta}{\mathrm{d}h_r\mathrm{d}h_s}\right]_{\mathbf{h}=\bar{\mathbf{h}}}+\mathfrak{A}_{\alpha b}\frac{\mathrm{d}^2\lambda_\gamma}{\mathrm{d}h_r\mathrm{d}h_s}+2\frac{\mathrm{d}\lambda_\gamma}{\mathrm{d}h_r}\mathfrak{B}_{\alpha sb}\right)E\left[\frac{\mathrm{d}\phi}{\mathrm{d}b_a}\right]\Bigg\} & \\
\times \quad \mathrm{Cov}(h_r,h_s) & \qquad (3.85)
\end{aligned}
$$

Eqs. (3.86)-(3.90) are substituting to Eq. (3.85), the covariances expression with including the

terms up to second order is obtained (Eq. 3.91)

$$
\begin{aligned}
\mathrm{Cov}\left(\frac{\mathrm{d}\phi}{\mathrm{d}b_a},\frac{\mathrm{d}\phi}{\mathrm{d}b_b}\right) &= \frac{\partial G}{\partial b_a}(\bar{\mathbf{h}})\frac{\partial G}{\partial b_b}(\bar{\mathbf{h}}) + \lambda_\gamma(\bar{\mathbf{h}})\frac{\partial G}{\partial b_a}(\bar{\mathbf{h}})\mathfrak{A}_{\gamma b} + \lambda_\alpha(\bar{\mathbf{h}})\frac{\partial G}{\partial b_b}(\bar{\mathbf{h}})\mathfrak{A}_{\alpha a} \qquad (3.86)\\
&+\lambda_\alpha(\bar{\mathbf{h}})\lambda_\gamma(\bar{\mathbf{h}})\mathfrak{A}_{\alpha a}\mathfrak{A}_{\gamma b}\\
&+\frac{1}{2}\left\{\left[\frac{\partial G}{\partial b_a}\frac{\partial^3 G}{\partial h_r\partial h_s\partial b_b} + \frac{\partial G}{\partial b_b}\frac{\partial^3 G}{\partial h_r\partial h_s\partial b_a} + 2\frac{\partial^2 G}{\partial h_r\partial b_a}\frac{\partial^2 G}{\partial h_s\partial b_b}\right]_{\mathbf{h}=\bar{\mathbf{h}}}\right.\\
&+\mathfrak{A}_{\gamma b}\left[2\frac{\partial^2 G}{\partial h_r\partial b_a}\frac{\mathrm{d}\lambda_\gamma}{\mathrm{d}h_s} + \frac{\partial G}{\partial b_a}\frac{\mathrm{d}^2\lambda_\gamma}{\mathrm{d}h_r\mathrm{d}h_s} + \lambda_\gamma\frac{\partial^3 G}{\partial h_r\partial h_s\partial b_a}\right]_{\mathbf{h}=\bar{\mathbf{h}}}\\
&+\lambda_\gamma(\bar{\mathbf{h}})\frac{\partial G}{\partial b_a}(\bar{\mathbf{h}})\left[\mathfrak{C}_{\gamma rsb} - \frac{\partial K_{\gamma\delta}}{\partial b_b}\frac{\mathrm{d}^2 q_\delta}{\mathrm{d}h_r\mathrm{d}h_s}\right]_{\mathbf{h}=\bar{\mathbf{h}}}\\
&+2\mathfrak{B}_{\gamma sb}\left[\lambda_\gamma\frac{\partial^2 G}{\partial h_r\partial b_a} + \frac{\partial G}{\partial b_a}\frac{\mathrm{d}\lambda_\gamma}{\mathrm{d}h_r}\right]_{\mathbf{h}=\bar{\mathbf{h}}} + 2\mathfrak{B}_{\alpha sa}\left[\lambda_\alpha\frac{\partial^2 G}{\partial h_r\partial b_b} + \frac{\partial G}{\partial b_b}\frac{\mathrm{d}\lambda_\alpha}{\mathrm{d}h_r}\right]_{\mathbf{h}=\bar{\mathbf{h}}}\\
&+\mathfrak{A}_{\alpha a}\left[2\frac{\partial^2 G}{\partial h_r\partial b_b}\frac{\mathrm{d}\lambda_\alpha}{\mathrm{d}h_s} + \frac{\partial G}{\partial b_b}\frac{\mathrm{d}^2\lambda_\alpha}{\mathrm{d}h_r\mathrm{d}h_s} + \lambda_\alpha\frac{\partial^3 G}{\partial h_r\partial h_s\partial b_b}\right]_{\mathbf{h}=\bar{\mathbf{h}}}\\
&+\lambda_\alpha(\bar{\mathbf{h}})\frac{\partial G}{\partial b_b}(\bar{\mathbf{h}})\left.\left[\mathfrak{C}_{\alpha rsa} - \frac{\partial K_{\alpha\beta}}{\partial b_a}\frac{\mathrm{d}^2 q_\beta}{\mathrm{d}h_r\mathrm{d}h_s}\right]_{\mathbf{h}=\bar{\mathbf{h}}}\right\}\\
&+\lambda_\alpha(\bar{\mathbf{h}})\lambda_\gamma(\bar{\mathbf{h}})\left(\mathfrak{A}_{\alpha a}\left[\mathfrak{C}_{\gamma rsb} - \frac{\partial K_{\gamma\delta}}{\partial b_b}\frac{\mathrm{d}^2 q_\delta}{\mathrm{d}h_r\mathrm{d}h_s}\right]_{\mathbf{h}=\bar{\mathbf{h}}} + 2\mathfrak{B}_{\alpha ra}\mathfrak{B}_{\gamma sb}\right)\\
&+\lambda_\alpha(\bar{\mathbf{h}})\lambda_\gamma(\bar{\mathbf{h}})\mathfrak{A}_{\gamma b}\left[\mathfrak{C}_{\alpha rsa} - \frac{\partial K_{\alpha\beta}}{\partial b_a}\frac{\mathrm{d}^2 q_\beta}{\mathrm{d}h_r\mathrm{d}h_s}\right]_{\mathbf{h}=\bar{\mathbf{h}}}\\
&+\mathfrak{A}_{\alpha a}\mathfrak{A}_{\gamma b}\left[\lambda_\alpha\frac{\mathrm{d}^2\lambda_\gamma}{\mathrm{d}h_r\mathrm{d}h_s} + \lambda_\gamma\frac{\mathrm{d}^2\lambda_\alpha}{\mathrm{d}h_r\mathrm{d}h_s} + 2\frac{\mathrm{d}\lambda_\alpha}{\mathrm{d}h_r}\frac{\mathrm{d}\lambda_\gamma}{\mathrm{d}h_t}\right]_{\mathbf{h}=\bar{h}}\\
&+2\left(\lambda_\alpha(\bar{\mathbf{h}})\frac{\mathrm{d}\lambda_\gamma}{\mathrm{d}h_r} + \lambda_\gamma(\bar{\mathbf{h}})\frac{\mathrm{d}\lambda_\alpha}{\mathrm{d}h_r}\right)\left.\left(\mathfrak{A}_{\alpha a}\mathfrak{B}_{\gamma sb} + \mathfrak{A}_{\gamma b}\mathfrak{B}_{\alpha sa}\right)\right\}\mathrm{Cov}(h_r,h_s)\\
&-\left\{\lambda_\alpha(\bar{\mathbf{h}})\mathfrak{A}_{\alpha a} + \frac{1}{2}\left(\lambda_\alpha(\bar{\mathbf{h}})\left[\mathfrak{C}_{\alpha rsa} - \frac{\partial K_{\alpha\beta}}{\partial b_a}\frac{\mathrm{d}^2 q_\beta}{\mathrm{d}h_r\mathrm{d}h_s}\right]_{\mathbf{h}=\bar{\mathbf{h}}}\right.\right.\\
&\left.\left.+\mathfrak{A}_{\alpha a}\frac{\mathrm{d}^2\lambda_\alpha}{\mathrm{d}h_r\mathrm{d}h_s} + 2\frac{\mathrm{d}\lambda_\alpha}{\mathrm{d}h_r}\mathfrak{B}_{\alpha sa}\right)\mathrm{Cov}(h_r,h_s)\right\}E\left[\frac{\mathrm{d}\phi}{\mathrm{d}b_b}\right]\\
&-\left\{\lambda_\gamma(\bar{\mathbf{h}})\mathfrak{A}_{\alpha b} + \frac{1}{2}\left(\lambda_\gamma(\bar{\mathbf{h}})\left[\mathfrak{C}_{\gamma rsb} - \frac{\partial K_{\gamma\delta}}{\partial b_b}\frac{\mathrm{d}^2 q_\delta}{\mathrm{d}h_r\mathrm{d}h_s}\right]_{\mathbf{h}=\bar{\mathbf{h}}}\right.\right.\\
&\left.\left.+\mathfrak{A}_{\alpha b}\frac{\mathrm{d}^2\lambda_\gamma}{\mathrm{d}h_r\mathrm{d}h_s} + 2\frac{\mathrm{d}\lambda_\gamma}{\mathrm{d}h_r}\mathfrak{B}_{\alpha sb}\right)\mathrm{Cov}(h_r,h_s)\right\}E\left[\frac{\mathrm{d}\phi}{\mathrm{d}b_a}\right]\\
&-\left(\frac{\partial G}{\partial b_a}(\bar{\mathbf{h}}) + \frac{1}{2}\left.\frac{\partial^3 G}{\partial h_r\partial h_s\partial b_a}\right|_{h=\bar{h}}\mathrm{Cov}(h_r,h_s)\right)E\left[\frac{\mathrm{d}\phi}{\mathrm{d}b_b}\right]\\
&-\left(\frac{\partial G}{\partial b_b}(\bar{\mathbf{h}}) + \frac{1}{2}\left.\frac{\partial^3 G}{\partial h_r\partial h_s\partial b_b}\right|_{h=\bar{h}}\mathrm{Cov}(h_r,h_s)\right)E\left[\frac{\mathrm{d}\phi}{\mathrm{d}b_a}\right]\\
&+E\left[\frac{\mathrm{d}\phi}{\mathrm{d}b_a}\right]E\left[\frac{\mathrm{d}\phi}{\mathrm{d}b_b}\right]
\end{aligned}
$$

3.6.2 Time Instant Sensitivity

In time instant sensitivity analysis the system response at the time $\tau = t$ is adopted as the series of successive impulses in infinitely small time (cf. Eq. (2.153))

$$\phi = \int_0^t G[q_\alpha(b_a, h_r, \tau); b_a]\delta(t-\tau)\mathrm{d}\tau, \tag{3.87}$$

where $t \in [0, T]$; $\beta = 1, 2, ..., N$; $a = 1, 2, ..., A$; $r = 1, 2, ..., \bar{r}$. The expression $\delta(t-\tau)$ denotes the Dirac-δ distribution. The function $G[q_\beta(b_a, \tau); b_a]$ is supposed to be continuous in the whole time interval $[0, T]$ and continuously differentiable with respect to q_α, b_a and h_r. Aiming to the time instant sensitivity by using the random variables, Eq. (2.89) is rewritten to

$$\begin{aligned} M_{\alpha\beta}(b_a; h_r)\ddot{q}_\beta(b_a; h_r; \tau) + D_{\alpha\beta}(b_a; h_r)\dot{q}_\beta(b_a; h_r; \tau) + K_{\alpha\beta}(b_a; h_r)q_\beta(b_a, h_r; \tau) \\ = Q_\alpha(b_a; h_r; \tau) \end{aligned} \tag{3.88}$$

with the initial conditions in the form

$$q_\alpha(b_a, h_r; 0) = 0; \quad \dot{q}_\alpha(b_a, h_r; 0) = 0 \tag{3.89}$$

Eq. (3.88) describes the equations of motion in the stochastic finite element method (SFEM). Differentiating Eq. (3.87) with respect to b_a by using the chain rule of differentiation leads to

$$\phi = \int_0^t \left(\frac{\partial G}{\partial b_a} + \frac{\partial G}{\partial q_\alpha}\frac{\mathrm{d}q_\alpha}{\mathrm{d}b_a}\right)\delta(t-\tau)\mathrm{d}\tau, \tag{3.90}$$

Because of $\tau = t$ in time instant sensitivity, we have

$$\int_0^t \frac{\partial G}{\partial b_a}(b_a, h_r, \tau)\delta(t-\tau)\mathrm{d}\tau = \frac{\partial G}{\partial b_a}(b_a, h_r, t) \tag{3.91}$$

Substituting Eq.(3.91) to Eq. (3.90) gives

$$\phi = \frac{\partial G}{\partial b_a}(t) + \int_0^t \frac{\partial G}{\partial q_\alpha}\frac{\mathrm{d}q_\alpha}{\mathrm{d}b_a}\delta(t-\tau)\mathrm{d}\tau; \quad t \in [0, T] \tag{3.92}$$

Following the same lines as in Sections 2.5.5 and 2.5.6 we received the adjoint equations of motion in the form as [35]

$$\begin{aligned} M_{\alpha\beta}(b_a, h_r)\ddot{\lambda}_\alpha(b_a, h_r; \tau) - D_{\alpha\beta}(b_a, h_r)\dot{\lambda}_\alpha(b_a, h_r; \tau) + K_{\alpha\beta}(b_a, h_r)\lambda_\alpha(b_a, h_r; \tau) \\ = \frac{\partial G}{\partial q_\beta}(b_a, h_r; t)\delta(t-\tau) \end{aligned} \tag{3.93}$$

with the terminal conditions

$$\lambda_\alpha(b_a, h_r; t) = 0; \quad \dot{\lambda}_\alpha(b_a, h_r; t) = 0; \quad \tau = [0, t]; \quad t = [0, T] \tag{3.94}$$

To avoid unnecessary derivations, we use the expression for dynamic sensitivity gradient in deterministic systems Eq. (2.160) and rewritten it including the random parameters to the form [35]

$$\begin{aligned} \frac{\mathrm{d}\phi}{\mathrm{d}b_a}(b_a, h_r; t) = \frac{\partial G}{\partial b_a}(b_a, h_r; t) + \int_0^t \lambda_\alpha(b_a, h_r, \tau)\Bigg[\frac{\partial Q_\alpha(b_a, h_r\tau)}{\partial b_a} \\ - \frac{\partial M_{\alpha\beta}(b_a, h_r)}{\partial b_a}\ddot{q}_\beta(\tau) - \frac{\partial D_{\alpha\beta}(b_a, h_r)}{\partial b_a}\dot{q}_\beta(\tau) - \frac{\partial K_{\alpha\beta}(b_a, h_r)}{\partial b_a}q_\beta(\tau)\Bigg]\mathrm{d}\tau \end{aligned} \tag{3.95}$$

for any fixed time $t \in [0, T]$.

Firstly, using Eq. (3.9), we expand the general coordinate vector and adjoint vector in Taylor series up to the second order around the mean values $\bar{h}_r$

$$\begin{aligned} q_\beta(b_a, h_r; \tau) &= q_\beta(\bar{\mathbf{h}}) + \left[\frac{\mathrm{d}q_\beta}{\mathrm{d}h_r}\delta h_r + \frac{1}{2}\frac{\mathrm{d}^2 q_\beta}{\mathrm{d}h_r \mathrm{d}h_s}\delta h_r \delta h_s\right]_{\mathbf{h}=\bar{\mathbf{h}}} \\ \lambda_\beta(b_a, h_r; \tau) &= \lambda_\beta(\bar{\mathbf{h}}) + \left[\frac{\mathrm{d}\lambda_\beta}{\mathrm{d}h_r}\delta h_r + \frac{1}{2}\frac{\mathrm{d}^2 \lambda_\beta}{\mathrm{d}h_r \mathrm{d}h_s}\delta h_r \delta h_s\right]_{\mathbf{h}=\bar{\mathbf{h}}} \end{aligned} \tag{3.96}$$

secondly, the second order expansions of their first and second derivatives are received

$$\begin{aligned} \dot{q}_\beta(b_a, h_r; \tau) &= \dot{q}_\beta(\bar{\mathbf{h}}) + \left[\frac{\mathrm{d}\dot{q}_\beta}{\mathrm{d}h_r}\delta h_r + \frac{1}{2}\frac{\mathrm{d}^2 \dot{q}_\beta}{\mathrm{d}h_r \mathrm{d}h_s}\delta h_r \delta h_s\right]_{\mathbf{h}=\bar{\mathbf{h}}} \\ \dot{\lambda}_\beta(b_a, h_r; \tau) &= \dot{\lambda}_\beta(\bar{\mathbf{h}}) + \left[\frac{\mathrm{d}\dot{\lambda}_\beta}{\mathrm{d}h_r}\delta h_r + \frac{1}{2}\frac{\mathrm{d}^2 \dot{\lambda}_\beta}{\mathrm{d}h_r \mathrm{d}h_s}\delta h_r \delta h_s\right]_{\mathbf{h}=\bar{\mathbf{h}}} \\ \ddot{q}_\beta(b_a, h_r; \tau) &= \ddot{q}_\beta(\bar{\mathbf{h}}) + \left[\frac{\mathrm{d}\ddot{q}_\beta}{\mathrm{d}h_r}\delta h_r + \frac{1}{2}\frac{\mathrm{d}^2 \ddot{q}_\beta}{\mathrm{d}h_r \mathrm{d}h_s}\delta h_r \delta h_s\right]_{\mathbf{h}=\bar{\mathbf{h}}} \\ \ddot{\lambda}_\beta(b_a, h_r; \tau) &= \ddot{\lambda}_\beta(\bar{\mathbf{h}}) + \left[\frac{\mathrm{d}\ddot{\lambda}_\beta}{\mathrm{d}h_r}\delta h_r + \frac{1}{2}\frac{\mathrm{d}^2 \ddot{\lambda}_\beta}{\mathrm{d}h_r \mathrm{d}h_s}\delta h_r \delta h_s\right]_{\mathbf{h}=\bar{\mathbf{h}}} \end{aligned} \tag{3.97}$$

then, the second-order power series is written for the functions $\partial G/\partial q_\alpha$, Q_α, $M_{\alpha\beta}$, $K_{\alpha\beta}$ and $D_{\alpha\beta}$ to obtain

$$\begin{aligned} \frac{\partial G}{\partial q_\alpha}(b_a, h_r; \tau) &= \frac{\partial G}{\partial q_\alpha}(\bar{\mathbf{h}}) + \left[\frac{\partial^2 G}{\partial h_r \partial q_\alpha}\delta h_r + \frac{1}{2}\frac{\partial^3 G}{\partial h_r \partial h_s \partial q_\alpha}\delta h_r \delta h_s\right]_{\mathbf{h}=\bar{\mathbf{h}}} \\ Q_\alpha(b_a, h_r; \tau) &= Q_\alpha(\bar{\mathbf{h}}) + \left[\frac{\partial Q_\alpha}{\partial h_r}\delta h_r + \frac{1}{2}\frac{\partial^2 Q_\alpha}{\partial h_r \partial h_s}\delta h_r \delta h_s\right]_{\mathbf{h}=\bar{\mathbf{h}}} \\ M_{\alpha\beta}(b_a, h_r) &= M_{\alpha\beta}(\bar{\mathbf{h}}) + \left[\frac{\partial M_{\alpha\beta}}{\partial h_r}\delta h_r + \frac{1}{2}\frac{\partial^2 M_{\alpha\beta}}{\partial h_r \partial h_s}\delta h_r \delta h_s\right]_{\mathbf{h}=\bar{\mathbf{h}}} \\ K_{\alpha\beta}(b_a, h_r) &= K_{\alpha\beta}(\bar{\mathbf{h}}) + \left[\frac{\partial K_{\alpha\beta}}{\partial h_r}\delta h_r + \frac{1}{2}\frac{\partial^2 K_{\alpha\beta}}{\partial h_r \partial h_s}\delta h_r \delta h_s\right]_{\mathbf{h}=\bar{\mathbf{h}}} \\ D_{\alpha\beta}(b_a, h_r) &= D_{\alpha\beta}(\bar{\mathbf{h}}) + \left[\frac{\partial D_{\alpha\beta}}{\partial h_r}\delta h_r + \frac{1}{2}\frac{\partial^2 D_{\alpha\beta}}{\partial h_r \partial h_s}\delta h_r \delta h_s\right]_{\mathbf{h}=\bar{\mathbf{h}}} \end{aligned} \tag{3.98}$$

Substituting Eqs. (3.96)-(3.18) into Eqs. (3.93) and (3.95), and comparing the terms with the same order leads to the hierarchical systems of equations for stochastic dynamic sensitivity problem [35]. That way, we obtain

— one pair of systems of N linear differential equations of the zeroth-order

$$\begin{aligned} M_{\alpha\beta}(b_a, \bar{\mathbf{h}})\ddot{q}_\beta(b_a, \bar{\mathbf{h}}; \tau) &+ D_{\alpha\beta}(b_a, \bar{\mathbf{h}})\dot{q}_\beta(b_a, \bar{\mathbf{h}}; \tau) + K_{\alpha\beta}(b_a, \bar{\mathbf{h}})q_\beta(b_a, \bar{\mathbf{h}}; \tau) \\ &= Q_\alpha(b_a, \bar{\mathbf{h}}; \tau) \\ M_{\alpha\beta}(b_a, \bar{\mathbf{h}})\ddot{\lambda}_\beta(b_a, \bar{\mathbf{h}}; \tau) &- D_{\alpha\beta}(b_a, \bar{\mathbf{h}})\dot{\lambda}_\beta(b_a, \bar{\mathbf{h}}; \tau) + K_{\alpha\beta}(b_a, \bar{\mathbf{h}})\lambda_\beta(b_a, \bar{\mathbf{h}}; \tau) \\ &= \frac{\partial G}{\partial q_\alpha}(b_a, \bar{\mathbf{h}}; t)\delta(t - \tau) \end{aligned} \tag{3.99}$$

— $\hat{r}$ pairs of systems of N linear differential equations of the first-order

$$\begin{aligned}
M_{\alpha\beta}(b_a,\bar{\mathbf{h}})\frac{\mathrm{d}\ddot{q}_\beta}{\mathrm{d}h_r}(b_a,\bar{\mathbf{h}};\tau) \;+\; & D_{\alpha\beta}(b_a;\bar{\mathbf{h}})\frac{\mathrm{d}\dot{q}_\beta}{\mathrm{d}h_r}(b_a,\bar{\mathbf{h}};\tau)+K_{\alpha\beta}(b_a,\bar{\mathbf{h}})\frac{\mathrm{d}q_\beta}{\mathrm{d}h_r}(b_a,\bar{\mathbf{h}};\tau)\\
=\;& \frac{\partial Q_\alpha}{\partial h_r}(b_a,\bar{\mathbf{h}};\tau)-\frac{\partial M_{\alpha\beta}}{\partial h_r}(b_a,\bar{\mathbf{h}})\ddot{q}_\beta(b_a,\bar{\mathbf{h}};\tau)\\
&-\frac{\partial D_{\alpha\beta}}{\partial h_r}(b_a,\bar{\mathbf{h}})\dot{q}_\beta(b_a,\bar{\mathbf{h}};\tau)-\frac{\partial K_{\alpha\beta}}{\partial h_r}(b_a,\bar{\mathbf{h}})q_\beta(b_a,\bar{\mathbf{h}};\tau)\\
M_{\alpha\beta}(b_a,\bar{\mathbf{h}})\frac{\mathrm{d}\ddot{\lambda}_\beta}{\mathrm{d}h_r}(b_a,\bar{\mathbf{h}};\tau) \;+\; & D_{\alpha\beta}(b_a;\bar{\mathbf{h}})\frac{\mathrm{d}\dot{\lambda}_\beta}{\mathrm{d}h_r}(b_a,\bar{\mathbf{h}};\tau)+K_{\alpha\beta}(b_a,\bar{\mathbf{h}})\frac{\mathrm{d}\lambda_\beta}{\mathrm{d}h_r}(b_a,\bar{\mathbf{h}};\tau)\\
=\;& \frac{\partial^2 G}{\partial h_r\partial q_\alpha}(b_a,\bar{\mathbf{h}};t)\delta(t-\tau)-\frac{\partial M_{\alpha\beta}}{\partial h_r}(b_a,\bar{\mathbf{h}})\ddot{\lambda}_\beta(b_a,\bar{\mathbf{h}};\tau)\\
&-\frac{\partial D_{\alpha\beta}}{\partial h_r}(b_a,\bar{\mathbf{h}})\dot{\lambda}_\beta(b_a,\bar{\mathbf{h}};\tau)-\frac{\partial K_{\alpha\beta}}{\partial h_r}(b_a,\bar{\mathbf{h}})\lambda_\beta(b_a,\bar{\mathbf{h}};\tau)
\end{aligned}$$

— one pair of systems of N linear differential equations of the second-order

$$\begin{aligned}
M_{\alpha\beta}(b_a,\bar{\mathbf{h}})\ddot{q}^{(2)}_\beta(b_a,\bar{\mathbf{h}};\tau) \;+\; & D_{\alpha\beta}(b_a,\bar{\mathbf{h}})\dot{q}^{(2)}_\beta(b_a,\bar{\mathbf{h}};\tau)+K_{\alpha\beta}(b_a,\bar{\mathbf{h}})q^{(2)}_\beta(b_a,\bar{\mathbf{h}};\tau)\\
=\;& Q^{(2)}_\alpha(b_a,\bar{\mathbf{h}};\tau)-\ddot{q}_\beta(b_a,\bar{\mathbf{h}};\tau)M^{(2)}_{\alpha\beta}(b_a,\bar{\mathbf{h}})\\
&-\dot{q}_\beta(b_a,\bar{\mathbf{h}};\tau)D^{(2)}_{\alpha\beta}(b_a,\bar{\mathbf{h}})-q_\beta(b_a,\bar{\mathbf{h}};\tau)K^{(2)}_{\alpha\beta}(b_a,\bar{\mathbf{h}})\\
&-2\Bigg[\frac{\partial M_{\alpha\beta}}{\partial h_r}(b_a,\bar{\mathbf{h}})\frac{\mathrm{d}\ddot{q}_\beta}{\mathrm{d}h_s}(b_a,\bar{\mathbf{h}};\tau)\\
&+\frac{\partial D_{\alpha\beta}}{\partial h_r}(b_a,\bar{\mathbf{h}})\frac{\mathrm{d}\dot{q}_\beta}{\mathrm{d}h_s}(b_a,\bar{\mathbf{h}};\tau)\\
&+\frac{\partial K_{\alpha\beta}}{\partial h_r}(b_a,\bar{\mathbf{h}})\frac{\mathrm{d}q_\beta}{\mathrm{d}h_s}(b_a,\bar{\mathbf{h}};\tau)\Bigg]\mathrm{Cov}(h_r,\,h_s)\\
M_{\alpha\beta}(b_a,\bar{\mathbf{h}})\ddot{\lambda}^{(2)}_\beta(b_a,\bar{\mathbf{h}};\tau) \;+\; & D_{\alpha\beta}(b_a,\bar{\mathbf{h}})\dot{\lambda}^{(2)}_\beta(b_a,\bar{\mathbf{h}};\tau)+K_{\alpha\beta}(b_a,\bar{\mathbf{h}})\lambda^{(2)}_\beta(b_a,\bar{\mathbf{h}};\tau)\\
=\;& \frac{\partial^3 G}{\partial h_r\partial h_s\partial q_\alpha}(b_a,\bar{\mathbf{h}};t)\delta(t-\tau)\mathrm{Cov}(h_r,\,h_s)\\
&-\ddot{\lambda}_\beta(b_a,\bar{\mathbf{h}};\tau)M^{(2)}_{\alpha\beta}(b_a,\bar{\mathbf{h}})-\dot{\lambda}_\beta(b_a,\bar{\mathbf{h}};\tau)D^{(2)}_{\alpha\beta}(b_a,\bar{\mathbf{h}})\\
&-\lambda_\beta(b_a,\bar{\mathbf{h}};\tau)K^{(2)}_{\alpha\beta}(b_a,\bar{\mathbf{h}})\\
&-2\Bigg[\frac{\partial M_{\alpha\beta}}{\partial h_r}(b_a,\bar{\mathbf{h}})\frac{\mathrm{d}\ddot{\lambda}_\beta}{\mathrm{d}h_s}(b_a,\bar{\mathbf{h}};\tau)\\
&+\frac{\partial D_{\alpha\beta}}{\partial h_r}(b_a,\bar{\mathbf{h}})\frac{\mathrm{d}\dot{\lambda}_\beta}{\mathrm{d}h_s}(b_a,\bar{\mathbf{h}};\tau)\\
&+\frac{\partial K_{\alpha\beta}}{\partial h_r}(b_a,\bar{\mathbf{h}})\frac{\mathrm{d}\lambda_\beta}{\mathrm{d}h_s}(b_a,\bar{\mathbf{h}};\tau)\Bigg]\mathrm{Cov}(h_r,\,h_s)
\end{aligned}$$

The mean value of Eq. (3.95) is expressed by the equation.

$$\begin{aligned}
E\left[\frac{\mathrm{d}\phi}{\mathrm{d}b_a}\right]=\;& E\left[\frac{\partial G}{\partial b_a}\right]+\int_0^t\Bigg(E\left[\lambda_\alpha\frac{\partial Q_\alpha}{\partial b_a}\right]-E\left[\lambda_\alpha\frac{\partial M_{\alpha\beta}}{\partial b_a}\ddot{q}_\beta\right]\\
&-E\left[\lambda_\alpha\frac{\partial D_{\alpha\beta}}{\partial b_a}\dot{q}_\beta\right]-E\left[\lambda_\alpha\frac{\partial K_{\alpha\beta}}{\partial b_a}q_\beta\right]\Bigg)\mathrm{d}\tau
\end{aligned}\tag{3.102}$$

for any fixed time $t \epsilon [\,0, T\,]$. To find the means of stochastic dynamic sensitivity gradient the functions $\partial G/\partial b_a$, $\partial Q/\partial b_a$, $\partial M/\partial b_a$ and $\partial D/\partial b_a$ are expanded in Taylor series up to second order

$$\begin{aligned}
\frac{\partial G}{\partial b_a}(b_a, h_r; t) &= \frac{\partial G}{\partial b_a}(\bar{\mathbf{h}}) + \left[\frac{\partial^2 G}{\partial h_r \partial b_a}\delta h_r + \frac{1}{2}\frac{\partial^3 G}{\partial h_r \partial h_s \partial b_a}\delta h_r \delta h_s\right]_{\mathbf{h}=\bar{\mathbf{h}}} \\
\frac{\partial Q}{\partial b_a}(b_a, h_r; \tau) &= \frac{\partial Q}{\partial b_a}(\bar{\mathbf{h}}) + \left[\frac{\partial^2 Q}{\partial h_r \partial b_a}\delta h_r + \frac{1}{2}\frac{\partial^3 Q}{\partial h_r \partial h_s \partial b_a}\delta h_r \delta h_s\right]_{\mathbf{h}=\bar{\mathbf{h}}} \\
\frac{\partial M}{\partial b_a}(b_a, h_r) &= \frac{\partial M}{\partial b_a}(\bar{\mathbf{h}}) + \left[\frac{\partial^2 M}{\partial h_r \partial b_a}\delta h_r + \frac{1}{2}\frac{\partial^3 M}{\partial h_r \partial h_s \partial b_a}\delta h_r \delta h_s\right]_{\mathbf{h}=\bar{\mathbf{h}}} \\
\frac{\partial D}{\partial b_a}(b_a, h_r) &= \frac{\partial D}{\partial b_a}(\bar{\mathbf{h}}) + \left[\frac{\partial^2 D}{\partial h_r \partial b_a}\delta h_r + \frac{1}{2}\frac{\partial^3 D}{\partial h_r \partial h_s \partial b_a}\delta h_r \delta h_s\right]_{\mathbf{h}=\bar{\mathbf{h}}}
\end{aligned} \tag{3.103}$$

The terms of Eq. (3.102) is obtained analogically to Eqs. (3.74) and (3.75) and for fixed time $t \epsilon [\,0, T\,]$ we have [35]

$$\begin{aligned}
E\left[\frac{\mathrm{d}\phi}{\mathrm{d}b_a}\right] = \left[\frac{\partial G}{\partial b_a}(t)\right]_{\mathbf{h}=\bar{\mathbf{h}}} & \\
+ \int_0^t \Bigg[& \lambda_\alpha(\bar{\mathbf{h}})\left(\frac{\partial Q_\alpha}{\partial b_a} - \frac{\partial K_{\alpha\beta}}{\partial b_a}q_\beta - \frac{\partial M_{\alpha\beta}}{\partial b_a}\ddot{q}_\beta - \frac{\partial D_{\alpha\beta}}{\partial b_a}\dot{q}_\beta\right) \\
& + \frac{1}{2}\lambda_\alpha^{(2)}\left(\frac{\partial Q_\alpha}{\partial b_a} - \frac{\partial K_{\alpha\beta}}{\partial b_a}q_\beta - \frac{\partial M_{\alpha\beta}}{\partial b_a}\ddot{q}_\beta - \frac{\partial D_{\alpha\beta}}{\partial b_a}\dot{q}_\beta\right. \\
& \left. - \frac{1}{2}\lambda_\alpha\left(\frac{\partial K_{\alpha\beta}}{\partial b_a}q_\beta^{(2)} + \frac{\partial M_{\alpha\beta}}{\partial b_a}\ddot{q}_\beta^{(2)} + \frac{\partial D_{\alpha\beta}}{\partial b_a}\dot{q}_\beta^{(2)}\right)\right. \\
& + \Bigg[\frac{1}{2}\lambda_\alpha\left(\frac{\partial^3 Q_\alpha}{\partial h_r \partial h_s \partial b_a} - \frac{\partial^3 K_{\alpha\beta}}{\partial h_r \partial h_s \partial b_a}q_\beta - \frac{\partial^3 M_{\alpha\beta}}{\partial h_r \partial h_s \partial b_a}\ddot{q}_\beta - \frac{\partial^3 D_{\alpha\beta}}{\partial h_r \partial h_s \partial b_a}\dot{q}_\beta\right. \\
& \left. - 2\frac{\partial^2 K_{\alpha\beta}}{\partial h_r \partial b_a}\frac{\mathrm{d}q_\beta}{\mathrm{d}h_s} - 2\frac{\partial^2 M_{\alpha\beta}}{\partial h_r \partial b_a}\frac{\mathrm{d}\ddot{q}_\beta}{\mathrm{d}h_s} - 2\frac{\partial^2 D_{\alpha\beta}}{\partial h_r \partial b_a}\frac{\mathrm{d}\dot{q}_\beta}{\mathrm{d}h_s}\right) + \frac{1}{2}\frac{\partial^3 G}{\partial h_r \partial h_s \partial b_a} \\
& + \frac{\mathrm{d}\lambda_\alpha}{\mathrm{d}h_r}\left(\frac{\partial^2 Q_\alpha}{\partial h_s \partial b_a} - \frac{\partial^2 K_{\alpha\beta}}{\partial h_s \partial b_a}q_\beta - \frac{\partial^2 M_{\alpha\beta}}{\partial h_s \partial b_a}\ddot{q}_\beta - \frac{\partial^2 D_{\alpha\beta}}{\partial h_s \partial b_a}\dot{q}_\beta - \frac{\partial K_{\alpha\beta}}{\partial b_a}\frac{\mathrm{d}q_\beta}{\mathrm{d}h_s}\right. \\
& \left. \left. - \frac{\partial M_{\alpha\beta}}{\partial b_a}\frac{\mathrm{d}\ddot{q}_\beta}{\mathrm{d}h_s} - \frac{\partial D_{\alpha\beta}}{\partial b_a}\frac{\mathrm{d}\dot{q}_\beta}{\mathrm{d}h_s}\right)\Bigg]\mathrm{Cov}(h_r, h_s)\Bigg]_{\mathbf{h}=\bar{\mathbf{h}}}\mathrm{d}\tau
\end{aligned} \tag{3.104}$$

Introducing the following notations

$$\begin{aligned}
\mathfrak{A}_{\alpha a}(\tau) &= \frac{\partial Q_\alpha}{\partial b_a}(\tau) - \mathfrak{D}_{\alpha a}(\tau) \\
\mathfrak{B}_{\alpha r s a}(\tau) &= \frac{\partial^3 Q_\alpha}{\partial h_r \partial h_s \partial b_a}(\tau) - \mathfrak{F}_{\alpha r s a}(\tau) - 2\mathfrak{H}_{\alpha r s a}(\tau) \\
\mathfrak{C}_{\alpha s a}(\tau) &= \frac{\partial^2 Q_\alpha}{\partial h_s \partial b_a}(\tau) - \mathfrak{K}_{\alpha s a}(\tau) - \mathfrak{L}_{\alpha s a}(\tau) \\
\mathfrak{D}_{\alpha a}(\tau) &= \frac{\partial K_{\alpha\beta}}{\partial b_a}q_\beta(\tau) + \frac{\partial M_{\alpha\beta}}{\partial b_a}\ddot{q}_\beta(\tau) + \frac{\partial D_{\alpha\beta}}{\partial b_a}\dot{q}_\beta(\tau) \\
\mathfrak{E}_{\alpha a}(\tau) &= \frac{\partial K_{\alpha\beta}}{\partial b_a}q_\beta^{(2)}(\tau) + \frac{\partial M_{\alpha\beta}}{\partial b_a}\ddot{q}_\beta^{(2)}(\tau) + \frac{\partial D_{\alpha\beta}}{\partial b_a}\dot{q}_\beta^{(2)}(\tau)
\end{aligned}$$

$$\begin{aligned}
\mathfrak{F}_{\alpha rsa}(\tau) &= \frac{\partial^3 K_{\alpha\beta}}{\partial h_r \partial h_s \partial b_a} q_\beta(\tau) + \frac{\partial^3 M_{\alpha\beta}}{\partial h_r \partial h_s \partial b_a} \ddot{q}_\beta(\tau) + \frac{\partial^3 D_{\alpha\beta}}{\partial h_r \partial h_s \partial b_a} \dot{q}_\beta(\tau) \\
\mathfrak{H}_{\alpha rsa}(\tau) &= \frac{\partial^2 K_{\alpha\beta}}{\partial h_r \partial b_a} \frac{\mathrm{d}q_\beta}{\mathrm{d}h_s}(\tau) + \frac{\partial^2 M_{\alpha\beta}}{\partial h_r \partial b_a} \frac{\mathrm{d}\ddot{q}_\beta}{\mathrm{d}h_s}(\tau) + \frac{\partial^2 D_{\alpha\beta}}{\partial h_r \partial b_a} \frac{\mathrm{d}\dot{q}_\beta}{\mathrm{d}h_s}(\tau) \\
\mathfrak{K}_{\alpha sa}(\tau) &= \frac{\partial^2 K_{\alpha\beta}}{\partial h_s \partial b_a} q_\beta(\tau) + \frac{\partial^2 M_{\alpha\beta}}{\partial h_s \partial b_a} \ddot{q}_\beta(\tau) + \frac{\partial^2 D_{\alpha\beta}}{\partial h_s \partial b_a} \dot{q}_\beta(\tau) \\
\mathfrak{L}_{\alpha sa}(\tau) &= \frac{\partial K_{\alpha\beta}}{\partial b_a} \frac{\mathrm{d}q_\beta}{\mathrm{d}h_s}(\tau) + \frac{\partial M_{\alpha\beta}}{\partial b_a} \frac{\mathrm{d}\ddot{q}_\beta}{\mathrm{d}h_s}(\tau) + \frac{\partial D_{\alpha\beta}}{\partial b_a} \frac{\mathrm{d}\dot{q}_\beta}{\mathrm{d}h_s}(\tau)
\end{aligned} \tag{3.105}$$

Eq. (3.108) is rewritten to the form

$$\begin{aligned}
E\left[\frac{\mathrm{d}\phi}{\mathrm{d}b_a}\right] = & \left[\frac{\partial G}{\partial b_a}(t)\right]_{\mathbf{h}=\bar{\mathbf{h}}} \\
& + \int_0^t \left[\left(\lambda_\alpha + \frac{1}{2}\lambda_\alpha^{(2)}\right)\mathfrak{A}_{\alpha a} - \frac{1}{2}\lambda_\alpha \mathfrak{E}_{\alpha a}\right. \\
& + \left.\left[\frac{1}{2}\lambda_\alpha \mathfrak{B}_{\alpha rsa} + \frac{1}{2}\frac{\partial^3 G}{\partial h_r \partial h_s \partial b_a} + \frac{\mathrm{d}\lambda_\alpha}{\mathrm{d}h_r}\mathfrak{C}_{\alpha sa}\right]\mathrm{Cov}(h_r, h_s)\right]_{\mathbf{h}=\bar{\mathbf{h}}} \mathrm{d}\tau
\end{aligned} \tag{3.106}$$

Analogically to the Eq. (3.110), the formula for $E[\mathrm{d}\phi/\mathrm{d}b_b]$ is given by

$$\begin{aligned}
E\left[\frac{\mathrm{d}\phi}{\mathrm{d}b_b}\right] = & \left[\frac{\partial G}{\partial b_b}(t_2) + \frac{1}{2}\frac{\partial^3 G}{\partial h_t \partial h_u \partial b_b}(t)\mathrm{Cov}(h_t,\ h_u)\right]_{\mathbf{h}=\bar{\mathbf{h}}} \\
& + \int_0^t \left[\left(\lambda_\beta + \frac{1}{2}\lambda_\beta^{(2)}\right)\mathfrak{A}_{\beta b} - \frac{1}{2}\lambda_\beta \mathfrak{E}_{\beta b}\right. \\
& + \left.\left[\frac{1}{2}\lambda_\beta \mathfrak{B}_{\beta tub} + \frac{\mathrm{d}\lambda_\beta}{\mathrm{d}h_t}\mathfrak{C}_{\beta ub}\right]\mathrm{Cov}(h_t, h_u)\right]_{\mathbf{h}=\bar{\mathbf{h}}} \mathrm{d}\upsilon
\end{aligned} \tag{3.107}$$

The cross-covariances at $\mathrm{d}\phi/\mathrm{d}b_a(t_1)$ and $\mathrm{d}\phi/\mathrm{d}b_b(t_2)$, by using Eq. (3.66), can be obtained from the following equation [35]

$$\begin{aligned}
& \mathrm{Cov}\left(\frac{\mathrm{d}\phi}{\mathrm{d}b_a}(t_1), \frac{\mathrm{d}\phi}{\mathrm{d}b_b}(t_2)\right) = \\
= & E\left[\left(\frac{\partial G}{\partial b_a}(t_1) + \int_0^{t_1} \lambda_\alpha(\tau)\left[\frac{\partial Q_\alpha(\tau)}{\partial b_a} - \frac{\partial M_{\alpha\beta}}{\partial b_a}\ddot{q}_\beta(\tau) - \frac{\partial D_{\alpha\beta}}{\partial b_a}\dot{q}_\beta(\tau) - \frac{\partial K_{\alpha\beta}}{\partial b_a}q_\beta(\tau)\right]\mathrm{d}\tau\right. \\
& \left. - E\left[\frac{\mathrm{d}\phi}{\mathrm{d}b_a}\right]\right)\left(\frac{\partial G}{\partial b_b}(t_2) + \int_0^{t_2} \lambda_\gamma(\upsilon)\left[\frac{\partial Q_\gamma(\upsilon)}{\partial b_b} - \frac{\partial M_{\gamma\eta}}{\partial b_b}\ddot{q}_\eta(\upsilon) - \frac{\partial D_{\gamma\eta}}{\partial b_b}\dot{q}_\eta(\upsilon)\right.\right. \\
& \left.\left. - \frac{\partial K_{\gamma\eta}}{\partial b_b}q_\eta(\upsilon)\right]\mathrm{d}\upsilon - E\left[\frac{\mathrm{d}\phi}{\mathrm{d}b_b}\right]\right)\Bigg]
\end{aligned} \tag{3.108}$$

3.7 Numerical Analysis of Truss and Beam Systems with Beat Effects

3.7.1 The Scope of the Analysis of Symmetry System

It is known that contemporary design rules in civil engineering resulted from many years of research and experiences. With the developments of computational hardware and software technology, state-of-the-art supersensitive measuring tools and computer codes nowadays serve the

purpose of thorough structural analysis conducted to obtain results that are more reliable. Furthermore, the cutting edge tools allow us to solve previously unreachable problems and discuss whether some traditional structural models are still valid.

According to what is known, the bar structures loaded only in main nodes are generally designed as a truss system, excluding the shear forces and bending moments out of the analysis. In this approach, one bar is modelled as a truss element in a finite element setting. Therefore, numerical computations include values of displacements and axial forces defined at end points of the element only, save verifying what happens along the bar between main nodes. The impact of these simplifications on the results of both the system statics and dynamics is very interesting. For this reason, the aim of the present chapter is to study the properties of the above-mentioned treatments in the context of the deterministic and stochastic analysis.

A purposeful action in this part of the paper is to select a symmetric type of structures as applied to data processing. During vibration of the structural systems with repeated segments, we frequently observe periodical changes of amplitude. They are called the beat effect and from the point of view the material fatigue can be regarded as a negative phenomenon in civil engineering, notwithstanding in this area only. Therefore, numerical computations in this section intend to identify this occurrence and go further to eliminate it by using damping and inputting added mass to the model. Success in this field may lead to the development of parallel studies in other areas, wherein the beat phenomenon is similarly undesirable.

3.7.2 The Model Bar Structure

With respect to aims listed in the previous section, we have chosen the dome consisting of 80 steel bars to undergo the analysis. Front and bird's eye view of the described structure is presented in Fig. 3.1 and 3.2, respectively. The geometrical dimensions of the scheme selected in the model creation are: hight – 5 m and base diameter – 10 m, compare [62,65].

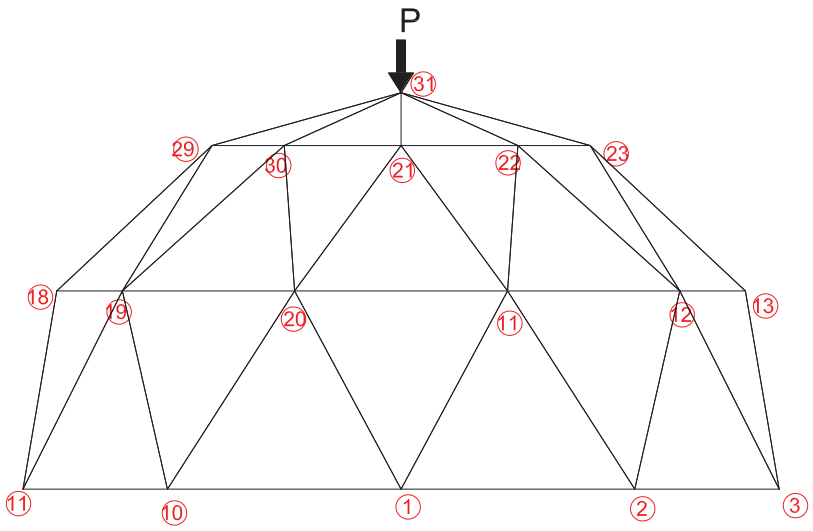

Figure 3.1 Finite element setting in front view

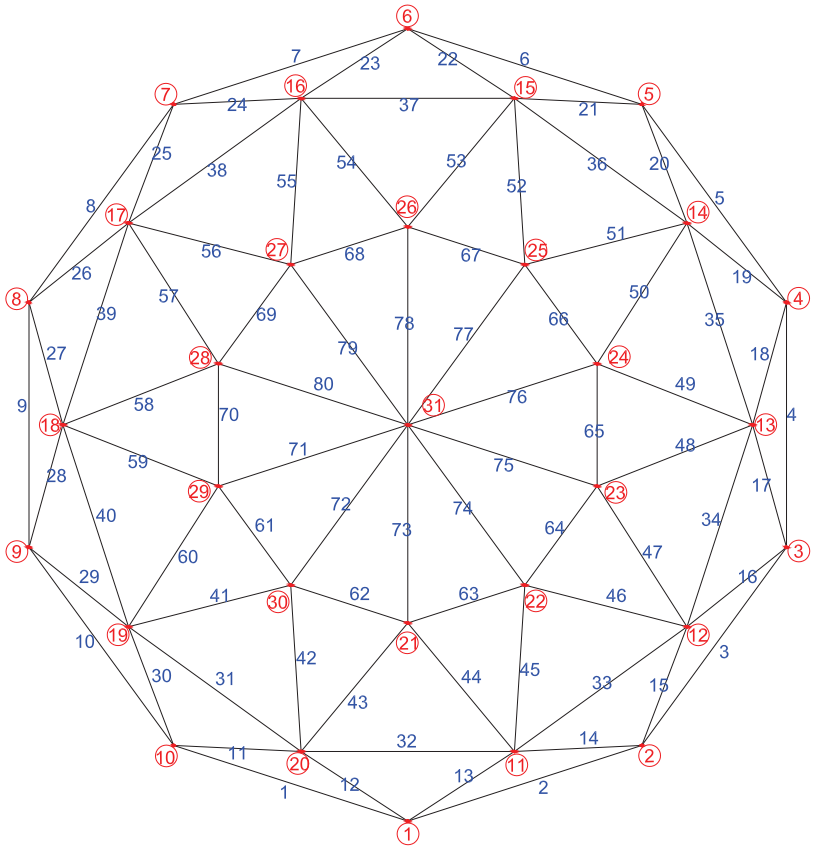

Figure 3.2 Finite element setting in bird's eye view

We adopted the pipe cross-section with the 20 cm^2 area in the numerical computation. Steel is selected as the structural material, therefore the following characteristics are assumed: the Young's Modulus — 205GPa, mass density — 7.85 kNs^2/m^4 and Poisson's ratio — 0.3. Nodes 1, 3, 5, 7 and 9 are defined as support points.

Geometric distribution of the elements and support placement makes the model fully symmetric, which is consistent with assumptions described in the scope of the chapter. During the subsequent data processing, four different models are created: 3D truss system, and three beam systems with various finite element settings. The results obtained in static, dynamic and sensitivity analysis are presented in consecutive sections.

3.7.3 A Truss System as an Example

3.7.3.1 Deterministic Statics

In the first stage of the studies, the bars are assumed to be joined by hinges while the nodes 1, 3, 5, 7 and 9 are supported by pins. These assumptions result in the creation of a 3D truss system. In accordance with the finite element method, each bar is modelled as a 3D truss element. Consequently, we obtain a system with 31 nodes and 80 elements. After applying the boundary conditions, the total number of degrees of freedom are equal to 171. Numbering of nodes and elements adopted in data processing is presented in Figs. 3.1 and 3.2.

In order to reach goals set out in detail in the first section of the chapter, we intentionally skipped the standard process of including dead and live load and load of snow and wind, in

the example for simplification purposes. As far as statics is concerned, only one vertical force of 1000kN put on the top of the dome is selected (compare Fig. 3.1.). The choice of the type of time-independent load is supposed to verify the geometry of the system. We will show that symmetric results of internal forces and displacements, obtained for corresponding nodes and elements will confirm the validity of the accepted model.

We address and solve deterministic statics independently by using two programs: POLSAP and ROBOT. The extreme values of received displacements and internal forces are summarized in Tables 3.1 and 3.2. The results presented in Table 3.1 are intentionally written with five-decimal-digit accuracy to show the difference between the value of nodal's displacement, otherwise they might be mistakenly regarded as identical.

Table 3.1 Extreme vertical displacements, [cm]

Node	Displacement		Difference
Number	POLSAP	ROBOT	[%]
31	-2.08558	-2.08424	0.064
10 and 2	-0.11594	-0.11979	3.214
4 and 8	-0.11593	-0.11978	3.214
6	-0.11592	-0.11977	3.214

Table 3.2 Extreme axial forces, [kN]

Element	Axial Force		Difference
Number	POLSAP	ROBOT	[%]
61 and 64	463.585	463.268	0.068
66 and 69	463.565	463.248	0.068
65 and 70	463.559	463.243	0.068
67 and 68	463.556	463.238	0.069
62 and 63	463.544	463.226	0.069

Upon comparing significant values of forces and displacements obtained by the above-mentioned programs, we observed a variance of 0.07%. Obviously, receiving bigger difference for much smaller vertical movement is a natural outcome. This difference stands at 3.2%, but it can still be applied to the structure.

Based on values presented in Tables 3.1 and 3.2 we observe that the analysis of symmetric nodes gives identical results. This can lay the foundations for the validity of the model input to the program.

3.7.3.2 Stochastic Statics

The stochastic analysis aims to define the material and geometrical characteristics as random variables and entering their means and cross-covariances matrix during data processing. Volatility of the values of the Youngh's modulus of steel seems to be hardly possible because contemporary industrial development is at such a high level. Therefore, to make the numerical computation more probable, the elements' cross-section areas A_b, $b = 1, 2, ..., 80$ are adopted as random variables.

The process of generating the covariance matrix is carried out based on examples illustrated in [35]. Below you will find excerpted program code used in the stochastic analysis. For the complete procedure, see Appendix C.

```
nrand=80                                !total number of random variables
a0=20.0d0                               !mean value of random variable
alpha=0.1d0                             !coefficient of variation
al2a02=alpha*alpha*a0*a0                !multiplier of correlation function
theta=200.0d0                           !dacay factor
                                        !generating the covariance matrix
k=0
do j=1,nrand
  do i=j,1,-1
  xij=-dabs((x(j)-x(i))/theta)
  yij=-dabs((y(j)-y(i))/theta)
  correlij=dexp(xij+yij)                !correlation function
  k=k+1
  cov(k)=al2a02*correlij
  enddo
enddo
```

In the above depiction, `x(i)` and `x(j)` are the x-coordinates of the mid points of the next two elements in the structure. Therefore `y(i)` and `y(j)` are the y-coordinates, respectively. A^0(`a0`) denotes mean values of the cross-sectional areas of the elements, which is 20cm^2.

"`theta`"(θ) designates the decay factor which clearly depends on the unit system used in computations. Selecting the value of θ aims at getting the non-zero and no diagonal covariance matrix of the random variables. After carrying out many trials for this example, θ =200 has been accepted for further analysis.

"`alpha`" (α) is designated as the coefficient of variation and is obtained experimentally. This factor is related to the degree of dispersion of the random variables. The necessary condition to applying in the analysis the Second Moment Perturbation Method is that, standard deviation $\sigma(x)$ of the expected values being less than 15%. Otherwise, we need to apply a more complicated statistical method such as Monte-Carlo Simulation increasing the difficulty of task's execution. It is known that from the definition $\sigma(x)^2 = \mathrm{Var}(x)$. According to the procedure of generating the covariance matrix applied during the analysis, the correlation function for the elements from main diagonal is 1.0, hence, the variance of specific elements depends directly on the correlation function multiplier. BecauseA^0 =20cm^2 and α equals 0.05, 0.10 or 0.15, are employed in the numerical computations in correspondence with the values of $\sigma(x)$: 5%, 10% and 15%. The synthesis of static displacements obtained by stochastic analysis described above is included in Table 3.3.

Table 3.3 Comparison the results of the vertical displacements obtained by POLSAP

Node Number	α	Expected Value [cm]	Deterministic Result [cm]	Difference [%]
	0.05	-2.09068		0.24
31	0.10	-2.10599	-2.08558	0.98
	0.15	-2.13150		2.20
	0.05	-0.11615		0.18
10 and 2	0.10	-0.11677	-0.11594	0.72
	0.15	-0.11780		1.60
	0.05	-0.11615		0.19
8 and 4	0.10	-0.11679	-0.11593	0.74
	0.15	-0.11785		1.66

We present the values given in Table 3.3 specifically with five-decimal-digit accuracy to show differences in values between points 10 and 2 as well as points 8 and 4. The nodes 10 and 2 are symmetric relative to each other and their displacements are equal and very similar, yet slightly different for nodes 8 and 4. A more concise presentation could be misleading, therefore the results seem to be identical.

As it is seen, for the α-coefficient equal 0.05 both types of analysis give very similar values, the difference is between 0.18 and 0.25%. However, that kind of situation is quite rare. For this reason the displacements for $\alpha = 0.10$ and $\alpha = 0.15$ are shown, for which the obtained results are also acceptable, the received values differ less than 2.20%. It is easily noticeable, that for the top of the dome, for which the vertical movement is significantly greater than in other nodes, the difference between deterministic and stochastic analysis is higher.

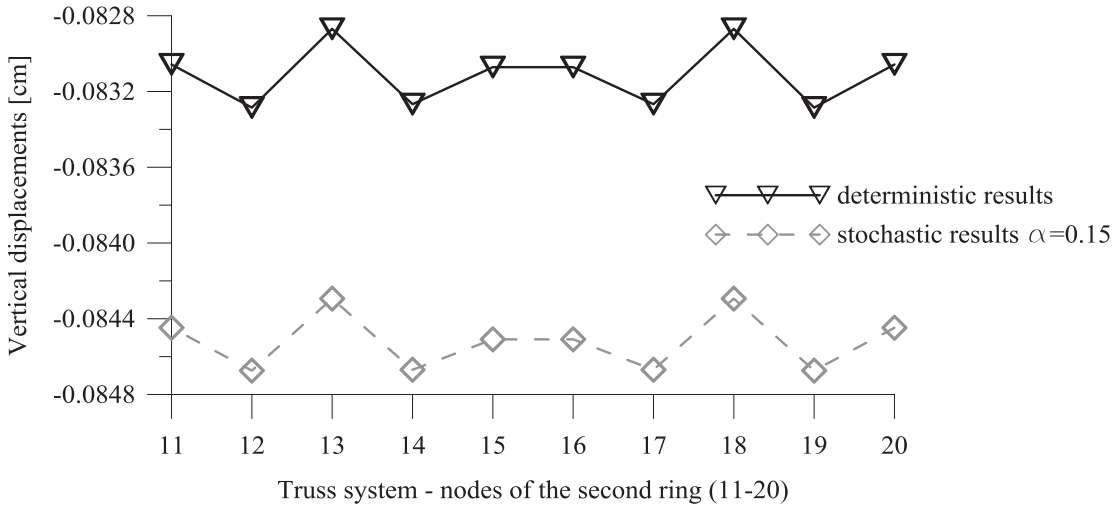

Figure 3.3 Truss System — Comparison of displacements for the nodes from the second ring

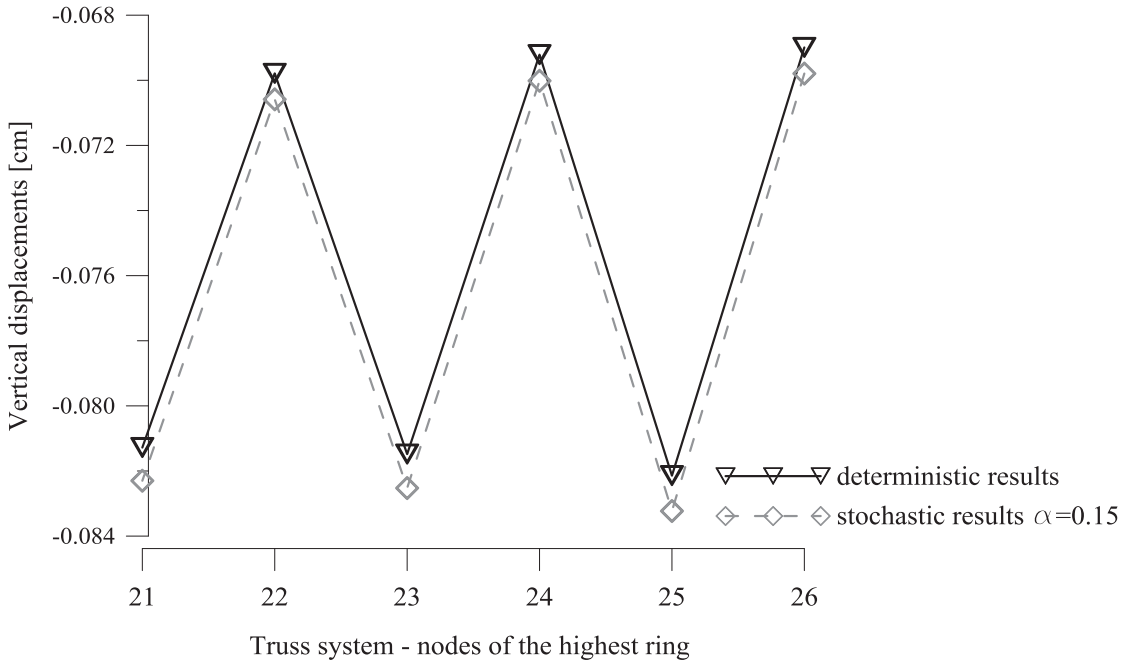

Figure 3.4 Truss System — Comparison of displacements for the nodes from the highest ring

In Figs. 3.3 and 3.4, we show displacements obtained for selected nodes from the second and the highest ring. For the clarity of presentation, apart from deterministic results, only the excepted values for α =0.15 are depicted. As seen in Fig. 3.3, values received for symmetric nodes are equal. It is also clear, that the greater the distance between nodes and the top of the dome, the lower the vertical movements.

3.7.3.3 Dynamic Analysis

With reference to the statics, dynamic analysis deals with the case of a sudden hit towards vertical direction on to the top of the dome. A constant impulse in value of 1000kN is applied during in time 2s, which is presented in Fig. 3.5.

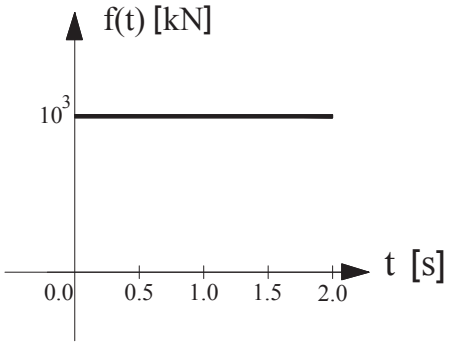

Figure 3.5 Dynamic force

The eigenproblem is solved for the first 18 eigenpairs, converged after 22 iterations. Maximum number of iteration required during the computation is 40. The tolerance convergence is 1.e-05. Naturally, it turned out that the largest displacement is on the top of the structure, i.e. at node 31, therefore we chose this point for further dynamic analysis. Table 3.4 presents natural frequencies of the truss system obtained independently by two programs: POLSAP and ROBOT. The differences between results oscillate around 0.02%, for every mode number.

Table 3.4 First 7 natural frequencies of the undamped truss system, [1/s]

Mode Number	POLSAP	ROBOT
1	44.6661	44.6581
2	44.6702	44.6621
3	67.2234	67.2113
4	73.5313	73.5180
5	73.5407	73.5275
6	75.6006	75.5869
7	75.6113	75.5975

The graph of the vertical displacements at the top of the dome under dynamic excitation, without including the damping during numerical computations, shows some regularity (compare Fig. 3.6). It is seen that amplitude vibration is changing periodically in time and has a course characteristic of systems with the beat phenomenon. The mentioned effect is the result of overlapping waves of slightly different frequencies. Looking at the numerical result shown in Table 3.4 two neighboring natural frequencies of the system are very similar because of dome segments' symmetric geometry and undoubtedly influences special course of the vibrations. For clarity of presentation, graphs below show time-dependent 1.0s long displacements.

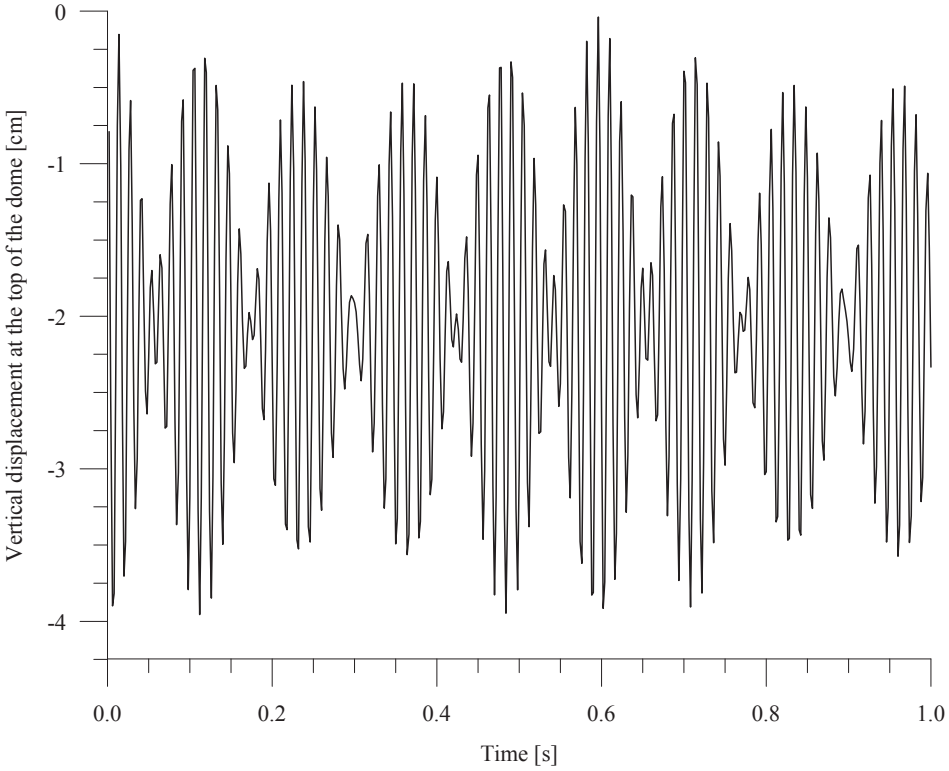

Figure 3.6 Deterministic results — time-dependent displacement for undamped truss system obtained by mode superposition

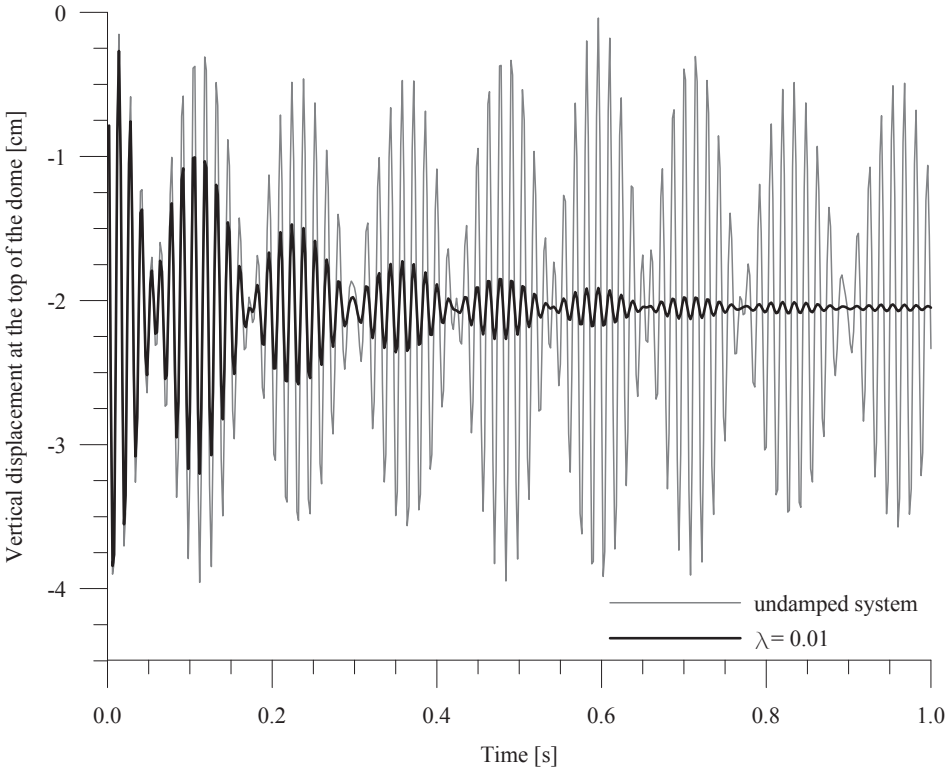

Figure 3.7 Deterministic results. Damping influence on vertical vibration — truss system

So far, we considered a damping-free system, yet such a structure does hardly exist on its own. Hence, further analysis is about the impact of damping factor on time-dependent displacements and internal forces and attempts to eliminate observed phenomenon.

Comparing graphs presented in Fig. 3.7, we see that applying the modal damping coefficient $\lambda = 0.01$ (compare Chapter 4) does not eliminate the beat phenomenon. In fact, it will only reduce the value of amplitude, while the periodic variability of the vibration remains unchanged. Therefore, we attempt to eliminate the beat effect by inserting added mass to the structure. After carrying out many tests and trials, most desired results are obtained for one mass input symmetrically on the top of the dome. It is sufficient to assume identical lumped mass coefficients, in all three translational degrees of freedom are equal to 0.01 inertia of elements' mass at that node. The simplified form of the spatial scheme with additional mass is shown in Fig. 3.8.

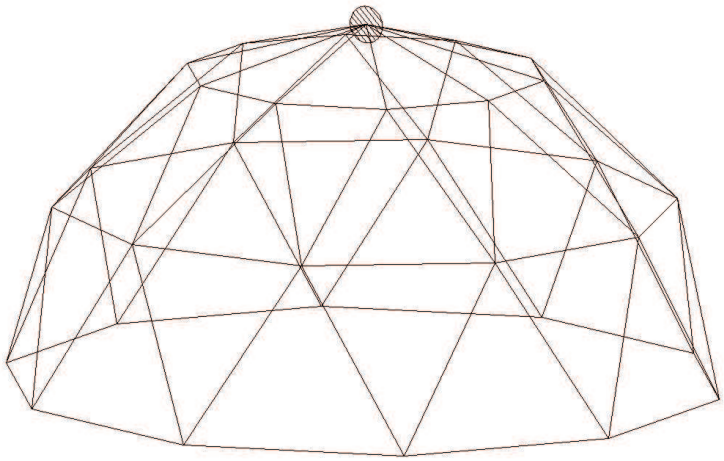

Figure 3.8 3D-view of the dome with added lumped mass location

Table 3.5 shows natural frequencies of the undamped system with and without mass. It is seen that inserting added mass to the structure results in significant reduction in first three frequencies within the system, the said being responsible for the occurrence of the beat phenomenon. This has effect on the disappearance of the periodic changes in the amplitude during the time-dependent displacement, see Fig. 3.9a.

Table 3.5 First 7 natural frequencies of the undamped truss system obtained by POLSAP, [1/s]

mode number	without added mass	with added mass
1	44.6661	31.3885
2	44.6702	34.5817
3	67.2234	34.5850
4	73.5313	70.5873
5	73.5407	72.9371
6	75.6006	72.9475
7	75.6113	75.6016

Considering that dynamic displacement, added mass and damping are all involved in the analysis and the former verified, structure's behavior can be observed in practice. Taking into account the coefficients of: modal damping $\lambda = 0.01$ and lumped mass to be 0.01 in all three directions of movement results in the elimination of the beat effect and greater reduction in amplitude, which makes the course of the vibrations more probable. To compare, see Fig. 3.9b.

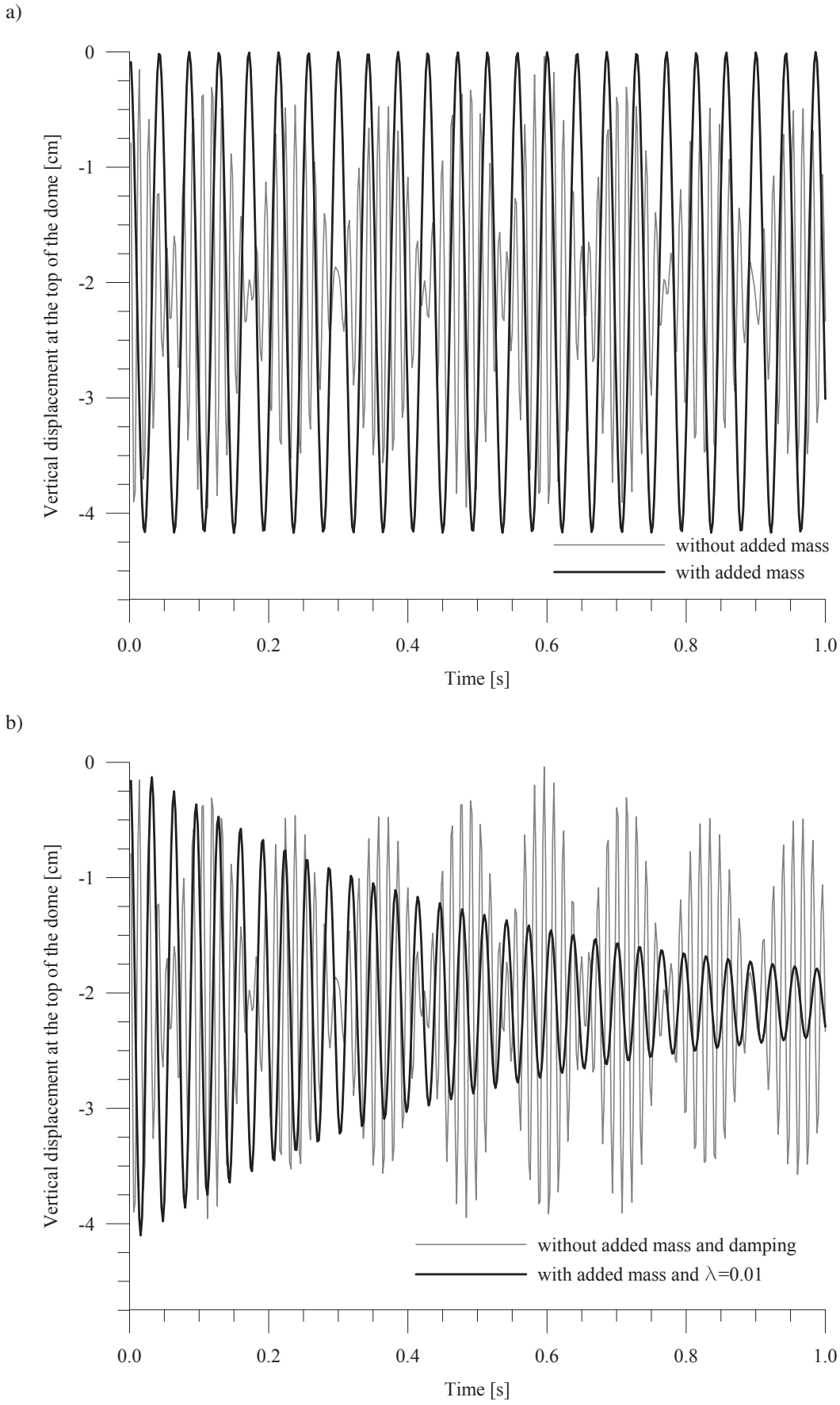

Figure 3.9 Truss model: a) added mass influence in undamped system; b) simultaneously effect of damping and added mass on vibration course

Including the uncertainties in the design random variables we can obtained a set of results in the form of expectations and their standard deviations. FEM mesh consists of 80 truss elements, whose cross-sectional areas are adopted as random variables. The stochastic analysis is made with using the 10 highest variables and including the following coefficients $\alpha = 0.05$ and $\theta = 200$, in the computations. The comparison of the received deterministic results in opposite to the excepted values are presented on fig. 3.10.

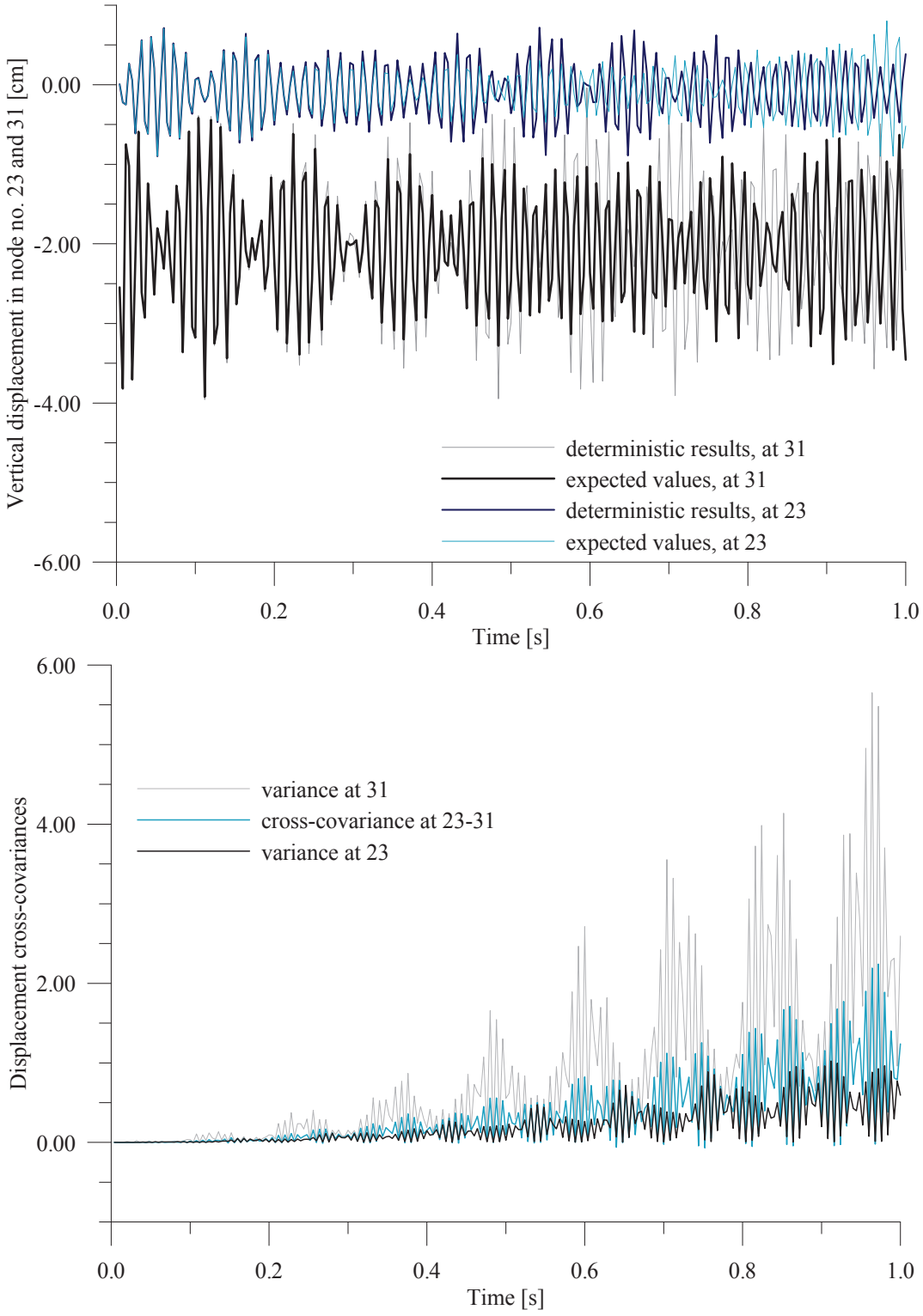

Figure 3.10 Displacement time response of the undamped system

3.7.3.4 Dynamic Sensitivity

The sensitivity analysis aims at verifying how the change of the cross-sectional areas of specific elements affect the vertical displacement in the design point. It turns out that as initially expected the top of the dome is the crucial point in the whole structure during data processing for truss system. In the sensitivity analysis, the functional of structural response takes the form

$$\phi = \frac{|q_\alpha|}{q_{\text{all}}} - 1 < 0 \tag{3.109}$$

where q_α, q_{all} stand for displacement of selected node and allowable displacement in this point respectively. The computation of dynamic response shows that the node 31 is the most sensitive with respect to the changing of the design variables of the elements in its domain. The whole graphs in this subsection present the dynamic z-displacement sensitivity of the top of the dome with respect to cross-sectional area of element no. 78. The limit value of the deflection is taken as 4 cm.

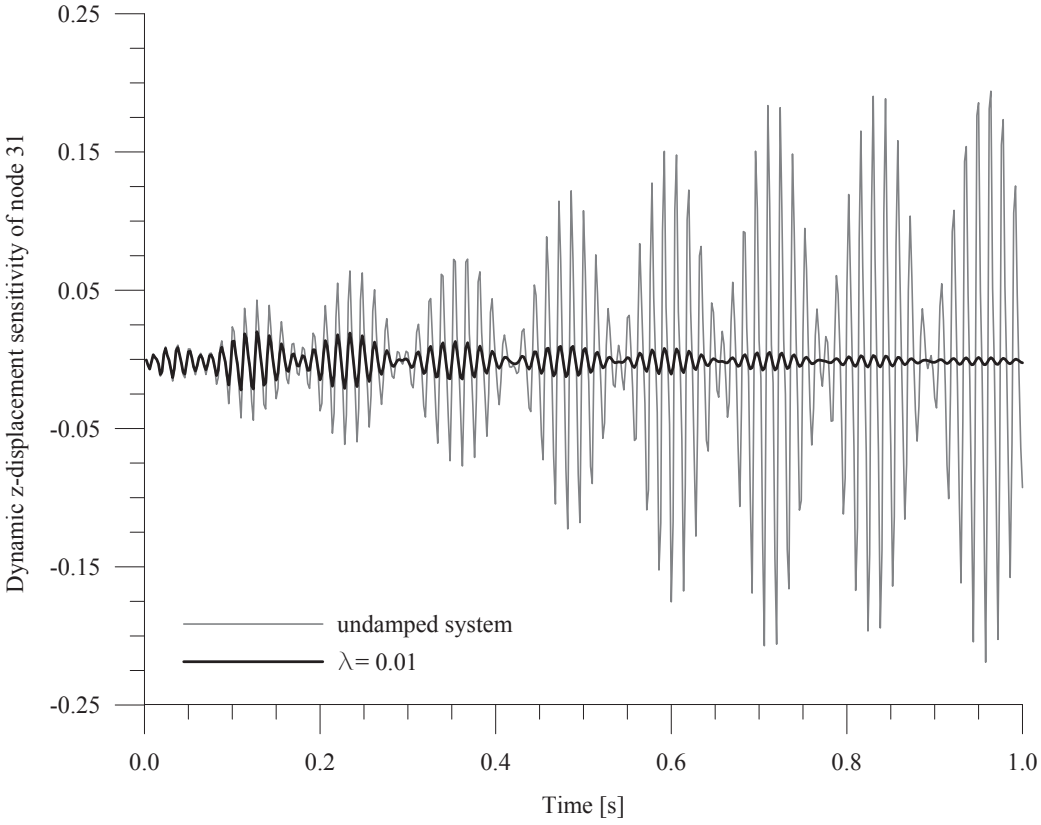

Figure 3.11 The damping effect to the dynamic sensitivity in truss system

As to Fig. 3.11 we can see that sensitivity response amplitude changes periodically and its value increases in time. Adding modal damping coefficient to the numerical computations results in the stabilization of maximum deflection value from the point of equilibrium and gradual reduction in the level of vibration, nevertheless the nature of time-dependent displacement remains unchanged. This only enforces the presence of the beat phenomenon in the system and leads to the confusion that damping is insufficient to eliminate the effect.

Inserting added mass in sensitivity analysis eliminates the beat phenomenon successfully. Fig. 3.12a shows time-dependent increases in sensitivity response values with amplitude stabilization and disappearance of periodic changes' characteristics. If simultaneous inclusion of damp-

ing and added mass occurs during the analysis, reduction in the beat effect and amplitude stabilization at a constant level will follow. To compare this vibration see Fig. 3.12b.

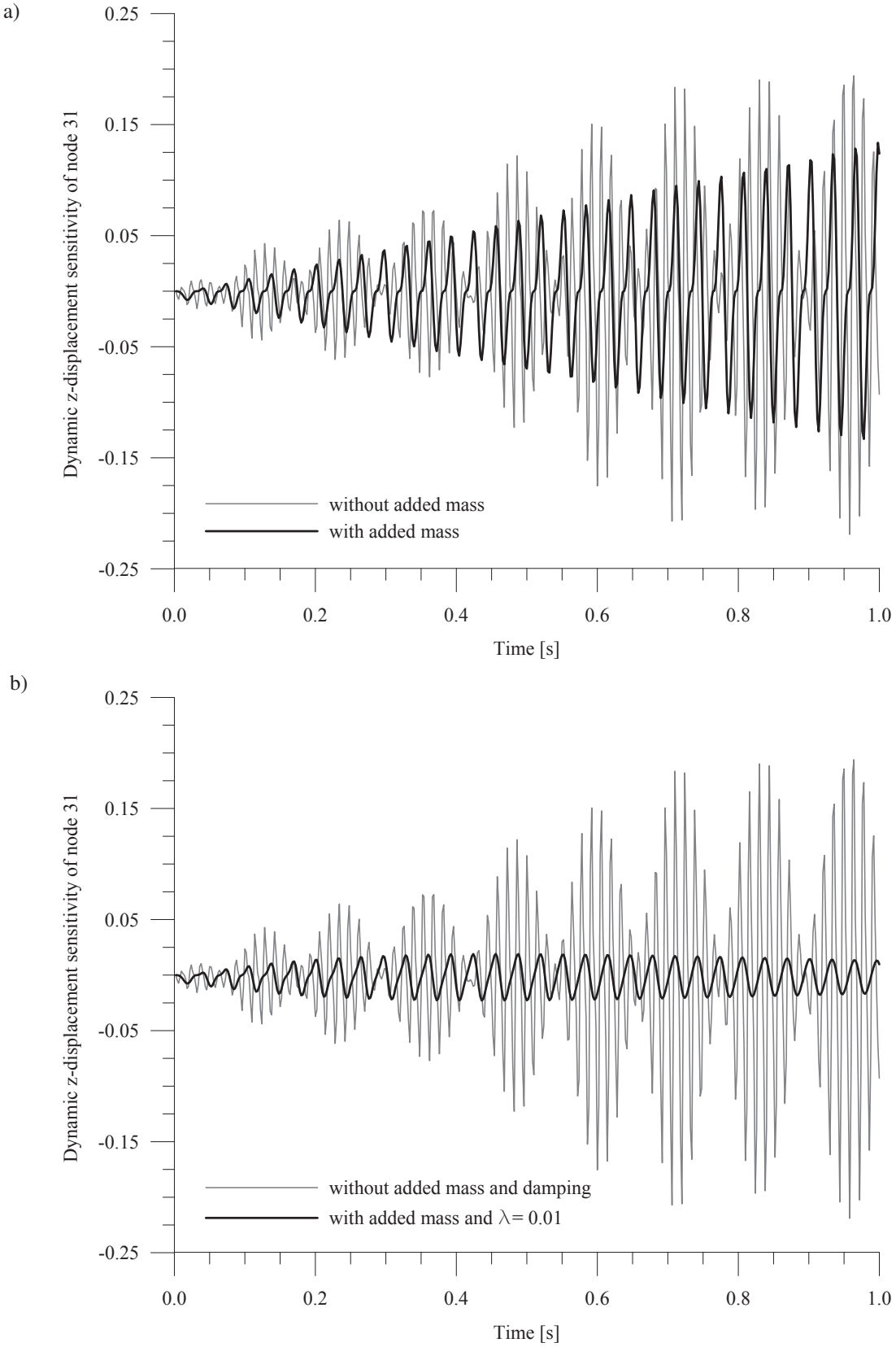

Figure 3.12 Truss system - design sensitivity with respect to cross sectional area of el. no 78 with influence of a) added mass in undamped system; b) added mass and damping

Including the stochastic analysis we obtained the expectations of dynamic sensitivity the displacement at node no. 31 with respect to the cross-sectional ares of element no. 78, and their cross-covariances — fig. 3.13. The coefficient using in the computations are equal $\alpha = 0.05$, $\theta = 200$. The results are received with taking into account 10 highest values of variables.

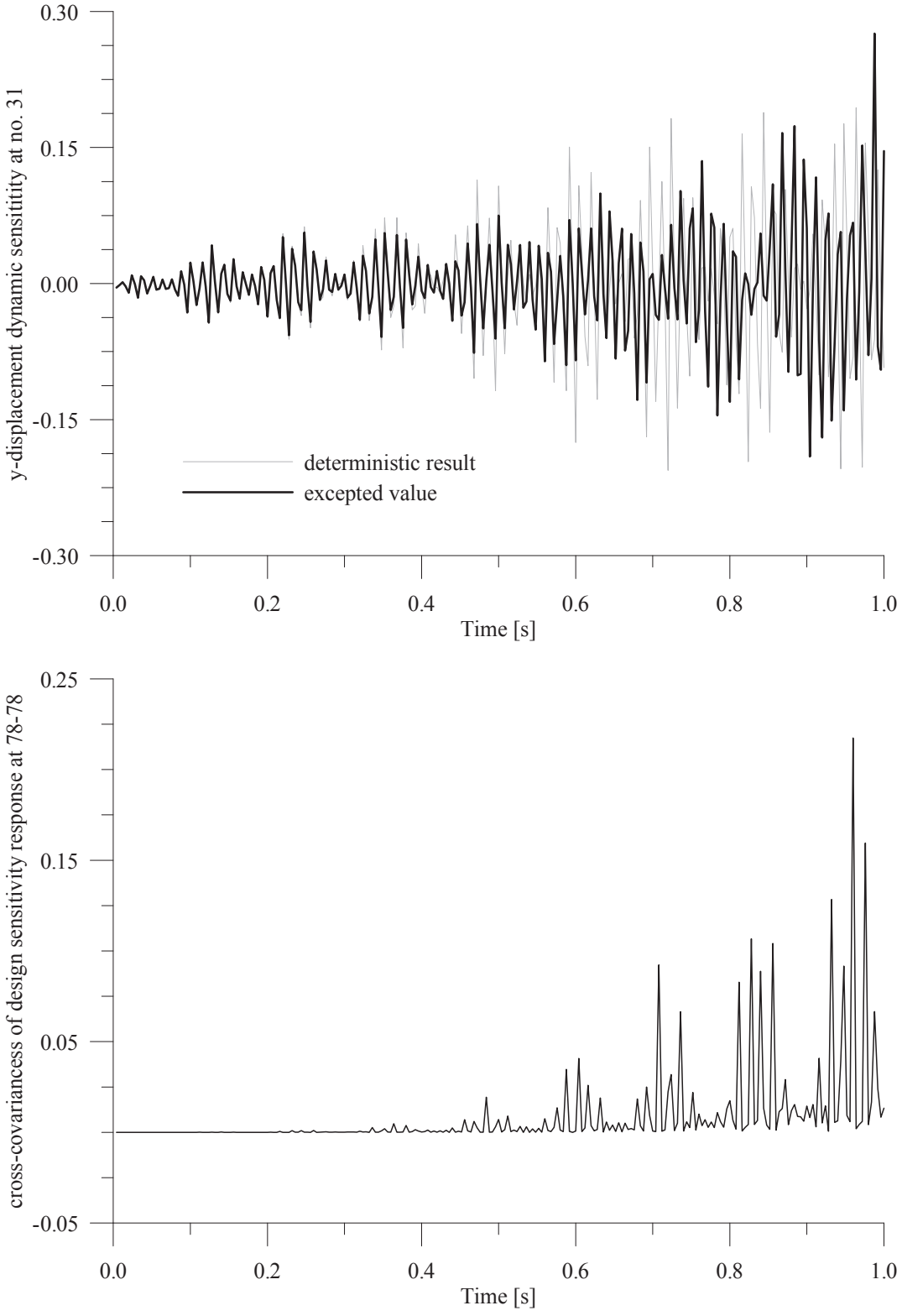

Figure 3.13 Time instant design sensitivity response

3.7.4 Comparison of Truss and Beam Systems

3.7.4.1 Statics Results

It is known that it is impossible to make perfect hinge joints for two or more elements in practice. It is due to several factors such as: friction force at the point of contact between materials, errors in the production stage of structure components, defects arisen by installing the elements, damping etc. This section is an attempt to address and answer the question if designing bar structures loaded only in nodes as 3D trusses for simplification purposes is wrong.

The goal of this part is to compare the truss and beam systems in different analysis. The second model has identical finite element setting as the first one, yet the bars are rigidly connected in nodes and so they are modeled as beam elements. Nodes 1, 3, 5 and 7 are supported by pins.

Static analysis shows insignificant values of the shear forces and bending moments in comparison to the axial forces. For that reason omitting them has no serious impact on the strength of calculation. As expected the largest displacement in the beam system is in node 31, but its value is lower than the truss one. The vertical movement obtained by deterministic and stochastic computations, for the top of the dome and for nodes from the first ring, are presented in Tables 3.6 and 3.7. The results obtained for other nodes are summarized in Figs. 3.14a and 3.14b.

Table 3.6 The vertical displacements at the top of the dome obtained by POLSAP

Node	α	Stochastic [cm]	Deterministic [cm]	Difference [%]
31	0.05	-2.05486	-2.04978	0.25
	0.10	-2.07012		0.99
	0.15	-2.09555		2.23

Table 3.7 Comparison of the displacements for the selected nodes received by POLSAP

Analysis	Node	Truss System [cm]	Beam System [cm]	Difference [%]
Deterministic	31	-2.08558	-2.04978	1.72
	10 and 2	-0.11594	-0.11585	0.08
	8 and 4	-0.11593	-0.11584	0.08
Stochastic				
α=0.05	31	-2.09068	-2.05486	1.71
	10 and 2	-0.11615	-0.11605	0.09
	8 and 4	-0.11615	-0.11605	0.09
α=0.10	31	-2.10599	-2.07012	1.70
	10 and 2	-0.11677	-0.11667	0.09
	8 and 4	-0.11679	-0.11669	0.09
α=0.15	31	-2.13150	-2.09555	1.69
	10 and 2	-0.11780	-0.11770	0.08
	8 and 4	-0.11785	-0.11775	0.08

Looking at Fig. 3.14 a) we can see that received displacement for nodes from the second ring is lower in beam system. Rigid connection between its constitutive elements cause this. For the

same reason, we can observe a different work of the particular elements in the structure in both models. In the beam scheme, the vertical movements on the top of the dome are lower because the nodes from the highest ring take greater part of the load than in the truss system, therefore, their displacements are larger (compare Fig. 3.14 b). What is important, the characters of graphs showing the selected points presented in above figures are parallel for the described two models. Results summarized in Table 3.7 show that biggest differences in vertical displacement between the truss and the beam system are visible on the top of the dome, meaning that the value is most significant as compared to other nodes.

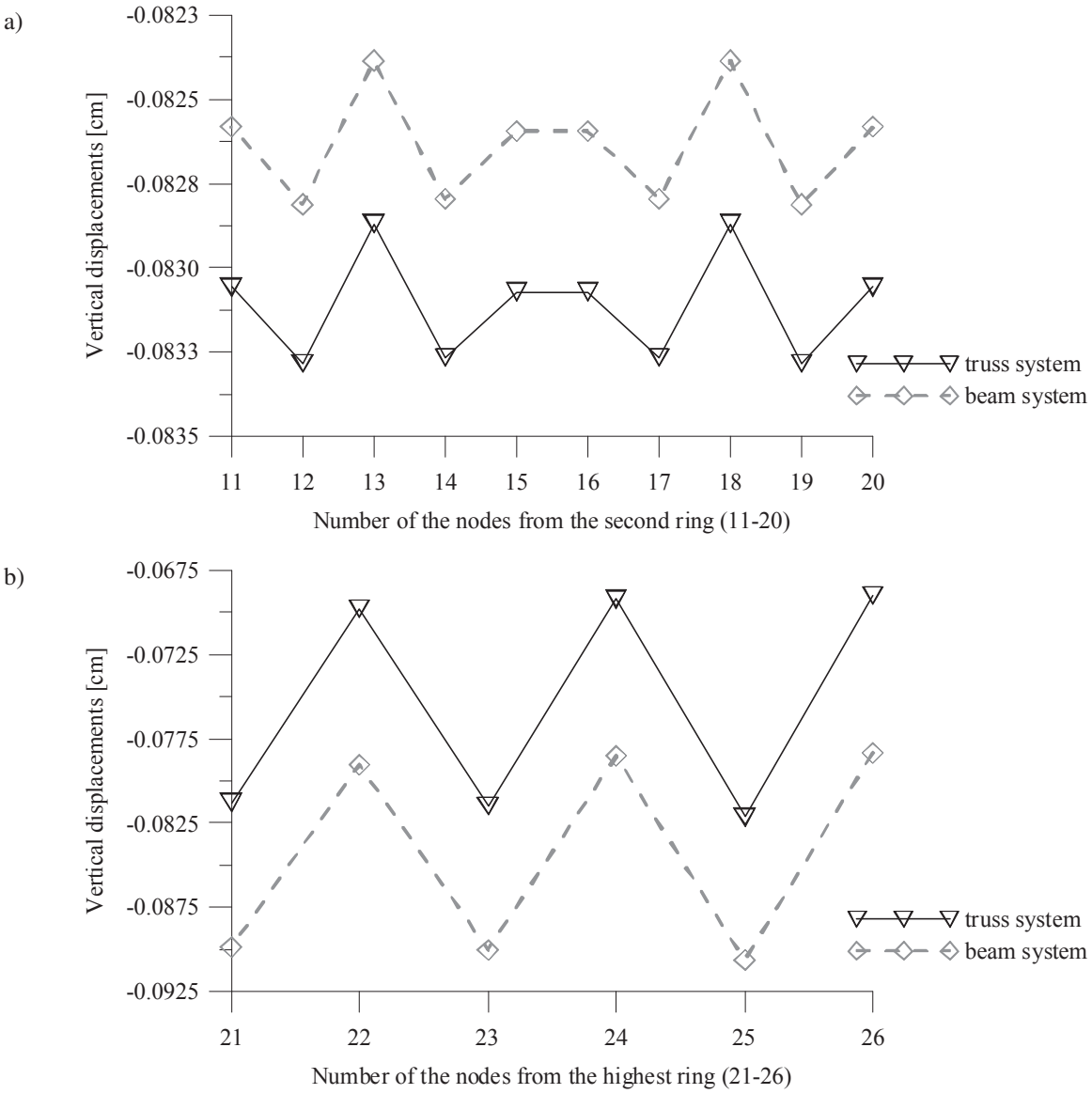

Figure 3.14 Comparison of the deterministic results gained for selected nodes from a) the second ring; b) the highest ring.

3.7.4.2 Dynamics Results

The same dynamic excitation as in previous section is put on the top of the structure (see Fig. 3.3). The comparison of node 31 vibration course for the truss and the beam systems is presented in Fig. 3.13.

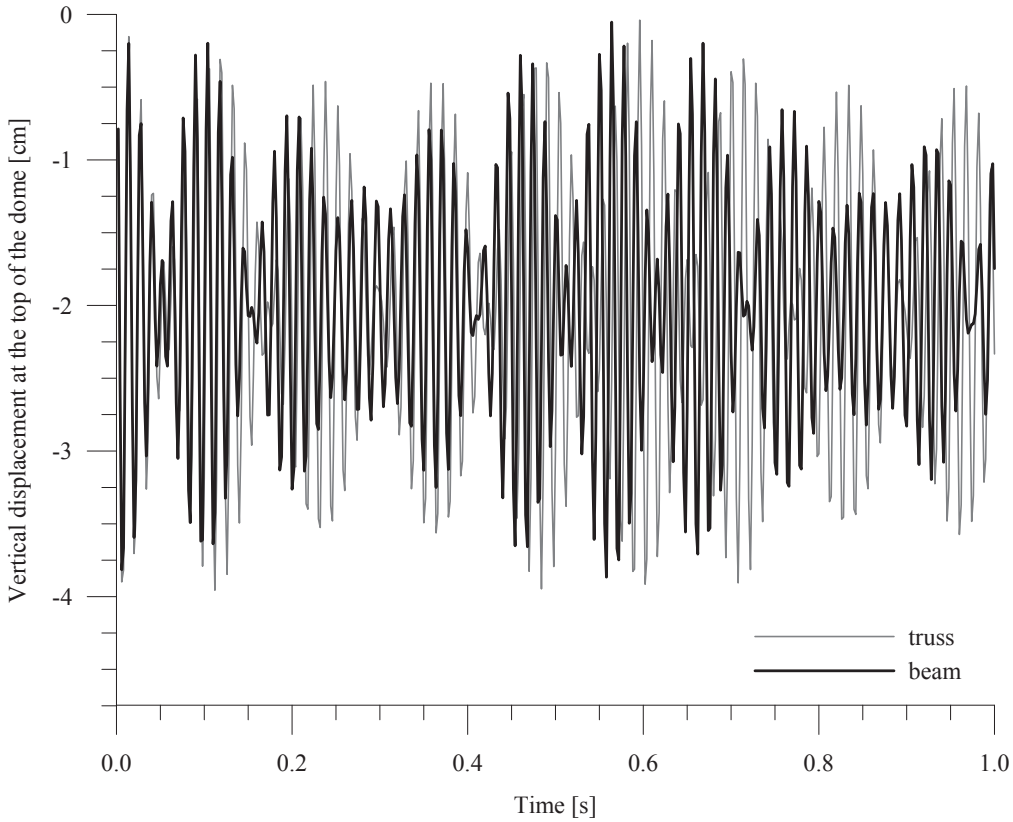

Figure 3.15 Comparison of the displacements obtained for undamped schemes

It turns out that the vertical dynamic displacements for the selected node are slightly smaller for the beam system and decay faster after taking the damping into account (compare Fig. 3.13). This is due to greater rigidity of the model, caused by different bars' connection. Obtained results suggest that second model describes the real conditions better than the first one. In practice, it is impossible to make a perfect joint by a hinge, therefore the beam scheme seems to reproduce the real structure work more reliably than the truss one. Looking at the course of vibration, it can be observed that the amplitude is changing periodically in time. Hence, we can get an impression that, in such a kind of repeatable symmetrical structures, the beat phenomenon is present regardless of the connection type between elements.

Table 3.8 First 7 natural frequencies of the undamped beam system, [1/s]

mode number	POLSAP	ROBOT
1	44.7814	44.7268
2	44.7845	44.7308
3	67.4297	67.3464
4	74.0473	73.9615
5	74.0515	73.9707
6	75.8421	75.8392
7	75.8452	75.8490

The natural frequencies of the system shown in Table 3.8 validate the above assumption about the beat effect, because of two neighboring frequencies having very similar values.

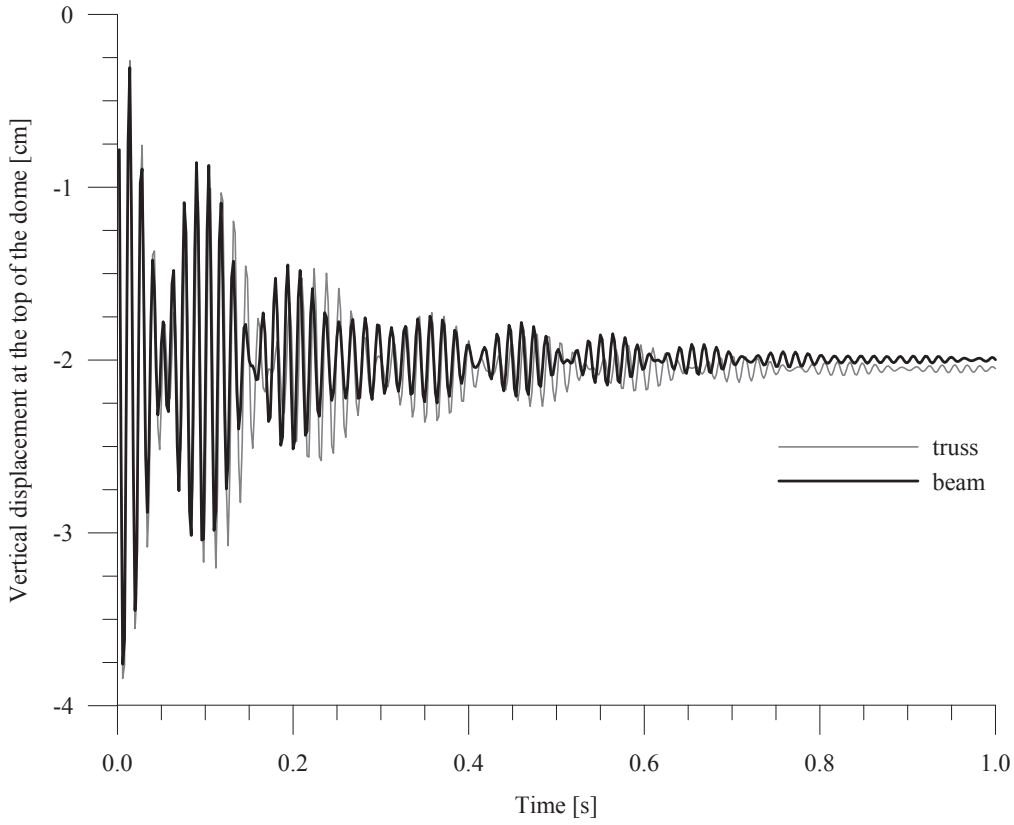

Figure 3.16 The time-dependent displacements received for systems with damping including

The use of damping during data processing does not change the periodical character of vibration regardless of the model. However, after inserting lumped mass coefficient into the system and putting it on the top of the dome, the beat effect has been eliminated successfully – for the comparison of displacements see Fig. 3.15.

After applying the added mass to the system in the analysis, the amplitude reaches constancy in time. Furthermore, two first frequencies of the system having greatest influence on the course of dynamic displacements in the model gain different values (see Table 3.9).

Table 3.9 First 7 natural frequencies of the undamped beam system obtained by POLSAP, [1/s]

mode number	without added mass	with added mass
1	44.7814	31.7814
2	44.7845	34.6728
3	67.4297	34.6742
4	74.0473	71.0842
5	74.0515	73.4878
6	75.8421	73.4946
7	75.8452	75.8421

Considering the modal damping coefficient and lumped mass simultaneously results in the elimination of the beat effect and gradual disappearance of the amplitude. Figs. 3.16-3.18 present the comparison of vertical displacements for system with and without damping and added mass.

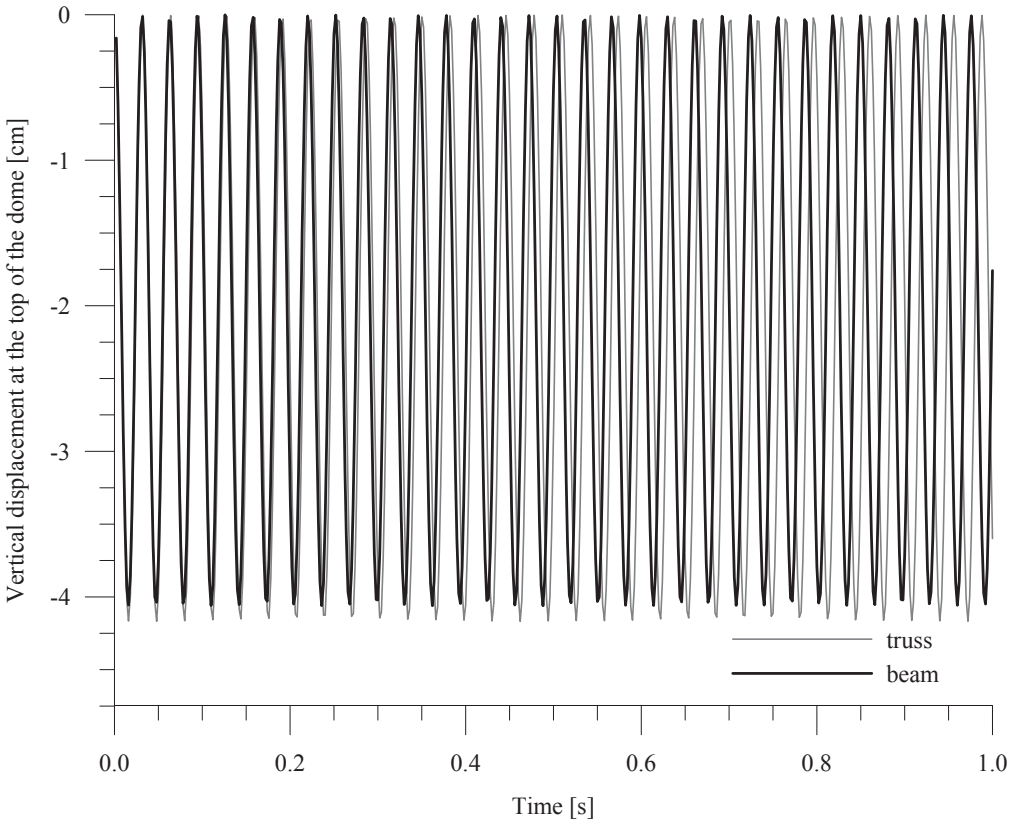

Figure 3.17 The added mass effect on the dynamic vibration in undamped systems

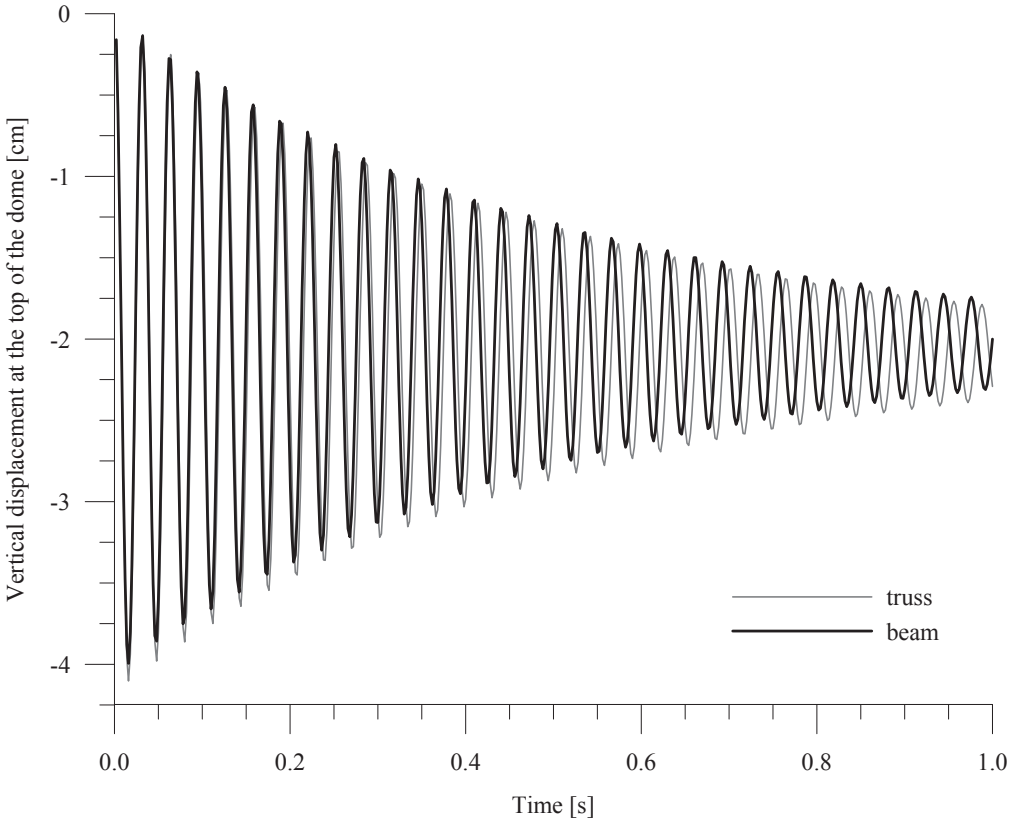

Figure 3.18 Displacement of node 31 in truss and beam systems — added mass and damping influence

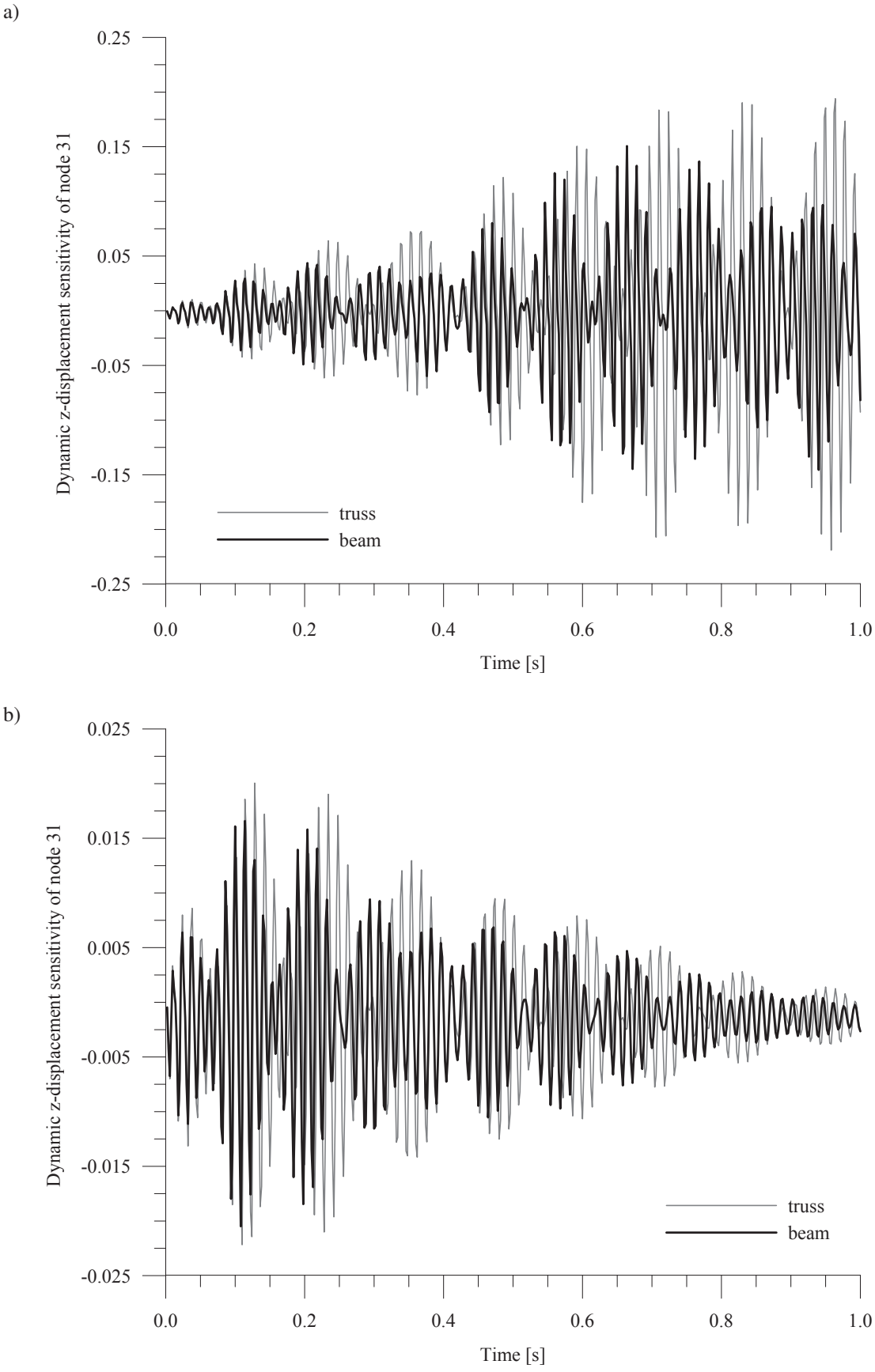

Figure 3.19 Comparison of the dynamic sensitivity with respect to cross sectional areas obtained for two models a) undamped systems; b) with modal damping coefficient λ=0.01

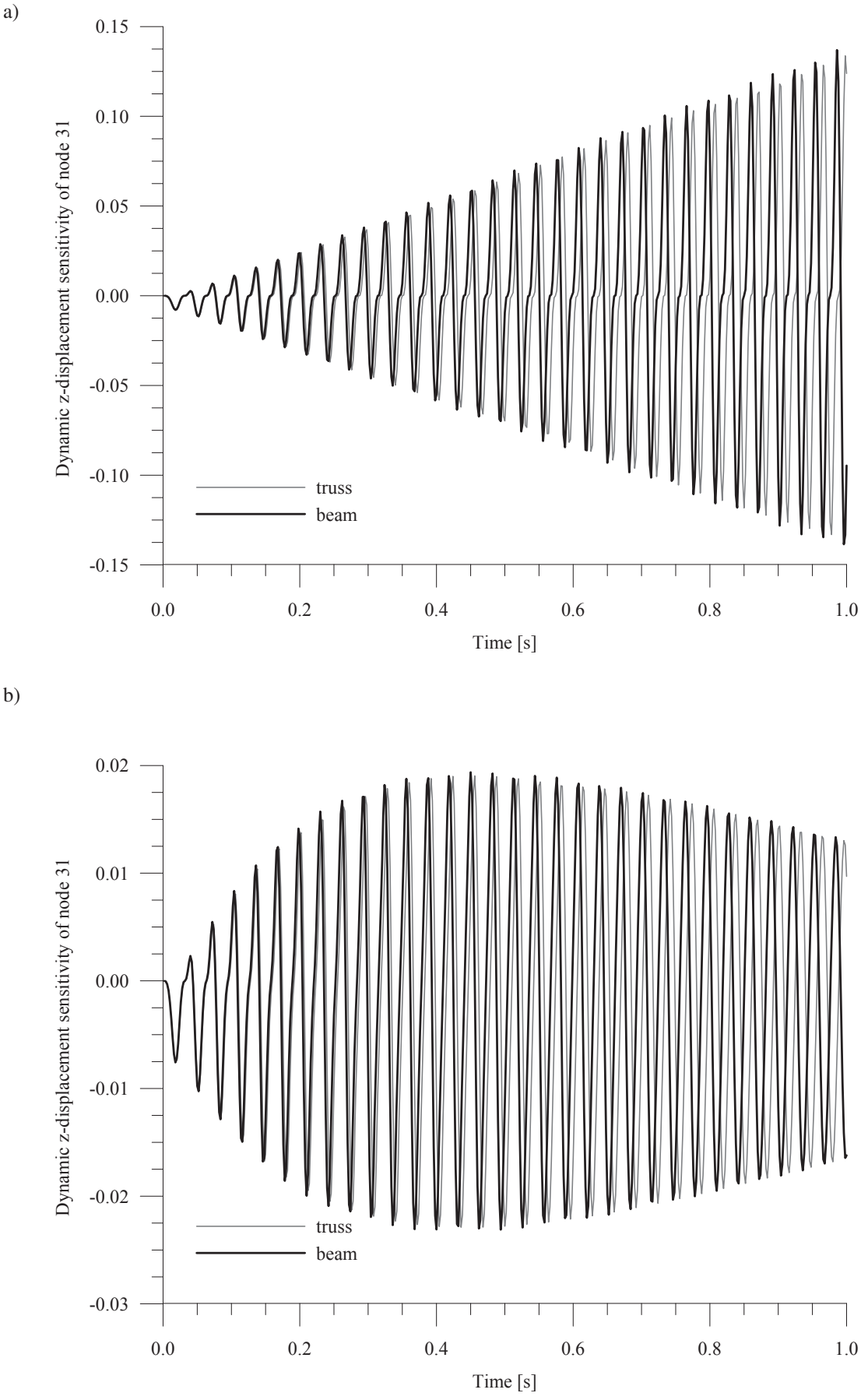

Figure 3.20 Dynamic sensitivity at node 31 - beam system: a) with added mass; b) with added mass and damping

3.7.4.3 Dynamic Sensitivity - Deterministic Results

For the possibility of comparing the sensitivity response received for two different models, conditions for the analysis are supposed to be identical. For that reason, time-dependent z-displacement sensitivity on the top of the dome with respect to the cross-section area of the element no. 78 is executed. We assumed the allowable deflection of 4 cm.

As predicted, the results obtained for beam scheme are analogous to the truss one. Inserting added mass to the system eliminates the beat effect while including damping, stabilizes the amplitude of vibration. However, as comparing dynamical responses for both models, it turns out that truss scheme is more sensitive to the change of the cross-sectional area of element no. 78 than the second one. It is due to lesser rigidity of connections between the particular elements, caused by using a hinge in the joints. Figs. 3.19 and 3.20 show the dynamic sensitivity of vertical displacement on the top of the dome with respect to the cross-sectional area of the 78-th element, for the beam system with and without inertial mass and damping.

Static and dynamic analysis of the mentioned object demonstrate that, it is not wrong to design the spatial dome under static lead as a truss system because of similar results obtained for both models. However, the beam system seems to describe the work of the structure more reliably. What is obtained in this scheme are small values of bending moments in nodes, and elements. Additionally, displacements received are smaller and vibration amplitude decays faster. Obtained results prove that adding lumped mass to such bar structures eliminates the beat phenomenon effectively.

3.7.5 Various Beam Systems

3.7.5.1 FEM Setting Selection

In the previous section, we analyzed the beam model consisting of 80 elements. However, it does not comply with all requirements of the FEM setting selection. This is because in the method, when the 3D beam system is considered, each bar should be divided into at least two parts. In fact, imputing axial forces, the influence of shear forces and bending moments as well as values of displacements and internal forces in mid-points of the element to the analysis, makes obtained results more precise. The way of reasoning seems necessary to the proper understanding of the structure's work.

It is commonly known that the greater number of elements included in such a numerical analysis the higher its cost. Therefore, there is a very important issue in this case, namely, the number of elements an individual bar should be divided to, for obtaining most optimal data processing — yielding accurate results with minimal computational time required. For that reason, this section contains two new beam models described, created on the basis of the same structure, consisting of between 160 and 320 elements respectively. In order to be able to compare new results with the previously obtained values for truss and 80-element beam systems, support conditions of the structure, the same as in the case of static and dynamic loads, are identical for each of the four considered models.

Figure 3.21 shows 160-element beam system that is the result of dividing each bar into two beam elements in FEM setting. In this way, the system with 112 nodes, 160 elements and 651

total number of degrees of freedom is received. The node 112, which is not seen in the mentioned figure, has all coordinates at zero value and it is located in the middle of the dome's base. This point is necessary for the correct orientation of local coordinate systems of particular elements.

We obtained the second scheme by dividing one bar into four beam elements. That gives the model with 272 nodes, 320 elements and 1611 total number of equations. For details concerning numbering see Fig. 3.22. Directional node is used for the proper orientation as regards to local systems' elements, has a number 272 and its location is the same as the position of the node 112 in the previous model.

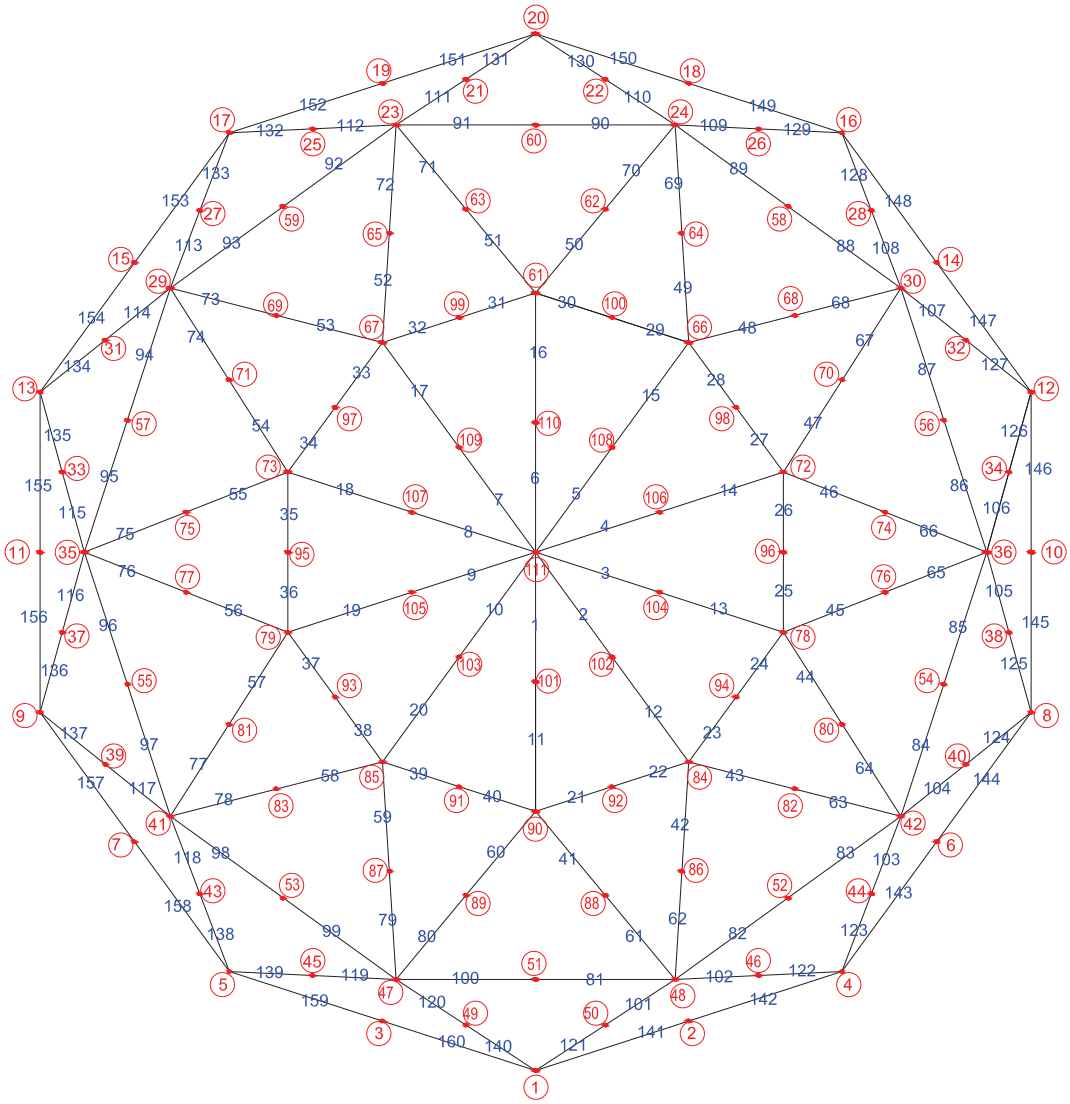

Figure 3.21 160-element beam system - finite element setting

The creation of the above models is very laborious yet it gives numerous advantages. What is most important for described schemes is that the values of displacements and internal forces for the nodes along the chosen bars can be received. It affects the accuracy of obtained results, for we simultaneously know what occurs inside the selected elements not only at their end-points. That provides us with a different view on the functioning of the considered structure.

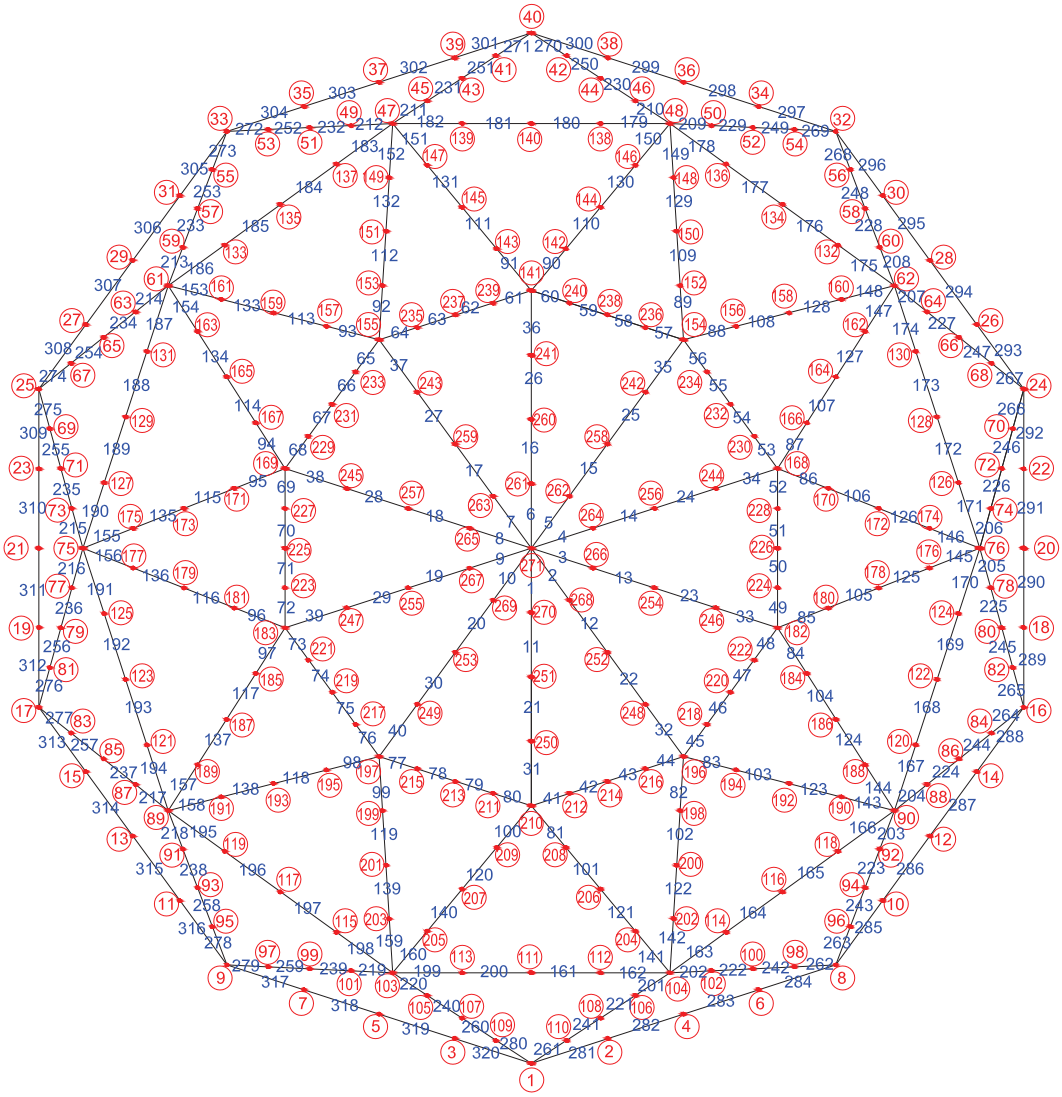

Figure 3.22 320-element beam system - finite element setting

The program code for generating nodal data for 160-element scheme is presented bellow:

```
do j=1,n
  do i=l(j),m(j),k(j)
    ri=dfloat(i)
    if ((k(j)).eq.6)then
       if((i/2*2-i).eq.0) then
       variable=theta(j)*xpi-fi/k(j)*(ri-l(j))
       else
       variable=theta(j)*xpi+fi/k(j)*(ri-l(j))
       endif
    else
       if((i/2*2-i).eq.0) then
       variable=theta(j)*xpi+fi/k(j)*(ri-l(j))
       else
       variable=theta(j)*xpi-fi/k(j)*(ri-l(j))
       endif
    endif
    x(i)=r(j)*dcos(variable)   !x-coordinate
    y(i)=r(j)*dsin(variable)   !y-coordinate
```

```
      z(i)=zn(j)                    !z-coordinate
    enddo
  enddo
```

Where `n` is the total number of the adopted rings, the variables `l(j)` and `m(j)` are the first and the last number of the point in the i-th ring, while `k(j)` is the computations' step. The radius of the concerned ring is assumes as `r(j)`. The expression `theta(j)*xpi` denotes the angle of the offset along the circle of the first point in considered ring, in radians. The variables `l(j), m(j), k(j), theta(j), r(j)` and `z(j)` are loaded from a different file during the analysis. For the whole procedure see Appendix C

3.7.5.2 Static Analysis

The static analysis is carried out independently twice for 160- and 320-element models, from a single vertical force with the value of 1000kN put on the top of the dome. The deterministic analysis of nodes' displacements and internal forces gives very similar values for both considered models but different from results received for the 80-element scheme.

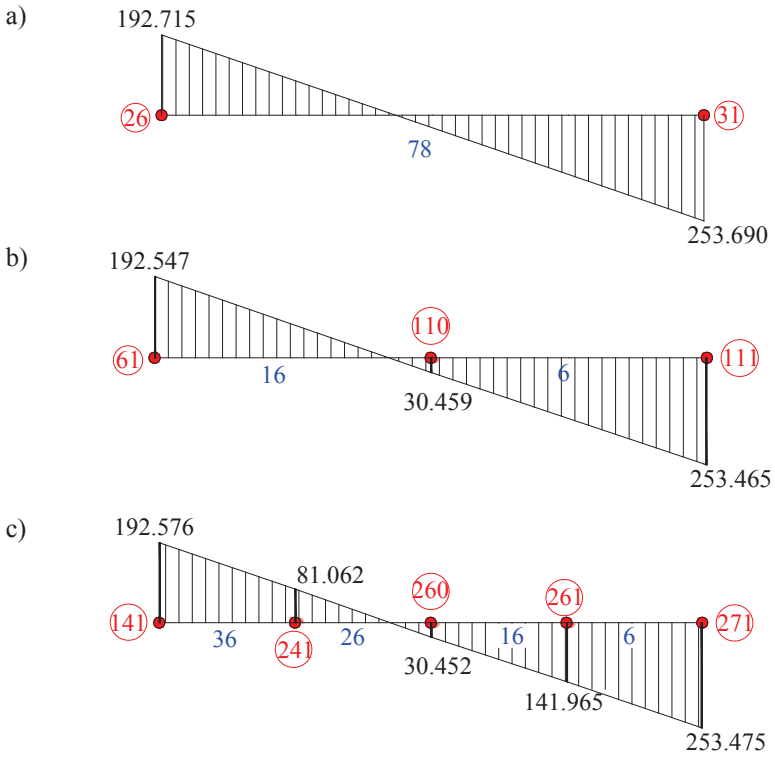

Figure 3.23 Deterministic results — bending moments obtained for the selected elements from a) 80-element; b) 160-element; c) 320-element scheme, [kNcm]

Creating models consisting of 160 or 320 elements is very laborious, yet it facilitates obtaining search values for the bars' mid-points. Therefore, as precise knowledge about deformation is available the same applies to the forces' distribution inside the element (compare Fig. 3.23). Having known the value of bending moments only for end nodes may lead to inadequate shape of internal forces' graph that could cause design flaws.

Table 3.10 Comparison the results of the vertical displacement at the choose nodes

Scheme	Node Number	α -coefficient	Stochastic Result [cm]	Deterministic Result [cm]	Difference [%]
a) The top of the dome					
80-element	31	0.05	-2.05486	-2.04978	0.25
		0.10	-2.07012		0.99
		0.15	-2.09555		2.23
160-element	111	0.05	-2.05386	-2.04875	0.25
		0.10	-2.06916		1.00
		0.15	-2.09467		2.24
320-element	271	0.05	-2.05390	-2.04878	0.25
		0.10	-2.06926		1.00
		0.15	-2.09487		2.25
b) The main point from the top ring					
160-element	96	0.05	-0.13743	-0.13718	0.18
		0.10	-0.13818		0.73
		0.15	-0.13944		1.65
320-element	226	0.05	-0.13745	-0.13720	0.18
		0.10	-0.13820		0.73
		0.15	-0.13945		1.64
c) The mid-point of el. from the top ring					
160-element	108	0.05	-1.20925	-1.20630	0.24
		0.10	-1.21810		0.98
		0.15	-1.23285		2.20
320-element	258	0.05	-1.20923	-1.20629	0.24
		0.10	-1.21807		0.98
		0.15	-1.23280		2.20
d) The mid-point of el. lying on the y-axis					
160-element	110	0.05	-1.20541	-1.20248	0.24
		0.10	-1.21421		0.98
		0.15	-1.22887		2.19
320-element	260	0.05	-1.20540	-1.20247	0.24
		0.10	-1.21420		0.98
		0.15	-1.22887		2.20

Parallel to the execution of deterministic analysis the stochastic analysis is performed. The equation for the covariance matrix is analogous to the expression from the section 3.7.3.2. Due to the complexity of covariance matrix's generation for the 160- and 320-element models specially created program is used in both cases. For the whole procedure see Appendix C

We adopted the mean value of cross-sectional area to be 20cm^2. The stochastic analysis is computed for three coefficients of variation, which equal to 0.05, 0.10 and 0.15 respectively. For all three beam systems 80-, 160- and 320-element, one average value of decay factor λ=200, is assumed during data processing. Using a different value of λ in the models could pose the question about the possibility of comparing the obtained results.

Table 3.11 Comparison the results of the y-direction displacement at the choose nodes

Scheme	Node Number	α -coefficient	Stochastic Result [cm]	Deterministic Result [cm]	Difference [%]
a) The main point from the lower ring					
80-element	15	0.05	0.15180	0.15146	0.22
		0.10	0.15283		0.90
		0.15	0.15455		2.04
160-element	24	0.05	0.15179	0.15143	0.24
		0.10	0.15285		0.94
		0.15	0.15461		2.10
320-element	48	0.05	0.15180	0.15144	0.24
		0.10	0.15286		0.94
		0.15	0.15463		2.11
b) The main point from the top ring					
80-element	25	0.05	0.22163	0.22106	0.26
		0.10	0.22334		1.03
		0.15	0.22618		2.32
160-element	66	0.05	0.22178	0.22121	0.26
		0.10	0.22349		1.03
		0.15	0.22633		2.31
320-element	154	0.05	0.22179	0.22122	0.26
		0.10	0.22350		1.03
		0.15	0.22636		2.32
c) The mid-point of el. from the top ring					
160-element	108	0.05	0.08131	0.08110	0.26
		0.10	0.08194		1.04
		0.15	0.08299		2.33
320-element	258	0.05	0.08132	0.08110	0.27
		0.10	0.08197		1.07
		0.15	0.08306		2.42
d) The mid-point of el. lying on the y-axis					
160-element	110	0.05	0.10141	0.10114	0.27
		0.10	0.10221		1.06
		0.15	0.10356		2.39
320-element	260	0.05	0.10142	0.10115	0.27
		0.10	0.10224		1.08
		0.15	0.10360		2.42

The values of received vertical and horizontal movements are summarized in Tables 3.10 and 3.11. The difference between deterministic and stochastic values of displacements for α=0.05 is about 0.18÷0.25%, for α=0.10 equal to 0.70÷1.10% and if α=0.15 it is 1.60÷2.42%. Looking at the obtained results, we can see that the percentage difference for most displacement values is higher than for the others.

During the process of generating covariance matrices for 160- and 320- element schemes, the coordinates of the beam elements' mid-points are loaded from an individual file. The procedure of receiving data can be found in Appendix C and it is analogous to determining the coordinates

of main nodes in mentioned models, presented at the beginning of this section. The mid-nodes of particular bars are lying on rings at different heights and radii. Obtaining the mid-point coordinates in each circle requires the input of the following data: number of first and last node of considered ring, computation step, circle's radius, z-coordinate and the angle of the offset – the first point along the circle. In order to facilitate numerical computation a new program is created and adopted to calculate necessary data prior to imputing first element node number in a given circle.

3.7.5.3 Dynamic Analysis

Dynamic analysis for 160- and 320-element beam system carried out independently by two methods: direct integration and mode superposition gave surprising results. The load has assumed the form of a constant vertical impulse with the value of 1000kN occurring during 2 second time interval put on the top of the dome. Looking at results, it turns out that it is impossible to eliminate the decay of amplitude vibration without including damping in the analysis. Ignoring the influence of the factors that can inhibit the vibration, the amplitude was supposed to be constant during the impulse. Only a thorough study of professional literature on the subject could provide the answer to the elaborate phenomenon. It turns out that the problem is about the wrong selection of time steps in numerical computations. In accordance to [Bathe], to get the correct results from dynamic analysis, the time step Δt chosen to the data processing should be less than $T_n/10$, where T_n denotes the smallest period of the considered system. As it is well known that FEM computations are approximate and in practice, for simplicity only first few natural frequency of the system are considered in analysis. Hence, the smallest period considered during the data processing may be several times higher than T_n, which leads to the false values of displacements.

Depending on the method of numerical integration which is used in computations, the percentage of amplitude decay is different. For example, for Wilson θ methods it ranges from 0 to 18% [3]. The comparison of the vertical time-dependent displacements obtained for different time steps in 160-element system is presented in Fig. 3.24.

The dynamic analysis of the described schemes by mode superposition method faced even greater obstacles. The problem turns out to be the symmetry and repeatable geometry of the considered structure. During data processing for the 80-element beam scheme through mode superposition method, only 18 initial values of the system's natural frequencies are taken into consideration. The density of FEM mesh gives slight differences between the values of the mentioned 18 initial frequencies ranging from 19.63 to 24.78Hz for 160-element beam system, and from 19.93 to 25.33Hz for 320-element model. The analysis of two last models by mode superposition method with the inclusion of account only 18 natural frequencies only gave a peculiar solution in the form of zero time-dependent displacements.

For receiving the proper course of vibration, the direct integration method for verification is used. To receive accurate results for dynamic analysis by mode superposition, 160 natural frequencies within 160-element scheme are to be included during data processing (compare Fig. 3.27), while for 320-element scheme this number is 470.

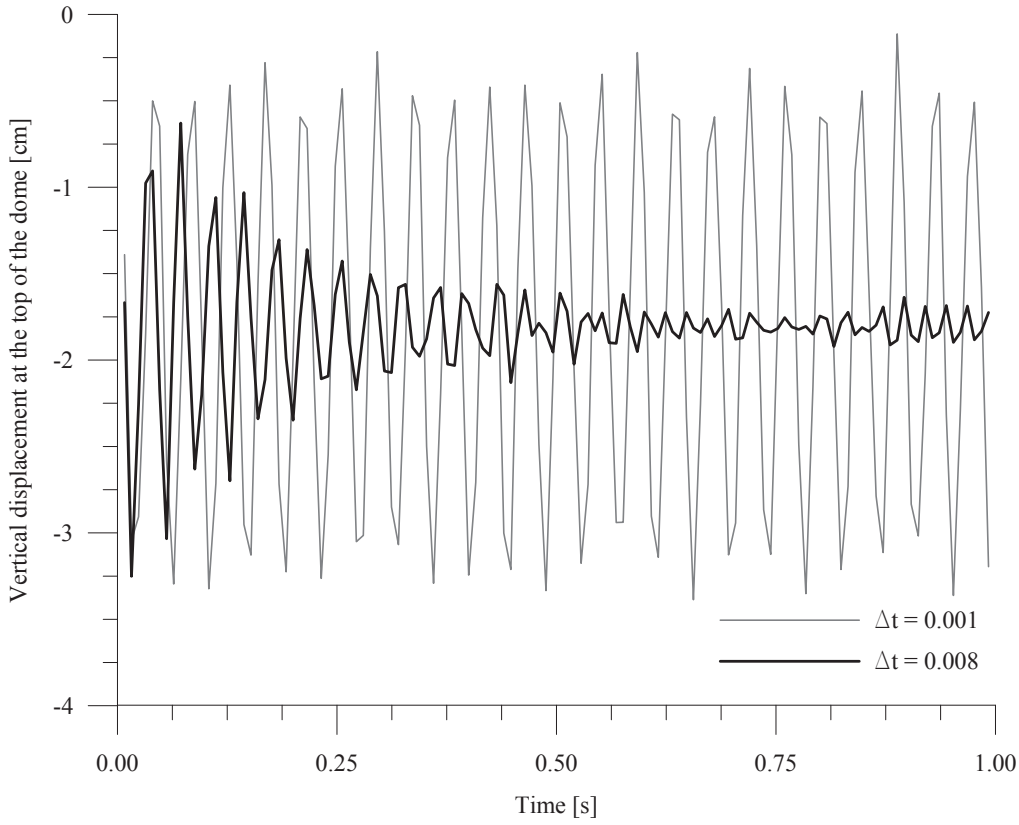

Figure 3.24 Influence the selection of the time step to the correctness of the vibrations

Not only are so many frequency values unlikely to be observed in reality but they would cause a significant increase in computational costs.

The comparison of time-dependent displacement on the top of the dome, for three described beam models without damping is summarized in Fig. 3.26. It is clear, that the increase in the number of elements in the system converges with the decrease in amplitude vibration however, the beat phenomenon is to be observed in all cases. For clarity of presentation, Figs. 3.26 and 3.27 present graphs encompassing short interval equaling 0.30s.

As in case of the previous models, taking into account added mass during data processing eliminates the beat effect successfully. Because in 160-element scheme the particular elements are shorter in comparison to the 80-element system, the lumped mass coefficients required to remove mentioned phenomenon are higher, i= 0.03. In Fig. 3.27 are presented the courses of vibration obtained for 160-element beam system for different values of lumped mass coefficients.

Fig. 3.28 presents vibration courses on the top of the dome for all three beam models including coefficients of damping $\lambda = 0.01$ and lumped mass i=0.03 in all three translational direction. Because of different lengths of elements connected in the main node, the added mass in this point varies in all described models, meaning that the values of inertial forces included during data processing are unequal.

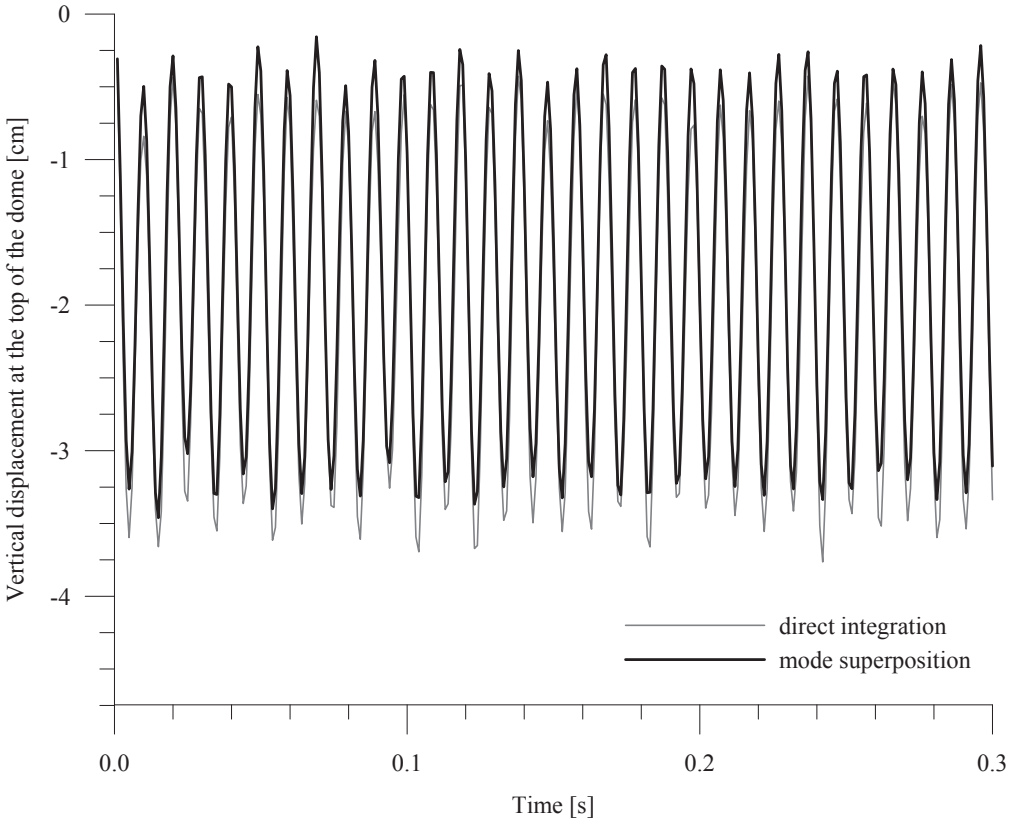

Figure 3.25 160-element scheme - obtained results for time step 0.0001s.

It turns out that the graphs for 160- and 320-element models overlap, and the values are very similar for the line of third scheme. For that reason, we assume that further increases in the coefficient of lumped mass are pointless, because the beat phenomenon was successfully eliminated and amplitude variation decays gradually over time.

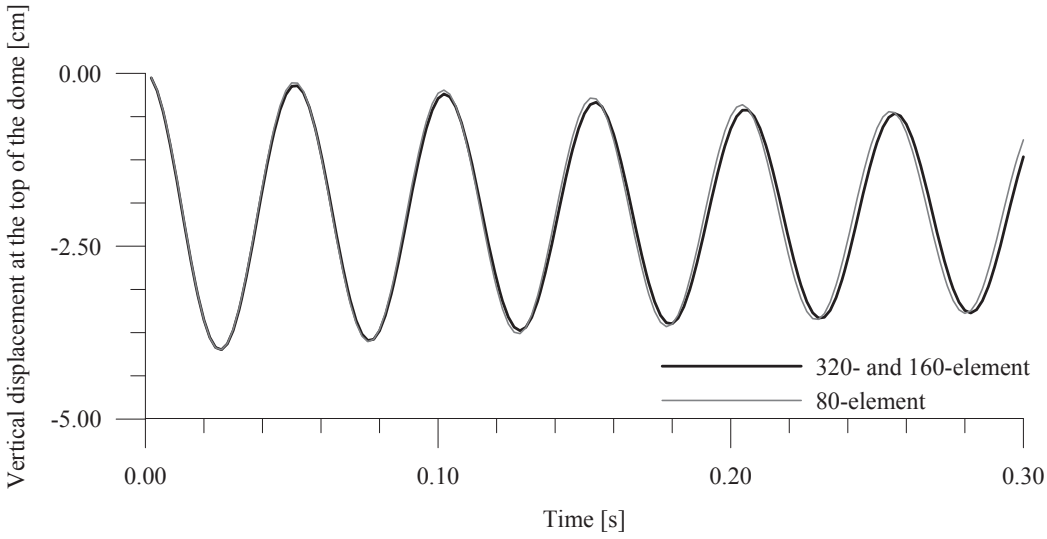

Figure 3.26 The influence of added mass and damping (λ=0.01) in two beam models.

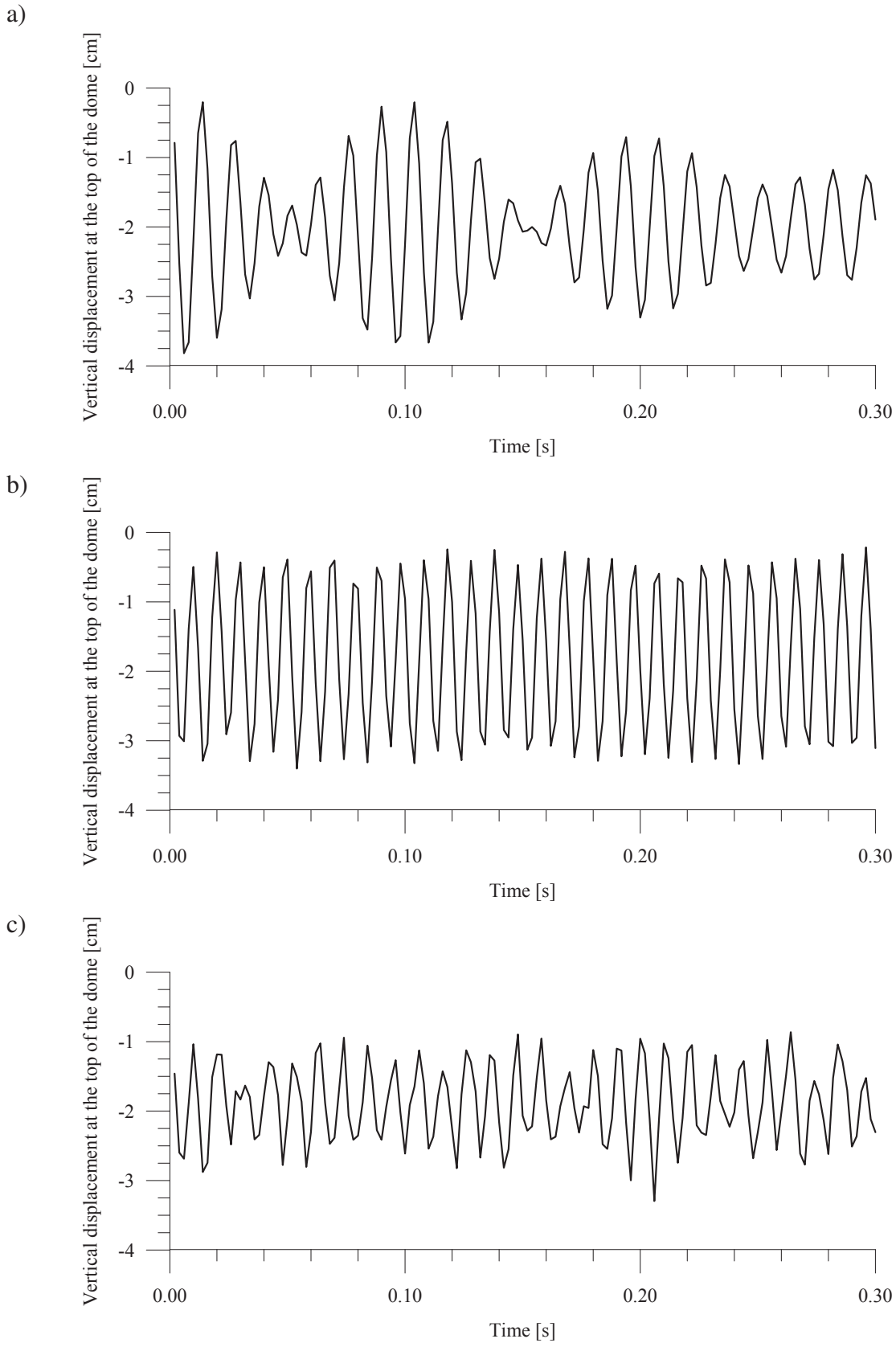

Figure 3.27 Comparison the dynamic displacement of undamped beam systems a) 80-element; b) 160-element; c)320-element, received by mode superposition.

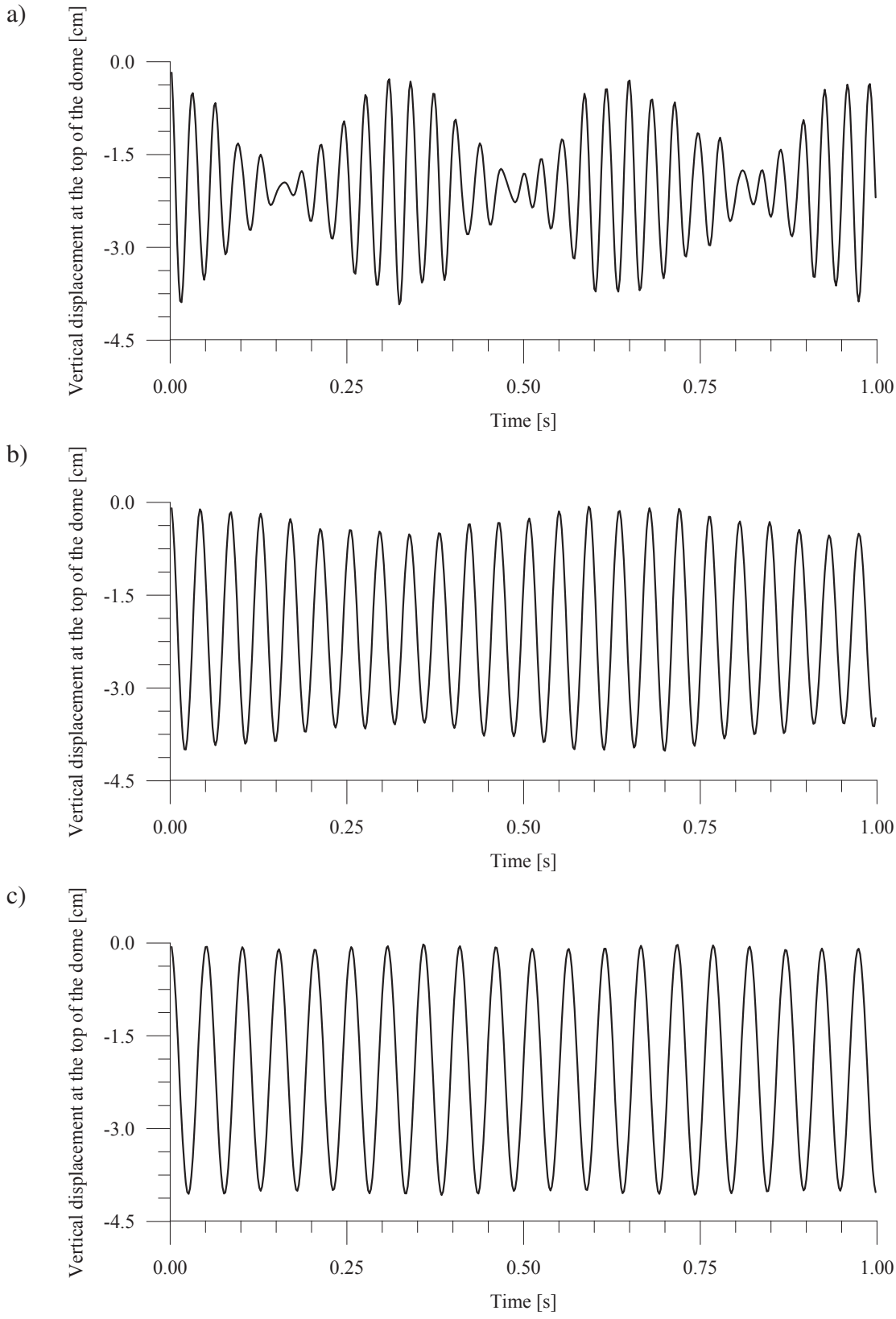

Figure 3.28 The course of vibration in the 160-element system, depending on the inertia of the added mass a) i=0.01; b) i=0.02; c) i=0.03.

3.7.5.4 Time-dependent Design Sensitivity - Deterministic Results

As we described in the previous section, the increase of elements' number in the FEM setting results in receiving slightly different values of initial periods of the system. Due to the repetitive frequency values within 160- and 320-element model, determining dynamic sensitivity without damping and added mass through superposition method failed to produce satisfactory results. The problem of numerical computation with this type of structures is widely described in the literature. Unfortunately, we did not manage to find a revealing solution to this issue meaning that including added mass on the top of the dome failed to produce sensitivity response by mode superimposition with 18 initial frequencies in both models.

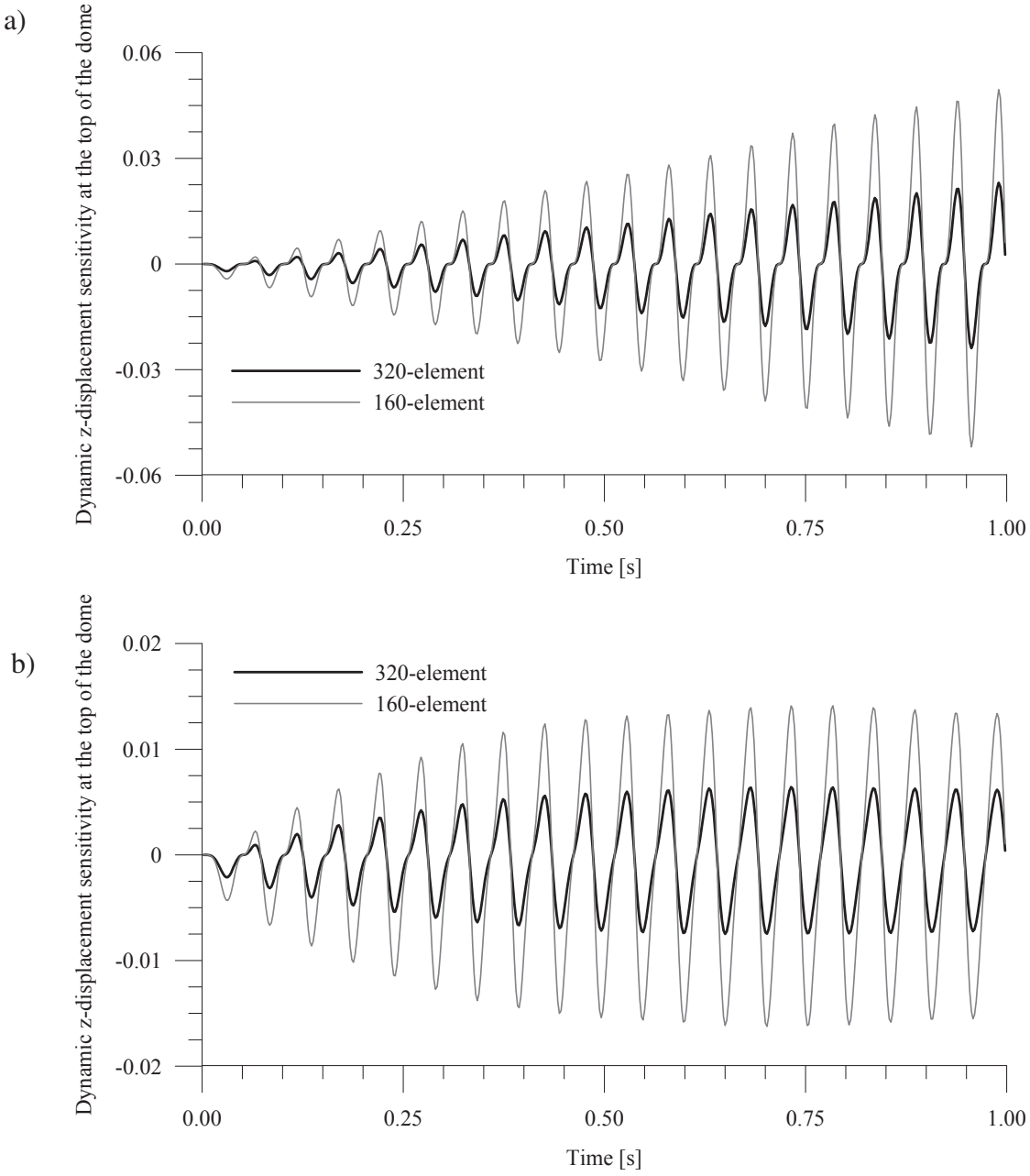

Figure 3.29 Comparison the results of design sensitivity with respect to cross sectional area of el. no 16 with influence of a) added mass; b) added mass and damping

Fig. 3.29 presents the result of dynamic sensitivity of z-direction displacement at the top of the dome with respect to cross-sectional area of element number 16. It turns out that for 320-

element model, sensitivity response design is lower than in the second one. This is because change of cross-sectional area of the component endures twice shorter than in the 160-element scheme. Therefore, the difference seems to be natural. Including added mass amounts to eliminating the beat phenomenon, however the amplitude of sensitivity response increases in time - compare Fig. 3.29.a). If we apply the damping coefficient $\lambda = 0.01$ the graph of sensitivity response gets stabilized (see Fig. 3.29b).

Despite mesh refinement bringing about numerous problems connected with obtaining correct results, addressing the former is advisable, because of advantages it could give. The analysis of 320-element beam model not only implies that the displacement of the selected node is most sensitive with respect to the change of cross-section of specific bar, but also specifies which part of this element is subject to displacement. It allows drawing the conclusion about the expected mechanism of the structure damage.

3.7.6 Stochastic Static Sensitivity in Beam Systems

We compute Stochastic Static Sensitivity for both vertical and horizontal displacements of selected nodes with respect to the cross-sectional areas of the specific elements. For better understanding of the types of data processing and results summarized in Tables 3.12 — 3.14, detailed drawings were created (see Figs. 3.28 and 3.31) presenting the fragment of FEM setting in considered beam models made of 80, 160 and 320 elements respectively.

Similarly as in the case of stochastic statics, numerical computations are made three times, for the coefficient of variation equal to 0.05, 0.10 and 0.15, respectively. The percentage differences between the deterministic and stochastic results depending on the value of the α-coefficient are summarized in Table 3.12. Tables 3.13 and 3.14 present deterministic results, excepted values and standard deviations of static displacement sensitivity response obtained for $\alpha = 0.15$. Other factors taken to the analysis are the same as in previous section, namely $\lambda = 200$ and $A^0 = 20\text{cm}^2$, for all three models. For adopted value of the coefficient of variation the differences between deterministic and stochastic results gained range between 5.40% to 8.20%, which in fact is the probable scenario. Only for the node no. 36 from 320-element beam scheme, we obtain the difference equal to 19.32%, which may be caused by very small values of displacement at this point, under 0.11cm and it is treated as a peculiar case. The static displacement sensitivity standard deviations is about $25 \div 32\%$ of the expectations, only for node no. 36 it is about 46%, which confirms the previous assumption.

It turns out that the highest values of the y-displacement sensitivity response in the selected nodes are obtained with respect to the cross-sectional areas of the elements in their own domain. The beam models consisting of 320 and 160 elements allow to examine the displacement sensitivity for the mid-points lying along chosen bars. Thanks to that we can find out which element part cross-section change makes the movement of a specific node most sensitive.

Table 3.12 The y-displacement static sensitivity with respect to the elements cross-sectional areas, for different α-coefficient values

Scheme	Node Number	Element Number	α -coefficient	Excepted Values	Deterministic Results	The percentage difference
80-element	15	67	0.05	0.01907	0.01893	0.74
			0.10	0.01951		3.06
			0.15	0.02023		6.87

a)

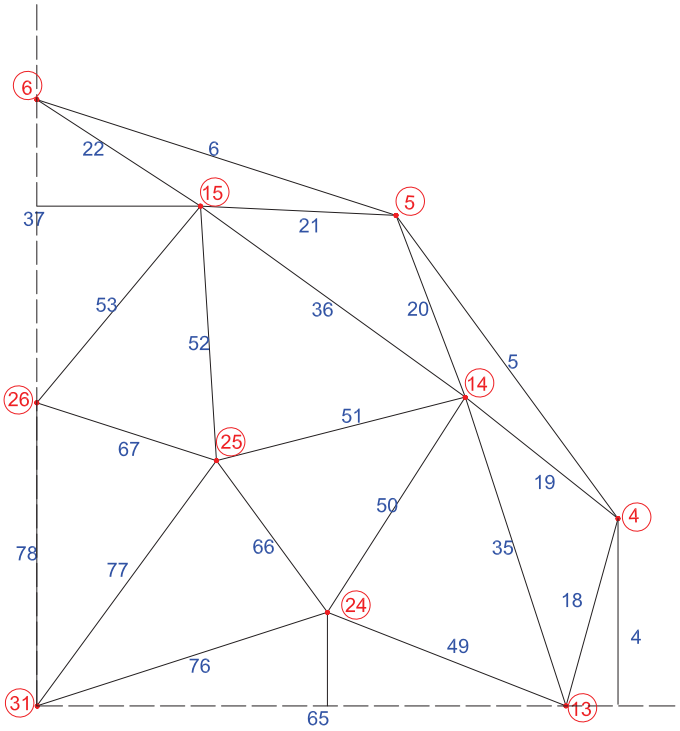

b)

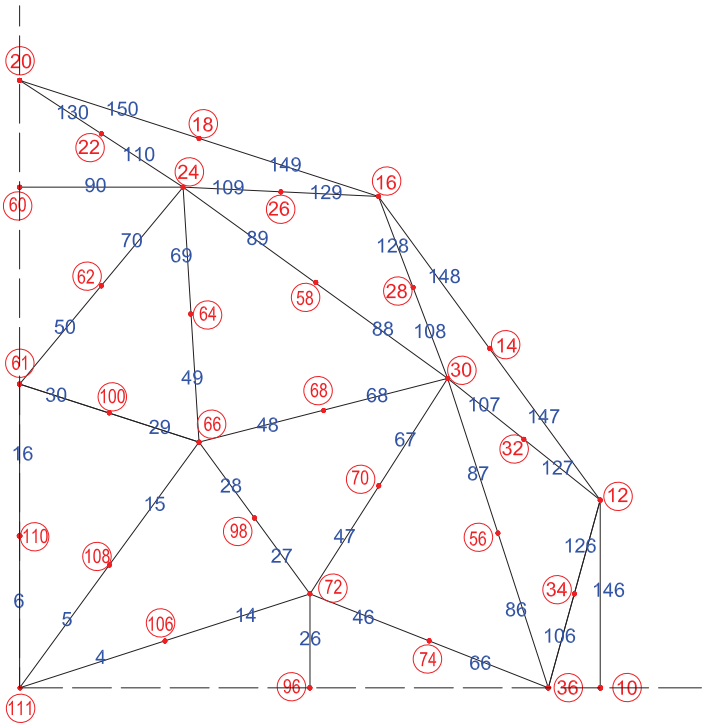

Figure 3.30 Finite element setting's fragments in beam models: a)80-element; b) 160-element;

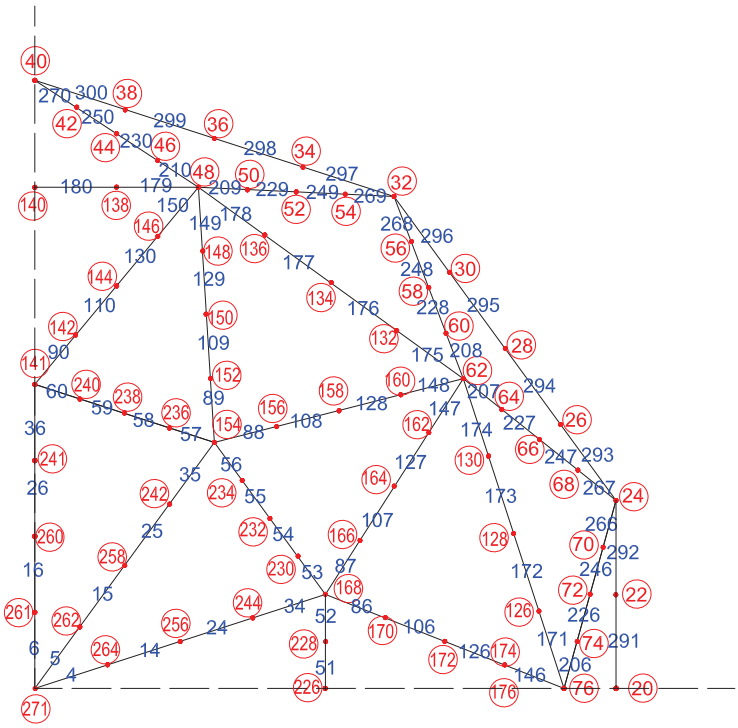

Figure 3.31 Finite element setting's fragments in 320-element beam scheme

Table 3.13 Static z-displacement sensitivity for the mid-point of element lying on y-axis with respect to cross-sectional area — $q_{all\{z\}} = 0.145$cm

Scheme	Node Number	Element Number	Deterministic Result	Excepted Values	Difference [%]	Standard Deviations
160-element	96	24	0.01533	0.01648	7.50	0.00465
		27	0.01497	0.01607	7.35	0.00451
		25	0.01423	0.01500	5.41	0.00439
		26	0.01408	0.01478	4.97	0.00425
320-element	226	49	0.01193	0.01291	8.21	0.00389
		52	0.01138	0.01228	7.91	0.00365
		48	0.00820	0.00887	8.17	0.00262
		53	0.00780	0.00841	7.82	0.00245

Considering the values presented in tables 3.13 and 3.14, it turns out, that the sensitivity obtained for selected node from the 320-element scheme is two times lower than in corresponding point from 160-element model and consequently four times lower than in from 80-element system. Subsequently, the following dependence can be set out: the higher the number of finite elements in the mesh of the considered model, the smaller the impact of changes within the cross-sectional area on bar's part. Therefore, the obtained regularity with the values of the sensitivity response in specific models seems to be natural.

The analysis of the stochastic sensitivity response, received for 160- and 320-element beam schemes, gives additional information on the change of which part of specific bars determines the results of displacements in selected nodes the most. In accordance with the above conclusion, the prescribed numerical computation in 320- and 160-element models gives a fresh insight into the structure's work. Except from the deterministic values we have the precision of

these results in the form of expectations and their standard deviations.

Table 3.14 Static y-displacement sensitivity with respect to cross-sectional areas

Scheme	Node Number	Element Number	Deterministic Result	Excepted Values	Difference [%]	Standard Deviations
a) The main point from the lower ring			$q_{all\{y\}} = 0.16$cm			
80-element	15	36	-0.02619	-0.02773	5.88	0.00718
		67	0.01893	0.02023	6.87	0.00570
		20	-0.01484	-0.01565	5.46	0.00387
		37	-0.01190	-0.01269	6.64	0.00354
160-element	24	89	-0.01311	-0.01392	6.18	0.00371
		88	-0.01309	-0.01387	5.96	0.00363
		30	0.00946	0.01011	6.87	0.00285
		29	0.00945	0.01010	6.88	0.00285
320-element	48	178	-0.00656	-0.00697	6.25	0.00188
		177	-0.00655	-0.00696	6.26	0.00185
		60	0.00473	0.00505	6.77	0.00143
		59	0.00473	0.00505	6.77	0.00143
b) The main point from the top ring			$q_{all\{y\}} = 0.24$cm			
80-element	25	77	0.03509	0.03747	6.78	0.01049
		66	-0.02250	-0.02403	6.80	0.00672
		76	-0.01900	-0.02031	6.89	0.00570
		65	-0.01064	-0.01137	6.86	0.00319
160-element	66	15	0.01760	0.01880	6.82	0.00531
		5	0.01746	0.01865	6.82	0.00526
		27	-0.01134	-0.01211	6.79	0.00338
		28	-0.01116	-0.01192	6.81	0.00335
320-element	154	25	0.00892	0.00953	6.84	0.00268
		35	0.00869	0.00928	6.79	0.00263
		15	0.00881	0.00949	7.72	0.00267
		5	0.00857	0.00916	6.88	0.00259
c) The mid- point of el. from the top ring			$q_{all\{y\}} = 0.085$cm			
160-element	108	5	0.03080	0.03073	0.23	0.00775
		27	-0.02003	-0.02138	6.74	0.00590
		14	-0.01885	-0.02006	6.42	0.00549
		28	-0.01714	-0.01811	5.66	0.00508
320-element	258	15	0.03573	0.03854	7.86	0.01210
		53	-0.01036	-0.01109	7.05	0.00307
		88	0.01084	0.01202	10.89	0.00384
		34	-0.00971	-0.01035	6.59	0.00286
d) The mid- point of el. lying on the y-axis			$q_{all\{y\}} = 0.11$cm			
160-element	110	6	0.02960	0.02964	0.14	0.00715
		29 and 32	-0.01520	-0.01620	6.58	0.00449
		30 and 31	-0.01407	-0.01496	6.33	0.00419
		15 and 17	-0.01320	-0.01398	5.91	0.00380
320-element	260	16	0.03433	0.03707	7.98	0.01142
		36	0.00828	0.00988	19.32	0.00462
		57 and 64	-0.00776	-0.00828	6.70	0.00229
		58 and 63	-0.00744	-0.00792	6.45	0.00219

3.8 Summarizing Remarks

The combination of stochastic analysis and design sensitivity give us the complex results in the form of deterministic values but also their means and cross-covariances. It seems to be very important in modern designing, because even small uncertainties in the design parameters may have a large influence on obtained values of displacements or internal forces.

The repeatable geometry in structures causes the presence of the beat phenomenon. Due to the material fatigue, it can be treated as negative effect and can be successfully eliminating by using added masses and damping.

The fully symmetry models selection should be avoided because of repeatable eigenvalues that makes the process of numerical computations complicated and in many cases impossible. For the same reason, the specific bars ought not to be divided into many finite elements in the mesh.

Chapter 4

Concluding Remarks

In this paper we are considering the problem of static and dynamic sensitivity of complex structures with including uncertainties in the design parameters. The computational results show a great importance of dynamic analysis in the contemporary designing. Most of the building objects are exposed to the dynamic force nowadays, therefore it is significant to include this type of load in the design process. The main reason is that the same system may behave quite differently under dynamic than static forces. For example, increasing the cross-sectional area of the element or thickness of the plate, undoubtedly advantageous from the point of view of static bearing capacity, may cause raising in the vibration amplitude which leads to the system destruction.

Presenting the numerical results, we prove the great importance of both static and dynamic sensitivity in the computations of the modern structures. It allows us to have a completely different look at the work of individual elements. This way, we can find the most sensitive point, that determines the stability of the entire system. Described in Section 2.6 the analysis of cable-stayed bridge, is a good example of that. The sensitivity results show a large impact of the changes in the cross-sectional areas of back cables supporting the pylon, to the displacements of span's middle-nodes. Due to the fact that these cables have no direct connections with the plate, they seem to have the secondary meaning in the analyzed displacements. Only the sensitivity results change the look at the work of the entire bridge and probable model of destruction.

By the combination of sensitivity analysis and random parameters, the computations of stochastic systems prove the great significance of even small uncertainties in the design parameters to the obtained results. In stochastic analysis the second moment perturbation method is used. The specific functions are expanded in Taylor series around the mean values of random variables, excluding the terms higher than second order. This way we obtain first two probabilistic moments of static and dynamic response and their sensitivities. This method requires small fluctuation of random variables, less than 15%. During the data processing of bar dome, presented in Section 3.7, the influence of the uncertainties values of random variables to the final displacements, are considered. It turns out, that when the randomness of the variables is under 15%, the difference between the deterministic and stochastic results is from 0.2 to 2.5% for displacements and 0.3 to 7.0% for sensitivities, in this type of structure. This way we obtained the set of results consisting of the deterministic values and the solution accuracy in the form of expectations and their cross-covariances.

During the computations of cable-stayed bridges the beat phenomenon was observed, that is the periodical changes of the amplitude in time. The analysis of different structural systems, confirmed the assumption that the repeatable geometry is largely responsible for appearing this effect in building objects. In this type of schemes, neighboring natural frequency have very similar values and their overlapping results in periodical changes of the amplitude. Because of the material fatigue point of view, the beat effect may be treated as negative phenomenon, so we tried to eliminate it by using the added mass in chosen nodes. Initially, the dynamic analysis shows that this is an effective method, however only careful sensitivity analysis proves that, to completely eliminate the beat phenomenon, the simultaneously including the added mass and damping is necessary. Considering the different type of numerical examples, we came to the conclusion that the added mass location is an individual issue for any structural scheme. However, in most cases the beat effect was eliminated effectively by putting added mass at the same node as dynamic force.

Presented method of eliminating the beat phenomenon by added masses and damping is examined and proved only by the numerical results. Developing the practical solution of this issue would be the culmination of the work on this problem and undoubtedly will be the focus of our future research.

The deterministic and stochastic analysis of structural system with many degrees of freedom by FEM, requires a lot of knowledge and experience to correctly interpret the results and locate possible errors. It is known, that FEM is an approximate method, thus there are many factors that determine obtaining the correct values of unknowns. At the beginning of the dynamic analysis of the described bar dome, the course of vibrations shows the amplitude decay without considering the damping in data processing and the node displacements are insensitive with respect to the cross-sectional areas of specific elements, which is impossible in reality. It turns out, that the wrong values of time step chosen in the analysis is responsible for this phenomenon. Only reduction of the time-step to several times gives a proper course of displacements and sensitivities during time.

At the stage of design the structural system we should try to avoid the full symmetry of object geometry, both in terms of the elements and supports arrangement. This type structures have the neighbouring natural frequencies with very similar values, which is a problem in numerical computations, that is widely prescribed in world literature [3]. During the data processing some eigenvalues are missing because of the seemingly identical values, that lead to confusing results. If we consider the statics of this type of dome, we can model each bar as divided into some beam elements. This gives more probable in reality results of displacements and internal forces, than for the truss system. However, aiming to the dynamic or sensitivity analysis, it is more appropriate to adopt the truss system, because using the dense mesh of beam elements leads to a peculiar problem. For the structure that has the symmetrical elements arrangement, it is sufficient to apply an asymmetrical setting of supports to avoid unnecessary numerical traps.

Analyzing structural system by FEM, an important part of computations is examining the correctness of the adopted model. It can be done for example by determining the condition number, [2,33,59] for instance. However, this method can only be used successfully for the system with small number of degrees of freedom. The aim of this paper is the analysis of MDOF structures. Finding the condition number for this type of system is a highly complicated numerical task and requires to develop an effective method of obtaining it. Therefore we intentionally exclude

this issue in the presented dissertation and decide to address this problem in further scientific research.

The static and dynamic sensitivity analysis with including the uncertainties in design parameters is an effective tool in designing the contemporary structures. Only the sensitivity in combination with the statics and dynamics of the considered system give a full view on the work of individual elements and on the structure as a whole. Additionally, including the random variables to the data processing results in obtaining the expectations and standard deviations, that in many cases have important meaning in designing. This type of analysis allows us to find the so-called design point, which means optimal solution with taking into account all relevant aspects.

Literature

1. G. Adomian
Stochastic Systems
Academic Press, 1983

2. Cz. Bajer
Metoda Elementów Czasoprzestrzennych w Obliczeniach Dynamiki Konstrukcji
IPPT PAN, 2008

3. K.-J. Bathe
Finite Element Procedures in Engineering Analysis
Prentice-Hall, 1982

4. R. Bąk, T. Burczyński
Wytrzymałość Materiałów z elementami ujęcia komputerowego
Wyd. WNT, 2009

5. T. Bednarek, W. Sosnowski
Multiple eigenvalue optimization problem for linear discrete systems using the DDM method
rozdz. w mon. *Knowledge acquisition for hybrid systems of risk assessment and critical machinery diagnosis*
W. Moczulski, K. Ciupke (eds.)
Publ. House of the Inst. for Sustain. Technolog., p.387-404, 2008

6. T. Bednarek, W. Sosnowski
Multiple eigenvalue optimization using direct differential method
rozdz. w mon. *Wybrane zagadnienia analizy modalnej konstrukcji mechanicznych*
T. Uhla(ed.)
Mat. Konf. XII Szkoła Analizy modalnej, p.15-28, 2008

7. J. Biliszczuk
Mosty podwieszone. Projektowanie i realizacja
Arkady, 2005

8. W. Bogucki, M. Żyburtowicz
Tablice do projektowania konstrukcji metalowych
Arkady, 1996

9. D. Bojczuk, Z. Mróz
Topological sensitivity derivative with respect to area, shape and orientation of an elliptic hole in a plate
Struct. Multidisc. Optim. 45, 153-169, 2012

10. Praca zb. pod kier. W. Buczkowskiego
Budownictwo Ogólne t. 4
Arkady, 2009

11. T. Chmielewski, H. Nowak
Wspomaganie komputerowe CAD CAM. Mechanika budowli. Metoda przemieszczeń. Metoda Crossa. Metoda elementów skończonych
WNT, 1996

12. K.K. Choi, Nam-Ho Kim
Structural Sensitivity Analysis and Optimization
Springer, 2010

13. R.W. Clough, J. Penzien
Dynamic of Structures
Mc Graw-Hill, 1975

14. R. Courant,
Variational methods for the solution of problems of equilibrium and vibrations
Bull. Amer. Math. Soc.,49, 1943

15. J.Ding, Z. Pan, L.Chen
Parameter identification of multibody systems based on second order sensitivity analysis
Int. J. of Non-Linear Mech. 47, 1105-1110, 2012

16. J. Drewko, T.D. Hien
First- and second-order sensitivities of beams with respect to cross-sectional cracks
Arch. Appl. Mech. 74, 309-324, 2005

17. M. Etzel, K. Dickinson
Digital Visual Fortran Programmer's Guide
Digital Press, 1999

18. G.S. Fishman,
Monte Carlo: Concepts, Algorithms, and Applications
Springer, 1995

19. K. Furtak, J. Śliwiński
Materiały budowlane w mostownictwie
Wyd. Komunikacji i Łączności, 2004

20. R.G. Ghanem, P.D. Spanos
Stochastic Finite Elements: A Spectral Approach
Springer, 1991

21. M. Giżejowski, J. Ziółko (eds.)
Budownictwo Ogólne t. 5
Arkady, 2010

22. M.S. Greene, Y. Liu, W. Chen, W. K. Liu
Computational uncertainty analysis in multiresolution materials via stochastic constitutive theory
Comput. Methods Appl. Mech. Engrg. 200, 309-325 , 2011

23. E.J. Haug, Kyung K. Choi, V. Komkov
Design Sensitivity Analysis of Structural Systems
Academic Pres, 1986

24. J.Heyman,
Elements of the Theory of Structures
Cambridge University Press, 1996

25. T.D. Hien
Deterministic and stochastic sensitivity in computational structural mechanics
habilitation thesis - IPPT, 1990

26. T.D. Hien,
Numerical Analysis of Stochastic Systems
Wyd. PS, 2003

27. T.D. Hien
Wybrane działy matematyki w ujęciu komputerowym
Wyd. PS, 1998

28. T.D. Hien, M. Kleiber
Computational Aspects in Structural Design Sensitivity Analysis for Statics and Dynamics
Computers & Structures Vol. 33. No. 4. pp. 939-950, 1989

29. T.D. Hien, M. Kleiber
POLSAP — A Finite Element Code for Deterministic and Stochastic Analyses of Large 3D Structures
IPPT PAN, 1990

30. T. Hisada, S. Nakagiri
Stochastic finite element method for structural safety and relability
Proc. 3rd Int. Conf. Struct. Safety Reliab., 395-402, 1981

31. A. Hrennikoff,
Solution of Problems of Elasticity by the Frame-Work Method
ASME J. Appl. Mech. 8,A619-A715, 1941

32. S. Jendo, J. Niczyj
Experimental identification of reliability of existing structural elements fuzzy sets
Num. mod. of uncert.: final program p.13, 1999

33. D Kincayd, W. Cheney
Analiza Numeryczna
Wyd. Nauk.-Tech. Wa-wa, 2006

34. M. Kleiber, T.D. Hien
Stochastic structural design sensitivity of static response
Int.J. Comput. Struct. 38, 659-667, 1991

35. M. Kleiber, T.D. Hien
The Stochastic Finite Element Method
Wiley, 1992

36. D.P. Kroese, T. Taimre, Z.I. Botev
Handbook of Monte Carlo Methods
John Wiley & Sons. p. 772, 2011

37. J. Kruszewski, S. Sawiak, E. Wittbrodt
Wspomaganie komputerowe CAD CAM. Metoda sztywnych elementów skończonych w dynamice konstrukcji
WNT, 1999

38. M. Kucharczyk, A. Mazurkiewicz, W. Żurowski
Nowoczesne Materiały Konstrukcyjne, wybrane zagadnienia
PR, 2008

39. K.M. Leet, Ch.-M. Uang, A.M. Gilbert
Fundamentals of Structural Analysis
fourth edition
Mc Graw-Hill, 2010

40. J. Li, J. Chen
Stochastic Dynamics of Structures
Wiley , 2009

41. L. Lichołai (ed.)
Budownictwo Ogólne t. 3
Arkady, 2008

42. W.K. Liu, T. Belytschko, A. Mani
Probabilistic finite elements for nonlinear structural dynamics
Comput. Methods Appl. Mech. Engrg. 56, 64-81, 1986

43. W.K. Liu, T. Belytschko, A. Mani
Random field finite elements
Int. J. Numer. Methods Eng., 23:1831-1845, 1986

44. M. Lubiński, A. Filipowicz, W. Żółtowski
Konstrukcje metalowe cz. I
Arkady, 2000

45. M. Lubiński, W. Żółtowski
Konstrukcje metalowe cz. II
Arkady, 2004

46. Cz. Machelski
Modelowanie Sprężenia Mostów
DWE, 2010

47. A. Madaj, W. Wołowicki
Podstawy projektowania budowli mostowych
Wyd. Komunikacji i Łączności, 2007

48. Z. Mróz, D. Bojczuk
Shape and topology sensitivity analysis and its application to structural design
Arch. Appl. Mech. 82, 1541-1555, 2012

49. Z. Mróz, R.T. Haftka
First- and second-order sensitivity analysis of linear and nonlinear systems
AIAA Jnl 24, 1187-1192, 1986

50. J. Niczyj
Relability-based optimization of trusses by fuzzy sets theory
Solid Struc. and Coup. Prob. in Eng.: 2nd Europ. Conf. on Comput. Mech.,p.26-29, 2001

51. J. Niczyj
Wielokryterialna optymalizacja niezawodnościowa oraz szacowanie stanu technicznego konstrukcji prętowych z zastosowaniem teorii zbiorów rozmytych
wyd. PS, 2004

52. M.E. Niezgodziński, T. Niezgodziński
Wzory Wykresy i Tablice Wytrzymałościowe
WNT, 1996

53. S. Rahman
Stochastic sensitivity analysis by dimensional decomposition and score functions
Probabilistic Engineering Mechanics 24, 278-287, 2009

54. G. Rakowski, Z. Kacprzyk
Metoda Elementów Skończonych w mechanice konstrukcji
Ofic. Wyd. PW, 2005

55. M. Rucka, K. Wilde
Dynamika Budowli z przykładami w środowisku MATLAB ®
Wyd. PG, 2008

56. K. Rykaluk
Zagadnienia Stateczności Konstrukcji Metalowych
DWE, 2012

57. P.W. Spence, C.J. Kenchington
The Role of Damping in Finite Element Analysis
NAFEMS, 1993

58. A. Sluzalec
Stochastic shape sensitivity in powder metallurgy processing
Appl. Math. Modelling 36, 3743-3752, 2012

59. W. Sosnowski, T. Bednarek, P. Kowalczyk
Badanie stabilności i jednoznaczności algorytmów teorii plastycznego płynięcia stosowanych w symulacji tłoczenia blach
Materiały XVII Konf. Informatyka w Technologii Metali
KomPlasTech, 2010

60. P.D.Spanos, R. Ghanem
Stochastic finite element expansion for random media
Eng. Mech., ASCE, 115:1035-1053, 1989

61. W. Szcześniak
Dynamika teoretyczna dla zaawansowanych
Ofic. Wyd. PW, 2007

62. H. Weber
Dynamic sensitivity of truss and beam systems with beat effects
Badania i analizy wybranych zagadnień z budownictwa ,
Wyd. PŚ., p. 583-591 , 2011

63. H. Weber
Static and Dynamic Analysis of Complex Structures by Finite Element Method
M.Sc. Thesis, 2008

64. H. Weber, T.D. Hien
Computational analysis of statics and dynamics of complex structures by finite element method
Pomiary, Automatyka, Kontrola Vol. 55, no.6 , p. 357-360 , 2009

65. H. Weber, T.D. Hien
Elimination of beat effects in structures by added lumped mass
Pomiary, Automatyka, Kontrola Vol. 56, no.6 , p. 617-619 , 2010

66. H. Weber, T.D. Hien
On the dynamic vulnerability of up-to-date structures
Pomiary, Automatyka, Kontrola Vol. 58, no.1 , p. 140-143 , 2012

67. W. Wojewódzki
Nośność graniczna konstrukcji prętowych
Ofic. Wyd. PW, 2012

68. O.C. Zienkiewicz, R.M. Taylor
The Finite Element Method
McGraw-Hill, 1991

69. PN-85/S-10030
Obiekty mostowe. Obciążenia

70. PN-82/B-02001
Obciązenia budowli. Obciązenia Stałe

71. PN-77/B-02011
Obciązenia w obliczeniach statycznych. Obciążenia wiatrem

72. *http://www.putrajaya.gov.my/tourist/attractions/bridge/jambatan_seri_wawasan*

Appendices

Appendix A

Selected Input and Output Printing for Suspended Bridge

```
P O L S A P  --  Deterministic and Stochastic Analysis for
Statics, Dynamics, Stability, Sensitivity and Optimization
of Medium- or Large-Scale Systems by Finite Element Method

   Dynamic analysis of structure of the suspended bridge.

   C O N T R O L   P A R A M E T E R S

   Number of nodal points.........................  736
   Number of finite element types.................    3
   Number of static load cases....................    1
   Number of requested frequencies................   18
   Analysis code .................................    2
   Deterministic options
   eq.0, Statics
   eq.1, Eigenproblem
   eq.2, Mode superposition
   eq.3, Response spectrum
   eq.4, Direct integration
   eq.5, Static sensitivity
   eq.6, Eigenvalue sensitivity
   eq.7, Buckling
   eq.8, Dynamic sensitivity
   eq.9, Optimization (Truss only)
   Stochastic options
    eq.10, Statics
   eq.11, Dynamics
   eq.12, Static sensitivity
   eq.13, Dynamic sensitivity
   Operation mode.................................0
   eq.0, Execution
   eq.1, Data check
   Number of subspace iteration vectors.....0
   Number of equations per block.....0
```

Structural Member

```
3 - D   T R U S S   E L E M E N T S

NUMBER OF TRUSS ELEMENTS                    =  154
NUMBER OF DIFFERENT ELEMENTS                =    2
FLAG FOR SENSITIVITY OR OPTIMIZATION
OR/AND STOCHASTIC ANALYSIS (ISENS)          =    0
EQ.0, NO
EQ.1, YES
DESIGN OR STOCHASTIC VARIABLE TYPE          =    0
EQ.0, IF ISENS.EQ.0
EQ.1, CROSS SECTIONAL AREA
EQ.2, YOUNG MODULUS
EQ.3, MASS DENSITY (NDYN.EQ.6,8,11,13)
EQ.4, LENGTH

MATERIAL AND GEOMETRIC PROPERTIES

TYPE      E        ALPHA      MASS       AREA      WEIGHT

1    2.000D+04  0.000D+00  7.850D-08  6.302D+01  0.000D+00
2    2.100D+04  0.000D+00  7.850D-08  1.018D+01  0.000D+00

ELEMENT CONNECTIONS

EL     I     J  TYPE      TEMP   BAND

 1   584   155     1      0.00   2115
 2   584   165     1      0.00   2065
 3   585   166     1      0.00   2066
 4   585   176     1      0.00   2016
 5   587   177     1      0.00   2023
 6   587   187     1      0.00   1973
 7   589   188     1      0.00   1980
 8   589   198     1      0.00   1930
 9   590   199     1      0.00   1931
10   590   209     1      0.00   1881
...  ...   ...   ...       ...    ...


3 - D   B E A M   E L E M E N T S

NUMBER OF ELEMENTS                              =  675
NUMBER OF GEOMETRIC PROPERTY SETS               =    3
NUMBER OF FIXED END FORCE SETS                  =    0
NUMBER OF MATERIALS                             =    2
FLAG FOR SENSITIVITY OR STOCHASTIC ANALYSIS (IS) =   1
EQ.0, NO
 EQ.1, YES
DESIGN SENSITIVITY OR STOCHASTIC VARIABLE TYPE  =    1
EQ.0, (IS.EQ.0)
EQ.1, CROSS SECTIONAL AREA
EQ.2, YOUNG MODULUS
 EQ.3, MASS DENSITY (NDYN.EQ.6,8,11,13)
EQ.4, LENGTH
```

MATERIAL PROPERTIES

MATERIAL NUMBER	YOUNG'S MODULUS	POISSON'S RATIO	MASS DENSITY	WEIGHT DENSITY
1	4.100D+03	2.000D-01	2.500D-08	0.000D+00
2	2.050D+04	3.000D-01	7.850D-08	0.000D+00

BEAM GEOMETRIC PROPERTIES

SECTION NUMBER	AXIAL AREA A(1)	SHEAR AREA A(2)	SHEAR AREA A(3)	TORSION J(1)	INERTIA I(2)	INERTIA I(3)
1	1.6000D+05	0.0000D+00	0.000D+00	9.0667D+09	4.5333D+09	4.5333D+09
2	3.2704D+03	0.0000D+00	0.000D+00	9.8454D+07	4.9227D+07	4.9227D+07
3	5.3200D+02	0.0000D+00	0.000D+00	3.4496D+06	3.3954D+06	5.4210D+04

BEAM NUMBER	NODE I	NODE J	NODE K	MATERIAL NUMBER	SECTION NUMBER	ELEMENT END LOADS A	B	C	D	END CODES I	J
1	736	127	325	1	1	0	0	0	0	0	0
2	127	573	325	1	1	0	0	0	0	0	0
3	573	574	325	1	1	0	0	0	0	0	0
4	574	575	325	1	1	0	0	0	0	0	0
5	575	576	325	1	1	0	0	0	0	0	0
6	576	577	325	1	1	0	0	0	0	0	0
7	577	578	325	1	1	0	0	0	0	0	0
8	578	579	325	1	1	0	0	0	0	0	0
9	579	580	325	1	1	0	0	0	0	0	0
10	580	581	325	1	1	0	0	0	0	0	0
...	...	...	...	...	...	...	...	...	...	...	...

T H I N P L A T E / S H E L L E L E M E N T S

ELEMENT TYPE = 6
NUMBER OF ELEMENTS = 510
NUMBER OF MATERIALS = 1
FLAG FOR SENSITIVITY OR STOCHASTIC ANALYSIS (IS) = 0
EQ.0, NO
EQ.1, YES
DESIGN SENSITIVITY OR STOCHASTIC VARIABLE TYPE = 0
EQ.0, (IS.EQ.0)
EQ.1, THICKNESS
EQ.2, YOUNG MODULUS
EQ.3, MASS DENSITY (NDYN.EQ.6,8,11,13)

MATERIAL PROPERTY TABLE

MATERIAL NUMBER	MASS DENSITY	THERMAL EXPANSION COEFFICIENTS ALPHA(X)	ALPHA(Y)	ALPHA(Z)
1	2.500D-08	0.000D+00	0.000D+00	0.000D+00

```
//ELASTIC CONSTANTS//

  C(XX)       C(XY)        C(XG)         C(YY)          C(YG)       G(XY)
1.067D+04   2.667D+03    0.000D+00     1.067D+04      0.000D+00   4.000D+03

THIN  PLATE/SHELL  ELEMENT DATA


ELEMENT                                          MATERIAL  AVERAGE    NORMAL
NUMBER NODE-I NODE-J NODE-K NODE-L NODE-O  NUMBER  THICKNESS  PRESSURE

   1     1      12     13      2      0         1  0.300D+02  -0.225D-02
   2     2      13     14      3      0         1  0.300D+02  -0.209D-02
   3     3      14     15      4      0         1  0.300D+02  -0.209D-02
   4     4      15     16      5      0         1  0.300D+02  -0.209D-02
   5     5      16     17      6      0         1  0.300D+02  -0.225D-02
   6     6      17     18      7      0         1  0.300D+02  -0.225D-02
  ...   ...     ...    ...    ...    ...       ...    ...          ...


S Y S T E M   P A R A M E T E R S
     Total number of equations.....................  3536
     Maximum half-bandwidth........................  2169
     Number of equations per block.................  3536
     Number of blocks..............................     1
```

Selected Types of Analysis

```
   E I G E N P R O B L E M   A N A L Y S I S
 CONTROL INFORMATION

     Flag for additional printing.....................    0
        eq.0, Suppress
        eq.1, Print
     Flag for Sturm sequence check....................    0
        eq.0, Check
        eq.1, Pass
     Maximum number of iterations required.............   20
    Convergence tolerance.............................  1.00D-05
     Cut-off frequency (cps)..........................  1.00D+08
     Number of starting iteration vectors
        to be read from File10 (Restart mode).........    0
     Flag for eigenvector printing....................    1
        eq.0, Print
        eq.1, Suppress
     Number of eigenvalues required...................   12

 (Convergence reached at iteration step 11)

 P R I N T   O F   E I G E N V A L U E S

  2.1875091047D+01  2.4749981516D+01  5.0976947247D+01  6.0367625090D+01
  1.3272178413D+02  1.6540672149D+02  1.7446069218D+02  2.1042679519D+02
          ...               ...               ...               ...
```

```
 P R I N T   O F   F R E Q U E N C I E S

   MODE   CIRCULAR FREQUENCY     CYCLIC FREQUENCY        PERIOD
 NUMBER         (RAD/SEC)            (CYCL/SEC)          (SEC)

      1   4.6770814668D+00   7.4438063468D-01    1.3433987310D+00
      2   4.9749353278D+00   7.9178554899D-01    1.2629682384D+00
      3   7.1398142305D+00   1.1363367275D+00    8.8002083868D-01
      4   7.7696605518D+00   1.2365798830D+00    8.0868208660D-01
      5   8.0648229946D+00   1.2835564448D+00    7.7908533286D-01
      6   1.0603493273D+01   1.6875983684D+00    5.9255805096D-01
     ...        ...                ...                  ...


 D Y N A M I C   A N A L Y S I S   B Y   M O D E   S U P E R P O S I T I O N S

 CONTROL INFORMATION
     NUMBER OF TIME FORCE FUNCTIONS...................    1
     FLAG FOR GROUND MOTION LOADING...................    0
       (EQ.0 - NO, EQ.1 - YES)
     NUMBER OF ARRIVAL TIMES..........................    1
     NUMBER OF TIME STEPS.............................  9999
     OUTPUT PRINTING INTERVAL.........................   10
     TIME INCREMENT...................................  4.000D-03
     DAMPING FACTOR...................................  0.000D+00
     FLAG FOR INTEGRATION OF UNCOUPLED EQUATIONS.......    0
       (EQ.0 - THETA WILSON, EQ.1 - NEWMARK
     FLAG FOR ELIMINATION OF SECULARITIES..............    0
       (EQ.0 - NO, EQ.1 - YES)
     FREQUENCY RANGE FACTOR FOR SECULAR ELIMINATION....  0.000D+00
       (WITH RESPECT TO FIRST NATURAL FREQUENCY)

 DYNAMIC NODAL FORCES/MOMENTS
              NODAL       TIME   ARRIVAL         TIME
   NODE   DEGREE OF   FUNCTION      TIME     FUNCTION
 NUMBER     FREEDOM     NUMBER    NUMBER   MULTIPLIER

    635           1          1         1     1.00D+00

 ARRIVAL TIME VALUES
  ENTRY   ARRIVAL TIME
 NUMBER          VALUE
      1       0.000000

 TIME FUNCTION NUMBER     =   1
 FUNCTION DESCRIPTION     =  Distributed Heaviside's function1
 NUMBER OF ABSCISSAE      =   2
FUNCTION SCALE FACTOR    =   1.00D+00

    TIME VALUE          FUNCTION    TIME VALUE          FUNCTION
   0.00000E+00  -1.000000000D+04   4.00000E+01  -1.000000000D+04

 DISPLACEMENT COMPONENT TIME HISTORY REQUESTS
   NODE   NODAL DEGREES OF FREEDOM
 NUMBER      *   *   *   *   *   *
    635      1   0   0   0   0   0
    580      1   0   0   0   0   0
    633      1   0   0   0   0   0
```

```
 CODE FOR DISPLACEMENT OUTPUT TYPE  =  1
   EQ.1,2, HISTORY AND MAXIMA
   EQ.3,   MAXIMA ONLY

SENSITIVITY COMPONENT TIME HISTORY REQUEST
   NODE NUMBER.....................=       635
   DEGREE OF FREEDOM...............=         1
   ALLOWABLE DISPLACEMENT..........= 1.000D+01
```

Appendix B

Selected Input and Output Printing for the Bar Dome

Structural Member in the Selected Models

```
Axial-symmetrical dome- truss system - stochastic statics

 C O N T R O L   P A R A M E T E R S

     Number of nodal points.........................   31
     Number of finite element types.................    1
     Number of static load cases....................    1
     Number of requested frequencies................    0
     Analysis code .................................   10
       Deterministic options
         eq.0, Statics
         eq.1, Eigenproblem
         eq.2, Mode superposition
         eq.3, Response spectrum
         eq.4, Direct integration
         eq.5, Static sensitivity
         eq.6, Eigenvalue sensitivity
         eq.7, Buckling
         eq.8, Dynamic sensitivity
         eq.9, Optimization (Truss only)
       Stochastic options
         eq.10, Statics
         eq.11, Dynamics
         eq.12, Static sensitivity
         eq.13, Dynamic sensitivity
     Operation mode.................................    0
         eq.0, Execution
         eq.1, Data check
         ..............
 3 / D   T R U S S   E L E M E N T S

 NUMBER OF TRUSS ELEMENTS                          =   80
 NUMBER OF DIFFERENT ELEMENTS                      =    1
```

```
 FLAG FOR SENSITIVITY OR OPTIMIZATION
        OR/AND STOCHASTIC ANALYSIS (ISENS)        =    1
   EQ.0, NO
   EQ.1, YES
 DESIGN OR STOCHASTIC VARIABLE TYPE               =    1
   EQ.0, IF ISENS.EQ.0
   EQ.1, CROSS SECTIONAL AREA
   EQ.2, YOUNG MODULUS
   EQ.3, MASS DENSITY (NDYN.EQ.6,8,11,13)
   EQ.4, LENGTH

 MATERIAL AND GEOMETRIC PROPERTIES

 TYPE       E       ALPHA        MASS        AREA      WEIGHT

   1  2.05000D+04 0.00000D+00 7.85000D-08 2.00000D+01 0.00000D+00


Axial-symmetrical dome - beam system - static sensitivity


 C O N T R O L   P A R A M E T E R S

     Number of nodal points.........................  112
     Number of finite element types.................    1
     Number of static load cases....................    1
     Number of requested frequencies................    0
     Analysis code .................................   12
       Deterministic options
         eq.0, Statics
         eq.1, Eigenproblem
         eq.2, Mode superposition
         eq.3, Response spectrum
         eq.4, Direct integration
         eq.5, Static sensitivity
         eq.6, Eigenvalue sensitivity
         eq.7, Buckling
         eq.8, Dynamic sensitivity
         eq.9, Optimization (Truss only)
       Stochastic options
         eq.10, Statics
         eq.11, Dynamics
         eq.12, Static sensitivity
         eq.13, Dynamic sensitivity
         ........

 3 - D   B E A M   E L E M E N T S

     NUMBER OF ELEMENTS                            =  160
```

```
     NUMBER OF GEOMETRIC PROPERTY SETS                =    1
     NUMBER OF FIXED END FORCE SETS                   =    0
     NUMBER OF MATERIALS                              =    1
     FLAG FOR SENSITIVITY OR STOCHASTIC ANALYSIS (IS) =    1
       EQ.0, NO
       EQ.1, YES
     DESIGN SENSITIVITY OR STOCHASTIC VARIABLE TYPE   =    1
       EQ.0, (IS.EQ.0)
       EQ.1, CROSS SECTIONAL AREA
       EQ.2, YOUNG MODULUS
       EQ.3, MASS DENSITY (NDYN.EQ.6,8,11,13)
       EQ.4, LENGTH

 MATERIAL PROPERTIES

    MATERIAL     YOUNG'S   POISSON'S      MASS      WEIGHT
      NUMBER     MODULUS      RATIO     DENSITY     DENSITY
           1  2.05000D+04   3.000D-01   7.850D-08  0.000D+00

 BEAM GEOMETRIC PROPERTIES

     SECTION   AXIAL AREA  SHEAR AREA  SHEAR AREA   TORSION   INERTIA
      NUMBER       A(1)        A(2)        A(3)        J(1)      I(2)
           1  2.0000D+01   0.0000D+00  0.0000D+00  1.4621D+02 8.6667D+01
        ...         ...         ...         ...         ...       ...
```

Parameters in Deterministic Dynamics

```
Axial-symmetrical dome - deterministic dynamic s

 C O N T R O L   P A R A M E T E R S

     Number of nodal points.........................   32
     Number of finite element types.................    1
     Number of static load cases....................    0
     Number of requested frequencies................   18
     Analysis code .................................    8
       Deterministic options
         eq.0, Statics
             ....
         eq.8, Dynamic sensitivity
             ....
     Number of design sensitivity constraints.......    1
             ....
 3 - D   B E A M   E L E M E N T S

     NUMBER OF ELEMENTS                               =   80
     NUMBER OF GEOMETRIC PROPERTY SETS                =    1
     NUMBER OF FIXED END FORCE SETS                   =    0
```

```
     NUMBER OF MATERIALS                                =    1
     FLAG FOR SENSITIVITY OR STOCHASTIC ANALYSIS (IS) =    1
       EQ.0, NO
       EQ.1, YES
     DESIGN SENSITIVITY OR STOCHASTIC VARIABLE TYPE   =    1
       EQ.0, (IS.EQ.0)
       EQ.1, CROSS SECTIONAL AREA             ....
 E I G E N P R O B L E M   A N A L Y S I S

 CONTROL INFORMATION

     Flag for additional printing.....................    0
        eq.0, Suppress
        eq.1, Print
     Flag for Sturm sequence check.....................    0
        eq.0, Check
        eq.1, Pass
     Maximum number of iterations required.............   40
     Convergence tolerance.............................  1.00D-05
     Cut-off frequency (cps)...........................  1.00D+08
     Number of starting iteration vectors
        to be read from File10 (Restart mode).........    0
     Flag for eigenvector printing.....................    1
        eq.0, Print
        eq.1, Suppress
     Number of eigenvalues required....................   18

 (Convergence reached at iteration step 23)

 P R I N T   O F   E I G E N V A L U E S

     7.8925200020D+04    7.8939427095D+04    1.7908251584D+05
     2.2641138818D+05    2.2956983822D+05    2.3175926150D+05
     ...                      ...                 ...
D Y N A M I C   A N A L Y S I S   B Y   M O D E   S U P E R P O S I T I O N S

 CONTROL INFORMATION

     NUMBER OF TIME FORCE FUNCTIONS....................    1
     FLAG FOR GROUND MOTION LOADING....................    0
       (EQ.0 - NO, EQ.1 - YES)
     NUMBER OF ARRIVAL TIMES...........................    1
     NUMBER OF TIME STEPS.............................. 9999
     OUTPUT PRINTING INTERVAL..........................   20
     TIME INCREMENT.....................................  2.000D-04
     DAMPING FACTOR.....................................  0.000D+00
     FLAG FOR INTEGRATION OF UNCOUPLED EQUATIONS.......    0
       (EQ.0 - THETA WILSON, EQ.1 - NEWMARK)
     FLAG FOR ELIMINATION OF SECULARITIES..............    0
```

```
       (EQ.0 - NO, EQ.1 - YES)
     FREQUENCY RANGE FACTOR FOR SECULAR ELIMINATION....  0.000D+00
       (WITH RESPECT TO FIRST NATURAL FREQUENCY)
```

Examples Design Constraints is Sensitivity Stochastic Analysis

```
 D E S I G N   C O N S T R A I N T S

   NODE   D.C.            X-AXIS            Y-AXIS            Z-AXIS
 NUMBER NUMBER       DISPLACEMENT      DISPLACEMENT      DISPLACEMENT
    110      1    0.000000000D+00    1.100000000D-01    0.000000000D+00

 STRUCTURE             ELEMENT    LOAD    MULTIPLIERS
 LOAD CASE            A         B         C         D
     1            0.000     0.000     0.000     0.000

 FLAGS FOR STOCHASTIC SOLUTION OUTPUT
 (EQ.0 - NO, EQ.1 - YES)

     READ INPUT COVARIANCES FROM A BINARY FILE...........=    1
     PRINTING EXPECTATIONS OF DISPLACEMENTS..............=    1
     PRINTING COVARIANCES OF DISPLACEMENTS...............=    0
     PRINTING ELEMENT STRESSES AT MEAN CONFIGURATION.....=    1

INPUT COVARIANCES ARE READ IN FROM FILE  160elnowa2.cov
E X P E C T A T I O N S   E ( N )   A N D   S T A N D A R D
D E V I A T I O N S   D ( N ) O F   S E N S I T I V I T I E S

(N = 1,..., NUMBER OF DESIGN VARIABLES)

 E(  1) = -3.023924927738D-03     E(  2) = -3.073606482801D-03
 D(  1) =  1.770134740409D-03     D(  2) =  1.450393582299D-03
... ...
```

Appendix D - Selected Fortran Computer Codes

```
!Program to generate the covariance matrix for the 80el. beam system

      implicit real*8 (a-h,o-z)
      Dimension x(80),y(80),z(80),cov(3240)

      nrand=80 !elements' number

      open (5,file='middlenodes80el1.txt',status='old')
      READ (5,'(3f10.3)') (x(j),y(j),z(j),j=1,nrand)

      a0=20.0d0 !mean value of random variable
```

```
      alpha=0.10d0 !coefficient determined by experimental method
      al2a02=alpha*alpha*a0*a0
      theta=200.0d0!scalling factor

      !generating the covariance matrix
      k=0
      do j=1,nrand
        do i=j,1,-1
          xij=-dabs((x(j)-x(i))/theta)
          yij=-dabs((y(j)-y(i))/theta)
          correlij=dexp(xij+yij)
          k=k+1
          cov(k)=al2a02*correlij
        enddo
      enddo
      open (6,file='xyz1.inp',status='unknown')
      write(6,'(1p3d20.10)') (x(i),y(i),z(i),i=1,80)

      open (4,file='80elnowa.cov',status='unknown',form='unformatted')
      rewind 4
      write (4) cov
      end


!Program to generate the coordinates of the middle of the elements in 80el.
!beam system

      implicit real*8 (a-h,o-z)
      integer fi
      Dimension l(8),m(8),k(8),theta(8),r(8),zn(8),
     *          x(80),y(80),z(80),a(80)
      xpi=0.01745329251994d0
      fi=36.0d0
      n=8
      nrand=80

      open (5,file='gen.middlenodes80el.txt',status='old')
      READ (5,'(3i10,3f10.5)') (l(j),m(j),k(j),theta(j),r(j),
     *                          zn(j),j=1,n)
      do j=1,n
        do i=l(j),m(j),k(j)
          ri=dfloat(i)
          variable=(theta(j)+(fi/k(j))*(ri-l(j)))*xpi
          x(i)=r(j)*dcos(variable)
          y(i)=r(j)*dsin(variable)
          z(i)=zn(j)
        enddo
      enddo

      do i=1,nrand
        a(i)=i
      enddo

      open (6,file='middlenodes80el.txt',status='unknown')
      write (6,'(1f10.0,3f10.3)') (a(i),x(i),y(i),z(i),i=1,nrand)
      end


!Program to generate the nodal coordinates for the 80el. beam system
```

```
      implicit real*8 (a-h,o-z)
     Dimension l(3),m(3),theta(3),r(3),zn(3),
     *          x(30),y(30),z(30),a(30)
     xpi=0.01745329251994d0
     fi=36.0d0
     n=3
     nrand=30
     open (5,file='gen.nodes80el.txt',status='old')
     READ (5,'(2i10,3f10.5)') (l(j),m(j),theta(j),r(j),
     *                         zn(j),j=1,n)
     do j=1,n
       do i=l(j),m(j)
         ri=dfloat(i)
         variable=(theta(j)+fi*(ri-l(j)))*xpi
         x(i)=r(j)*dcos(variable)
         y(i)=r(j)*dsin(variable)
         z(i)=zn(j)
       enddo
     enddo

     do i=1,nrand
       a(i)=i
     enddo

     open (6,file='coordinates80el.txt',status='unknown')
     write (6,'(1f10.0,3f10.3)') (a(i),x(i),y(i),z(i),i=1,nrand)
     end


!Program to generate the covariance matrix for the 160el. beam system

     implicit real*8 (a-h,o-z)
     Dimension a(160),x(160),y(160),z(160),cov(12880)

     nrand=160 !elements' number
     open (5,file='middlenodes160el.txt',status='old')
     READ (5,'(1f10.0,3f10.3)') (a(j),x(j),y(j),z(j),j=1,nrand)

     a0=20.0d0 !mean value of random variable
     alpha=0.15d0 !coefficient determined by experimental method
     al2a02=alpha*alpha*a0*a0
     theta=200.0d0 !scalling factor

     !generating the covariance matrix
     k=0
     do j=1,nrand
       do i=j,1,-1
         xij=-dabs((x(j)-x(i))/theta)
         yij=-dabs((y(j)-y(i))/theta)
         correlij=dexp(xij)*dexp(yij)
         k=k+1
         cov(k)=al2a02*correlij
       enddo
     enddo

     open (6,file='160elnowa2.cov',status='unknown',form='unformatted')
     rewind 6
     write (6) cov
```

```
      open (7,file='macierz.txt', status='unknown')
      write (7,'(10f10.3)') (cov(k),k=1,12880)
      end


!Program to generate the coordinates of the middle of the elements
!in 320el. beam system

      implicit real*8 (a-h,o-z)
      integer fi
      Dimension l(32),m(32),k(32),theta(32),r(32),zn(32),
     *          x(320),y(320),z(320),a(320)
      xpi=0.01745329251994d0
      fi=36.0d0
      n=32
      nrand=320 !elements' number

      open (5,file='gen.middlenodes320el.txt',status='old')
      READ (5,'(3i10,3f10.5)') (l(j),m(j),k(j),theta(j),r(j),
     *                          zn(j),j=1,n)
      do j=1,n
        do i=l(j),m(j),k(j)
          ri=dfloat(i)
          variable=(theta(j)+(fi/k(j))*(ri-l(j)))*xpi
          x(i)=r(j)*dcos(variable)
          y(i)=r(j)*dsin(variable)
          z(i)=zn(j)
        enddo
      enddo

      do i=1,nrand
        a(i)=i
      enddo

      open (6,file='middlenodes320el.txt',status='unknown')
      write (6,'(1f10.0,3f10.3)') (a(i),x(i),y(i),z(i),i=1,nrand)
      end


!Program to generate the coordinates of the middle-point of the choosen
!elements in 320el. beam system

      implicit real*8 (a-h,o-z)
      real xn,yn,zn,an,bn,rn,thetan,cn
      Dimension x(270),y(270),z(270),a(270)

      xpi=0.01745329251994d0
      an=284 !element number
      k=6 !number of first node in the element
      l=8 !number of second node in the element

      open (5,file='Coordinates320el.txt',status='old')
      READ (5,'(1f10.0,3f10.3)') (a(j),x(j),y(j),z(j),j=1,270)

      xn=0.5*(x(k)+x(l))!x-coordinate of the middle of the an-element
      yn=0.5*(y(k)+y(l))!y-coordinate of the middle of the an-element
      zn=0.5*(z(k)+z(l))!z-coordinate of the middle of the an-element
      bn=xn*xn+yn*yn
```

```
rn=SQRT(bn)!radius of the circle
cn=xn/rn
thetan=asin(cn)/xpi+270.0d0 !the offset angle

open (6,file='wyniki.txt',status='unknown')
write (6,'(1f10.0,5f10.5)') an,xn,yn,thetan,rn,zn
end
```